Author/s:
Bruell, Shoni Denise Rega

Title:
Mechanism of activation of the relaxin family peptide receptors RXFP1 and RXFP2

Date:
2019

Persistent Link:
https://hdl.handle.net/11343/233642

Mechanism of activation of the relaxin family peptide receptors RXFP1 and RXFP2

Shoni Denise Rega Bruell
ORCID: 0000-0002-8419-6711

Submitted in total fulfilment of the requirements of the degree of Doctor of Philosophy

Under the supervision of Associate Professor Paul Gooley and Professor Ross Bathgate

Department of Biochemistry and Molecular Biology
The University of Melbourne

September 2019

ABSTRACT

The relaxin family peptide receptors RXFP1 and RXFP2 are the cognate receptors for the peptide hormones relaxin and INSL3 respectively, best known for their roles in reproductive biology. Being GPCRs, these receptors are members of the largest family of membrane-bound receptors known in the human genome, but they are unique within this family due to the existence of a single low-density lipoprotein type A (LDLa) module on the N-terminus of their large ectodomain. The LDLa module is imperative to normal receptor signalling and is hypothesised to be a tethered ligand, interacting with the receptor transmembrane domain (TMD) to bring about an active conformation. This module is connected to the leucine-rich repeats that make up the remainder of their extracellular domain by a stretch of amino acids 32 long in RXFP1 and 25 in RXFP2. These linking residues have been termed the linker, and a series of accidental and intentional discoveries led to the notion that the linker plays an important role within the activation mechanism of both RXFP1 and RXFP2 in response to their peptide ligands. The work presented within this thesis delves into the details of this activity, exploring the various regions of the linker, as well as the LDLa modules, with the use of mutagenesis and the construction of chimeras of the two receptors. The mutants and chimeras were systematically tested in stably or transiently transfected HEK293T cells in a series of ligand binding, activity (focussing on their ability to prompt an accumulation of intracellular cAMP) and cell surface/total expression assays. By comparing the behaviour of the mutant and chimeric receptors to that of their wild-type counterparts we have been able to paint a detailed picture of the binding and activation mechanisms of RXFP1 and RXFP2 in response to either active peptide ligand, adding our findings to a growing understanding of their activity quickly emerging from the lab and the field at large.

Complementing the data generated from cell-based assays are nuclear magnetic resonance (NMR) studies performed concurrently using recombinantly expressed and purified RXFP1 and RXFP2 LDLa-linker proteins in titrations with relaxin as well as the receptor extracellular loops, as expressed on a soluble scaffold based on thermostabilized protein GB1. While the NMR experiments were carried out by a collaborating student, the RXFP2 LDLa-linker and soluble scaffold proteins were designed and characterized for use in NMR during this PhD project, and the details are outlined herein.

In Chapter 2 the LDLa modules of the two receptors were swapped, such that RXFP1 contained the LDLa module from RXFP2 and vice versa. We found that while ligand-induced

activity was weakened in the chimeric receptors, they were able to produce a robust signal, and for RXFP2 (but not RXFP1) the signal was slightly closer to wild-type levels upon subsequent swapping of the TMDs, such that they would match the non-native LDLa module [1]. The result contradicted previous findings in which RXFP1 with the LDLa module from RXFP2 was shown to be incapable of signalling upon relaxin stimulation. We rationalized this discrepancy as being due to the differing design in the cloning of the chimeric constructs. While our versions swapped only the LDLa modules themselves, the previous versions had also swapped a large portion of the neighbouring linker residues. This alerted us to a possible function being carried out by the linker and guided our future work.

We proceeded to mutate residues of the linker to alanine, carrying out an extensive scan of the RXFP1 linker that is presented in Chapter 3. We discovered that the initial residues formed something of a motif with the sequence GDNNGW, and when mutated – the residues Asp_2, Gly_5 and Trp_6 in particular – the receptors lost their ability to stimulate cAMP production and bind relaxin effectively. This information along with NMR data led to the conclusion that this motif made up an activation region that was involved in the tethered ligand activation mechanism of RXFP1. Of note, we observed that the fold-difference in affinity for relaxin exhibited by the mutants of the activation domain was not commensurate with the enormous weakening in potency in relaxin signalling assays shown by the same mutants. This contrasted with mutants of the central part of the linker, in particular Phe54 and Tyr58, which when mutated individually or together displayed similar fold-differences from wild-type in relaxin potency and affinity. Coupled with compelling NMR data we concluded from this evidence that the central portion of the linker constituted a relaxin binding site that had hitherto never been described [2].

We pursued a similar investigation focussing on the linker of RXFP2 in Chapter 4. The supposed activation region is largely conserved in the similar receptor, with the initial sequence of the linker GDTSGW. Indeed, mutation to alanine of these residues and the Phe found three residues along showed that both relaxin and INSL3 activation was dependent on equivalent residues to those identified in the RXFP1 mutagenesis campaign. Similarly, relaxin binding was severely compromised in the mutant receptors, while INSL3 binding was not. This result mirrored prior knowledge coming from mutagenesis and A-chain truncations of the relaxin and INSL3 peptides and highlighted a differing mode of action on RXFP2 in response to the two similar agonists. We postulated that the activation region of RXFP2 consisted of the linker residues from the GDxxGW motif found in both receptors, but they

were assisted or accompanied by the actions of the N-terminal residues of the INSL3 A-chain [3].

We further investigated the relaxin binding site from the RXFP1 linker by creating another two chimeras, in which the implicated residues were inserted into an equivalent position in the RXFP2 linker. The linker of RXFP2 is shorter than that of RXFP1 and hence a relaxin binding site had not been identified at a similar position, but by including the residues we supposed to be contributing to this binding site we were able to increase the potency and affinity for relaxin of the chimera to more closely resemble the behaviour of RXFP1 with its native ligand. In addition, the dissociation kinetics of the interaction, measured using a NanoBRET assay, resembled more closely the case of RXFP1 than RXFP2. This information helped us to confirm the existence of the relaxin binding site and highlight major differences between the two receptors with a focus on the linker [4].

The work presented in this thesis gives a deep and detailed look at an integral part of the binding and activation mechanisms of RXFP1 and RXFP2 in response to the peptide hormones relaxin and INSL3, paving the way for their use in a therapeutic setting. The resolution of the role that the LDLa module plays has altered the prevailing view about receptor activation in a number of aspects. Firstly, the complex binding mode of both relaxin and INSL3 has been defined more thoroughly, and secondly, we now know to focus on the linker when defining TM interactions. It therefore highlights the utility of using a combination of approaches – cell-based assays partnered with mutagenesis and chimeras alongside protein expression and NMR – to reach valid conclusions about molecular systems.

DECLARATION

This is to declare that:

1) This thesis comprises only my original work towards the PhD except where indicated in the preface
2) Due acknowledgement has been made in the text to all other material used
3) The thesis is fewer than 100,000 words in length

Shoni Denise Rega Bruell

PREFACE

The following work was carried out in collaboration:

Chapter 2. The chapter comprises a published work entitled “Chimeric RXFP1 and RXFP2 receptors highlight the mechanism of activation utilizing their N-terminal low-density lipoprotein class A modules”. It was published in the journal Frontiers in Endocrinology in 2013.

Roy Kong made and tested the chimeric receptors RXFP211 and RXFP212 that are presented in Chapter 2, and RXFP1-Ins A40-41 in Chapter 3.

Ashish Sethi performed all of the NMR experiments presented in Chapters 3 and 4, as well as purifying all $RXFP1_{(1-72)}$, and multiple batches of $RXFP2_{(1-65)}$, GB1-$RXFP2_{(1-65)}$, ssRXFP1 and ssRXFP2.

Sharon Layfield and Tania Ferrero performed Eu^{3+}-relaxin binding assays on the single-point RXFP1 mutants presented in Chapter 3.

Nicholas Smith made and tested RXFP2 linker mutants presented in Chapter 4.

Bradley Hoare made Nluc-RXFP1 and performed the NanoBRET assays for RXFP1 presented in Chapter 4.

Work contributing to a prior degree:

The double mutants RXFP1 G41A/D42A, N43A/N44A and G45A/W46A presented in Chapter 3 were made and initially tested during my Honours project (2011-2012).

PUBLICATIONS

Hoare, BL., **Shoni Bruell**, Michael J Lew, Mohammed A Hossain, Asuka Inoue, Daniel J Scott, Ross AD Bathgate
Multi-component mechanism of H2 relaxin binding to RXFP1 through NanoBRET Kinetic analysis
iScience, 2019, 11, p.93-113.

Bruell, S., Ashish Sethi, Nicholas Smith, Daniel J Scott, M Akhter Hossain, Q.P. Wu, Z.Y. Guo, Emma J Petrie, Paul R Gooley, Ross AD Bathgate
Distinct activation modes of the Relaxin Family Peptide Receptor 2 in response to insulin-like peptide 3 and relaxin.
Scientific reports, 2017, *7*(1), p.3294.

Sethi, A., **Shoni Bruell**, Nitin Patil, M Akhter Hossain, Daniel J Scott, Emma J Petrie, Ross AD Bathgate and Paul R Gooley
The complex binding mode of the peptide hormone H2 relaxin to its receptor RXFP1.
Nature communications, 2016, *7*, p.11344.

Kong, RCK., Ross AD Bathgate, **Shoni Bruell**, John D Wade, Paul R Gooley, Emma J Petrie
Mapping key regions of the RXFP2 low-density lipoprotein class-A module that are involved in signal activation.
Biochemistry, 2014, Vol 53(28):4537-48

Bruell, S., Roy CK Kong, Emma J Petrie, Brad Hoare, John D Wade, Daniel J Scott, Paul R Gooley, Ross AD Bathgate
Chimeric RXFP1 and RXFP2 Receptors Highlight the Similar Mechanism of Activation Utilizing Their N-Terminal Low-Density Lipoprotein Class A Modules.
Frontiers in Endocrinology (Lausanne), 2013, Vol 4: 171.

ORAL AND POSTER PRESENTATIONS

Oral:

- *Investigating the activation mechanism of RXFP2*
  Relaxin and Related Peptides conference, Cabo San Lucas, Mexico, May 2018
- *The secret life of proteins*
  3-minute thesis (3MT) competition, Biochemistry Department and University of Melbourne competitions, July and August 2016
- *RXFP1 – an unusual member of a large family*
  Seminar presentation at *l'Institut Genomique Fonctionelle*, Montpellier, France, 2015
- Students of the Florey Institute (SOFI) talks: 2016, 2018
- Biochemistry Retreat student talks: 2013, 2015

Posters:

- Molecular pharmacy of GPCRs (MPGPCR) meeting, Melbourne, Australia, December 2018
- Early-career scientists forum on GPCRs (ECSF-GPCR), Berlin, Germany, July 2018
    - Chaired a session at ECSF-GPCR, Berlin
- Relaxin and Related Peptides conference, Cabo San Lucas, Mexico, May 2018
- Relaxin and Related Peptides Meeting, Kuching, Malaysia, October 2015
- ASCEPT-MPGPCR meeting, Melbourne, Australia, 2014

AWARDS AND PRIZES

- Biochemistry department travel award to attend ECSF-GPCR in Berlin, Germany (2018)
- Geoff Tregear travel fund for attending Relaxin and Related Peptides conferences in Mexico (2018) and Malaysia (2015)
- Biochemistry department 3MT competition winner, 2016
- Structural biology prize for oral presentation at Biochemistry department graduate retreat, 2015
- Stipend equivalent in value to an APA scholarship from the Florey Institute of Neuroscience and Mental Health for the duration of my PhD
- Melbourne Research Fee Remission Scholarship, 2013 – 2019

ACKNOWLEDGEMENTS

The day I met Paul Gooley, back in 2011, he asked me if I knew what a GPCR was, to which I replied, “Well, I know what PCR is.” Despite this less-than-ideal show of my scientific chops, he took me on as an Honours student and introduced me to his collaborator Ross Bathgate, who blew me away with his passion and enthusiasm about this amazing hormone called Relaxin. “What a great name for a protein”, I thought to myself, and, with the idea of following my dream of finding out as much as I could about how molecules communicate with each other, I signed on to the project.

I could never have imagined all the highs and lows this decision would lead me to, but the advantages of working for over eight years in the Gooley and Bathgate labs have far outweighed the crushing blows of failed purifications and wasted reagents. I’ve found working with Ross and Paul to be both challenging and satisfying, and I thank them for their endless patience and support. Being a part-time student with two interruptions for maternity leave during my candidature has meant my project has taken a long, meandering path, and the collaborations that supported its different aspects have added to the scope of the story I’ve been able to tell, so I also express the deepest gratitude to all those who are mentioned within these pages, and who share authorship on the five publications that contain work from this PhD: Roy Kong, Bradley Hoare, Ashish Sethi and Nicholas Smith. My work was guided in a very real sense by the post-docs and senior lab members who were always available to provide help and advice, and whose work on the structure and function of RXFP1 and RXFP2 gave my work its starting point: Emma Petrie, Dan Scott (also a committee member) and Martina Kocan. My training in tissue culture and cell-based assays was carried out (and still continues) by the steadfast research assistants Sharon Layfield and Tania Ferraro, and they also helped complete my data sets in order to reach publication while I was away on leave. In protein expression and purification, I was taught by Patrick Shilling, Jesse Mobbs, Natalie Diepenhorst, Jason Ling and Ashish Sethi. Huge thanks to all those who gave me the lab skills I needed to do this work and sometimes even understand it.

But of course one of the best things about being in a lab is being surrounded by clever people all day long, and I’ve shared the labs and offices with so many fun and interesting colleagues, some of whom have already been mentioned, but so many more besides: Samantha Lagaida, Adam Valkovic, Bruce Ngo, Lilian Wong, Feng Jie Wu, Fabian Bumbak, Riley Cridge, Kelvin Yong, Natalie Gunn, Tasneem Vaid, Alice Whitehead, Lisa Williams, Jonathan Siah, Fei Yan, Alamgir Hossain and Jing Yu Zhan to name just a few.

Special thank you to Marie Bogoyevitch, my committee chair. Good luck with the next chapter in your story!

Another large debt of thanks goes to Ross for the financial support he has been able to give me. Thanks also to Leon Helfenbaum and Amber Willems-Jones for giving me the opportunity to supplement this with demonstrating work, and to the friends I made on that side of the uni in Izabela Szambelanczyk Orval, Renu Shankar and Kim Ia (among others). Teaching the next generations of undergrads second- and third-year techniques also helped my own understanding of molecular biology no end.

And it wouldn't be an acknowledgement section without mention of my beautiful friends and family: my friends Sha, Faith, Becca and Shane, who may be a little silly sometimes, but only in the best ways; and my family who are also really my best friends too – sisters Misha and Pandora and brother Baillie, each living life in their own very special way, and my mother Jacquie, who has spent a good proportion of my PhD time circumnavigating the world single-handed, showing us all the power of having a dream and a strong will. I'll also mention my father Peter and babcia (grandmother) Anna, who are no longer with us, but helped shape me in so many ways. Babcia was a huge part of my life until just last year, and always supportive of my chosen path and life choices (except when I was driving buses – she was not OK with that!) I'm sure she would be extremely pleased to see me finally graduate.

I thank my kids Félix and Joey for giving me perspective and forcing me to work efficiently and quickly. Also, for being super fun and adorable and teaching me to get by on minimal sleep. I hope that I can succeed in teaching you wisdom, resilience and resourcefulness in a changing world.

And my final and most heartfelt thanks go to partner Pierre, without whom it would have been a very different journey, and perhaps never have arrived at this point. Merci mon amour, je t'adore!

Not just a post-script: Thanks to the infinite, the universe, the greater power that makes all things possible.

ABBREVIATIONS

2R	2 rounds of whole genome duplication
AC	Adenylate Cyclase
AHF	Acute heart failure
Akt	Protein kinase B
ANOVA	Analysis of variance
AT_1R	Angiotensin type 1 receptor
AT_2R	Angiotensin type 2 receptor
ATP	Adenosine Triphosphate
β-gal	Beta galactosidase
BRET	Bioluminescence resonance energy transfer
BSA	Bovine serum albumin
cAMP	Cyclic 3'-5' adenosine monophosphate
CD	Circular dichroism
cGMP	Cyclic guanosine monophosphate
CPRG	Chlorophenol red-β-D-galactropyranoside
CRE	cAMP response element
CREB	CRE-binding protein
CTRP	C1q/tumour necrosis factor-related protein
DMEM	Dulbeccos' modified Eagle medium
DMSO	Dimethyl sulphoxide
ECD	Extracellular domain
EL	Extracellular loop
ELISA	Enzyme-linked immunosorbent assay

ERK1/2	Extracellular signal regulated kinase 1/2
EST	Expressed sequence tag
Eu	Europium
ExLink	Extended linker
FACS	Fluorescence activated cell sorting
FBS	Foetal bovine serum
FSHr	Follicle-stimulating hormone receptor
Fu-CRD	Furin-like cysteine rich domain
GABA	Gamma aminobutyric acid
GB1	B1 immunoglobulin binding domain of streptococcal protein G
GPCR	G-protein coupled receptor
GPHR	Glycoprotein hormone receptor
GR	Glucocorticoid receptor
GREAT	GPCR associated with testicular descent
GTP	Guanosine triphosphate
HEK	Human embryonic kidney
hetNOE	Heteronuclear nuclear Overhauser effect
HF	Heart failure
HPLC	High performance liquid chromatography
HSQC	Heteronuclear single quantum coherence
IGF	Insulin-like growth factor
IGFR	IGF type 1 receptor
INSL	Insulin-like peptide
IPTG	Isopropyl-D-1-thiogalactopyranoside

IR	Insulin receptor
LB	Luria-bertani broth
LDLa	Low-density lipoprotein module type A
LDLR	Low-density lipoprotein receptor
LGR	Leucine-rich repeat containing GPCR
LHr	Luteinizing hormone receptor
LRR	Leucine-rich repeat
LSD	Least squares deifference
MAPK	Mitogen-activated protein kinase
mGR	Membrane-associated GR
ML290	2-isopropoxy-*N*-(2-(3-(trifluoromethylsulfonyl)phenylcarbamoyl)phenyl)benzamide
MMP	Matrix metalloproteinase
MRE	Mean residue ellipticity
NI	Nucleus incertus
Nluc	Nanoluc™/Nanoluciferase
NMR	Nuclear magnetic resonance
NO	Nitric oxide
NOS	Nitric oxide synthase
PAGE	Polyacrylamide gel electrophoresis
PAR	Protease-activated receptor
PBS	Phosphate-buffered saline
PCR	Polymerase chain reaction
PEI	Polyethylenimine
PI3K	Phosphatidylinositol 3 kinase

PKC	Protein kinase C
PPARγ	Peroxisome proliferator-activated receptor gamma
RXFP	Relaxin family peptide receptor
SALPR	Somatostatin and angiotensin-like peptide receptor
SDS	Sodium dodecyl sulphate
SEC	Size-exclusion chromatography
SEM	Standard error of the mean
sGC	Soluble guanosine cyclase
sTyr	Sulphated tyrosine
TamRLX	TAMRA-labelled relaxin
TBS	Tris-buffered saline
TM/TMD	Transmembrane/Transmembrane domain
TSHr	Thyroid stimulating hormone receptor
VEGF	Vascular endothelial growth factor
WGD	Whole genome duplication

LIST OF AMINO ACIDS

Amino acid	3-letter abbreviation	1-letter abbreviation
Alanine	Ala	A
Arginine	Arg	R
Asparagine	Asn	N
Aspartic acid	Asp	D
Cysteine	Cys	C
Glutamic acid	Glu	E
Glutamine	Gln	Q
Glycine	Gly	G
Histidine	His	H
Isoleucine	Ile	I
Leucine	Leu	L
Lysine	Lys	K
Methionine	Met	M
Phenylalanine	Phe	F
Proline	Pro	P
Serine	Ser	S
Threonine	Thr	T
Tryptophan	Trp	W
Tyrosine	Tyr	Y
Valine	Val	V

TABLE OF CONTENTS

LIST OF FIGURES

LIST OF TABLES

Chapter 1 General Introduction

1.1 Relaxin family peptides and their receptors: overview

Relaxin is a peptide hormone descended from an ancestral insulin gene that gave rise not only to modern insulin and relaxin, but also an array of insulin-like growth factors (IGF), insulin-like peptides (INSL) and relaxin family peptides, all of which contain a similar structural fold, characterized by a conserved "cysteine knot" (Figure 1.1). These are divided into two major families, with one branch containing insulin and the IGFs, and the other the INSL and relaxin peptides [5]. The single relaxin-like gene that gave rise to the various numbers and variations of the peptide found in most vertebrate species known today was subject to a series of duplication events, beginning with two rounds (2R) of whole genome duplication (WGD) around 550 million years ago [6]. The relaxin- and insulin-like peptide signalling axis is actually much more ancient however, and this class of peptide has been identified in various forms in species ranging from primates to invertebrates including starfish and drosophila [7-9], working in both reproductive and other capacities through G protein-coupled receptors (GPCRs) related to the modern relaxin family peptide (RXFP) receptors. In humans there are seven relaxin family peptides and four receptors present in the modern genome [8]. These are the hormones relaxin-1, relaxin-2, relaxin-3, and insulin-like peptides (INSL) INSL3, INSL4, INSL5 and INSL6, and the four receptors, RXFP1-4 (Figure 1.2).

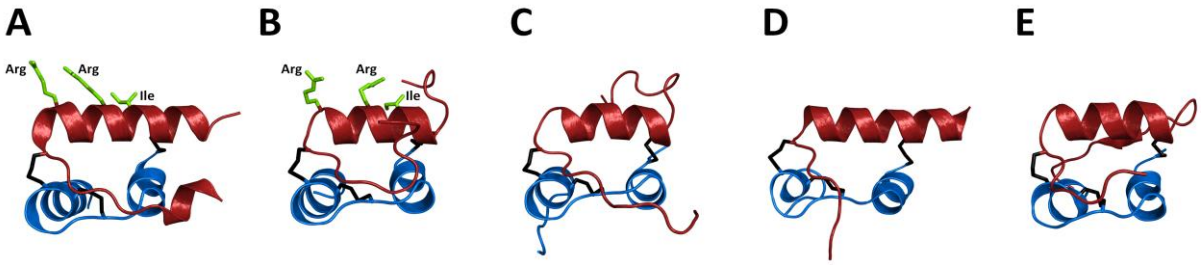

F

```
Relaxin-1       MP-RLFLFHLLEFCLLLNQFSRAVA-AKWKDDVIKLCGRELVRAQIAICGMSTWSKRSLS  58
Relaxin-2       MP-RLFFFHLLGVCLLLNQFSRAVA-DSWMEEVIKLCGRELVRAQIAICGMSTWSKRSLS  58
Relaxin-3       MA-RYMLLLLLAVWVLTGELWPGAE-ARAAPYGVRLCGREFIRAVIFTCGGSRWRRSDIL  58
INSL3           MDPRLPAWALVLLGPA---LVFALGPAPTPEMREKLCGHHFVRALVRVCGGPRWSTEARR  57
INSL4           MA-SLFRSYLPAIWLLLSQLLRES-----LAAELRGCGPRFGKHLLSYCPMPEKTFTTTP  54
INSL5           MKGSIFTLFLFSV-------LFAIS-EVRSKESVRLCGLEYIRTVIYICASSRWRRHQEG  52
INSL6           MP-RLLRLSLLWLGLLLVRFSRELS-D--ISSARKLCGRYLVKEIEKLCGHANWSQFRFE  56
                *        *  .                      : **    :     *

Relaxin-1       QEDAPQTPRPVAEIVPSFINKDTETIIIMLEFIANLPPELKAALS---------------  103
Relaxin-2       QEDAPQTPRPVAEIVPSFINKDTETINMMSEFVANLPQELKLTLS---------------  103
Relaxin-3       AHEAMGDTFPDADADEDSLA-----------------GELDEAMG-------SSEWLALT  94
INSL3           PATGGD-----REL-----LQWLERRHLLHGLVADSNLTLGPGLQ---------------  92
INSL4           GGWLLESG-RPKEMVSTSNNKDGQALGTTSEFIPNLSPELKKPLS---------------  98
INSL5           IPQAQQA-----ETGNSF------QLPHKREFSEENPAQNLPKVDASGE---DRLWGGQ-  97
INSL6           EETPFS------RL----IAQASEKVEAYSPYQFESPQTASPARG-RGTNPVSTSWEEAV  105


Relaxin-1       ---E--RQPSLPELQQYVPALKDSN--------LSFEEFKKLIRNRQSEAADSNPSELKY  150
Relaxin-2       ---E--MQPALPQLQQHVPVLKDSS--------LLFEEFKKLIRNRQSEAADSSPSELKY  150
Relaxin-3       K---------S---------------------------PQAFYRGRP-----------SW  107
INSL3           ------------------------------------------------------------PL  94
INSL4           ---E--GQPSLKKIILS-------------------------------------------  110
INSL5           ------------------------------------------------------MPTEELW  104
INSL6           NSWEMQSLPEYKDKKGYSPLGKTREFSSSHNINVYIHENAKFQKKRR-----NKIKTLSN  160


Relaxin-1       LGLDTHSQKKRRPYVALFEKCCLIGCTKRSLAKYC---------------------      185
Relaxin-2       LGLDTHSRKKRQLYSALANKCCHVGCTKRSLARFC---------------------      185
Relaxin-3       QGTPGVLRGSRDVLAGLSSSCCKWGCSKSEISSLC---------------------      142
INSL3           PQTSHHHRHHRAAATNPARYCCLSGCTQQDLLTLCPY-------------------      131
INSL4           -------RKKRSGRHRFDPFCCEVICDDGTSVKLCT--------------------      139
INSL5           KS-KKHSVM---SRQDLQTLCCTDGCSMTDLSALC---------------------      135
INSL6           LFWGHHPQRKRRG---YSEKCCLTGCTKEELSIACLPYIDFKRLKEKRSSLVTKIY     213
                                 **    *        *
```

Figure 1.1. Structure and sequence of relaxin family peptides.

Solved structures of A) H2 relaxin [10]; B) H3 relaxin [11]; C) INSL3 [12]; D) INSL5 [13] and E) insulin. A-chain is shown in blue and B-chain in red, while stabilizing disulphide bonds are shown in black. The relaxin arginine cassette sidechains are in green with residues labelled. Adapted from [14]. F) Clustal OMEGA Sequence alignment of human relaxin-like peptides extracted from UniProtKB and manually annotated to show signal peptide in bold, B-chain in yellow, C-chain, then A-chain in magenta. Residues of the relaxin arginine cassette are in bold and underlined. Conserved residues are marked with *, and similar residues with one or two points below.

The peptide hormone relaxin was discovered by Frederick Hisaw in 1926 when he observed the relaxation of the pubic ligaments of virgin guinea pigs after being injected by serum from pregnant rabbits [15], and it has since been studied extensively, revealing an important role in mammalian physiology not limited to its activity during pregnancy. It was later revealed that although primates possess a homologous relaxin gene, *RLN1*, the active peptide is the product of the *RLN2* gene, an orthologue not found in lower species, called H2 relaxin [16], and simply referred to as relaxin herein. Other members of the relaxin family were discovered much later through various searches for insulin-like peptides. INSL3 was isolated from boar testes and tentatively called Leydig Insulin like (Ley I-L) peptide [17], while INSL5 and INSL6 were found through screening of expressed sequence tag (EST) databases [18, 19]. The neuropeptide relaxin-3 (H3 relaxin in humans) was identified by searching human and mouse genome databases [20] and erroneously described as the ancestral peptide of the family [21]. Later paleogenomic analysis revealed that the diversification of the ancestral (pre-vertebrate) relaxin into subfamilies occurred earlier than previously thought [8].

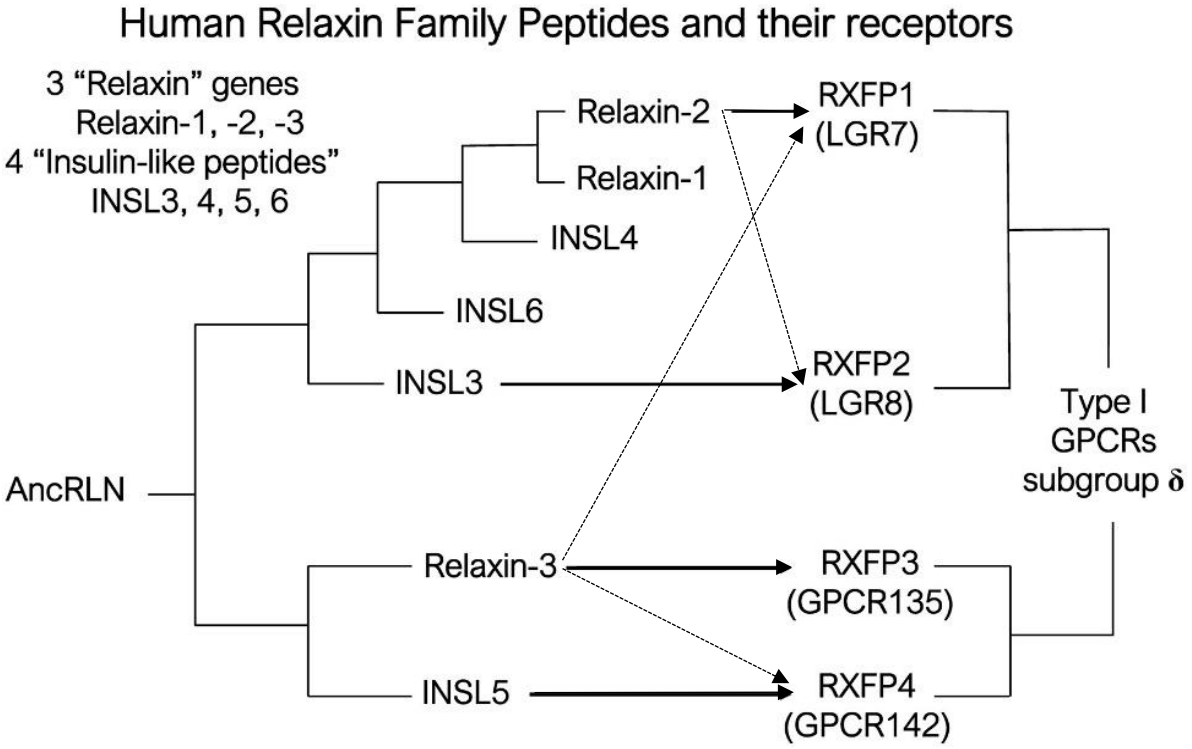

Figure 1.2. Diagram showing phylogenetic relationships between human relaxin family peptides and their receptors.

Activation possibilities are shown with arrows connecting hormones to four RXFP receptors. Solid arrows indicate cognate pairings. Dashed arrows indicate activation possibilities outside of cognate pairings. Figure adapted from [6].

The relaxin family of peptides share a similar structural fold to insulin, in that they have a two-chain structure, stabilized by two inter-chain disulphide bonds, and an additional intra-chain disulphide bond in the A-chain (Figure 1.1A-E). They are produced as a pre-prohormone with a signal sequence and a C-chain connecting the two chains, and these are cleaved to give the mature form [22] (Figure 1.1F). The relaxins are distinguished from the INSL peptides due to the presence of a so-called arginine cassette, containing the conserved binding motif R-x-x-x-R-x-x-I/V (where x is any residue) on the B-chain α-helix [23] (Figure 1.1).

Unlike insulin and IGFs that signal through tyrosine kinases [24], the relaxin family peptide receptors are class A GPCRs, belonging to the δ branch of the rhosopsin-like subfamily. They all contain the requisite 7 transmembrane (TM) alpha (α) helices, and in addition RXFP1 and RXFP2 possess large ectodomains that consist of 10 leucine-rich repeats (LRRs) as well as a single low-density lipoprotein class A (LDLa) module at their N-terminus (Figure 1.3). RXFP1 (formerly known as LRR-containing GPCR 7 (LGR7)) and RXFP2 (LGR8 or GREAT [25]) are descended from a single pre-2R ancestral RXFP1/2 gene [26], and they are the cognate receptors for relaxin and INSL3 respectively. Conversely, RXFP3 (previously known as GPCR135 or somatostatin and angiotensin-like peptide receptor (SALPR) [27]), the relaxin-3 receptor, and RXFP4 (previously GPCR142 [28]), the receptor for INSL5, have a structure similar to type 1 small peptide receptors in that their extracellular portion is relatively long, but unstructured [29] (Figure 1.3), and they came from a separate, RXFP3/4 ancestor, being more associated with neuroendocrine function than reproduction [26] (Figure 1.2). The remaining peptides from the family INSL4 and INSL6 are still unpaired with receptors.

There is much variation in how the different peptides bind to and activate the different receptors that exist across species [26], and in the human receptors, there is some cross reactivity with various members of the peptide family (Figure 1.2), although outside of the cognate relationships outlined here, the physiological relevance of the interactions is unclear [29].

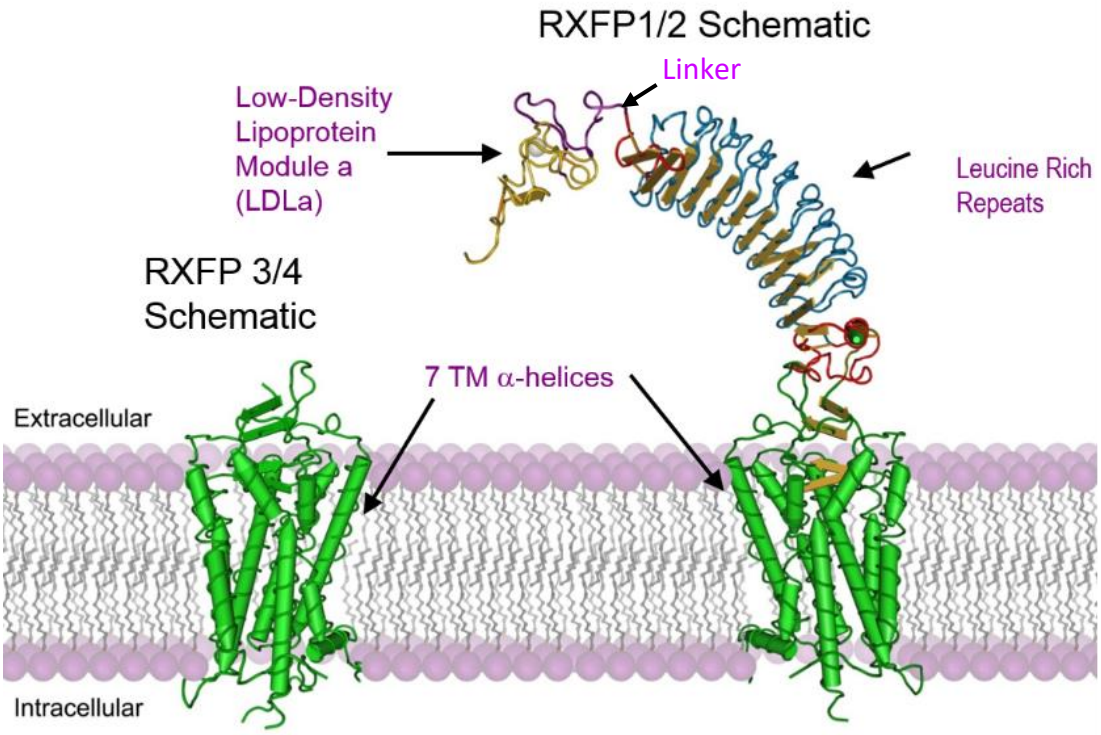

Figure 1.3. Schematic representation of RXFP1/RXFP2 (right) and RXFP3/RXFP4 (left) showing domain organisation.

7TM domain common to both is in green. Leucine-rich repeats are in blue with yellow arrows representing β-sheets, and terminal caps in red. LDLa module is in yellow with grey sphere representing calcium ion. Linker is in purple. C-terminus is intracellular, and N-terminus is extracellular. Figure adapted from [29].

1.2 Relaxin and RXFP1 distribution and function

Each month, the human ovary becomes host to an additional organ that will produce a great array of hormones in preparation for the possible fertilization of the oocyte being released. This organ, called the corpus luteum is one of the largest producers of hormones relative to size in the body, and it is the major source of circulating relaxin in females [30]. If fertilization does not occur, the relaxin is released into the circulation, leading to a small peak in relaxin immunoreactivity in the plasma around 10 days after ovulation [31], and the corpus luteum is destroyed. If however, the oocyte is destined to become a zygote, then the corpus luteum remains active and relaxin levels peak in the first trimester, reaching three to four times greater quantities than those seen in the luteal phase of menstruation [32], before declining to a steady level of about 0.5 ng/ml from around week 24 [33]. This peak corresponds to marked increases in cervical length and diameter [34]. Eventually the corpus luteum is degraded and hormone production is taken over by the placenta [35]. In rats, mice and pigs the corpus luteum is the main source of relaxin as in humans [29], although in rats relaxin levels gradually increase throughout pregnancy, peaking before a rapid decline in the hours or day before birth [36]. Other species that have been studied, including horse, hamster, cat and dog, produce most of their relaxin in the placenta [29]. Relaxin is produced in other reproductive tissues of both sexes, including breast [37], testis and prostate [38, 39]. Reflecting its role as cognate receptor, RXFP1 mRNA and protein is localized to various reproductive tissues such as uterus, vagina and cervix [40], and knocking out RXFP1 affects the development of the rat and mouse reproductive tracts [41, 42], as well as nipple development [18]. Many species require relaxin for the increased flexibility of the interpubic ligament required for successful birth [43] and the relaxation of the uterus is mediated by relaxin in rat, mouse, guinea pig and pig [44]. In humans however, these actions are not confirmed [45, 46] and the fact that levels are highest at the beginning of pregnancy suggests a role in implantation [47, 48], although the hormone is not essential to this process since women can become pregnant in the absence of ovaries and with undetectable levels of circulating relaxin [49]. Other important roles for relaxin in pregnancy are becoming increasingly clear, particularly in the renal and cardiovascular systems, where it contributes to vasodilation and matrix remodelling [50], showing its inherent utility as a modulator of heart and/or kidney function (discussed in section 1.5). To this end it reached Phase 3 clinical trials for the treatment of acute heart failure (AHF) [51] (see section 1.9).

While it is most pronounced in pregnancy, the activities mediated by relaxin also occur in males and non-pregnant females. Non-reproductive tissue plays host to relaxin and RXFP1, including

the brain, heart, kidney and pancreas [14, 29]. Relaxin knockout mice show notable fibrosis [52] and a scleroderma-like phenotype [53]. Actions mediated by relaxin at RXFP1 include the remodelling of joints and tissues through a modulation of matrix macromolecules [54], as well as a reduction in vascular resistance via nitric oxide (NO) synthesis [55, 56]. Relaxin also has a role in bone metabolism, since it can stimulate osteoclastogenesis *in vitro* [57]. It is a mediator of skeletal development in mice, working by activation of RXFP1, but also of RXFP2, although this mechanism has yet to be shown to occur *in vivo* [58]. The hormone's activity on bone development appears to function in a classic endocrine manner, since relaxin itself is not expressed in either osteoclasts or osteoblasts [59]. Relaxin also has a role in the development and protection of skeletal muscle, both via its well-known anti-fibrotic actions and through stimulation of vasodilation via angiogenesis [60]. Interestingly, the peptide is also capable of activating glucocorticoid receptor (GR), resulting in alterations in gene expression on a number of targets, which implies that the peptide may be capable of translocation across the cell membrane [61]. However, the discovery of a membrane-associated GR (mGR) could shed more light on how and where this interaction occurs [62]. It has been suggested that cell-impermeable hormones could activate these mGR receptors via an unknown mechanism [63]. The relaxin activation of GR may be instrumental in connective tissue metabolism as well as the vasodilator effects of relaxin [64].

RXFP1 is expressed in the rat and mouse brain [65, 66], where it may be activated by relaxin, although whether relaxin is located in precisely the same areas as its receptor is still unclear [67]. More recently, a novel factor called C1q/tumour necrosis factor-related protein 8 (CTRP8) was found to bind to and activate RXFP1 in human glioblastoma cells, causing cell migration and metastasis [68] (see section 1.7).

1.3 INSL3 and RXFP2 distribution and function

INSL3 was discovered in 1993 [17] and its receptor was de-orphanized in 2002 by the same group who paired relaxin with RXFP1 [69]. It is associated primarily with a role in the male reproductive tract, and erroneous expression of either ligand or receptor leads to abnormal testicular descent (cryptorchidism) [70-72]. This is due to faulty development of the gubernacular ligament, which is required for the trans-abdominal migration of developing testis. INSL3 protein is detectable in the amniotic fluid from women carrying a male foetus, with maximal levels around weeks 12-14, around the same time as the first phase of testicular

descent [73]. While several mutations have been discovered in the INSL3 and RXFP2 genes in formally cryptorchid patients, few are deemed sufficient to be the sole cause of the condition [74, 75]. The rare T222P mutation within the RXFP2 LRR domain may be associated with testicular maldescent, probably as a result of poor receptor expression on cell surfaces [76]. More recently, a recessive variant of the Rxfp2 gene containing a Gly to Glu mutation in TM3 was shown to give rise to non-functional protein, and be the apparent cause of cryptorchidism in four boys from the same family [77]. In addition to its role in the developing male, INSL3 is secreted into circulation from puberty with serum concentration in adults around 1000 pg/ml [78] and it has been recommended as a marker of Leydig cell function [79]. This large quantity of circulating peptide, coupled with the high transcript number of INSL3 mRNA found in the Leydig cells [20] points to an important physiological function in adult males. Indeed, RXFP2 expression has additionally been mapped to the brain where it may influence sensorimotor function [80], as well as in muscle, bone [59] and kidney [81]. RXFP2 expressed in osteoblasts were found to contribute to a bone anabolic activity in response to externally produced INSL3, and mutations in the peptide could contribute to osteoporosis [82].

Also produced in the ovary in mammalian females, INSL3 is thought to inhibit cells of the follicle and corpus luteum from entering the apoptotic pathway [83]. Indeed, the hormone probably acts to promote germ cell survival in both sexes [84, 85]. Female mice and rats homologous for Insl3 knockout were fertile, however litter sizes were reported to be smaller than average and oestrous cycles much longer [71]. In females it works as an autocrine/paracrine factor to determine the production of estradiol through the follicular phase within an antral follicle, as well as being secreted into the circulation where it acts as a biomarker monitoring follicle growth [86]. Circulating INSL3 is detectable in women only between puberty and menopause, at levels around 10 times lower than those found in post-pubescent males [87].

1.4 Other relaxin family peptide distribution and function

Relaxin-3 was for a long time thought to be the evolutionary ancestor of the relaxin family peptides, since homologues of the RLN3 gene have been identified in all characterized genomes [88]. It is a neuropeptide, being expressed in GABA neurons of the brain stem, particularly in the area known as the nucleus incertus (NI) [20, 89] and projecting to various areas in the forebrain. While its promiscuous activation profile meant that it was identified as

a ligand for each of RXFP1 [90], RXFP3 [91] and RXFP4 [92] separately, the predominant overlapping expression pattern of RXFP3 in the brain led to this receptor being paired with relaxin-3. The extent of the relaxin-3/RXFP3 function are still emerging, but they have been implicated in a wide range of behaviours and physiologies including stress response, sleep/wake states and circadian rhythms, metabolism and emotional memory (reviewed in [93]).

INSL5, the cognate ligand for RXFP4 [94], is not as well studied as the relaxins and INSL3, but it is highly expressed in the rectum and colon [18], with lower levels in the thymus, pancreas and eye [95]. Knockout mice indicate a role in glucose homeostasis [96] with reports attributing it an orexigenic effect [97]. As mentioned above, RXFP4 can also be activated by relaxin-3, and both ligands show a similar signalling profile, promoting phosphorylation of a number of targets as well as cell proliferation, and inhibiting adenylyl cyclase, although these effects are observed with differing potencies [98].

The final two known relaxin family peptides, INSL4 and INSL6 are still unpaired to receptors, and their functions remain elusive. INSL4 has been localized to the placenta and uterus [99], while INSL6 is thought to be involved in sperm function [100] and may have utility as a therapeutic against autoimmune diseases due to its ability to hinder T- and/or B-cell activation [101].

1.5 Signalling pathways activated by RXFP1

Relaxin acts primarily through its receptor, RXFP1, to activate a vast array of different signalling pathways leading to the variety of physiological responses discussed above (Figure 1.4). The signal cascades activated depend on cellular background, as well as timing, and the different activation partners involved. The most well-elucidated pathway involves receptor coupling to $G\alpha_s$ subunits to cause an accumulation of cyclic 3'-5' adenosine monophosphate (cAMP) [40], which is synthesised from adenosine triphosphate (ATP) by adenylate cyclases (AC) [102]. The cAMP pathway was first described in transfected human embryonic kidney (HEK) 293T cells and it was found that both in these and THP-1 cells – a leukemia cell line that natively expresses RXFP1 – the response is biphasic. The first, $G\alpha_s$-stimulated phase of cAMP production is inhibited by $G\alpha_{oB}$ subunit, and then a second phase involves $G\alpha_{i3}$ proteins which stimulate phosphatidylinositol 3 kinase (PI3K), leading to an activation of protein kinase C (PKC). PKC subsequently activates the membrane-associated AC5, such that the second

wave of cAMP accumulation may occur [103]. The first phase of cAMP production, but not the second, was detectable using a cytoplasmically expressed bioluminescence resonance energy transfer (BRET)-based biosensor activated by cAMP, indicating that $G\alpha_{i3}$ induced cAMP accumulation may be restricted to specific intracellular compartments [104]. Nevertheless, monophasic cAMP responses have also been recorded for RXFP1 in human myometrial cells [105], human skin Colo 16 cells and in human breast T-47D cells [106], confirming that relaxin signals in a cell-type specific manner to promote a broad range of physiological responses.

While the production of cAMP is the most well-characterized of its effects, it does not promote cAMP accumulation in fibroblasts, in contrast to its actions in the vasculature [107]. Relaxin nevertheless contributes to other pathways. Another major second messenger activated by the hormone is nitric oxide (NO), which has been implicated in both the anti-fibrotic activity as well as the vasodilation associated with relaxin signalling [108]. The NO pathway leads to the production of cyclic guanosine monophosphate (cGMP) via soluble guanosine cyclase (sGC), leading to regulation of matrix metalloproteinases (MMPs) to inhibit fibrosis [109]. Furthermore, NO inhibits transforming growth factor β (TGFβ) and prevents associated collagen production and myofibroblast differentiation in several organs, typically via the prevention of Smad2 phosphorylation [110, 111]. NO is a potent vasodilator that is activated by relaxin through the different isoforms of nitric oxide synthase (NOS) to promote relaxation of vascular smooth muscle cells, while concurrently reducing Ca^{2+} levels [56]. Indeed, the ability to relax cells of the vasculature via NO has been reported in many organs and tissues, both reproductive and other (reviewed in [112]). Similarly, relaxin activation of human umbilical arterial smooth muscle cells and human cardiac fibroblasts gave evidence of a cardioprotective role for relaxin through phosphorylation of extracellular signal regulated kinase 1/2 (ERK1/2) and cGMP signalling leading to increased levels of vascular endothelial growth factor (VEGF) and MMPs 2 and 9 [113].

RXFP1 activation is also modulated by a number of other receptors via specific crosstalk which depends on cell-type and timing. For example, relaxin's actions in fibroblasts are dependent on oligomerisation and/or functional crosstalk with the angiotensin receptor type 2 (AT_2R), since an antagonist to AT_2R blocks relaxin's anti-fibrotic actions both *in vitro* and *in vivo* [114]. It has since been found that the angiotensin receptor type 1 (AT_1R), which is known to have opposing actions to the related AT_2R [115], can form heteromers with both AT_2R and RXFP1 in myofibroblasts, and the three receptors may even form a complex which reduces fibrosis in

cultured cells as well as *in vivo* models [116]. As mentioned above, the TGF-β receptor is modulated by RXFP1, an action that is instrumental in the anti-fibrotic actions of relaxin via MMPs. Notch-1 can be activated by relaxin, both to decrease Smad3 phosphorylation and down-regulate TGF-β signalling to prevent fibrosis [117] and to produce cardioprotective effects [118] and inhibit oxidative stress [119]. Relaxin can also lead to the ligand-independent activation of peroxisome proliferator-activated receptor gamma (PPARγ) [120], another inhibitor of TGFβ that has anti-fibrotic properties, among others [121]. A multi-protein complex named the RXFP1 signalosome that can signal at attomolar relaxin concentration has been defined [122]. While the sub-picomolar levels of relaxin that activate the complex may resemble physiological levels more closely than those used in many assays [123], the signalosome has yet to be demonstrated to exist *in vivo*.

RXFP1 is generally not present in great numbers on cells, but small numbers of receptor are able to produce relatively large surges of cAMP, as observed in THP-1 cells where around 260 receptors per cell were able to induce similar levels of cAMP (~100 pmol per hour) to luteinizing hormone (LH) receptors, expressed at around 40,000 per cell, implying some secondary positive feedback mechanism [124]. Temporal aspects of relaxin signalling reveal that the various responses induced by the hormone are already evident within two minutes [125], with the first wave of cAMP production, but that effects can continue for several hours or even days [126]. Indeed, the maintenance of high levels of cAMP within cells is important in multiple tissues, notably during pregnancy [127, 128]. The prolonged activity of RXFP1 is compounded by an absence of β-arrestin recruitment and receptor internalisation [129].

A simplified overview of the signalling pathways of RXFP1 in the vasculature (A) and fibroblasts (B) is displayed in Figure 1.4.

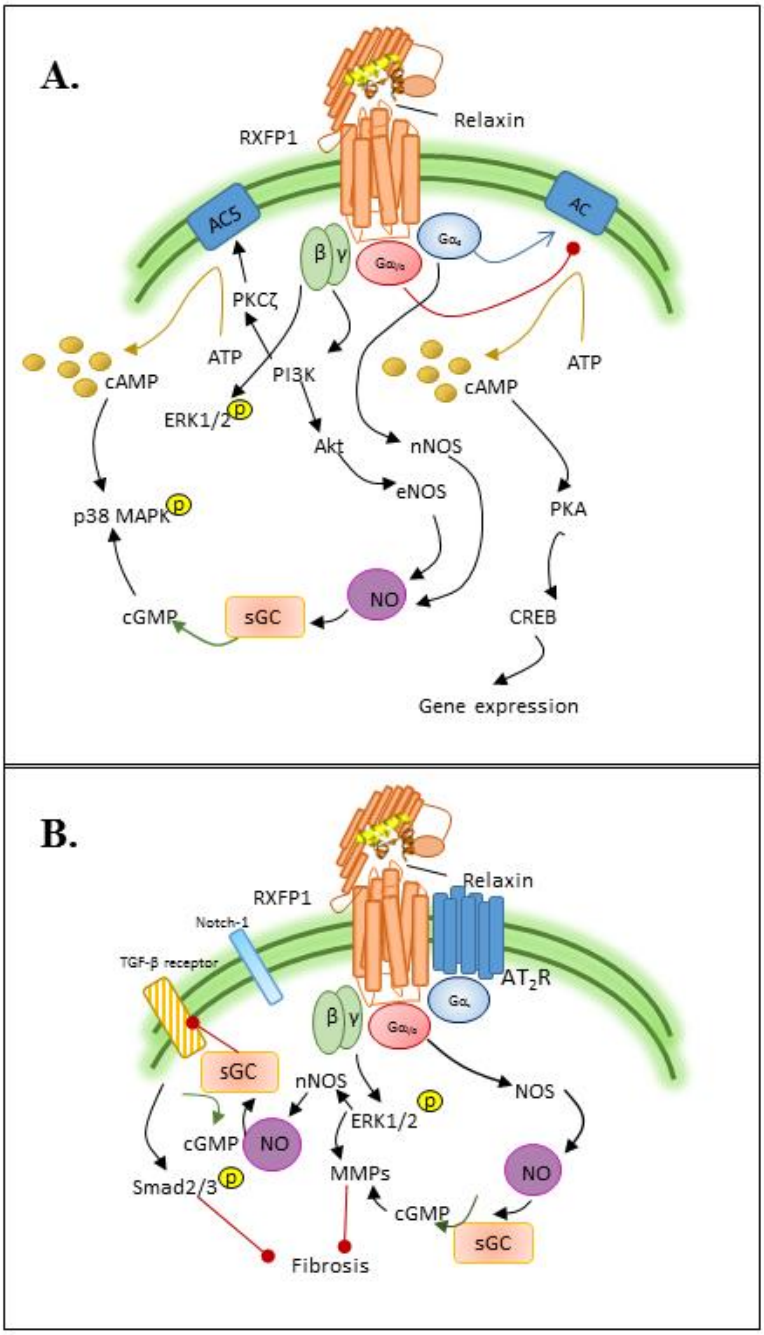

Figure 1.4. Overview of canonical relaxin signalling at RXFP1

A. The vasculature. RXFP1 (orange) couples to stimulatory (blue) and inhibitory (red) G proteins to produce a biphasic wave of cAMP accumulation. NO and cGMP activation also occur via NOS and soluble GC respectively. B. Fibroblasts. Differential signalling in fibroblasts in which RXFP1 works in conjunction with AT_2R. cAMP does not accumulate, but NO activation leads to cGMP signalling, including activation of MMPs and inhibition of TGF-β to prevent fibrosis. Yellow circles indicate phosphorylation.

1.6 Signalling pathways activated by RXFP2

RXFP2 activation appears less complex, although it is much less well-studied than the RXFP1 signalling profile. Human RXFP2 can be activated by either INSL3 or relaxin, and in transfected HEK293T cells this activation leads to the stimulation or inhibition of cAMP accumulation through coupling to $G\alpha_s$ or $G\alpha_{oB}$ proteins respectively [84, 130]. The same G-protein isoforms are also activated in cells natively expressing RXFP2, such as gubernacular cells, which produce cAMP and incorporate thymidine in response to INSL3 or relaxin treatment *in vitro* [69]. While the potency of the two agonists have long been known to differ, the aforementioned BRET biosensor (see section 1.5) showed that the temporal pattern of activation by the two peptides is also different, with INSL3 inducing a slow increase in cAMP, and relaxin giving a fast accumulation that reached a maximum within 5 minutes of peptide application [104]. It should be noted however that relaxin is not a ligand of RXFP2 in all species, since rat and mouse relaxin do not activate their equivalent RXFP2 receptors [131, 132].

Pathways involving RXFP2 in the reproductive tract include Wnt/Beta-catenin and Notch-1 to bring about correct gubernacular development [133]. RXFP2 has also been identified as important in bone development in males [82]. A mitogen-activated protein kinase (MAPK) signalling pathway was identified that could be activated by the increase in cAMP brought about by INSL3 stimulation of RXFP2, leading to multiple downstream actions including osteoblast proliferation and differentiation, collagen deposition, matrix protein deposition, mineralization and osteoclastogenesis [60, 134]. Like RXFP1, RXFP2 has been observed to elicit prolonged signalling, potentially explained by its lack of β-arrestin recruitment and internalization in response to ligand activation [129].

1.7 Pharmacology of RXFP1 and RXFP2

RXFP1 and RXFP2 are both activated by their respective cognate ligands, relaxin and INSL3, with affinity around 1 nM [135]. Furthermore, relaxin can activate RXFP2 robustly at a concentration of 10 nM, while INSL3 is practically inactive at RXFP1 (Figure 1.2). These characteristics facilitate the exploration of the mechanism of activation of the two receptors in comparison to each other, as does the existence of other molecules capable of activating one or both receptors, as outlined here.

The discovery that RXFP1 could be activated by CTRP8 (see section 1.2) followed a screening process in which short linear peptides were tested for bioactivity, and two of these, termed p74 and p59 were active at both RXFP1 and RXFP2 [136]. The p74 peptide (or CGEN25009) was further seen to activate fibroblasts and THP-1 cells *in vitro*, as well as improve fibrotic phenotypes *in vivo* [137]. The metastatic actions of CTRP8 could be disrupted by a small competitor peptide derived from the related factor CTRP6, and the authors proposed a mechanism of interaction in which the protein would interact with RXFP1 at LRR7 and LRR8 [138], although this has yet to be shown experimentally [68].

Another peptide able to activate RXFP1 is the single-chain relaxin derivative B7-33 [139], which was designed and synthesised in order to improve the clinical profile of relaxin, as it was undergoing clinical trials for the treatment of acute heart failure [140] (see section 1.9). The B-chain only peptide was able to promote MMP-2 levels in human cardiac fibroblasts and rat renal myofibroblasts in similar amounts to relaxin, despite only exhibiting weak potency on HEK293T-RXFP1 cells. Positive actions of B7-33 in mouse models included a reduction in cardiac and lung fibrosis and improved heart and airway function, without any associated tumorigenic activity [139].

RXFP1 is also activated by the small molecule 2-isopropoxy-*N*-(2-(3-(trifluoromethylsulfonyl)phenylcarbamoyl)phenyl)benzamide (ML290), which was isolated following a high throughput screen and subsequent optimization campaign [141], although it activates the receptor in an allosteric manner that does not compete for relaxin binding [142]. The molecule shows specificity, as it does not activate RXFP2, and it is also species selective, activating human, monkey and pig receptor, but not rat or mouse, making it difficult to test on model organisms. However, the species specific nature of its activity allowed sequence comparison to help map the binding site, which was first localised to EL3 and then mapped to a pocket involving helix 7 of the TM domain [143]. The fact that ML290 acts specifically at RXFP1 in an allosteric, non-competitive manner makes it an ideal tool for testing various RXFP1 mutants with reduced H2 relaxin binding for correct fold and trafficking. The signalling profile of ML290 differs from that of relaxin however. It is a biased agonist in all cell types studied, prompting a robust cGMP response preferentially over that of cAMP, and not activating pERK1/2 at any of the time-points assessed [107].

1.8 Signalling pathways activated by RXFP3 and RXFP4

Relaxin-3 and INSL5 activation of their native receptors differs from relaxin and INSL3 in that they inhibit cAMP production. RXFP3 activation is linked to $G_{i/o}$ coupling, upon whose stimulation cAMP accumulation is reduced following the phosphorylation of ERK1/2 and receptor internalization and compartmentalization into lipid-rich environments [144]. This pathway involves the activation of a PKC-dependent pathway, including PI3K and Src tyrosine kinases. While RXFP3 can also be activated by relaxin, (see section 1.1) it displays signal bias, meaning that the different ligands stabilize different conformations of the receptor, leading to different signalling profiles [145]. While relaxin-3 activation prompts receptor coupling to $G\alpha_{i2}$, $G\alpha_{i3}$, $G\alpha_{oA}$ and $G\alpha_{oB}$, to instigate AP-1 and NFκB transcription via distinct pathways, relaxin can only recruit $G\alpha_{i2}$ and $G\alpha_{oB}$ leading to activation of a subset of the same signalling molecules and transcription factors [146]. Additionally, relaxin lacks the ability to promote RXFP3/β-arrestin interactions.

The gut hormone INSL5 mediates its activity at RXFP4 through G-proteins including $G\alpha_{i2}$, $G\alpha_{oA}$ and $G\alpha_{oB}$. It inhibits cAMP accumulation and increases phosphorylation of ERK1/2, p38MAPK, Akt Ser^{473}, Akt Thr^{308} and S6 ribosomal protein, and is internalised following activation [147].

1.9 Clinical potential of relaxin

The actions of relaxin during pregnancy include several beneficial phenotypes that are notable in a therapeutic setting. Given the hormone's capacity to remodel tissue, protect organs including the kidneys, and ameliorate pressure in the cardiovascular system [44] it was a logical step to imagine that it could perform these functions more generally. Indeed, many of the phenotypes associated with changes in the female during pregnancy that are attributed at least in part to the actions of relaxin, were demonstrated to be replicated in preclinical models, including anti-fibrosis and renal protection [148], vasodilation and cardiac protection [149, 150]. These findings subsequently prompted clinical investigation of relaxin for a number of pathologies including scleroderma [151], orthodontics [152] and heart failure [153]. All of these trials failed to move into commercial development, although intravenous administration of serelaxin (recombinant human relaxin-2) passed Phase IIIa clinical trials for acute heart failure (AHF) [97]. The drug showed high safety and a reduced mortality at 180 days post treatment when compared with placebo [154], however the results were not replicated on a

broader scale in the Phase IIIb trial [155]. This result called into question the design of a number of AHF trials in which the dose was consistently limited to a single 48-hour perfusion of parental therapy in comparison to placebo or an active drug, and led to suggestions of a re-evaluation of how novel agents are tested for HF [156].

Relaxin's ability to improve vasoconstriction was recently tested in the treatment of renal dysfunction in cirrhosis, with preliminary results showing promise [157]. It has also been suggested as a candidate for lung preservation due to its ability to protect rat lungs from ischemia-reperfusion injury [158]. Pregnant rats are more resistant to kidney injury, and the kidneys of pregnant rats contain twice the levels of relaxin as non-pregnant counterparts [159]. It is also recommended as a potential treatment of pre-eclampsia given its capacity to prevent endothelial dysfunction [160], an action that was also brought about by the single chain agonist B7-33 (see section 1.7) [161]. The fact that B7-33 does not show a cancer-promoting phenotype is significant, since relaxin has been implicated in various different cancers including prostate [162], ovarian [163], endometrial [164] and breast [165]. This in turn infers the potential for the development of RXFP1 antagonists in the fight against cancer.

The inherent difficulties of using peptides as therapeutics led to the search for and identification of small molecule agonists of RXFP1. ML290 displays many advantages as a therapeutic, including specificity, oral bioavailability and a long half-life [166], all attributes lacking in relaxin [167]. Its biased signalling profile away from pERK1/2 and towards cGMP could lead to positive vasodilator and anti-fibrotic actions, all without associated angiogenesis and hypertrophy [107], although further testing is required, including analysis of the temporal aspect of ERK signalling.

1.10 Clinical potential of INSL3

Sarcopenia and osteoporosis are two examples of pathologies that are associated with hypogonadism [168] and the recent elucidation of a role for INSL3 in bone and muscle metabolism supports the idea that it may be useful in their treatment [59]. The utility of INSL3 as a therapy is most pronounced in cases where reduced Leydig cell function leads to a loss of bone or muscle mass, in order to avoid negative effects often ascribed to use of exogenous testosterone [169]. It has also been suggested as a marker of Leydig cell function [170]. Not limited to its role in male physiology, high INSL3 levels, as well as polymorphisms and haplotypes of the gene have been reported in women with polycystic ovary syndrome, which

correlates with the increased number of follicles present and may indicate a role for INSL3 in the development of the disease, although more work is required to confirm this hypothesis [171, 172]. It may also be of use as a biomarker of antral follicle growth or in hormone replacement therapy and in-vitro fertilization (IVF) [173]. Notably, the levels of INSL3 in amniotic fluid are predictive of future pre-eclampsia and birthweight [174]. INSL3 and RXFP2 are differentially expressed in a number of cancer cell lines, including thyroid [175], testicular [176], prostate [177] and ovarian [178]. While the INSL3/RXFP2 system has thus far been overlooked as a potential therapeutic target, as more information is garnered about its multi-faceted range of activity, it will almost certainly come to light in the future.

1.11 Other factors influencing RXFP1 and RXFP2 function

1.11.1 The role of dimerization

Dimerization is emerging as an important regulatory mechanism in the activity of a number of GPCRs [179-181]. Other LGRs have been shown to function as homo- and hetero-dimers as well as existing in more complex multimeric complexes [182, 183]. Binding of insulin to its receptor requires multiple domains of a pair of dimers [184], and the formation of homo- and heterodimers contributes to the complex interplay between insulin and IGFs with their respective receptors [185] to produce vastly different responses on a cellular level [186]. Evidence from bioluminescence resonance energy transfer (BRET) experiments has indicated that RXFP1 [187] and RXFP2 [188] form homodimers and/or heterodimers. Comparing the rates of dissociation of ligand from receptor with or without the addition of an excess of unlabelled competitor indicated the presence of negative cooperativity at both receptors. Trafficking of both receptors to the cell surface requires the formation of dimers in the endoplasmic reticulum, and the dimerization surface is stated to involve the receptor TMD and be stabilised by the extracellular domain in both cases. It is possible in this case that activation could occur in a trans fashion, with ligand binding occurring on one receptor and the LDLa module of one dimer partner activating the TM domain of the other [14]. This has not been proven however, and indeed the functional significance of dimerization is still questionable [189]. As mentioned above (section 1.5) a heterodimer of RXFP1 and AT_2R has been identified, and the pair function, possibly in conjunction with AT_1R, to reduce renal interstitial fibrosis via a cGMP pathway [109, 114]. The discovery of the RXFP1 signalosome indicates

that different combinations of receptor with other membrane-associated proteins could exist [190], although as yet the physiological relevance of the protein complex is not clear [108].

1.11.2 Post-translational modification

Most GPCRs, once activated, are targeted for phosphorylation and in this way β-arrestins and clathrin are recruited, leading to internalisation [191]. However, this does not occur with RXFP1 or RXFP2 [129], and these atypical GPCRs therefore show unusually prolonged signalling in many systems [192-194]. Nevertheless, they are the subject of glycosylation at multiple asparagine sites, which are identified based on sequence analysis [195] and confirmed experimentally for RXFP1 [196]. These sites include one in the LDLa module and five in the LRR domain and they are essential for correct trafficking of receptors to the cell surface and signalling *in vitro*. Many of these sites are conserved in RXFP2, and indeed, mutation to alanine of the LDLa N-glycosylation site Asn15 resulted in significantly reduced cell surface expression, implying a similar functionality in both receptors [197].

1.11.3 Splice variants

RXFP1 and RXFP2 contain 18 exons each, being among the most intron-rich genes in the human genome, and therefore the possibilities for different splice variants being expressed is great [198]. Indeed, mRNA analysis on human and rodent tissues have revealed the presence of many different variants, some of which encode the TM domain, and others the truncated extracellular region [199-201]. With the exception of the receptors lacking the LDLa module, these receptors do not generally bind ligand, but many display the capacity to modulate receptor functioning via dimerization, sequestration of full-length receptor within cells [201], or functional antagonism [200]. The co-expression of a multitude of splice variants may therefore represent an important regulatory mechanism in the activation of these receptors.

1.12 Binding and activation of RXFP3 and RXFP4

The smaller, type A GPCRs RXFP3 and RXFP4 (Figure 1.3) are structurally distinct from RXFP1 and 2, but they are closely related to one another, sharing around 50% sequence identity [202]. Given the lack of a large ectodomain, it stands to reason that the binding event is mediated largely by a single chain of their respective cognate ligands relaxin-3 and INSL5, in

this case the B-chain [91, 203, 204]. While relaxin-3 can activate both RXFP3 and RXFP4 as well as RXFP1 with high affinity, INSL5 is specific to RXFP4, and is in fact a weak antagonist at RXFP3, inhibiting the binding of relaxin-3 [94]. Despite this difference however, their mechanisms for activation are fairly similar. For relaxin-3, residues ArgB12, IleB15, ArgB16, IleB19 and PheB20 on the central α-helix of the B-chain are all essential for binding, while ArgB26 and TrpB27 towards the C-terminus are required for receptor activation despite only contributing to binding to a small degree [205]. The receptor binding surface spans extracellular loops 1 and 2, with residues Glu244, Leu246, Asp145 and Leu248 being specifically involved [206], and this mechanism is common between relaxin-3 and the recently characterized single-chain antagonist R3 B1-22R [207]. The binding site is nevertheless distinct as relaxin-3 forms a "lid" over the extracellular surface of the receptor, with C-terminal residues Arg-B26 and Trp-B27 inserting into the binding pocket to activate the receptor, while the non-native Arg23 of the antagonist is postulated to be sandwiched between Trp138 and Glu141 in TM2, locking the receptor in its inactive state [206].

The INSL5 peptide contains a receptor binding patch consisting of C-terminal residues ArgB23 and TrpB24 as well as IleB16, with more central residues GluB10, IleB12, ArgB13, TyrB17, SerB21 and SerB22 also contributing to receptor function [208]. Chimeric and mutagenesis data implicate the N-terminus and EL2 in RXFP4 ligand binding, with TM2, 3 and 5 being involved in activation [202]. The A-chain probably fulfils a stabilizing role, since B-chain only relaxin-3 analogues can agonise the receptor if they are held to a helical formation by hydrocarbon stapling, for example [209, 210]. Nevertheless, the A-chain is necessary for relaxin-3's affinity for RXFP1, since if it is replaced with the INSL5 A-chain, it loses the capacity for an interaction [211]. The specificity of INSL5 for RXFP4 has been pinpointed to four specific determinants, GluB2, LeuB9, TyrB17 and a rigid B-chain C-terminus, all of which contribute to the lack of affinity of this peptide for RXFP3 [212].

1.13 Binding and activation of Type A and Type B LGRs

Leucine-rich repeats (LRR) are protein domains commonly found to be involved in ligand binding and protein-protein interactions [213]. GPCRs that have LRRs on their extracellular domains are termed LGRs, and there are eight members in humans (Table 1.1). They are divided into three classes according to the number of repeats and ligand class. Type A LGRs

are the glycoprotein hormone receptors (GPHR) [214, 215], while Type B LGRs 4, 5 and 6 are activated by R-spondins that signal through Wnt pathways [216, 217].

Table 1.1 List of members of LGR family and their ligands.

Name	Alternative name	Ligand	No. of LRRs	Residues per repeat	Ligand affinity (K_d)	PDB
Type A						
LGR1	FSHr	Follicle stimulating hormone	9	21-25	0.03-3 nM [218]	1XWD, 4AY9, 4MQW
LGR2	LH/CGr	Lutropin or choriogonadotropic hormone	6	22-31	0.3-0.5 nM [219]	
LGR3	TSHr	Thyroid stimulating hormone	7	20-31	0.25 nM [220]	3XWT, 3GO4
Type B						
LGR4	LGR4	Rspondin 1-4	17	20-25	56 nM [221]	4KT1, 4QXE, 4QXF
LGR5	LGR5	Rspondin 1-4	17	21-26	3 nM [216]	4BSR, 4BSS, 4BST
LGR6	LGR6	Rspondin 1-4	17	21-25	0.5-7 nM [222] (IC_{50})	4BSU, 4KNG
Type C						
LGR7	RXFP1	Relaxin	10	24-25	9.2-9.8 ($pK_{d/i}$) [108]	2JM4 (LDLa module)
LGR8	RXFP2	INSL3	10	24	9.3-9.7 ($pK_{d/i}$) [108]	2M96 (LDLa module)

Table adapted from [223].

In the context of trying to understand RXFP1 and 2 binding it is important to compare to the other members of the LGR family, since they share the same leucine-rich repeat-containing ligand-binding domain (Figure 1.3). The Type A receptors follicle-stimulating hormone receptor (FSHr) and Thyroid stimulating hormone receptor (TSHr) both follow a two-step binding mechanism, in which ligand binding to the LRRs in a "handclasp" fashion involving multiple β-strands of the receptor, exposes an essential tyrosine residue within the hinge region that connects the LRRs to the TMD. This tyrosine is then sulphated and inserted into a hydrophobic pocket on the hormone [183, 224] (Figure 1.5), which lifts part of the hinge that is a hairpin loop acting as an inhibitor to receptor activation, thus relieving the inhibitory action [225, 226]. While the luteinizing hormone receptor (LHr) also contains the sulphated tyrosine (sTyr) site in its hinge region [227], its mechanism of activation is thought to be different from the other two Type A LGRs as removal of its ectodomain does not result in constitutive activation [228].

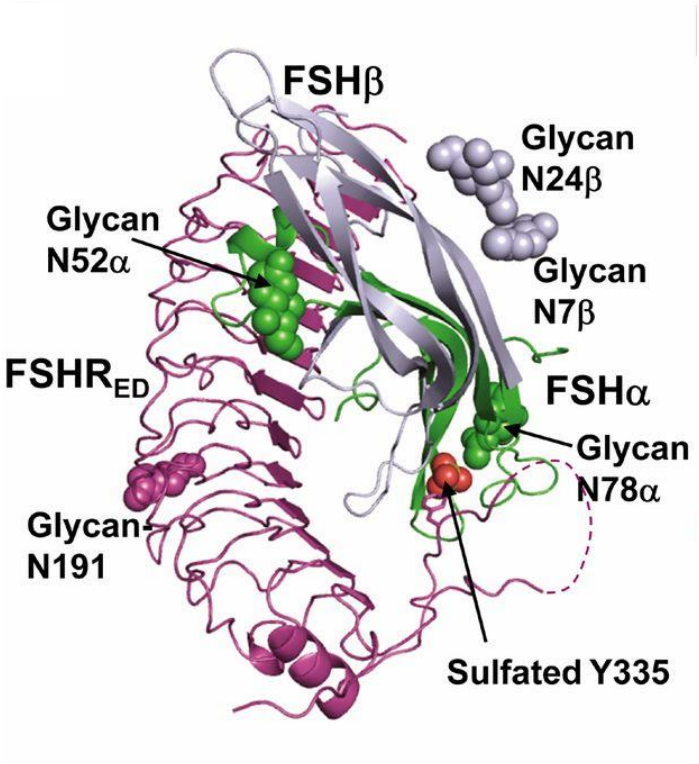

Figure 1.5. Structure of human FSH in complex with ectodomain of FSHr.

FSH α-subunit and β-subunit and FSHr are coded grey, green and purple respectively. The side chain of sulphated Y335 is shown as sticks for the tyrosine stem and orange balls for the sulphate group. Carbohydrates are shown as balls. Insertion of the sTyr at position 335 into a pocket on the hormone lift the hinge hairpin loop away from its inhibitory state, allowing activation of the TMD. Figure taken from [225].

The precise details of how the R-spondins (RSPOs) activate the Type B LGRs LGR4-6 are not entirely clear, however structural studies have revealed that the ligands bind over a relatively large surface area involving multiple LRRs using electrostatic and hydrophobic interactions [221, 229]. The four RSPOs contain two tandem furin-like cysteine-rich domains (Fu-CRD) that are involved in binding to two separate regions of the LRRs, leading to a flattening of the two repeats of the ligand, which sit at 90° from one-another in their apo-state [230, 231] (Figure 1.6A, B). The mechanism appears largely conserved between LGRs4-6, which may explain the lack of specificity between receptors and ligands [223]. This notwithstanding, a role for the hinge region in these receptors has not been found [232].

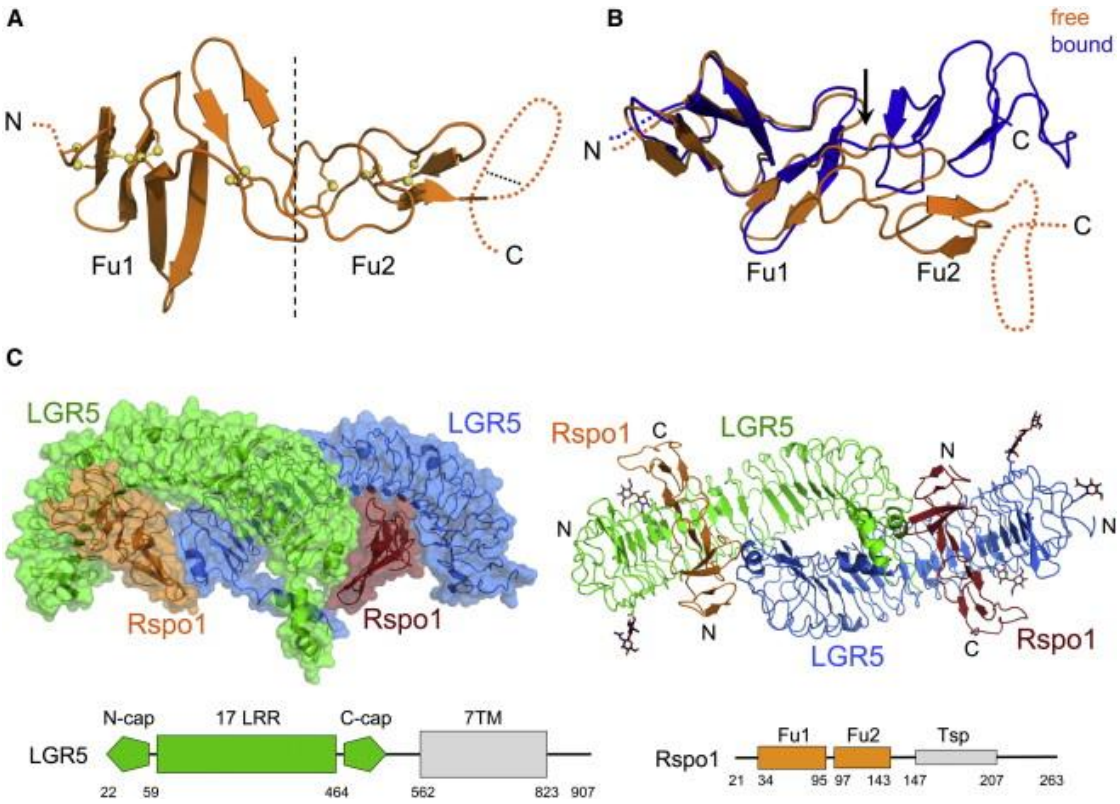

Figure 1.6. Structure and binding mode of Rspo1 to LGR5.

A) Structure of RSPO1 in apo state. Disulphide bonds are shown as ball and stick, and disordered residues are dashed. B) Overlay of Rspo1 free (yellow) and bound (blue). Arrow shows hinge around which Fu1 and Fu2 domains move by around 90° upon binding. C) LGR5 ectodomain in complex with RSPO1 Fu1-Fu2 domains at 3.2 Å resolution in two views. Domain structure of LGR5 and RSPO1 are shown beneath, with coloured regions highlighting regions isolated in crystal structures. Figure taken from [231].

1.14 Binding and activation of insulin and IGF

Insulin and insulin-like growth factors (IGF) 1 and 2 are the other members of the insulin superfamily of hormones. While they signal through membrane-bound tyrosine kinases and not GPCRs, the knowledge that the peptides interact with a large, multi-domain extracellular portion of their receptor invites comparison with the relaxin system. The insulin and IGF1 type 1 receptors (IR and IGFR) are closely related to one another and they present on cell surfaces as covalent dimers, where each partner is identical and the unbound receptor is thus symmetrical [233] (Figure 1.7). The extracellular portion consists of two leucine-rich repeat containing large domains (L_1 and L_2) separated by a cysteine-rich (CR) domain, and three fibronectin type III (Fn_{1-3}) domains [234-236]. Each receptor monomer has two ligand-binding surfaces, one within the L_1 domain, which combines with a 12 amino-acid peptide from the insert in Fn_2 (CT peptide), and the other on the opposite side of the molecule in the C-terminal portion of L_2 and in the Fn_1 and Fn_2 modules (summarised in [186]). The CT peptide is very important to both insulin and IGF binding [237] and it is adjacent to another stretch of 12 amino acids that can be alternatively spliced. Its presence leads to improved affinity for IGF, while insulin binds equally well to both variants [238]. There are therefore four ligand binding sites within a single dimer unit, and they exhibit negative cooperativity and ligand-dependent dissociation rates [239]. The structure of the IR ectodomain has been solved by crystallography [233, 240, 241], and it supports a model of bivalent crosslinking, in which two of the receptor sites are partially bound by two separate sites on the insulin molecule. The precise molecular details of this complex system go beyond the scope of this thesis; however, two points of interest can be raised when comparing to the RXFP system: that insulin and IGF bind to LRR domains within their receptor ectodomains, and that a tethered peptide is important for the full binding interaction with this first site. This mechanism may in fact resemble the respective roles of the LRR domain (that has been well-characterized) and the RXFP1 linker, the theme of thesis Chapter 3.

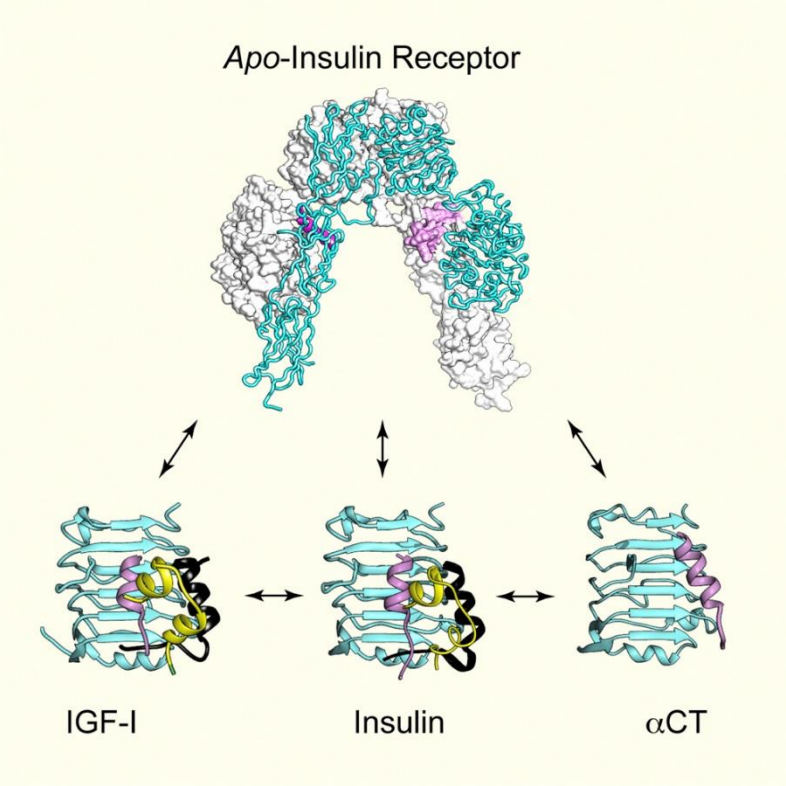

Figure 1.7. Schematic representation of binding modes of IGF-1 and Insulin to Insulin receptor dimer.

Apo- receptor is shown with one partner as ribbon and the other as space-filling model. The binding site is made up of LRR domain from one partner and αCT (violet) of the other. Ligands are depicted in black (B-chain) and yellow (A-chain). Figure taken from [242].

1.15 Binding and activation of RXFP1 and RXFP2

RXFP1 and RXFP2 are very closely related, sharing 60% amino acid sequence homology, and an overall domain structure that is nearly identical (Figure 1.3) [40]. Peptide ligand-binding and activation occurs in a complex fashion involving a highly specific interplay between the different regions of the hormone and receptor, which is largely similar between the two receptors and can be divided into a simplified three-component mechanism. The first is the high-affinity binding between the B-chain of the circulating hormone and the receptor leucine-rich repeats, and the second is a lower-affinity interaction between the peptide A-chain and receptor extracellular loops/TM domain. Finally, an active conformation is brought about through the involvement of the receptor LDLa module, with a mechanism whose details are elucidated to some degree within the pages of this thesis. Indeed, work done within this project has helped to clarify and extend upon the current understanding of a number of these mechanisms. While these components are often described in a given order, it is becoming clearer that the different binding mechanisms probably occur in a coordinated, and not step-wise manner.

1.15.1 Binding of hormone B-chain to receptor leucine-rich repeats

RXFP1 and RXFP2 make up the Type C LGRs, and similarly to Type A and B counterparts (see section 1.13), the primary binding of hormone to receptor has been mapped to the LRRs, which form linkages to the residues of the relaxin B-chain. In the case of relaxin, the B-chain residues involved make up the binding cassette [243]. Specifically, ArgB17 interacts with Asp231 and Glu233 in LRR6 and ArgB13 with Glu277 and Asp279 in LRR8, while IleB20 forms hydrophobic contacts with Trp180, Ile182 and Leu204, which are spread over LRRs 4 and 5 (Figure 1.8B).

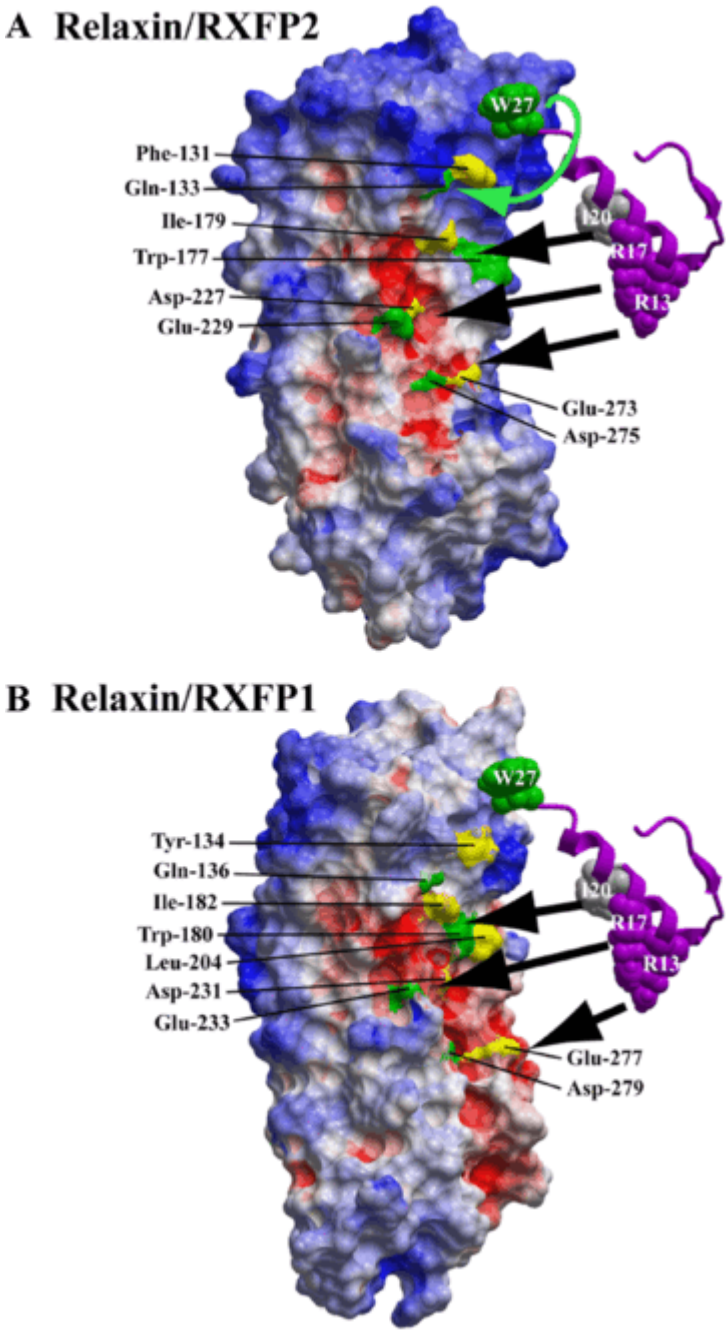

Figure 1.8. Surface-rendered homology model of the LRR domain of A. RXFP2 and B. RXFP1

Models are coloured according to surface charge where red indicates negative and blue positively charged areas, with predicted binding modes of relaxin B-chain (purple) binding on each. Residues of the binding cassette participate in electrostatic and hydrophobic interactions on the concave surface of each receptor binding site. Figure adapted from [244].

The B-chain of INSL3 also binds receptor LRRs, but in a manner distinct from that of relaxin [245]. The relaxin binding cassette is absent from INSL peptides, however B-chain residues are involved in binding, specifically INSL3 ArgB16 to RXFP2 Asp227, INSL3 HisB12 with RXFP2 Trp177, INSL3 ValB19 with RXFP2 Ile179 and INSL3 ArgB20 with RXFP2 Asp181 and Glu229 [246]. In addition, the INSL3 Trp B27 residue binds to RXFP2 Phe131 and Gln133, meaning that the RXFP2 LRR binding surface spans at least LRRs 2-7 and therefore is more extended and in a different orientation to that of RXFP1 [245] (Figure 1.9). Relaxin contains a Trp at position B28 which has been found to be important to the peptide's capacity to bind RXFP2 [247] (Figure 1.8A). Rhesus monkey and rat relaxin lack this residue and are unable to activate the related receptor [248], and the absence of an equivalent LRR residue to RXFP2's Phe131 may partially explain INSL3's low affinity for RXFP1. Additionally, arginine residues in the INSL3 B-chain, while separated by three amino acids, are positioned closer to the N-terminus than in relaxin from humans or other species that display high affinity for RXFP1, and the Ile/Val residue that completes the cassette is missing entirely [135] (Figure 1.1F). The relaxin binding residues are all conserved between RXFP1 and RXFP2, indicating that relaxin may bind to RXFP2 in a manner similar to how it binds its native receptor [40], however mutagenesis and modelling data suggests that its binding mechanism more closely resembles that of INSL3 on RXFP2 [244]. In an effort to understand the different binding and activation mechanisms of the two receptors, a 2012 study saw individual LRR β-sheets cloned from one receptor into the other, and the replacement of the RXFP1 LRR1 (four amino acid substitutions) by that from RXFP2 was sufficient to allow high affinity binding of INSL3 to the resulting ectodomain [245], indicating that binding necessitates an even larger portion of the LRR surface than previously thought. Despite this, when the ectodomain was attached to the RXFP1 or RXFP2 TM domain, the chimeric receptor was not activated by INSL3, indicating that the combined influence of the various RXFP2 binding surfaces are working together to produce a fully active receptor. Complementary mutation data from the relaxin and INSL3 peptide B-chain residues mentioned above as individuals or in combination with one another confirms their involvement in binding [249, 250].

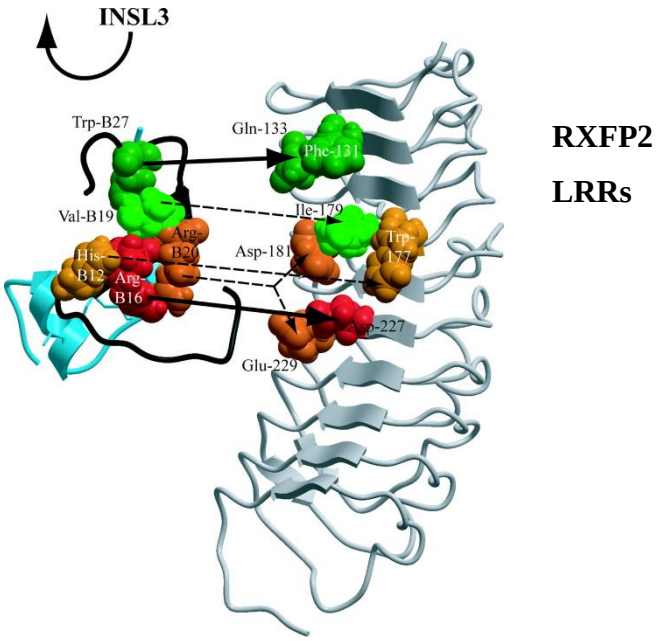

Figure 1.9. Model of the interaction between INSL3 B-chain and RXFP2 LRRs.

Bold arrows indicate confirmed interactions between INSL3 Arg B16 and RXFP2 Asp277 as well as INSL3 Trp B27 and RXFP2 Phe131/Gln133. Inferred pairings are indicated by dashed arrows. Figure adapted from [246].

1.15.2 Binding of hormone to receptor transmembrane domain

The hormone A-chain has been suggested to interact with the extracellular loops (EL) of the receptor transmembrane (TM) domain in both RXFP1 and RXFP2. This has been shown using RXFP1/RXFP2 chimeric receptors combining the TM domain from one receptor with the ectodomain of the other as well as ectodomain only constructs that are bound to single transmembrane helices from protein CD8. Binding and activation was tested in response to peptide ligands from both human and other species and it was found that functional TM domains in conjunction with matching ectodomains were necessary for optimal activity [90, 248]. The affinity of relaxin-3 for RXFP1 is mediated by A-chain interactions at EL2 [90], and while INSL3 can bind to the RXFP1 ectodomain, it has extremely low affinity for the whole receptor, again implicating the TM domain and ELs [135]. In order to test the binding of relaxin to the RXFP1 extracellular loops, EL1 and EL2 were cloned into a soluble scaffold formed by the B1 immunoglobulin binding domain of streptococcal protein G (GB1), and this construct was used in nuclear magnetic resonance (NMR) titration experiments with relaxin. An interaction was found to require EL2, in particular residue Phe564, as well as a conserved disulphide linkage between EL1 and EL2 [251]. Nevertheless, the fact that the B-chain only construct B7-33 can activate RXFP1 in many contexts implies that the A-chain interaction may not be imperative to receptor activation [6]. This is in opposition to B-chain only variants of INSL3, as these, and B-chain dimers, act as antagonists at RXFP2 [252, 253]. Indeed, alterations to peptide A-chains reveal that truncation of the INSL3 A-chain by nine residues or less results in a hormone capable of binding RXFP2 but that acts as an antagonist to activation, pointing to the existence of an activation domain in the INSL3 A-chain [254]. In contrast, truncation of the H2 or H3 relaxin A-chains by up to 4 residues gives peptides that can still bind and activate receptor but any further truncation leads to a concurrent reduction in both binding affinity and potency [255]. The different behaviour of relaxin and INSL3 at RXFP2 is a major theme of thesis Chapter 4.

1.15.3 LDLa-induced receptor activation

The final active receptor conformation is not reached without the involvement of the LDLa module, since if it is cleaved or misfolded, although the resulting receptors are expressed at the cell surface at levels equivalent to wild type, and they are able to bind ligand normally, they cannot signal [200, 256, 257]. Indeed, the soluble scaffold protein displaying RXFP1 EL2 also interacts with a recombinant RXFP1 LDLa module [251]. This action involves several

conserved hydrophobic residues on the module surface that are thought to interact specifically with areas on the ELs to induce an active conformation [257]. This was discovered using a two-pronged approach, in which residues on the native module were mutated to alanine, to achieve a loss of function, while equivalent gain-of-function studies were carried out on a non-functional chimeric receptor that had its native LDLa module replaced with the second ligand binding domain from the low-density lipoprotein receptor (LDLR), called LB2. Residues Leu7, Tyr9 and Lys17 were implicated, although neither a complete loss- or gain-of-function was seen in these experiments, indicating that the precise sequence of events had not been entirely elucidated. An attempt to replicate these experiments for RXFP2 was made, however no conclusive result was produced, implying that the binding surface on RXFP2 is distinct to that of RXFP1 [197], despite two of the three implicated LDLa residues being conserved (Figure 1.10C).

1.16 The LDLa module: a unique domain

GPCRs are notoriously difficult to purify, and the presence of the ectodomain on RXFP1 and RXFP2 means that structural studies have taken a "divide and conquer" approach. Sequence homology of the TM domain places the receptors into the Class A GPCR family, while the LRRs associate them with the LGR branch. Nevertheless, the two receptors are classed apart as the only two type C LGRs due to the presence of the N-terminal LDLa module (Table 1.1). These are the only regions of the receptors whose structures have been solved to date, both by solution NMR [197, 258] (Figure 1.10).

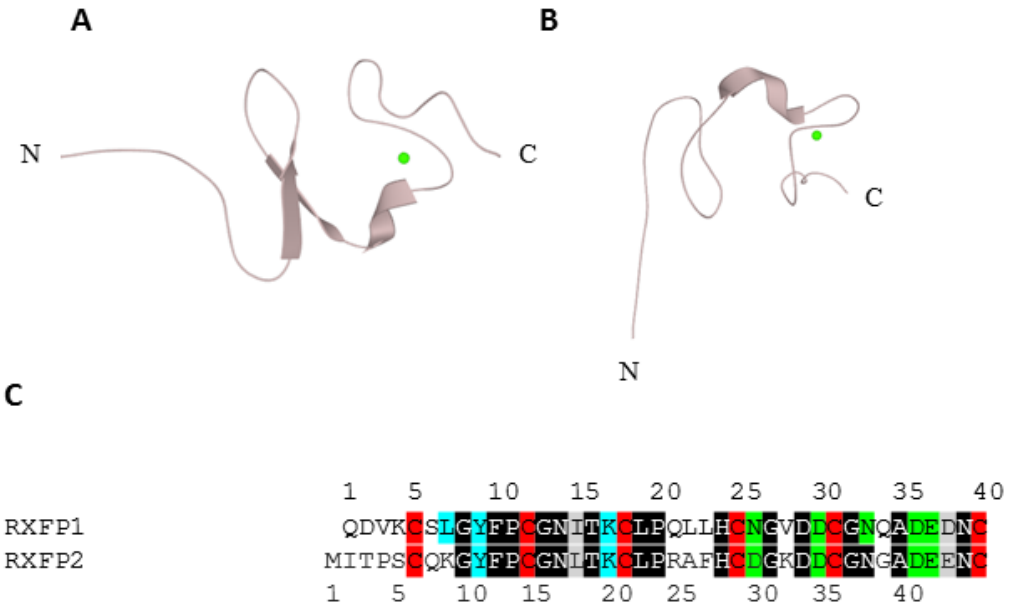

Figure 1.10. Structures and sequence of the RXFP1 and RXFP2 LDLa modules.

Solved structures of the A) RXFP1 LDLa module (PDB: 2JM4) [258] and B) RXFP2 LDLa module (PDB: 2M96) [197] as grey ribbon. Calcium ions are shown as green spheres and N-terminus and C-terminus are labelled. C) Sequence alignment of RXFP1 and RXFP2 LDLa modules with identical residues shaded in black and similar residues in grey. Cysteine residues involved in disulphide bonds are coloured red. Residues involved in calcium ligation are green. Cyan colouring indicates residues implicated in activation surface of RXFP1 and RXFP2 equivalents.

The module is so-named thanks to its homology to regions by the same name typically found in multiple repeats in low-density lipoprotein receptor (LDLR) family members [259], where it was first identified for its role in lipid metabolism [260]. They are sometimes referred to as cysteine-rich modules as they are stabilized by 6 conserved cysteine residues that form three disulphide bonds as well as a single calcium ion bound by a conserved series of acidic residues in the C-terminus [261, 262]. They are involved in a number of varied functions, including viral entry [263], cell differentiation [264] and ligand binding [265]. Notably, in many LDLR proteins the same residues are thought to be involved in both calcium ligation and ligand interactions [266, 267]. As mentioned above, the LDLa modules on RXFP1 and RXFP2 are imperative to signalling, but not binding, and they are thought to act as a "tethered ligand", interacting with and driving the final active conformation of the TM domain, thus allowing it to couple to G-proteins and initiate signal cascades. The binding of the RXFP1 LDLa module to EL2 may be mediated by residues towards the N-terminus (see section 1.15.3), while a similar binding surface on the RXFP2 LDLa module has not been found [197]. The calcium-binding residues may also be involved in interactions with the TM domain of the receptor. This is difficult to prove since mutagenesis of these residues compromises the expression and/or function of the receptor [268]. Tethered ligands are also reported on other GPCRs including the protease-activated receptors (PARs) and adhesion GPCRs, although in both these cases the cleavage of parts of the extracellular domain is required to expose the portion that activates the receptor [269-271]. In contrast, the LDLa module acts in response to exogenous ligand binding, and the peptide ligand must remain bound for the receptor to continue to signal. If expressed recombinantly the RXFP1 LDLa module can act as an antagonist, and this functioning may be a real mechanism of receptor modulation, since an RXFP1 splice variant encoding only the LDLa module and part of the linker is expressed in the uteri of pregnant mice [200]. The precise details of how the LDLa modules of RXFP1 and RXFP2 bring about receptor activation are gradually being uncovered using various techniques and strategies.

1.17 The hinge and linker

There are two outstanding regions within the RXFP1 and 2 domain architecture that have hitherto been overlooked when it comes to any functional importance. These are the hinge region that joins the TM with the LRR domain, and the linker region that forms a connection between the LRR domain and LDLa module (Figure 1.3). The hinge is so-called because it connects the TM domain to the large ectodomain, and it may perform a role in receptor

activation as is the case for the equivalent region in some Type A LGRs (see section 1.13) but so far it has not been investigated in any depth. Despite the very large differences between the hinge regions of the GPHRs and those of RXFP1 and 2, it may well be found to play an intrinsic role in these Type C LGRs in future work. It is quite well-conserved in species ranging from insects through to mammals (Figure 1.11), showing around 30% identity irrespective of whether the orthologue corresponds to RXFP1 or RXFP2. Whatever mechanism is being fulfilled by this region is likely to be shared, since the human RXFP1 and 2 sequences are 78% identical. This may be an important next step in the understanding of receptor activation.

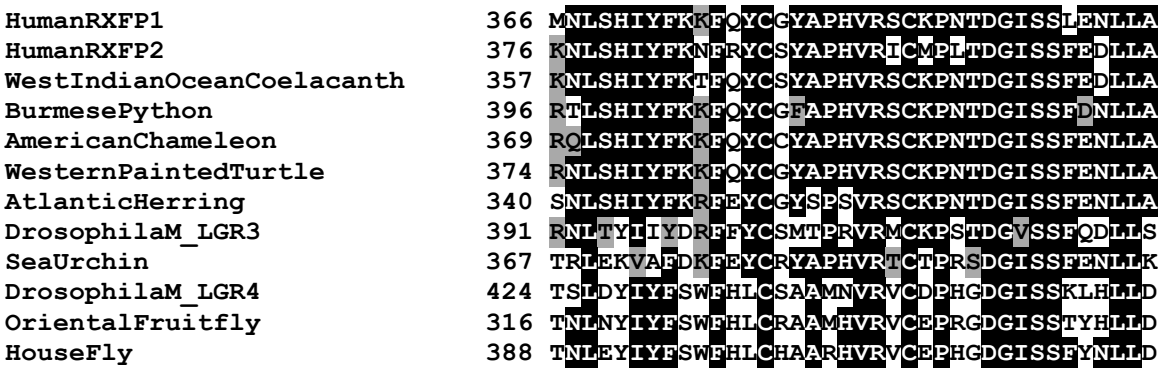

Figure 1.11. Sequence alignment from hinge region of relaxin family peptide receptors from various vertebrate and non-vertebrate species including fish, reptiles and insects as compared to human RXFP1 and RXFP2.

The linker also remained unexplored prior to the beginning of my Honours and PhD projects. It is a stretch of amino acids 32 residues long for human RXFP1 and 25 for RXFP2, and the sequence similarity between the two linkers is quite low (see Chapter 2, Figure 2.1). Nevertheless, in the years leading up to the start of my PhD project a string of evidence began to emerge that would indicate that this region is in fact incredibly important to both the binding and activation mechanisms of RXFP1 and RXFP2. It was found that RXFP1 lost all activity if its LDLa module was replaced by that of RXFP2 [256], but we noted with interest that the authors had also replaced a large portion of the linker, leading to a shorter, and sequentially distinct linker being present. Furthermore, an accidental discovery in our lab showed that a single alanine residue inserted between the LDLa module and linker abolished activity (Figure

3.1). Within my own honours work, preliminary mutagenesis data proved that mutation of the first six residues of the RXFP1 linker as three double mutants (G41A/D42A, N44A/N44A and G45A/W46A) had a drastic effect on signalling (see Chapter 3). These and other clues led us to the conclusion that further investigation was warranted on this previously underestimated stretch of amino acids.

1.18 Thesis aims and organisation

The project involves the use of different techniques and approaches to study two GPCRs and their ligands that have garnered a lot of attention in recent years, RXFP1 and RXFP2. This is mostly due to the success of relaxin in clinical trials for AHF, and although the phase IIIb of this trial was unsuccessful, the potential of relaxin or the targeting of RXFP1 for the treatment of pathologies characterised by fibrosis in particular remains valid [6]. The peptide itself does not have great drug-like properties and so the need to develop small-molecule functional analogues, especially for chronic disease treatment, is higher than ever. Likewise, the utility of INSL3 or an alternative to target RXFP2 is likely to prove useful for the treatment of bone disorders among others. The specific aims focus my work on the extracellular domain of the receptors, looking particularly at the linkers and LDLa domains, and how they work in similar or dissimilar ways between the two human receptors. The receptors have been primarily studied in stably or transiently transfected human embryonic kidney 293T (HEK293T) cells. We chose to use these cells since they are an effective model system that have been used historically to evaluate RXFP1 and RXFP2 structure and function. They can be transfected to express the receptors at high levels and produce signalling responses representative of their activity in some native contexts, allowing us to evaluate the activity of mutant and chimeric receptors compared to wild-type equivalents. They do not contain endogenous RXFP1 and RXFP2, but mRNA transcripts for potential dimerization partners AT_1R and AT_2R have been reported [272].

The thesis is separated into three research chapters as follows:

1.18.1 Chapter 2: Chimeric RXFP1 and RXFP2 receptors highlight the similar mechanism of activation utilizing their N-terminal low-density lipoprotein class A modules

Chapter by publication [1]. The paper outlines how we were able to maintain robust activity at both RXFP1 and RXFP2 where each had their own LDLa module replaced with that of the sister receptor. Our chimeras were distinct from those made by Kern et. al. [256] as we were careful not to swap any of the associated linker residues, rather cleaving the receptors

immediately C-terminally to the final Cysteine of the respective LDLa domain. Note that the paper has been formatted to a thesis chapter for consistency, but that the content is unchanged from the publication.

1.18.2 Chapter 3: Investigating the role of the RXFP1 linker

I performed mutagenesis studies on the RXFP1 linker, focussing on the conserved N-terminal region as well as specific residues implicated in concurrent NMR analyses from the central portion of linker. Insertion and deletion mutants were also produced to explore the role of length and specific spacing on the linker function. This work was published in 2016 [2].

1.18.3 Chapter 4: Investigations into the INSL3 receptor - RXFP2

This chapter spans two published works, from 2017 [3] and 2018 [4]. The first part describes a mutagenesis survey of the RXFP2 linker using both active ligands, relaxin and INSL3, while the second returns to the use of chimeras, this time with a portion of the RXFP1 linker being inserted into RXFP2 at an equivalent position. The resulting receptor was used to explore relaxin binding and kinetics. Together the data paints a picture of how the two different peptides act in distinct ways at RXFP2, as well as underlining the functional importance of the RXFP1 linker.

The final thesis chapter brings the work together in a general discussion, exploring how the linkers, far from being simple unstructured and unimportant lengths of amino acids serving the sole purpose of joining together two receptor domains, fulfil important roles that are functionally distinct between the two. Given that this work is already published in several peer-reviewed papers, it is contributing to the expansive knowledge base of RXFP1 and RXFP2 mechanism of action for both binding and activation as we continue to add pieces to the puzzle.

Chapter 2 Chimeric RXFP1 and RXFP2 receptors highlight the similar mechanism of activation utilizing their N-terminal low-density lipoprotein class A modules

Shoni Bruell[1,2,5], Roy CK Kong[1,2,5], Emma J Petrie[2,3], Bradley Hoare[1], John D Wade[1,4], Daniel J Scott[1,2], Paul R Gooley[2,3], and Ross AD Bathgate[1,2,*]

[1]Florey Institute of Neuroscience and Mental Health and Florey Department of Neuroscience and Mental Health, [2]Department of Biochemistry & Molecular Biology, [3]Bio21 Molecular Science and Biotechnology Institute, [4]School of Chemistry, The University of Melbourne, Vic, Australia.

Preface:

Since Chapter 2 is an unaltered publication, many of the methods used are described only briefly herein. I therefore give full accounts of the methodology for cell culture and cell-based assays in Chapter 3, in which the same methods have been used.

Abstract

Relaxin family peptide (RXFP) receptors 1 and 2 are unique G-protein coupled receptors in that they contain an N-terminal low-density lipoprotein type A (LDLa) module which is necessary for receptor activation. The current hypothesis suggests that upon ligand binding the LDLa module interacts with the transmembrane (TM) domain of a homodimer partner receptor to induce the active receptor conformations. We recently demonstrated that three residues in the N-terminus of the RXFP1 LDLa module are potentially involved in hydrophobic interactions with the receptor to drive activation. RXFP2 shares two out of three of the residues implicated, suggesting that the two LDLa modules could be interchanged without adversely affecting activity. However, in 2007 it was shown that a chimera consisting of the RXFP1 receptor with its LDLa swapped for that of RXFP2 did not signal. We noticed this construct also contained the RXFP2 region linking the LDLa to the leucine-rich repeats. We therefore constructed chimeric RXFP1 and RXFP2 receptors with their LDLa modules swapped immediately C-terminally to the final cysteine residue of the module, retaining the native linker. In addition, we exchanged the TM domains of the chimeras to explore if matching the LDLa module with the TM domain of its native receptor altered activity. All of the chimeras were expressed at the surface of HEK293T cells with ligand binding profiles similar to the wild-type receptors. Importantly, as predicted, ligand binding was able to induce cAMP based signalling. Chimeras of RXFP1 with the LDLa of RXFP2 demonstrated reduced H2 relaxin potency with the pairing of the RXFP2 TM with the RXFP2 LDLa necessary for full ligand efficacy. In contrast the ligand mediated potencies and efficacies on the RXFP2 chimeras were similar suggesting the RXFP1 LDLa module has similar efficacy on the RXFP2 TM domain. Our studies demonstrate the LDLa modules of RXFP1 and RXFP2 modulate receptor activation via a similar mechanism.

2.1 Introduction

Relaxin family peptide receptor (RXFP) 1 and RXFP2 are class A G-protein coupled receptors (GPCR). They are therefore members of the largest gene family in humans [273], and GPCRs are currently the target of more directed drugs than any other gene family [274]. While RXFP1 and RXFP2 both possess the representative 7 transmembrane (TM) spanning α-helices, they also contain a large extracellular domain, consisting of 10 leucine-rich repeats (LRR) tethered

to a single low density lipoprotein type A (LDLa) module [275] by an uncharacterized linker. The LRRs are the primary binding site for the cognate ligands, relaxin (RXFP1) and insulin-like peptide 3 (INSL3) (RXFP2), while the LDLa module is essential for signalling [200]. As the receptors have been shown to form constitutive homodimers [276, 277] it is hypothesised that the LDLa module acts as a secondary ligand, possibly interacting with the extracellular loops of the transmembrane (TM) region of a homodimer partner receptor to induce the conformational change necessary for signalling [278]. RXFP1 and RXFP2 are the only known mammalian GPCRs to contain an LDLa module and thus the potential role of this module in signal activation is unique. The module itself requires the formation of three disulfide bonds between six conserved cysteine residues, as well as the presence of a single bound calcium ion to maintain its active, globular structure [258]. Replacing the native LDLa module of RXFP1 with the structurally similar but functionally distinct LB2 module from the low-density lipoprotein receptor (LDLR) gives rise to a chimera that can bind ligand like the wild type, but cannot signal [257, 258]. The RXFP1-LB2 chimera was used to identify key residues needed for signalling in a gain-of function study complemented with equivalent loss-of-function mutations and a detailed structural analysis [257]. In this way a prospective binding surface was identified involving Leu7, Tyr9 and Lys17, which are proposed to contribute to the activation of RXFP1 using hydrophobic contacts.

A similar mechanism of action of the LDLa module by the two receptors is implied by the degree of sequence similarity they share. The LDLa modules of RXFP1 and RXFP2 share 60% sequence similarity (Figure 1), each possessing features common to other LDLa modules characterized from the LDLR including the six cysteines that form disulphide bonds, and the motif AspxxxAspxxAspxxAspGlu (where x is any residue) that binds a calcium ion. Many LDLa modules characterised from the LDLR utilize this motif to not only ligate the calcium ion but contribute to protein-protein interactions [279], while residues important to RXFP1 function have been mapped to the N-terminal region of the LDLa [280]. Two residues key to the function of RXFP1, Tyr9 and Lys17, are conserved in the RXFP2 LDLa module and it is reasonable to assume they function in a similar manner to induce signal activation. Importantly, it has been shown that chimeras, named RXFP1/2 and RXFP2/1, in which the entire ectodomain of the receptors are swapped are still able to signal, albeit with lowered activity compared to wild-type [135]. This implies that the LDLa module of RXFP2 can compensate for the module of RXFP1 and vice versa. It would seem reasonable to assume then that simply swapping the LDLa modules between RXFP1 and RXFP2 would also yield chimeras capable

of signalling. However, in a study by Kern and colleagues in 2007 where they replaced the RXFP1 LDLa module with that of RXFP2, they reported that the chimera did not signal, concluding that the cAMP signalling function of RXFP1 was only possible with its native LDLa module [256].

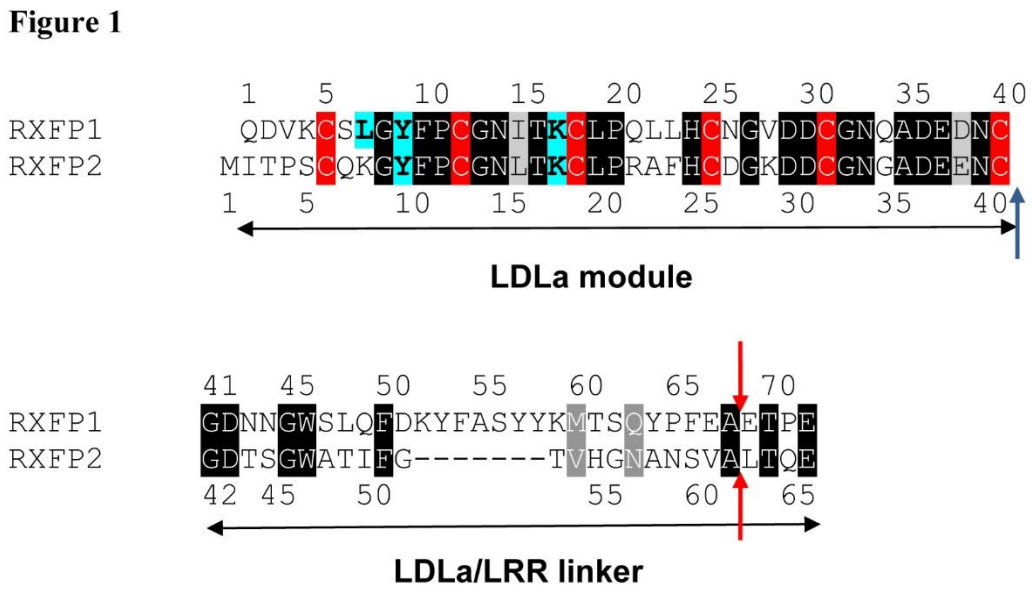

Figure 2.1. Alignment of the RXFP1 and RXFP2 LDLa module sequences.

Identical residues are boxed in black and similar residues are boxed in grey while the conserved cysteine residues are boxed in red. The residues recently identified as being involved in RXFP1 ligand-mediated activation [257] are highlighted in blue in both RXFP1 and where they are conserved in RXFP2. A blue arrow shows where our swapped modules are cleaved. Red arrows show the point of cleavage for the swapped modules in the chimera made by Kern et al. [256].

The present study aims to further investigate this seeming contradiction, and establish why an ectodomain-swapped chimera of RXFP1 with RXFP2 can signal, while an equivalent LDLa-swapped chimera cannot. Upon scrutiny of the constructs made by Kern et al., it would appear that the point chosen to swap the LDLa modules was twenty seven residues C-terminally to the final cysteine (Cys40) necessary for LDLa structural integrity for RXFP1. Importantly, the equivalent region of RXFP2 which was replaced in the chimera is seven amino acids shorter (Figure 1), meaning that the resulting chimera had a shorter stretch of amino acids linking the LDLa module to the LRRs than wild type RXFP1. We therefore designed chimeric constructs of both RXFP1 and RXFP2 that had their LDLa modules swapped immediately C-terminally to the aforementioned cysteine similar to our RXFP1-LB2 chimera [258], meaning that only the LDLa module itself was swapped, and none of the adjoining linker residues. We call these constructs RXFP211 and RXFP122 (Figure 2). As further investigation into the possibility of a receptor-specific interaction between the LDLa module and the TM domain, we also matched the LDLa module with the complementary TM domain, to establish if an improvement in signalling activity would be observed. These constructs are named RXFP212 and RXFP121 (Figure 2). The resulting chimeras were tested for surface expression, binding of ligand and cAMP-based signalling.

Figure 2

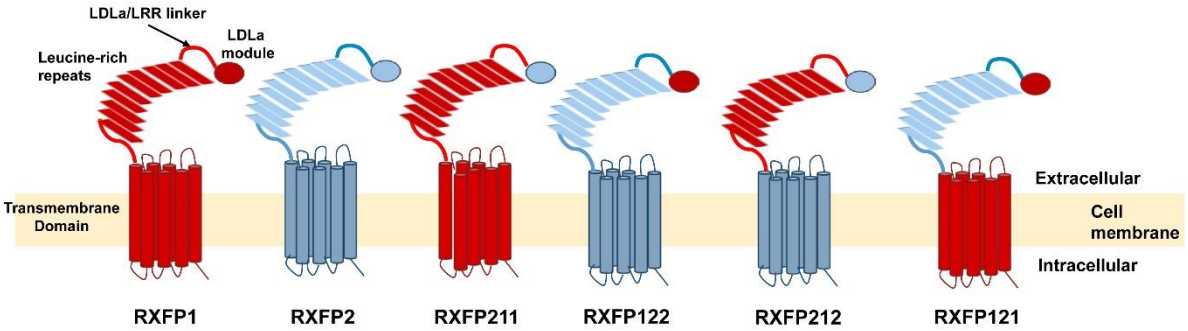

Figure 2.2. Schematic representation of the RXFP1 and RXFP2 receptors compared to the RXFP211, RXFP122, RXFP212, and RXFP121 chimeric receptors.

The domains of receptors are labelled on the RXFP1 receptor. RXFP1 domains are in red while RXFP2 domains are in blue.

2.2 Materials and Methods

2.2.1 Hormones and cell lines

Recombinant human gene-2 relaxin (H2 relaxin) peptide was kindly provided by Corthera and human INSL3 was chemically synthesized as previously described [11]. Human embryonic kidney (HEK) 293T cells (ATCC #CRL-1573; American Type Tissue Culture Collection) used to express receptors were maintained in Dulbeccos' modified eagle medium (DMEM) supplemented with 10% fetal bovine serum (FBS), 1% l-glutamine and 1% penicillin/streptomycin (referred to as complete DMEM) in incubators (Thermo scientific) maintained at 37 °C, with 5% CO_2 and 85% humidity.

2.2.2 Receptor constructs

RXFP1, RXFP2 and chimeric constructs were cloned into a pcDNA3.1^{TM}/Zeo+ AmpR mammalian expression vector (Invitrogen, Carlsbad CA) which contained an N-terminal FLAG tag and a bovine prolactin signal sequence [275] and has been shown not to interfere with receptor activity [90]. The chimeric receptor constructs were made using overlap PCR. The LDLa modules were first generated using the relevant LDLa module as template and PCR primers that would anneal to the two ends of the LDLa module (Table 1). The amplification PCR mixture contained 100 ng of DNA template, 10 µl of 10x PCR buffer, 1 µl of each primer, 0.5 µl of dNTP mix, 2 µl of $MgCl_2$, 0.5 µl of Taq (Bioline Velocity) and distilled, deionized water to make up to a total of 50 µl. PCR conditions were 2 minutes (min) at 98 °C, then 30 cycles of 98 °C (30 seconds (sec)), 58 °C (30 sec), 72 °C (15 sec) followed by a 7 min extension at 72 °C. The LRR/TM regions of each construct were similarly amplified (Table 1) and the two sections of DNA were annealed together in a PCR reaction consisting of 200 ng of LDLa DNA, 50 ng of LRR/TM DNA, 10 µl of 5x PCR buffer, 1 µl of dNTP mix, 0.25 µl of Taq polymerase (Bioline Velocity) and made up to 50 µl with distilled, de-ionized water. The conditions used were 98 °C (2 min) then 10 cycles of 98 °C (30 sec), 50 °C (25 min), 72 °C (5 min). The final annealed product was then amplified using the same protocol as in the other amplification steps, except that the 72 °C step was carried out for 30 sec instead of 15 sec. Primers used were the forward (sense) primer used to amplify the LDLa sequence and the reverse (antisense) primer used to amplify the LRR/TM sequence for each construct (Table 1). The DNA was then digested with BamHI and XhoI to create sticky ends that would correspond

to sites in fresh, verified and digested pcDNA3.1 Zeo+ vector. Ligation was carried out using T4 DNA ligase (Promega) at 4 °C overnight or at room temperature for 3 hours. The vectors were then transformed into DH5α *E. coli* cells using the heat shock method and resultant colonies were picked and grown before isolating the plasmid DNA using a PureLink® Quick Plasmid Miniprep Kit. The entire insert of successful clones were sequenced to ensure the desired end product was correct, with no unintentional mutations incorporated.

2.2.3 Receptor expression on HEK 293T cells

Transient transfections were performed using lipofectAMINE^{TM} 2000 (Invitrogen) according to the manufacturer's instructions. For competition binding assays chimeric receptors were selected for semi-stable expression and compared with cells stably expressing RXFP1 or RXFP2 [280]. Semi-stable expression was achieved by selection of cells with Zeocin after transient transfection followed by fluorescence activated cell sorting (FACS) using a fluorescently tagged FLAG antibody one week later. For FACS analysis, cells were seeded in 10 cm dishes at 3 x 10^6 cells, and grown overnight. The following day the cells were washed and resuspended in 1% FBS in phosphate buffered saline (PBS) (Gibco) (FBS/PBS) medium. Alexa 647 labelled anti-FLAG antibody (Invitrogen) was added at a 1:1000 dilution in FBS/PBS and cells were incubated on ice for 30 mins, then passed through a filter and sorted using FACS (Becton Dickinson FACS Aria III). Only the top 10% of cells with fluorescence levels significantly higher than the background fluorescence in non-transfected HEK293T control cells were collected. The sorted cells were grown in complete DMEM in the presence of 200 µg/ml Zeocin until confluent. HEK293T cells stably expressing wild type (WT) RXFP1 were used as a positive control in the FACS sort.

2.2.4 Cell surface expression assays

The presence of the chimeric receptors at the surface of cells was assessed in triplicates, exploiting the FLAG epitope on their N-terminus using the method described previously [196]. Briefly, cells were transfected with receptor of interest for 24 hours. Next, cells were fixed with 3.7% formaldehyde solution (Sigma-Aldrich), blocked with bovine serum albumin (BSA) and incubated with an anti-FLAG mouse monoclonal primary antibody (Sigma-Aldrich). Goat anti-mouse Alexa Fluor 488 was used as secondary antibody (Invitrogen). Finally, cells were lysed and transferred into black-walled 96-well plates for measurement using a BMG plate

reader (Omega) at 495nm excitation and 519nm emission wavelengths. Data were analysed using GraphPad PRISM (Graphpad Software, Inc.) and presented as mean percentage of wild type RXFP1 or RXFP2 expression ± SEM of at least three independent experiments. Significance of receptor expression above background and compared to wild type was assessed using one-way ANOVA and uncorrected Fisher's LSD multiple comparison test.

2.2.5 Ligand binding assays

Competition binding assays were performed on whole cells as described previously, using Europium labelled INSL3 (Eu-INSL3) [281] and Europium labelled H2 relaxin (Eu-H2 relaxin) [282]. Increasing concentrations of unlabelled ligand were used in conjunction with labelled equivalents, and nonspecific binding was established using 1 µM unlabelled ligand. Readings were taken in triplicate and read on a BMG plate reader (Omega) in clear-bottomed, opaque-walled 96-well plates (PerkinElmer). Data were analysed using GraphPad PRISM and presented as mean percentage specific binding ± SEM of at least three independent experiments. A nonlinear regression one-site binding curve was then fitted and resulting pIC_{50} values were subjected to one-way ANOVA and uncorrected Fisher's LSD comparison test.

2.2.6 cAMP activity assays

Cells were assayed for cAMP signalling by co-transfection of receptors with a pCRE β-galactosidase (β-gal) reporter construct as previously described [283]. Cells were stimulated for 6 hours at 37 °C with H2 relaxin or INSL3 at dilutions varying from 1 µM to 0.001 nM. Pooled data from at least 3 separate experiments, each performed in triplicate were presented as percentages of the maximum response induced by 5 µM Forskolin ± SEM. A nonlinear regression sigmoidal dose-response curve was then fitted using GraphPad PRISM and resulting pEC_{50} and maximum response (Emax) values were subjected to one-way ANOVA and uncorrected Fisher's LSD comparison test.

Table 2.1. Primers used in overlap cloning

Construct component	Template DNA	Primer (5' to 3' DNA sequence)
RXFP2 LDLa	RXFP2 LDLa module	Sense: CATCATGGATCCGCCACCATGGACAGCAAAG
		Antisense: CAGAGACCATCCATTGTTGTCTCCACAGTTCTCTTCGTCCGCCCC
RXFP1 LDLa	RXFP1 LDLa module	Sense: CATCATGGATCCGCCACCATGGACAGCAAAG
		Antisense: CGCCCATCCACTAGTGTCACCACAGTTGTCCTCATCGGCCTG
RXFP211 LRR and TM	RXFP1	Sense: GGGGCGGACGAAGAGAACTGTGGAGACAACAATGGATGGTCTCTG
		Antisense: GAGAGCTCGAGTCATGAATAGGAATTGAGTCTCGTTG
RXFP212 LRR and TM	RXFP1/2	Sense: GGGGCGGACGAAGAGAACTGTGGAGACAACAATGGATGGTCTCTG
		Antisense: CATCATCATCTCGAGCTAGGAAACTGGTTTCATTATACTGTC
RXFP122 LRR and TM	RXFP2	Sense: CAGGCCGATGAGGACAACTGTGGTGACACTAGTGGATGGGCG
		Antisense: CATCATCATCTCGAGCTAGGAAACTGGTTTCATTATACTGTC
RXFP121 LRR and TM	RXFP2/1	Sense: CAGGCCGATGAGGACAACTGTGGTGACACTAGTGGATGGGCG
		Antisense: GAGAGCTCGAGTCATGAATAGGAATTGAGTCTCGTTG

2.3 Results

Table 2.2. Pooled binding affinity (pIC50), cell surface expression and cAMP activity (pEC50 and Emax) data for RXFP211 and RXFP212 in comparison to RXFP1

Receptor	Eu-H2 relaxin competition binding (pIC_{50})	Cell Surface expression % RXFP1	cAMP activity data	
			pEC_{50}	Emax (%Forskolin)
RXFP1	8.77 ± 0.10 (7)	100 ± 3.23 (8)	10.89 ± 0.07 (4)	102.4 ± 3.3 (3)
RXFP211	8.64 ± 0.15 (8)	141.2 ± 11.3 (7)**	10.28± 0.15 (3)	64.5 ± 3.4 (3)*
RXFP212	8.43 ± 0.17 (4)	109.7 ± 14.7 (5)	9.19 ± 0.03 (3)**	99.9 ± 5.3 (3)

*p<0.05; **p<0.01 vs RXFP1

Table 2.3. Pooled binding affinity (pIC50), cell surface expression and cAMP activity data (pEC50 and Emax) data for RXFP122 and RXFP121 in comparison to RXFP2

Receptor	Eu-INSL3 competition binding (pIC_{50})	Cell Surface expression % RXFP2
RXFP2	8.79 ± 0.06 (6)	100 ± 3.5 (4)
RXFP122	8.35 ± 0.08 (6)**	94.5 ± 10.7 (4)
RXFP121	8.43 ± 0.17 (3)*	91.0 ± 9.8 (5)

	INSL3 stimulation		H2 relaxin stimulation	
Receptor	**pEC50**	**Emax (%Forskolin)**	**pEC50**	**Emax (%Forskolin)**
RXFP2	10.26 ± 0.42 (3)	115.1 ± 9.2 (3)	9.13 ± 0.06 (3)	102.6 ± 16.5 (3)
RXFP122	9.67 ± 0.20 (5)	93.9 ± 3.6 (5)	7.95 ± 0.10 (6)**	109.8 ± 5.0 (6)
RXFP121	10.40 ± 0.34 (5)	93.7 ± 14.6 (5)	8.22 ± 0.17 (4)*	101.4 ± 8.8 (4)

*p<0.05; **p<0.01 vs RXFP2

2.3.1 Characterization of RXFP211 and RXFP212

Cell surface expression assays on the chimeric constructs showed that all receptors were expressed at the cell membrane, since their fluorescence profiles were consistently equal to or greater than that displayed by the wild-type receptors (Figure 3).

Figure 3

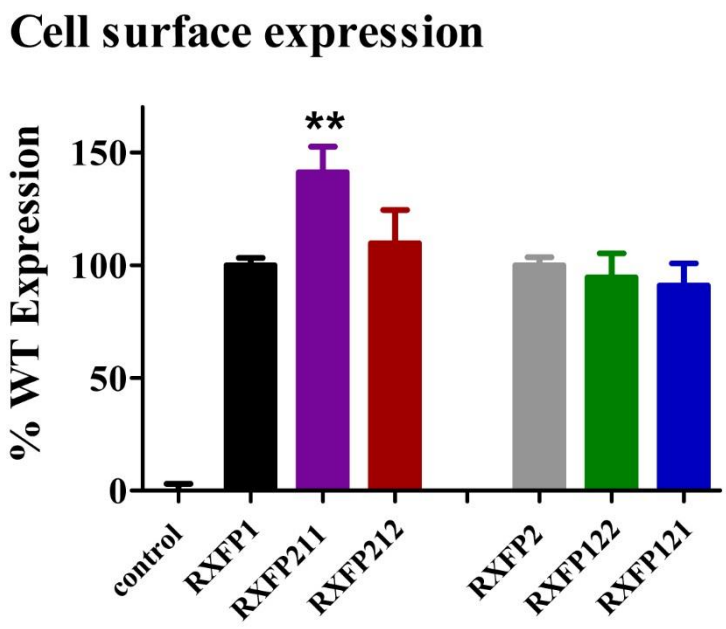

Figure 2.3. Cell surface expression of chimeric receptors compared to the RXFP1 and RXFP2 wild-type (WT) receptors.

Data are expressed as mean ± S.E.M of triplicate determinations from at least three independent experiments. **p<0.01 compared to RXFP1.

Both RXFP211 and RXFP212 were expressed more highly than wild-type RXFP1, which is consistent with findings by Kern et al. for their LDLa-swapped chimera [256]. However, only RXFP211 showed significantly ($p < 0.01$) higher expression than RXFP1 (141.2 ± 11.3% of RXFP1 expression) (Figure 3, Table 2).

The construct RXFP211 is made up of the LDLa module from RXFP2 and the LRRs and TM domain of RXFP1. RXFP212 contains the same domains except that the TM domain is from RXFP2 (Figure 2). As high affinity ligand binding is driven by the LRRs, binding was assessed

in comparison to RXFP1 using a competition binding assay with Eu-H2 relaxin. As expected binding was unaltered in comparison to wild-type as the LRR sequence was equivalent to the native receptor in each of the constructs (Figure 4a).

Figure 4

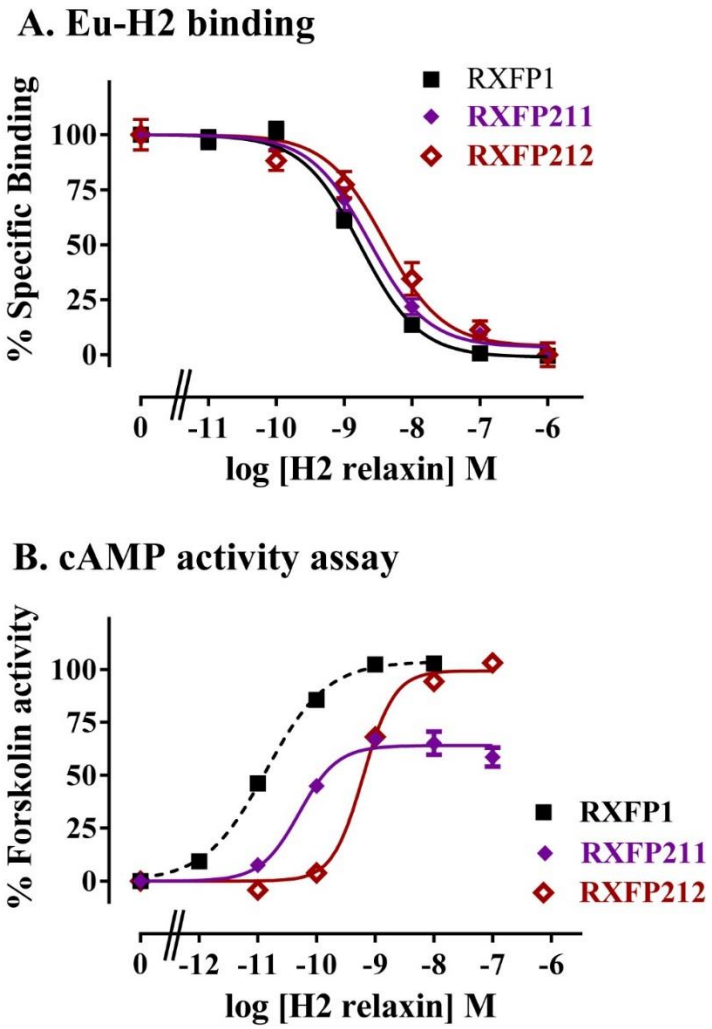

Figure 2.4. Activity of RXFP1 chimeric receptors compared to RXFP1.

A. Competition binding using Eu-labelled H2 relaxin. B. H2 relaxin-induced cAMP responses. cAMP activity is expressed as the percentage of the 5 µM forskolin-stimulated response for each receptor. Note the data for the RXFP211 receptor has been normalized for cell surface expression (see text for details). Data are expressed as mean ± S.E.M of triplicate determinations from at least three independent experiments.

The two LDLa swapped receptors were tested for cAMP production using a reporter gene assay. As the RXFP211 chimera had significantly different cell surface expression to RXFP1 the results have been normalized to cell surface expression for this construct only. While both chimeras were able to induce cAMP activity in response to H2 relaxin, the potency was reduced, with the pEC_{50} of H2 relaxin on RXFP211 being 10.28 ± 0.15, and that of H2 relaxin on RXFP212 9.19 ± 0.03, the latter of which is significantly different ($p < 0.01$) from wild-type RXFP1 (pEC_{50} 10.89 ± 0.03) (Figure 4b, Table 3). Importantly the efficacy of H2 relaxin induced cAMP responses at RXFP211 was significantly reduced compared to RXFP1 with a maximum Forskolin response of 64.02 ± 3.4% compared with 102.4 ± 3.3% ($p < 0.05$). The replacement of the RXFP1 TM domain with that of RXFP2 in RXFP212 restored the H2 relaxin stimulated efficacy to 99.9 ± 5.3% Forskolin response (Figure 4b, Table 3).

2.3.2 Characterisation of RXFP122 and RXFP121

RXFP122 has the TM and LRR domains from RXFP2 and the LDLa module from RXFP1. RXFP121 has the LDLa module and the TM region from RXFP1 and the LRRs from RXFP2 (Figure 2). Cell surface expression for these two constructs was not significantly different from WT RXFP2 levels (Figure 3, Table 3). Binding assays also showed similar patterns of binding to RXFP2, although pIC50 values for INSL3 binding were found to be significantly different from RXFP2 ($p < 0.05$ for RXFP121 and $p < 0.01$ for RXFP122) (Figure 5a, Table 3). Given that the constructs had the LRR region from RXFP2, we tested them for signalling with both INSL3 and H2 relaxin, as these ligands are both known to activate RXFP2 [275]. While the pEC50 values were not significantly different from RXFP2 on INSL3 stimulation, they were reduced from the 9.13 ± 0.06 seen in RXFP2 on response to H2 relaxin to 7.95 ± 0.10 for RXFP122 ($p < 0.01$) and 8.22 ± 0.17 for RXFP121 ($p < 0.05$) (Figure 5b, Table 3). Importantly, ligand mediated maximum responses (Emax) did not differ significantly from RXFP2.

Figure 5

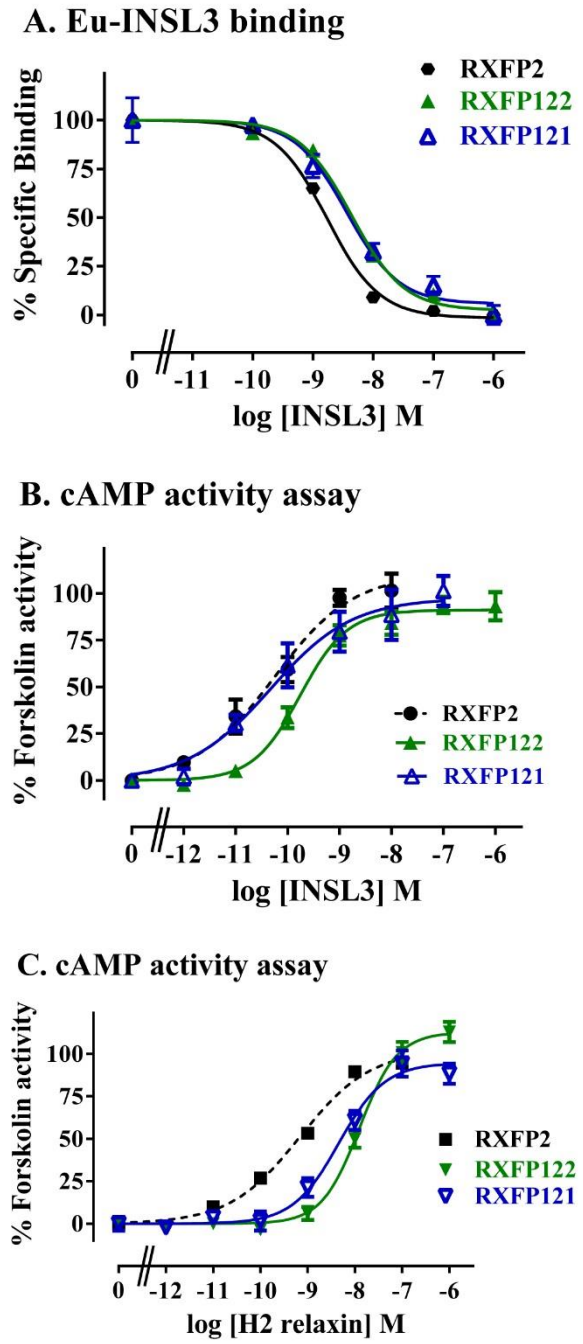

Figure 2.5. Activity of RXFP2 chimeric receptors compared to RXFP2.

A. Competition binding using Eu-labelled INSL3. B. INSL3-induced cAMP responses. B. H2 relaxin-induced cAMP responses. cAMP activity is expressed as the percentage of the 5 µM forskolin-stimulated response for each receptor. Data are expressed as mean ± S.E.M of triplicate determinations from at least three independent experiments.

2.4 Discussion

The activation mechanisms of RXFP1 and RXFP2 represent a unique paradigm in GPCR functioning, since these are the only two mammalian GPCRs that possess an LDLa module. When found in the LDLR and related receptors, these modules are typically involved in protein-protein interactions, and are thus involved in a variety of interactions both with peptides and other molecules [284]. The evidence suggests that the LDLa modules on the RXFP receptors are also involved in protein interaction, although rather than being involved in ligand binding, we have hypothesized that the LDLa module binds with another domain on the receptor, and that this interaction is necessary to induce the conformational changes needed for signalling to occur [278]. Nevertheless, while in most LDLR family receptors the binding surface of the LDLa modules seems to involve C-terminal residues, which are also involved in Ca^{2+} binding [279, 285], the RXFP1 LDLa module appears to have a binding surface that involves residues in the N-terminal region, and the hydrophobic regions of the side-chains of Leu7, Tyr9 and Lys17 have been implicated in mutational investigations on RXFP1 [280]. Both Tyr9 and Lys17 are conserved between RXFP1 and RXFP2 (Figure 1), and although they may interact differently in each case, their presence implies a similar mechanism of activation in the two receptors, also suggesting the LDLa modules of each receptor could be swapped with limited effect on receptor activation. It was therefore surprising that it was reported that when the LDLa module of RXFP2 was swapped into RXFP1 that the chimeric receptor was inactive [256]. However upon investigation of the chimeric receptor design we noted that the authors had designed the chimeric construct with additional amino acid residues from the RXFP2 linker region C-terminal of the LDLa module. Importantly this region of RXFP2 is shorter than that in RXFP1 and therefore when the chimera was produced the linker between the LRRs and the LDLa of the chimeric RXFP1 receptor was seven amino acids shorter. In this study we therefore first designed a chimeric RXFP1/RXFP2 receptor construct whereby the RXFP2 LDLa module was swapped at the C-terminal cysteine residue of the module. By reducing the swapped domain to its functional minimum length and size, we were able to produce a functional RXFP211 receptor as hypothesised, although the efficacy of signalling was reduced compared to the native receptor. Hence it is likely that the inactivity of the Kern chimeric RXFP1 construct was due to the shortening of the linker region between the LRRs and LDLa rather than the swapping of the LDLa modules.

While Kern et al. only made the RXFP1 chimera with the LDLa module of RXFP2 attached, we sought to characterise both this and the equivalent RXFP2 construct with the LDLa from RXFP1. We hypothesised that such chimeras would be informative in relation to common and distinct mechanisms of activation by the LDLa module. Additionally, we explored the concept that the LDLa is exerting its effect by interacting with the TM domain of the receptor in a specific manner by creating LDLa chimeras with matched TM domains in RXFP121 and RXFP212. The chimeric receptors were all expressed at the cell surface indicating they were folded correctly and able to be trafficked to the cell surface. The RXFP211 chimera had significantly higher cell surface expression as previously demonstrated for the chimera produced by Kern et al. [256]. Binding affinities of both RXFP1 and RXFP2 chimeras were slightly lower than the wild-type receptors with only the RXFP2 chimeras being statistically different. These differences are likely due to the lower expression levels of the receptors in the cells used for ligand binding. The sensitivity of the binding assays requires stable or semi-stable cell lines and the expression levels of the RXFP1 and RXFP2 stables were considerably higher as they were high expressing monoclonal stable lines (data not shown). These lower expression levels would influence the pIC_{50} values and unfortunately there was not sufficient Eu-labelled ligand to perform saturation binding to obtain K_d values. However, we have previously demonstrated that RXFP1 and RXFP2 receptors lacking the LDLa module bind ligand normally [200]. Hence the slight reductions in pIC_{50} values are unlikely to be related to the LDLa module swaps.

As anticipated the chimeric receptors did show differences in ligand mediated cAMP activity compared to the wild-type receptors. This was most obvious for the RXFP1 chimeras where H2 relaxin demonstrated both decreased potency as well as decreased % maximum Forskolin activity on RXFP211. The shift in pEC_{50} was similar to what we have previously demonstrated when the key RXFP1 LDLa residue Leu7 is mutated to Lysine as it is in the RXFP2 LDLa module [280]. The decreased E_{max} values may reflect the mismatch of the LDLa with the TM domain resulting in the RXFP2 LDLa module acting like a partial agonist on the RXFP1 receptor. Notably, we have seen similar decreases in E_{max} with multiple mutations of the RXFP1 LDLa module [258, 280]. Furthermore, H2 activation of RXFP1-LB2 gain-of-function receptors also resulted in lower E_{max} values compared to RXFP1 [280]. Interestingly the replacement of the TM domains with that from RXFP2 in the chimera RXFP212 resulted in full H2 relaxin stimulated but coupled with lower potency. Hence the RXFP2 LDLa module is now acting more like a full agonist as potentially the matching of the LDLa module and the

TM domain allows for optimal interactions to increase the probability of the receptor becoming fully activated. The decreased ligand potency on RXFP121 may be due to subtle differences in the LRRs that confer decreased coupling efficiency between ligand binding and LDLa mediated activation. Similarly, because RXFP1 and 2 are multi-domain receptors, it is these subtle mismatches that lead to the changes in ligand potency and efficacy seen in all the chimeric receptors. Our previous studies with RXFP2 LRR chimeric receptors have highlighted that changes in the ectodomain structure have profound effects on ligand mediated activation [286]. Furthermore, as indicated above in the gain-of-function analysis using the RXFP1-LB2 construct, full restoration of signalling was not obtained, despite inclusion of sequence that corresponded to the three-dimensional structure of the interactive surface of the RXFP1 LDLa module [280]. In contrast the RXFP2 chimeric receptors had more modest effects on receptor activity with only a slight decrease in the potency of H2 relaxin at both chimeras which may reflect the different mechanism by which H2 relaxin binds and activates RXFP2 [255, 286]. The similar activity of the two chimeras is in contrast to the RXFP1 chimeras and may reflect the fact that H2 relaxin is a ligand of both receptors and the RXFP2-INSL3 interaction evolved more recently [88, 287]. Hence the RXFP1 LDLa module may have equal efficacy on the RXFP2 TM domains. This hypothesis is supported by the similar efficacy of ligands on the previously reported RXFP1/2 chimera [135] which matches an RXFP1 LDLa with the RXFP2 TM domain in addition to the reduced ligand efficacy on the RXFP2/1 chimera in this same study [135] again highlighting a partial agonist effect of the RXFP2 LDLa on the RXFP1 TM domain.

Taken together, this study has shown that the LDLa modules of RXFP1 and RXFP2, which are unique among GPCRs, behave in a comparable fashion to one another, and that their mechanism of action must therefore be closely related. Additionally it is clear that the length of the linker region between the LRRs and the LDLa module is important for RXFP1 function. This information can be used to further elucidate a model of activation, as we gradually clarify the myriad of different elements that come into play upon binding and activation of these complex receptors. Given that relaxin has been implicated in various pathologies including cancer [288] and that it is has recently successfully completed a phase 3 clinical trial for the treatment of chronic heart failure [289] any knowledge of the activation of its cognate receptor and family members leads us closer to the development of small molecule analogues and antagonists that may be therapeutically relevant.

2.5 Acknowledgements

The authors thank Sharon Layfield and Tania Ferraro for technical assistance and Corthera for provision of recombinant H2 relaxin. This research was supported by National Health and Medical Research Council of Australia project grants 628427 and 1043750 (RADB and PRG) and by the Victorian Government Operational Infrastructure Support Program. RADB and JDW are recipients of NHMRC (Australia) Research Fellowships, DJS is a recipient of an NHMRC CJ Martin Fellowship, RCKK is the recipient of a University of Melbourne International Research Scholarship and University of Melbourne International Fee Remission Scholarship and EJP is the recipient of a Melbourne Research Fellowship (Career Interruptions).

Chapter 3 Investigating the role of the RXFP1 linker

3.1 Introduction

This chapter will present data from the 2016 publication in Nature Communications, in which we explore the role of the linker between the LDLa module and LRR domain of RXFP1 [2]. While the binding and activation domains of RXFP1 had previously been identified as the LRRs and LDLa module respectively [243, 290], this organization did not entirely explain certain phenotypes observed. For example, it was found that an insertion of two amino acids constituting an EcoRI cleavage site between the LDLa module and neighbouring residues (between Cys40 and Gly41 – see Figure 3.3) was sufficient to abrogate signalling entirely (Figure 3.1 – blue curve). Upon mutating both residues to alanine, activation was not restored (Figure 3.1 – red curve), and even when one alanine was removed so that the sequence was identical to wild type bar a single alanine insertion no signalling was observed (Figure 3.1 – green curve).

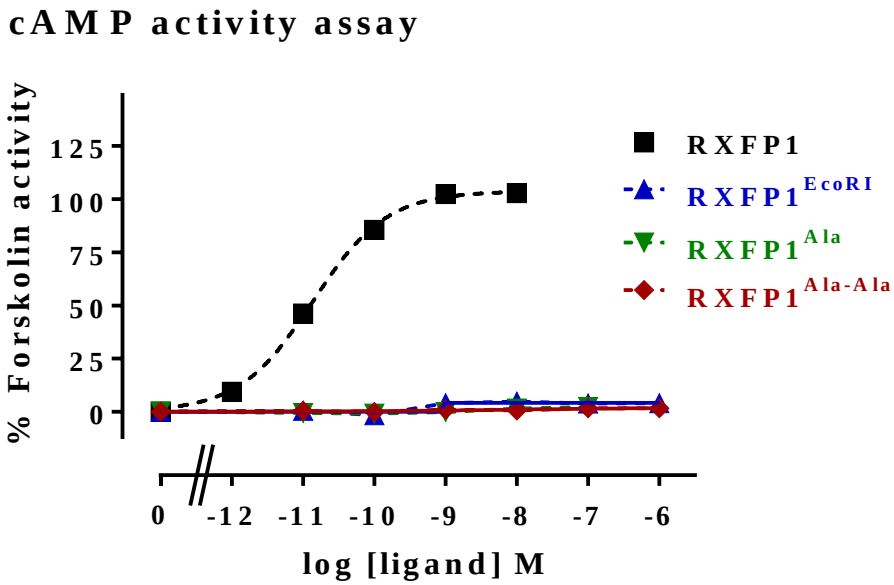

Figure 3.1 Activity curves from insertion mutants compared to RXFP1 wild-type receptor.

Data is represented as mean ± SEM and is taken from a minimum of three repeated experiments involving triplicate measures of each data point. Data from Roy Kong.

NMR data in the form of a HSQC spectrum from a titration of relaxin into a solution of recombinant RXFP1 LDLa module displayed unexplained differences compared to a construct that also contained 32 residues from the linker (not shown). Other information gathered in our lab also indicated a greater role for the linker than that previously attributed to it. During my honours year I set about mutating linker residues to alanine, in groups of two, starting with the first six residues, GDNNGW. Surprisingly, all three double mutants were signalling deficient to some extent (Figure 3.2A), despite being correctly trafficked and presented on the HEK293T cell surfaces (Figure 3.2B). Competition binding assays were attempted unsuccessfully, using transiently transfected receptors, leaving the binding capacity of the mutants unknown at that time.

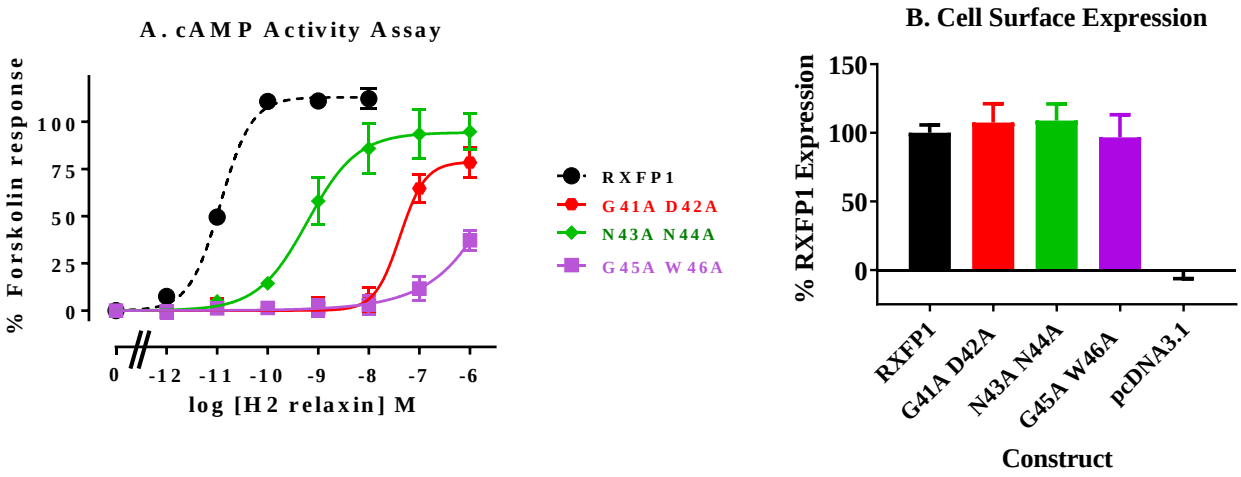

Figure 3.2. A. Activity and B. cell surface expression data from RXFP1 double mutants compared to wild-type RXFP1.

All data are presented as mean ± SEM from a minimum of three independent experiments each performed in triplicate.

With all of this tantalizing evidence emerging from the lab, we decided to investigate the role being played by the RXFP1 linker in much greater detail. The subsequent exploration formed the basis for the current thesis chapter, as well as the associated publication [2], which combined my work with that of close collaborator, Ashish Sethi.

The double mutants G41A/D42A, N43A/N44A and G45A/W46A were transfected stably into HEK293T cells using the Zeocin resistance conferred by the pcDNA3.1 plasmid to select for successfully transfected cells. They were then tested for binding using a saturation binding assay with Eu^{3+}-labelled relaxin (Eu-relaxin), as well as signalling in response to the small molecule RXFP1 agonist ML290 [291].

Close appraisal of the linker sequence revealed that this initial section was among the most highly conserved between mammalian species of RXFP1, and that residues further toward the C terminus were much more variable (Figure 3.3).

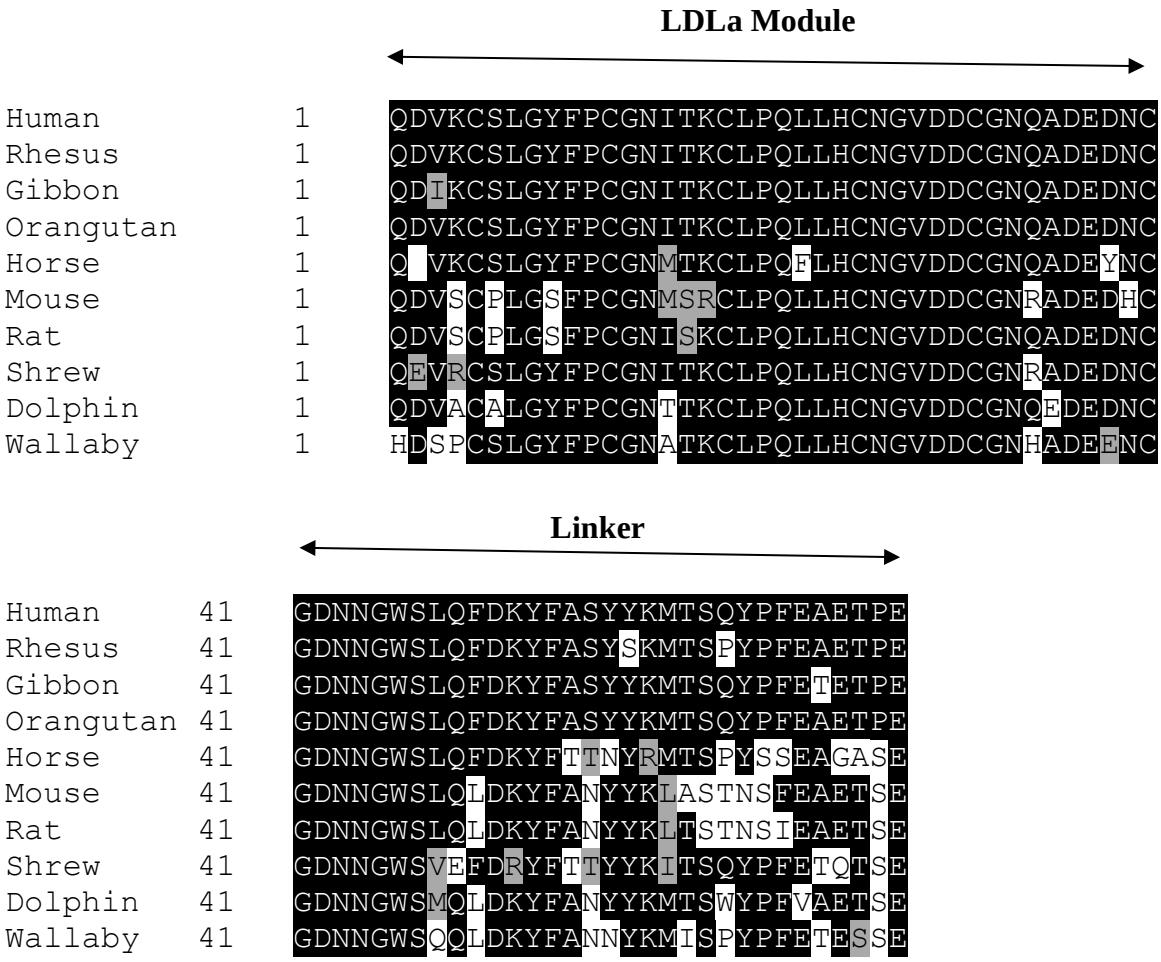

Figure 3.3. Sequence alignment of mammalian RXFP1 LDLa module and linker

Alignment is coloured using BoxShade such that conserved residues are black and conservative substitutions are grey.

Collaborator Ashish Sethi used the segment of human RXFP1 encompassed by the sequence shown in Figure 3.3 for the design of a construct that could be expressed and purified in *E.coli* using an N-terminal purification tag, the thermostabilized B1 immunoglobulin binding domain of the streptococcal protein G (GB1). The construct, named $RXFP1_{(1-72)}$, was used in the absence of any structural data for RXFP1 apart from the LDLa module itself, which was solved by solution NMR in 2007 [258] (Figure 1.10B). By using a recombinant protein with the addition of the 32-residue linker we hoped to gather new information about the binding mechanism of relaxin to RXFP1 beyond the well-characterized LRR binding site. $RXFP1_{(1-72)}$ was expressed as a ^{15}N-labelled peptide and heteronuclear single quantum coherence (HSQC) spectra were collected before and after the addition of increasing concentrations of relaxin. The subsequent chemical shifts were observed as they changed in intensity and/or position, and those with the greatest change were selected as a starting point for performing an alanine scan on the linker in the whole receptor (Figure 3.4). The mutagenesis data collected makes up the remaining contents of this chapter.

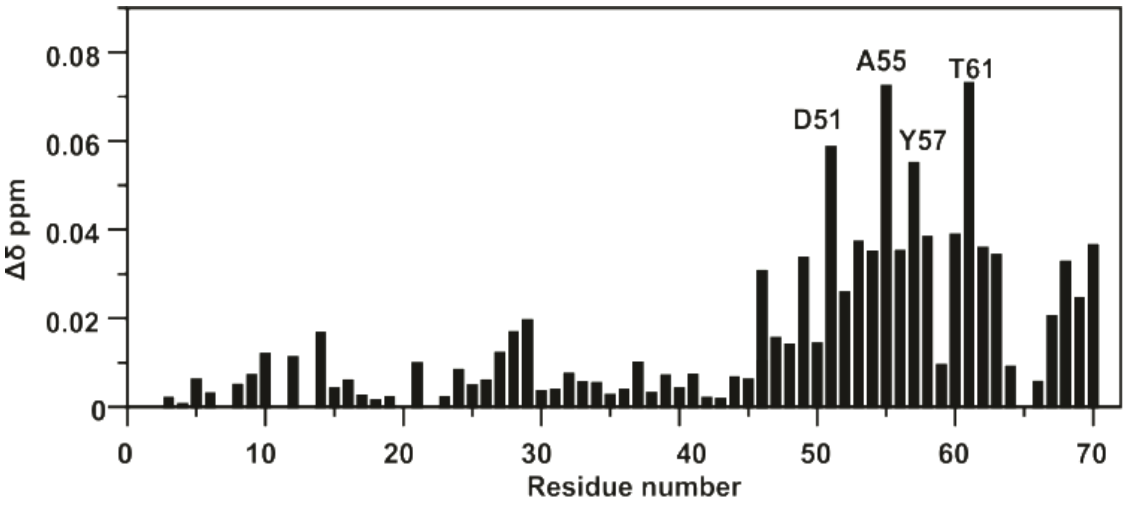

Figure 3.4. Chemical shift difference plot for residues of 50 µM 15N-labelled RXFP1$_{(1-72)}$ following titration of nine equivalents of relaxin.

Figure taken from [2].

The mutant receptors were transfected into HEK293T cells and tested for cell surface expression levels, cAMP activation and binding to relaxin, and also ML290 activity if changes were seen in comparison to wild-type responses. We also tested two different insertion mutants, placing additional alanine residues at specific points along the linker, one after Phe50 and the other after Glu67, as well as a deletion of Ala68 in order to test the effect of changing linker length and altering flexibility. In this way, the NMR investigation occurring on the RXFP1 linker was supported by the information garnered from cellular assays and together we were able to paint a detailed picture of the role being played by the heretofore unnoticed RXFP1 linker [2].

3.2 Materials and Methods

3.2.1 Sequence Analysis

Protein sequences were extracted from UniProtKB in FASTA format, and aligned first using Clustal Omega® through the EMBL-EBI website, and then the BoxShade™ server to highlight conservation of residues between species.

3.2.2 Expression of receptors on cultured HEK293T cells

Receptors were transiently or semi-stably expressed in HEK293T cells (ATCC #CRL-1573; American Type Tissue Culture Collection) which were maintained in DMEM (Gibco, ThermoFisher Scientific, Waltham, MA) that was supplemented with 10% FBS, 1% l-glutamine and 1% penicillin/streptomycin. Cells were grown in 175 cm^3 flasks in incubators maintained at 37 °C with 5% CO_2 and 85% humidity and passaged every two to three days. Transfections were performed using lipofectAMINE 2000 (Invitrogen) typically a day after cells had been plated out on Cellbind (Costar, Corning) or poly-l lysine precoated View plates (Perkin-Elmer) at an appropriate density. Vector containing our protein of interest was placed into OptiMEM (Gibco) at 0.25 µg per well for 96-well plates, or 1 µg per well for 24-well plates and after a 5 minute incubation added to an equal volume of OptiMEM containing 0.5 µl of lipofectAMINE per well for 96-well plates, or 2 µl per well for 24-well plates. The mixture was incubated for 20-40 minutes at room temperature before being added to wells (25 µl/100 µl per well). Plates were then returned to incubators for a further 18-24 hours' growth.

3.2.3 Mutagenesis

Single point mutations were introduced into wild-type RXFP1 which had previously been cloned into a pcDNA3.1™/Zeo+ AmpR mammalian expression vector (Invitrogen), such that it would contain an N-terminal FLAG tag and a bovine prolactin signal sequence, all of which do not interfere with receptor function [90]. Mutants were made using PrimeStar polymerase (TaKaRa, Kusatsu, Japan) using primers that were made according to the method described in [292]. Primers for insertion and deletion mutants were produced using the methodology described in [293]. In both methods a short overlapping region of forward and reverse primer spanned the desired mutation and non-overlapping extensions were included on the 5' end of each to reduce primer dimerization and encourage correct binding to template (Table 3.1). A PCR mix typically contained the following constituents: 5x PrimeStar buffer (10 µl); forward

and reverse primers @ 25 µM (1 µl each); template plasmid DNA (50-100 ng); dNTPs @ 2.5 µM each (4 µl); PrimeStar polymerase (1 µl); dH2O to 50 µl total volume. For point mutations the T_m was calculated using the portion of primer 5' of the mutation with the online server from Harvard University (http://mbcf149.dfci.harvard.edu/docs/oligocalc.html). The PCR protocol was designed according to PrimeStar recommendations and consisted of 30 seconds at 95 °C, 25 cycles of 95 °C (30 sec); T_m - 2 °C (typically 53 °C; 5-10 sec); 68 °C (1 min per kb of vector) followed by a 4 °C hold. Insertion and deletion mutations were made using the same general make-up of PCR mix, but the protocol was described in [293] and varied according to primers' calculated overlapping (pp) or non-overlapping (no) T_m's: 5 minutes at 95 °C; 12 cycles of 95 °C (1 min), T_m(no) - 2 °C (1 min), 68 °C (12 min); 1 min at T_m(pp) - 2 °C followed by a further extension step at 68 °C for 30 min, and a 4 °C hold. Upon completion of the PCR cycling, 20 µl of the total 50 µl reaction was placed into a separate tube with 1 µl of DpnI enzyme (Promega) in order to remove template plasmid, and 10 µl were then used to transform into DH5α strain of *Escherichia coli* (*E.coli*) and grow on Amp-containing LB-Agar plates overnight. Colonies were screened by sequencing, and once a mutant had been identified the entire insert segment was sequenced to ensure no accidental mutations had been incorporated. Mutant Ins A40-41 was made by Roy Kong.

3.2.4 Establishing stable cell lines of the double mutants G41A/D42A, N43A/N44A and G45A/W46A

The protocol for achieving semi-stable expression of the first three linker mutants was simpler than that described in the Chapter 2 (section 2.2.3). Rather than sorting the cells using FACS, cells were simply transfected and re-seeded into smaller flasks where they were grown in the presence of 200 µg/ml Zeocin (Gibco) to eliminate any untransfected cells in the culture, since the pcDNA3.1 vector possesses Zeocin selectivity. After several rounds of passaging with Zeocin positive media, it was assumed that only transfected cells would survive, and cell-surface expression assays were performed to assess relative levels.

3.2.5 Cell surface expression assays

We tested levels of expression of the various mutants using the same method as described in section 2.2.4. The plate-based enzyme-linked immunosorbent assay (ELISA) assay was performed over two days, using cells seeded and transfected in 24-well plates on the two

preceding days. Buffer used was tris buffered saline (50 mM Tris pH 7.4, 150 mM NaCl) supplemented with 1 mM $CaCl_2$ (TBS/$CaCl_2$). Primary antibody was anti-FLAG M1 monoclonal antibody (Sigma-Aldrich), which was incubated at room temperature with cells after their being washed with buffer, fixed with 3.7% paraformaldehyde and then blocked with 1% bovine serum albumin (BSA) in buffer. Two washes followed, and then we carried out a further, shorter blocking step and a 1-hour incubation with secondary antibody (goat anti-mouse Alexa Fluor 488; Sigma-Aldrich) suspended in 1% BSA/TBS/$CaCl_2$. After three more washes the plates were aspirated and frozen at -80 °C for at least 24 hours. On the final day we lysed the cells in lysis buffer (TBS with 1 mM ETDA and 0.25 % Triton X-100) by incubation with shaking in low light, and then manually scraped the cells using a pipette tip and distributed them into individual wells of a 96-well black plate (Corning) to be read on an Omega POLARstar plate reader (BMG labtech) with excitation at 490 nm and emission at 520 nm. Data were normalized against expression levels of wild-type RXFP1 (100%) and background as measured by cells transfected with equivalent amounts of vehicle (empty pcDNA3.1 vector) (0%). We present these and all data from cell-based assays in this thesis (unless stated otherwise) as mean ± standard error of the mean (SEM) from at least three individual experiments each performed in triplicate. Pooled data was analysed in GraphPad PRISM (La Jolla, CA) with one-way analysis of variance and uncorrected Fisher's least square difference (LSD) multiple comparison test.

3.2.6 Eu^{3+}-labelled H2 relaxin binding assays

Similarly to the competition binding assays described in the chapter 2 (section 2.2.5), the binding affinity of mutants to H2 relaxin was established using europium-labelled peptide (Eu-relaxin) in saturation binding assays. We carried out the assays in 96-well plates which were seeded and transfected as described above, and on the third day they were washed with phosphate buffered saline (40mM Na_2HPO_4, 1.5 mM KH_2PO_4, 150 mM NaCl) (PBS) and then incubated with increasing concentrations of Eu-relaxin for 1 hour at room temperature. Non-specific binding was established by incubating a second set of wells with the same concentrations of Eu-relaxin in the presence of an excess of unlabelled H2 relaxin (1 µM) and then subtracting values as base-line. Buffer used was relaxin receptor binding buffer (RRBB; 20 mM HEPES pH 7.5, 1.5 mM $CaCl_2$, 50 mM NaCl) with 1% BSA. After a one-hour incubation in low light, cells were washed with PBS and 100 µl of Delfia Enhancement solution (PerkinElmer, Waltham, MA) was added to each well. Plates were shaken for around 20

minutes to remove europium from its cage and then read on the Omega POLARstar plate reader (BMG Labtech, Offenburg, Germany) using time-resolved fluorescence and an excitation wavelength of 340 nm and emission of 614 nm. Data was plotted in GraphPad Prism and curves were fit to One site – Specific Binding saturation curves, after subtraction of baseline. K_d and B_{max} values were extracted and significant differences between wild-type and mutants were calculated using one-way ANOVA and uncorrected Fisher's LSD multiple comparison test. Some of the binding assays were carried out by myself, and others by lab assistant Tania Ferraro.

3.2.7 cAMP activity assays

We measured the capacity of mutant receptors to activate a cAMP response after stimulation with either relaxin or ML290 using the reporter gene β-galactosidase (β-gal) which is inserted into the pBLUESCRIPT plasmid under the control of multiple copies of cAMP-response element (CRE). It is transfected with receptors in 1:1 proportion into HEK293T cells seeded in CellBind plates (Corning). The method has been characterised in [294] and relies on the fact that cAMP within cells will phosphorylate cAMP response element binding protein (CREB), leading to the translation of β-gal in response to a large array of cAMP-forming pathways. In this way we hope to capture a broad spectrum of activation possibilities with a single assay, and the β-gal present will cause a dose-dependent colour change in the substrate chlorophenol red-β-D-galactopyranoside (CPRG; Roche) that can be measured at absorbance of 570 nm. The cells were seeded and transfected as described above, and on the third day they were stimulated at 37 °C for 6 hours with increasing concentrations of relaxin in complete DMEM or ML290 suspended in minimal DMEM (0.5% FBS) with 1% dimethyl sulphoxide (DMSO) to improve solubility of ML290. Comparative assays were conducted with RXFP1 in minimal DMEM/DMSO to ensure that this variable did not alter experimental outcomes. One set of wells was used for vehicle (media only) and another for 5 µM Forskolin, which acts as a positive control as it activates adenylate cyclase (AC) directly, and these would serve as a 0% and 100% mark for normalisation of results. At the end of the incubation time media was aspirated from all wells and plates were frozen overnight at -80 °C. We then developed plates on the final day, first by lysing cells by incubation with shaking for 10 minutes in assay buffer 1 (100 mM Na_2HPO_4, 0.2 mM $MgSO_4$, 0.01 mM $MnCl_2$ (pH 8.0); 25 µl per well), then 10 minutes in assay buffer 2 (100 mM Na_2HPO_4, 2 mM $MgSO_4$, 0.1 mM $MnCl_2$, 0.5% Triton X-100, 40 mM β-mercaptoethanol (pH 8.0); 100 µl per well), and finally 25 µl per well of the β-

gal substrate CPRG (1 mg/ml in assay buffer 1) was added and plates continued to shake as colour change was visually monitored and readings were performed when a clear difference between vehicle and Forskolin wells could be seen. Readings were taken on a Benchmark Plus Microplate Reader (Bio-Rad) at 570 nm. Some of the ML290 assays were performed by Sharon Layfield and Tania Ferraro. Data was normalized to vehicle and forskolin controls and fit to a sigmoidal dose-response curve using Graphpad Prism 7. Multiple repeats of assays were pooled and E_{max} and pEC_{50} values extracted. Significant differences between mutant and wild-type responses were identified using one ANOVA and uncorrected Fisher's LSD multiple comparison test.

Table 3.1. Mutagenic primers used for site-directed mutagenesis.

Mutant	Sense primer 5' – 3'
	Antisense primer 5' – 3'
G41A D42A	CTGTGCCGCCAACAATGGATGGTCTCTGCAATTTGACAAATATTTTG
	GTTGGCGGCACAGTTGTCCTCATCGGCCTG
N43A N44A	GACGCCGCCGGATGGTCTCTGCAATTTGACAAATATTTTGCC
	CATCCGGCGGCGTCTCCACAGTTGTCCTCATCGG
G45A W46A	CAATGCCGCCTCTCTGCAATTTGACAAATATTTTGCCAGTTACTAC
	GAGAGGCGGCATTGTTGTCTCCACAGTTGTCCTCATCG
F54A Y58A	GTTACGCCAAAATGACTTCCCAATATCCTTTTGAGGCAG
	CATTTTGGCGTAACTGGCAGCATATTTGTCAAATTGCAG
F54A Y58A M60A	GTTACGCCAAAGCGACTTCCCAATATCCTTTTGAGGCAGAAACAC
	GGAAGTCGCTTTGGCGTAACTGGCAGCATATTTGTCAAATTGCAGAG
G41A	CTGTGCCGACAACAATGGATGGTCTCTGCAATTTGACAAATATTTTG
	CTGGGCACAGTTGTCCTCATCGGCCTG
D42A	GGAGCCAACAATGGATGGTCTCTGCAATTTGACAAATATTTTG
	GTTGGCTCCACAGTTGTCCTCATCGGCCTG
N43A	GACGCCAATGGATGGTCTCTGCAATTTGACAAATATTTTGCC
	CCATTGGCGTCTCCACAGTTGTCCTCATCGG
N44A	CAACGCCGGATGGTCTCTGCAATTTGACAAATATTTTGCC
	CATCCGGCGTTGTCTCCACAGTTGTCCTCATCGG
G45A	CAATGCCTGGTCTCTGCAATTTGACAAATATTTTGCCAGTTACTAC
	CCAGGCATTGTTGTCTCCACAGTTGTCCTCATCG
W46A	GGAGCCTCTCTGCAATTTGACAAATATTTTGCCAGTTACTAC
	GAGAGGCTCCATTGTTGTCTCCACAGTTGTCCTCATCG
F50A	GCAAGCTGACAAATATTTTGCCAGTTACTACAAAATGACTTCCC
	AATATTTGTCAGCTTGCAGAGACCATCCATTGTTGTCTCC
D51A	CAATTTGCCAAATATTTTGCCAGTTACTACAAAATGACTTCC
	CAAAATATTTGGCAAATTGCAGAGACCATCCATTGTTGTCTC
K52A	GACGCATATTTTGCCAGTTACTACAAAATGACTTCCCAATATC
	CAAAATATGCGTCAAATTGCAGAGACCATCCATTGTTGTC
F54A	CAAATATGCTGCCAGTTACTACAAAATGACTTCCCAATATC
	CTGGCAGCATATTTGTCAAATTGCAGAGACCATCCATTGTTG
A55L	CAAATATTTTCTCAGTTACTACAAAATGACTTCCCAATATCCTTTTGAG
	GTAACTGAGAAAATATTTGTCAAATTGCAGAGACCATCCATTGTTGTC
Y57A	CAGTGCCTACAAAATGACTTCCCAATATCCTTTTGAGGCAG
	GTAGGCACTGGCAAAATATTTGTCAAATTGCAGAGACCATC
Y58A	GCCAGTTACGCCAAAATGACTTCCCAATATCCTTTTGAGGCAGAAACAC
	CATTTTGGCGTAACTGGCAAAATATTTGTCAAATTGCAGAGACCATCCATTGTTG
T61A	CAAAATGGCTTCCCAATATCCTTTTGAGGCAGAAACACC
	GGAAGCCATTTTGTAGTAACTGGCAAAATATTTGTCAAATTGCAG
F66A	CCTGCTGAGGCAGAAACACCTGAATGTTTGGTC
	CTCAGCAGGATATTGGGAAGTCATTTTGTAGTAACTGGC
E67A	CTTTTGCGGCAGAAACACCTGAATGTTTGGTCGG
	CTGCCGCAAAAGGATATTGGGAAGTCATTTTGTAGTAACTGG
Ins Ala 50-51	GGTCTCTGCAATTTGCCGACAAATATTTTGCCAGTTACTACAAAATG
	GGCAAATTGCAGAGACCATCCATTGTTGTCTCCACAGTTG
Ins Ala 67-68	CAATATCCTTTTGAGGCCGCAGAAACACCTGAATGTTTGG
	GGCCTCAAAAGGATATTGGGAAGTCATTTTGTAGTAACTGG
Del Ala 68	CCTTTTGAGGAAACACCTGAATGTTTGGTCGGTTCTGTGCC
	CAGGTGTTTCCTCAAAAGGATATTGGGAAGTCATTTTGTAGTAACTG

Template used was pcDNA3.1 FLAG-RXFP1.

3.3 Results

3.3.1 Double mutants RXFP1-G41A/D42A, N43A/N44A and G45A/W46A

Firstly, we established semi-stable cell lines expressing the mutants in order to more categorically assess their binding capacity. The transfected cells were grown in the presence of Zeocin to ensure that only those that had successfully taken up the pcDNA3.1 Zeo(+) vector containing the receptors were able to survive. To assess the success of the method we measured the levels of receptor compared with stably expressing RXFP1 cells as positive control, and untransfected HEK293T cells as negative control (Figure 3.5; Table 3.2). While levels were lower than the stable RXFP1-expressing cells, all three double mutants were indeed being expressed at high levels, and the cells were therefore considered appropriate for use in subsequent binding assays.

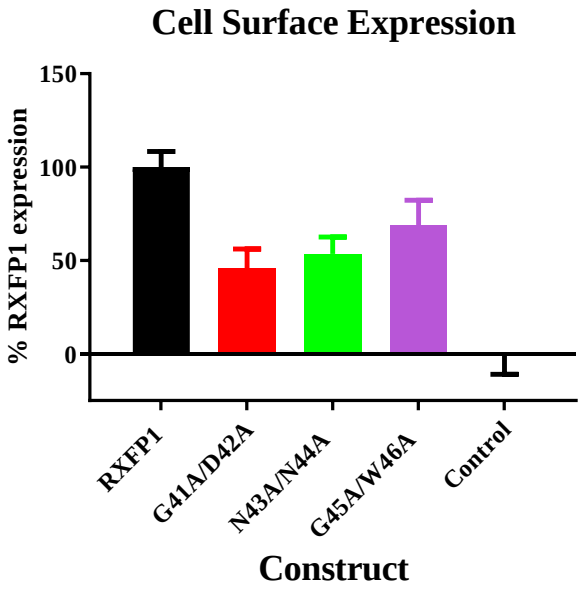

Figure 3.5. Relative cell surface expression of semi-stably expressed double mutants compared to stably expressed RXFP1 (100%) and untransfected HEK293T cells (0%).

All data are displayed as mean ± SEM of at least three independent experiments, each performed in triplicate.

Binding assays were done using a saturation protocol, such that we could quantify and compare K_d values and thereby have a conclusive measure of affinity. We imagined that the mutants should bind ligand similarly to wild-type, since the signalling deficient LDLa-free RXFP1 variant characterised in the past had shown close to normal binding [200]. However, contrary to our expectations, the mutants bound relaxin very weakly, especially G41A/D42A (K_d > 20) and G45A/W46A (K_d > 20), but also N43A/N44A to a significant degree (K_d = 3.28 ± 0.57) (Figure 3.6; Table 3.2).

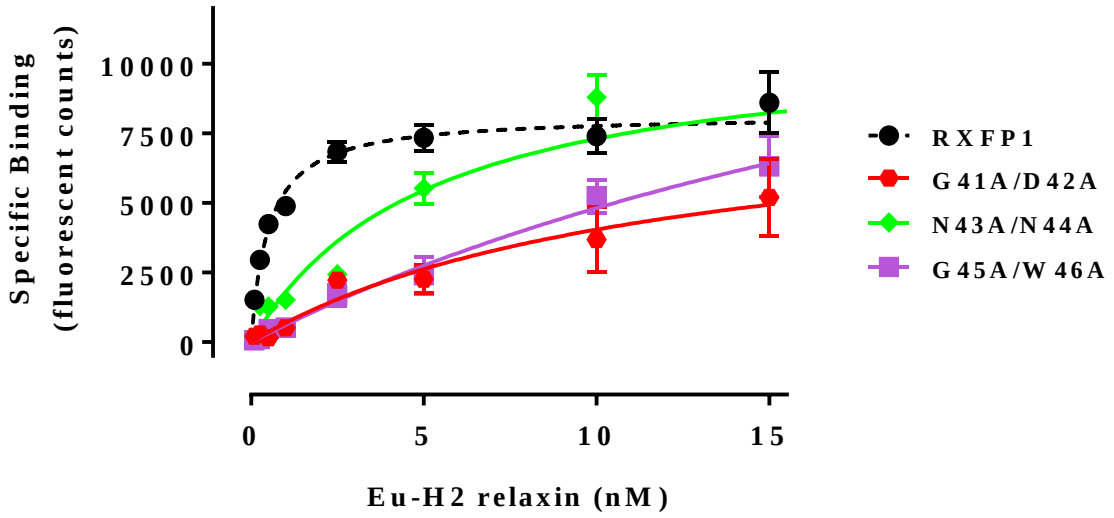

Figure 3.6. Saturation binding curves of RXFP1 compared to double mutants G41A/D42A, N43A/N44A and G45A/W46A.

Data are representative of mean ± SEM of at least three separate experiments each performed in triplicate.

Fortunately we had the small molecule ML290 at our disposal, which had been shown to activate the RXFP1 TM domain independently of the ectodomain [166] and hence we could test mutants for signalling competency using this novel tool. Testing with ML290 revealed that the double mutants were capable of signalling like wild-type (Figure 3.7; Table 3.2).

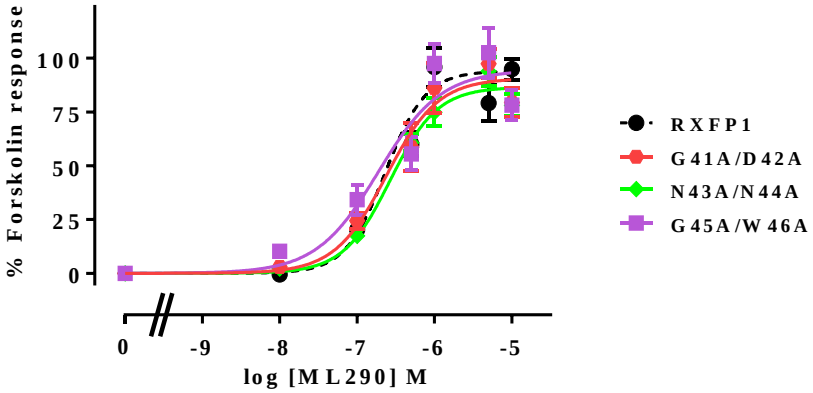

Figure 3.7. Activation of RXFP1 and mutants by ML290 as percentage of Forskolin response.

Data points are mean ± SEM of at least three independent experiments each performed in triplicate.

We also tested RXFP1 in a minimal, DMSO-containing media to ensure that results were not altered when the experiment was performed in the same way as for ML290, and the curves recapitulated those we had seen when using complete DMEM, albeit with slightly (but not significantly) higher efficacy (Figure 3.8).

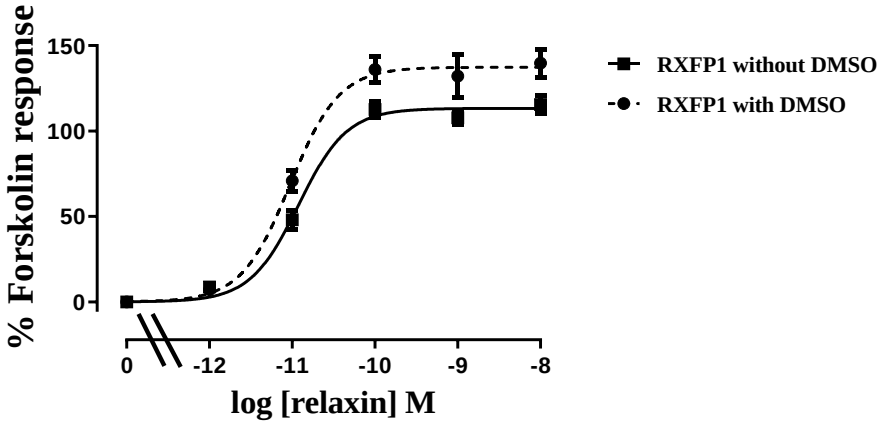

Figure 3.8. cAMP activity assay for wild-type RXFP1 in complete DMEM without addition of DMSO compared to minimal DMEM with 1% DMSO.

Data points are mean ± SEM of at least three separate experiments each performed in triplicate.

3.3.2 Single-point mutants from the GDNNGW motif

The single-point mutants were assayed following transient transfection into HEK293T cells in order to find out whether one or both residues contributed the most to the phenotypes observed in the double mutants. Activity assays revealed that Asp42 was more important to receptor function than Gly41 (Figure 3.9A); Asn43 was more destructive after mutation than Asn44 (Figure 3.9B); and both Gly45 and Trp46 were necessary, although W46A caused a slightly greater perturbation in signal (Figure 3.9C; Table 3.2).

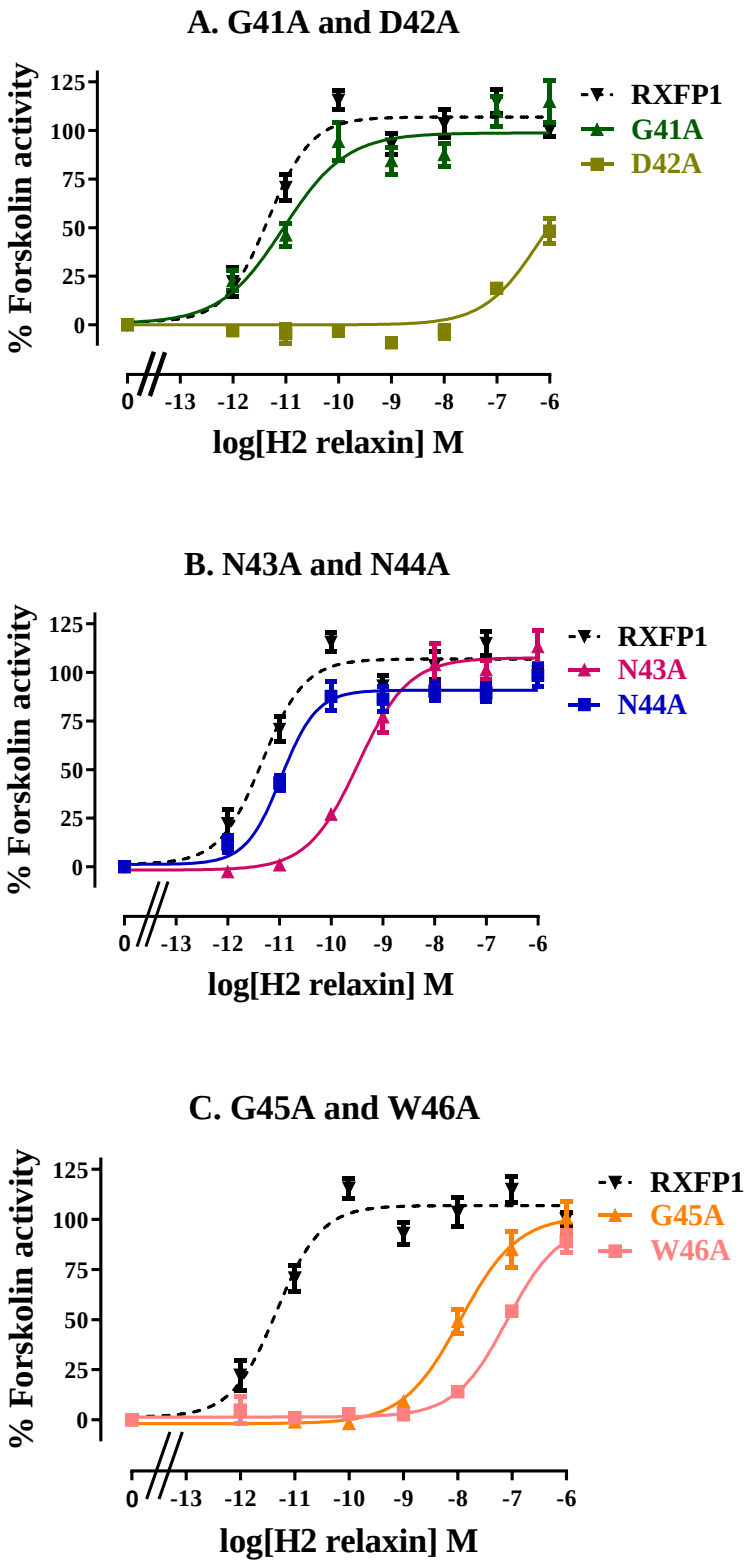

Figure 3.9. cAMP activity of single-point mutants from GDNNGW sequence of RXFP1 linker, separated into A. G41A and D42A, B. N43A and N44A, C. G45A and W46A.

All data are presented as mean ± SEM of at least three independent experiments, each performed in triplicate.

Saturation binding assays were once again used to see if a correlation between loss of activity and relaxin binding could be seen, and this seemed to be the case. While none of the single-point mutants had binding as severely perturbed as the double mutants, D42A (K_d = 20.7 ± 3.5), G45A (K_d = 19.1 ± 3.07), W46A (K_d = 12.26 ± 1.36) and to an extent N43A (K_d = 2.55 ± 0.55) all had reduced affinity for H2 relaxin (Figure 3.10; Table 3.2).

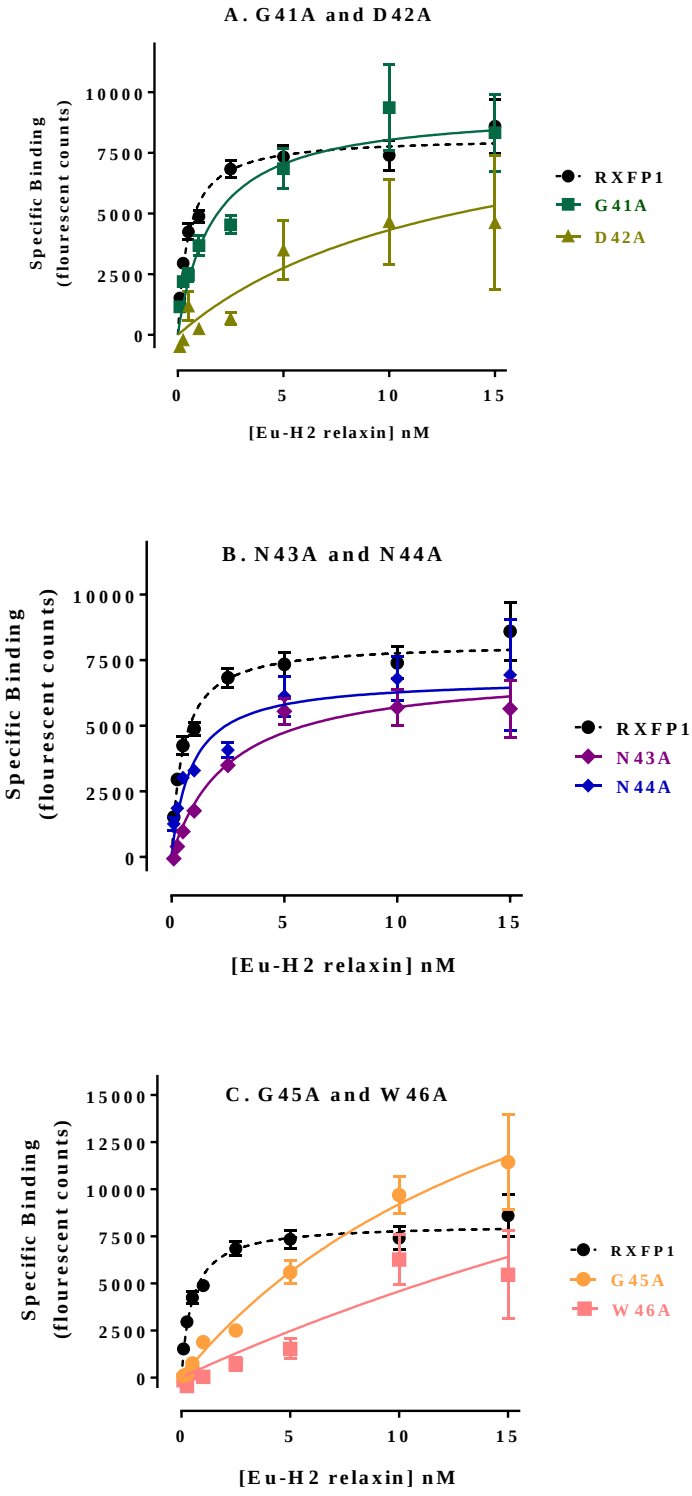

Figure 3.10. Saturation binding curves for single point mutants in the GDNNGW sequence of RXFP1 linker compared to wild-type RXFP1.

Data points are mean ± SEM from at least three independent experiments each performed in triplicate.

In radioligand saturation binding assays, the B_{max} gives a read-out of the available receptor binding sites in the system [295]. This parameter is therefore indicative of relative cell surface expression, and the data presented here would suggest that the receptors were indeed being robustly expressed (Figure 3.10, Table 3.2). Nevertheless, for completeness I checked the levels of all of the mutants using the cell surface expression assay. In this way we could be sure that any differences we saw from wild-type activity and binding was not due to a lack of adequate protein found at the cell surface. Indeed, we found that none of the mutants tested had significantly different expression than wild-type RXFP1 (Figure 3.11; Table 3.2).

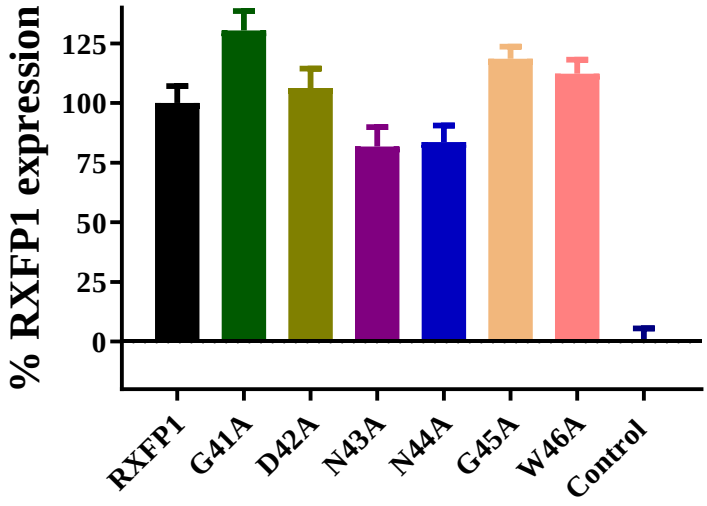

Figure 3.11. Relative cell surface expression of single-point mutants

Expression is displayed as a percentage of transiently transfected RXFP1 expression levels with empty vector pcDNA3.1 serving as negative control (0%). Data are shown as mean ± SEM of at least three independent experiments each performed in triplicate.

Since ML290 had activated the double mutants similarly to wild-type we did not test the single-point mutants using this molecule.

3.3.3 Other single-point mutants from the linker

Moving on from the first six residues of linker, we decided to focus on residues that showed the greatest chemical shift change in NMR titrations of $RXFP1_{(1-72)}$ with recombinant H2 relaxin (Figure 3.4). Residues mutated were Phe50, Asp51, Lys52, Phe54, Ala55, Tyr57, Tyr58, Met60, Trp61, Phe66 and Glu67. We chose to mutate to alanine, in order to eliminate any function performed by the natural side-chain otherwise present at a given amino acid [296]. Any residues that were already alanine were mutated to both serine for a change from hydrophobic to polar, and leucine for an extension in length. None of the mutants showed phenotypes as striking as those seen within the GDNNGW motif, and activity in response to both H2 relaxin and ML290 was like wild-type (H2 relaxin pEC_{50} = 10.97 ± 0.05; E_{max} = 116.3 ± 4.2) (Figure 3.11; Table 3.2; ML290 graphs not shown) with the exception of F50A, with reduced H2 relaxin potency (pEC_{50} = 9.45 ± 0.07) and efficacy (E_{max} = 91.9 ± 2.1), as well as a loss of affinity (K_d = 6.48 ± 0.76); F54A, with reduced relaxin potency (pEC_{50} = 10.23 ± 0.13) and affinity (K_d = 2.43 ± 0.46); and F58A with reduced relaxin affinity (1.56 ± 0.09) (Figure 3.12; Table 3.2). Interestingly, F50A also had a slightly reduced efficacy in response to ML290 (E_{max} = 65.6 ± 5.6). While the mutants were all expressed normally on the surface of cells according to the cell surface expression assay (Figure 3.13; Table 3.2), some of them had reduced B_{max} values compared to wild-type RXFP1 in saturation binding assays (F54A = 5626 ± 12.9, M60A = 3886 ± 500.08, T61A = 5850 ± 196.22 vs RXFP1 = 8496.75 ± 625; Figure 3.13B,C, Table 3.2). While not significant, this trend suggests that not all the receptors at the cell surface were able to fully bind ligand perhaps due to structural perturbations relating to the mutations. A small reduction in binding competent receptors would not necessarily be measurable in the signalling assay, since a small proportion of total receptor is capable of eliciting a full response (see Chapter 4), although the reduced relaxin potency at F54A may be a reflection of this phenomenon (Figure 3.12A, Table 3.2).

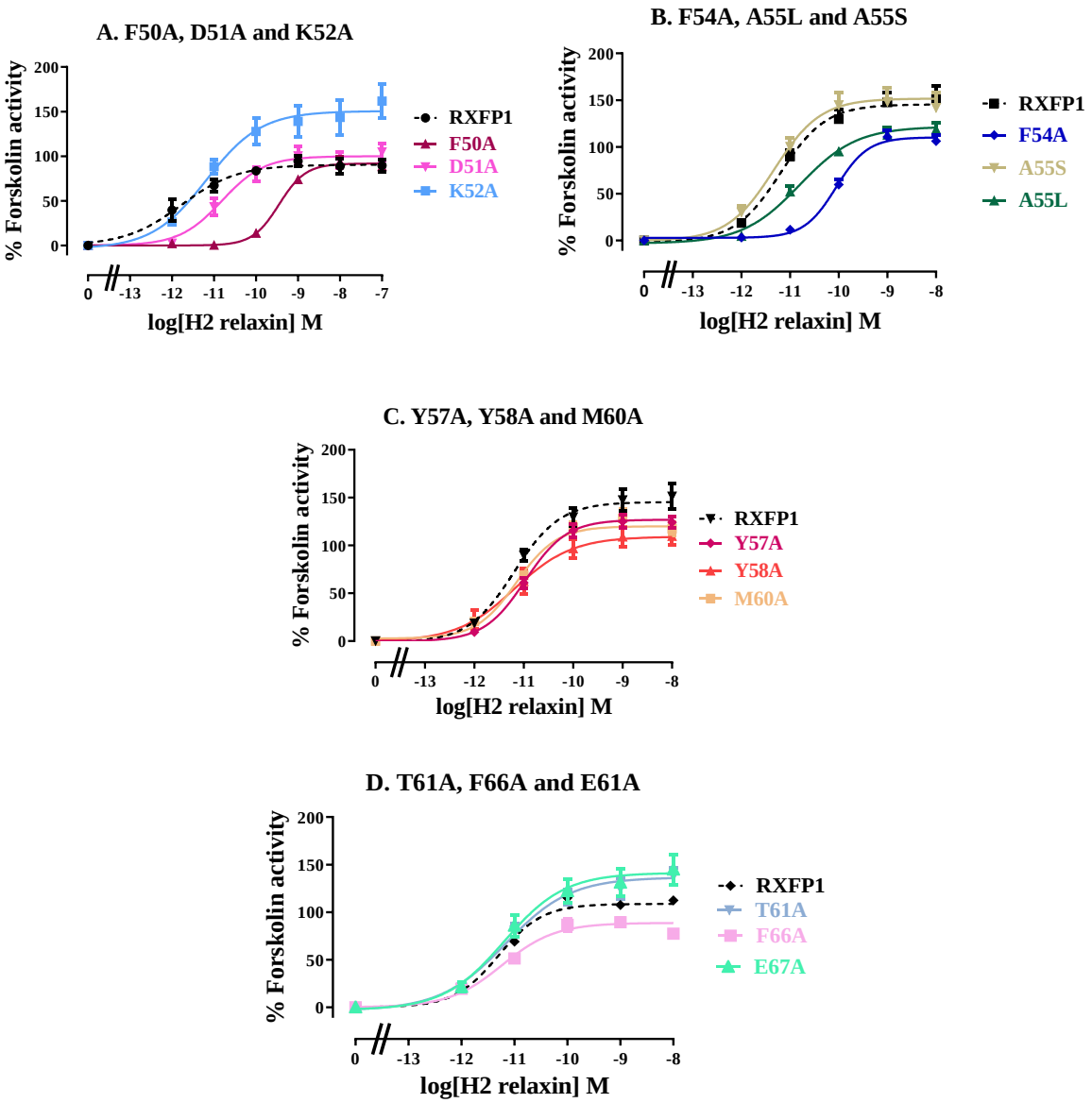

Figure 3.12. cAMP activity assay of single-point mutants from within the RXFP1 linker as compared to RXFP1 wild-type.

Note that some variation of RXFP1 efficacy is seen between experiments, and that significance is calculated in a head-to-head manner, comparing mutants to wild type on the same plate, and hence different versions of RXFP1 are seen here. Data are shown as mean ± SEM of at least three independent experiments each performed in triplicate.

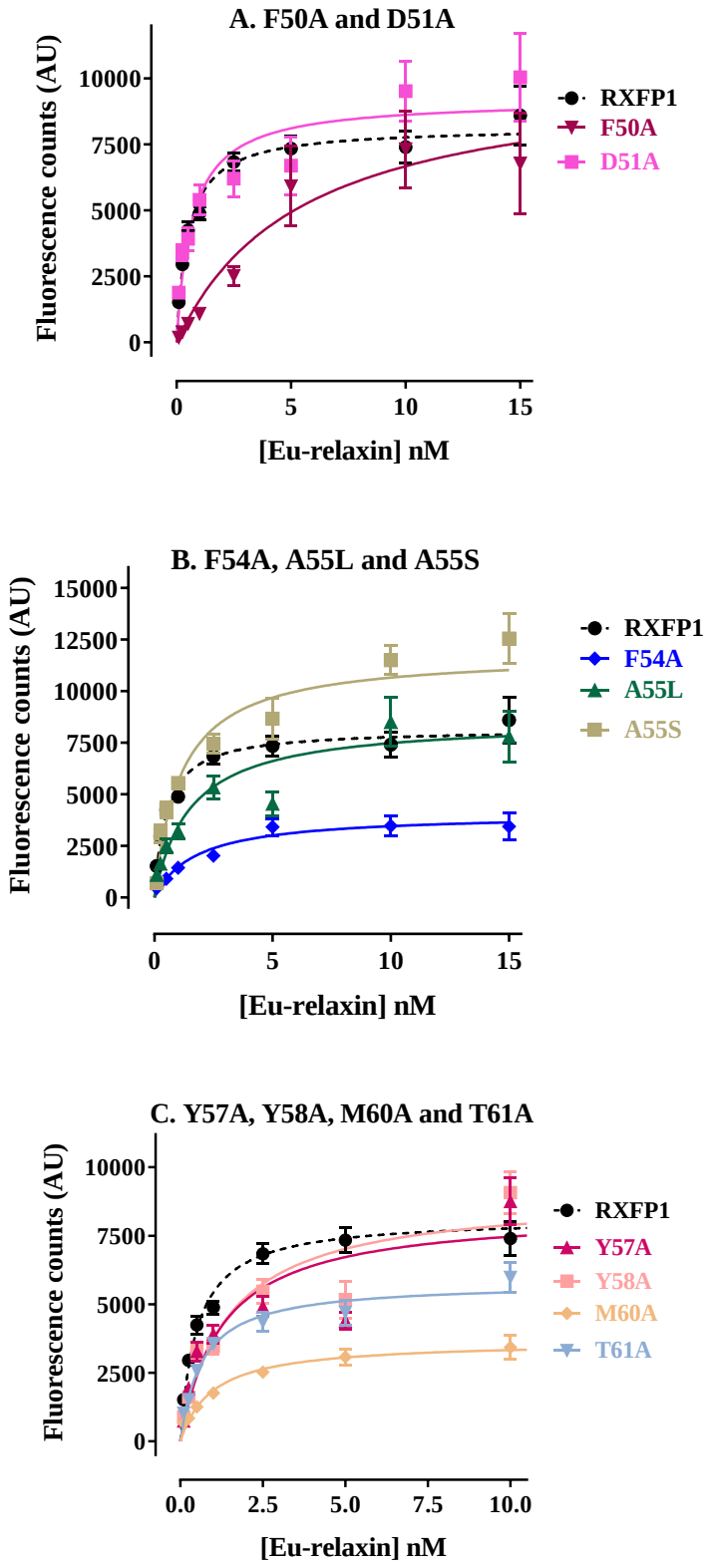

Figure 3.13.Saturation binding plots for single-point linker mutants compared to wild-type RXFP1.

Data are shown as mean ± SEM of at least three independent experiments each performed in triplicate.

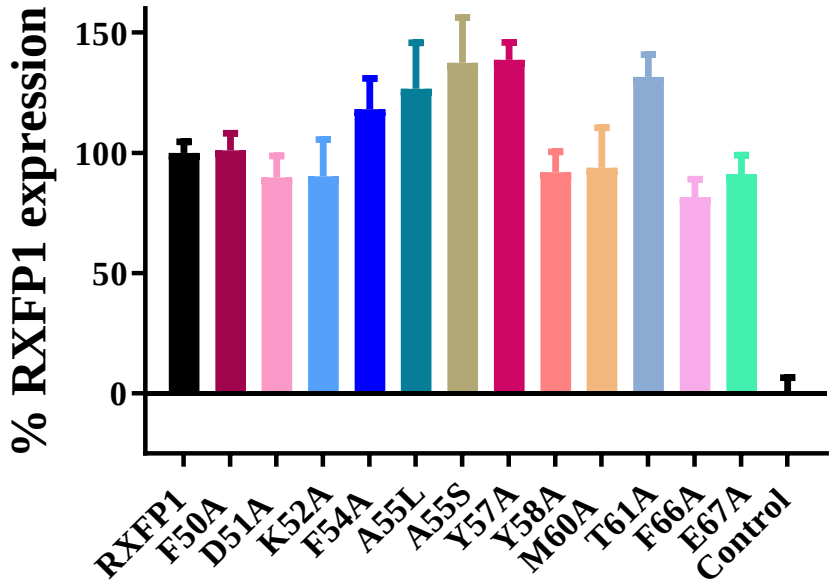

Figure 3.14. Relative cell surface expression of single-point mutants from the linker region of RXFP1.

Expression is displayed as a percentage of transiently transfected RXFP1 expression levels with empty vector pcDNA3.1 serving as negative control (0%). Data are shown as mean ± SEM of at least three independent experiments each performed in triplicate.

3.3.4 Other double/triple mutants from the linker and LDLa module

While none of the mutations made in the central linker region had as profound an influence on signalling and binding as those in the N-terminal region, some single-point mutants did have reduced potency and affinity for relaxin, in particular F54A and Y58A. Notably, these are amino acids with large aromatic sidechains, and they are separated by three residues within the linker, and we considered that they may combine to form a binding surface for relaxin. We therefore joined F54A and Y58A into a double mutant, as well as comparing any contribution made by M60A in a triple mutant. We found that combining F54A and Y58A did indeed cause an accumulative loss of signal and binding, with the K_d increasing approximately 3-fold on either of the single mutants, to 6.51 ± 1.33, and the pEC_{50} also decreasing by a log unit to 9.87 ± 0.08 (Figure 3.15; Table 3.2). The addition of M60A to the double mutant did not significantly change the phenotype (Figure 3.14; Table 3.2).

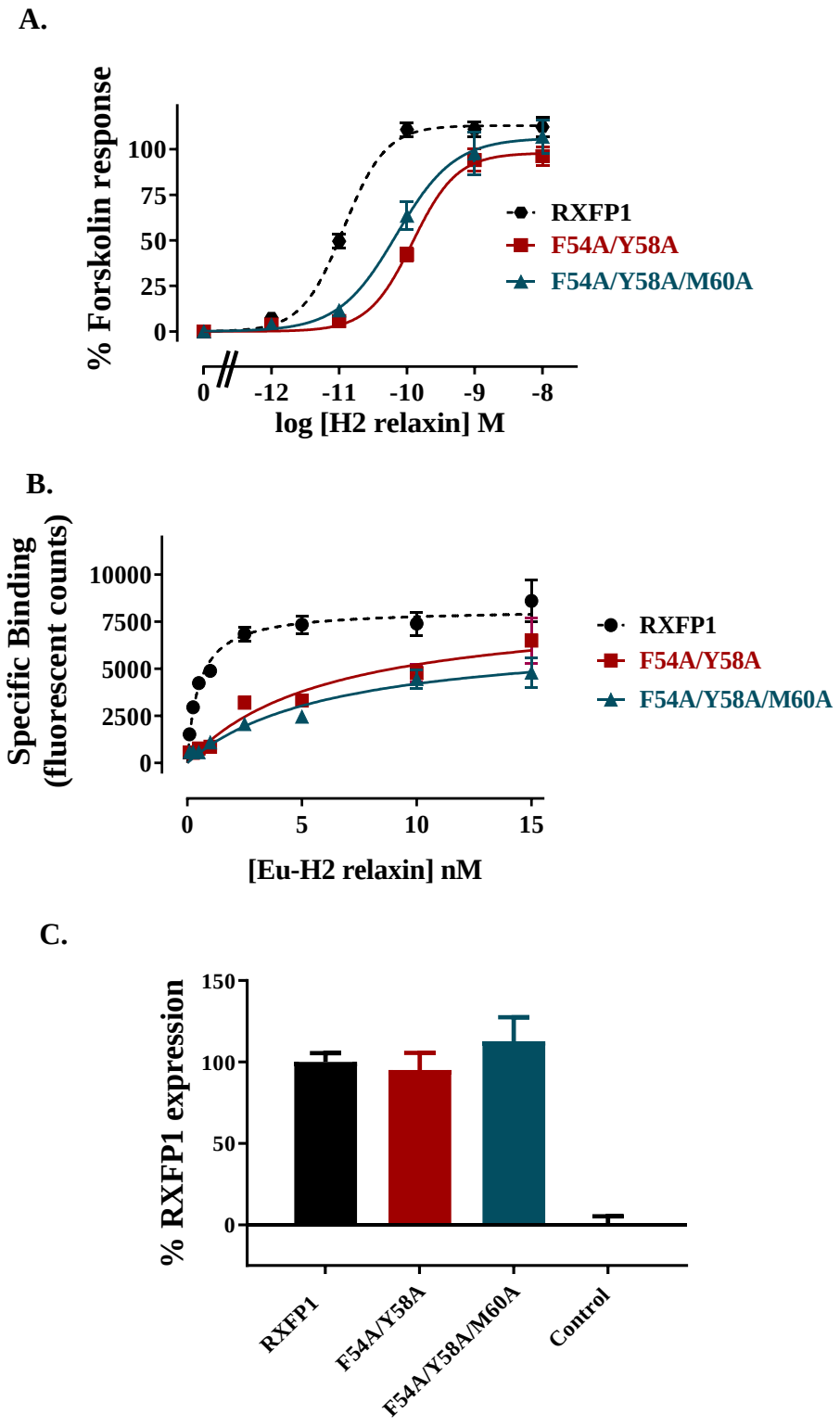

Figure 3.15. A. Activity, B. binding and C. cell surface expression data for F54A Y58A and F54A Y58A M60A as compared to wild-type RXFP1.

Data are shown as mean ± SEM of at least three independent experiments each performed in triplicate.

3.3.5 Insertion and deletion mutants

Given the dramatic loss of signal seen previously with the insertion of an alanine residue immediately preceding the linker we decided to probe whether the effect we were seeing was a result of the placement of the insertion or a more general response to a lengthening of the linker. We chose two other insertion points, one between residues Phe50 and Asp51, and the other between Glu67 and Ala68. We also shortened the linker by deleting residue Ala68. We observed that any change towards the C-terminal end of linker – Ins A67-68 and Del A68 had no significant effect on signalling or cell surface expression, while the insertion after Phe50 did have reduced activity against relaxin (pEC_{50} = 9.41 ± 0.13) as well as a large reduction in affinity (K_d = 16.7) (Figure 3.16; Table 3.2). It was interesting to note that the insertion after Cys40 had a smaller effect on K_d (3.92 ± 0.82), despite the signal from that mutant being abrogated entirely. All insertion and deletion mutants were expressed normally on the cell surface and those tested (Ins A40-41 and Ins A50-51) could signal normally in response to ML290 (graph not shown; Table 3.2)).

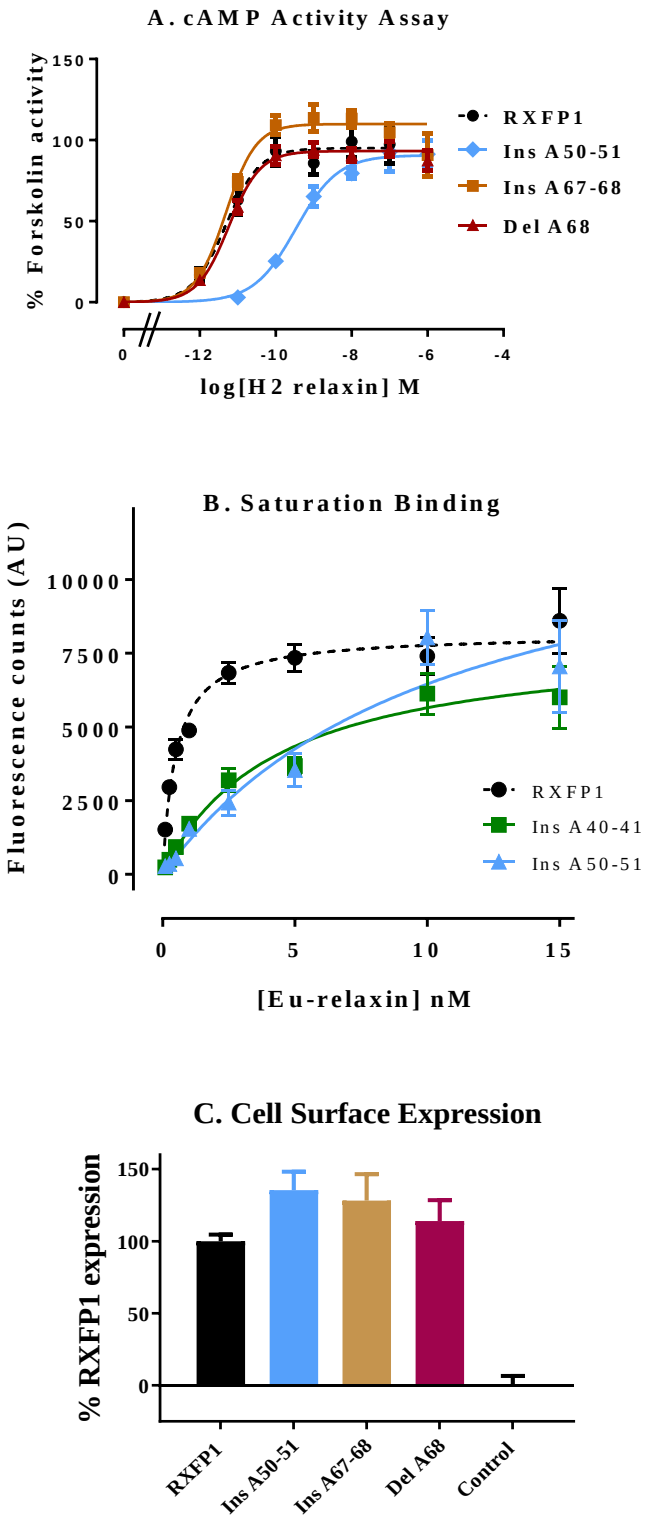

Figure 3.16. A. Activity, B. binding and C. cell surface expression data for insertion mutants Ins A50-51 and Ins A67-68 and deletion mutant Del A68 as compared to wild-type RXFP1.

Binding was tested for Ins A50-51 only and compared to wild-type and Ins A40-41. Data are shown as mean ± SEM of at least three independent experiments each performed in triplicate.

3.3.6 Numerical summary of data presented in this chapter

Table 3.2. Activity data for RXFP1 mutants compared to wild-type RXFP1.

Receptor construct	Cell surface Expession (% RXFP1)	Eu-relaxin binding		H2 relaxin activation		ML290 activation	
		K_d nM	B_{max} (AU)	E_{max} (% Forsk.)	pEC_{50}	E_{max} (% Forsk.)	pEC_{50}
Controls							
RXFP1	100 ± 4.58	0.64 ± 0.05 (7)	8496.75 ± 624.72	121.96 ± 7.84 (24)	11.25 ± 0.07	ND	
RXFP1 with DMSO	ND	ND		141.33 ± 16.52 (3)	11 ± 0.03 (3)	91.1 ± 6.3 (5)	6.82 ± 0.15 (5)
GDNNGW Double Mutants							
G41A/D42A	107.48 ± 13.69 (4)	ND		106.8 ± 46.67 (3)	7.26 ± 0.32 (3)***	ND	
• **Transient**							
• **Semi-stable**	45.65 ± 3.03 (4)****	>15 (3)	9007 ± 2440			81.9 ± 3.9 (3)	6.96 ± 0.04 (3)
N43A/N44A	108.97 ± 12.03 (4)	ND		118.90 ± 12.81 (3)	8.29 ± 0.63 (3)**	ND	
• **Transient**							
• **Semi-Stable**	53.50 ± 2.62 (4)****	3.3 ± 0.57 (5)***	11427 ± 1737.1			84.51 ± 7.6 (3)	6.69 ± 0.02 (3)
G45A/W46A	96.76 ± 13.37 (4)	ND		-	<5 (3)	ND	
• **Transient**							
• **Semi-Stable**	68.92 ± 3.84 (4)****	>15	12056 ± 5570			85.4 ± 16.5 (4)	7.29 ± 0.17 (4)*
Single Linker Mutants							
G41A	130.5 ± 8.05 (3)	0.95 ± 0.13 (4)	8925 ± 1725	104.7 ± 1.65 (3)	11.13 ± 0.1 (3)	ND	
D42A	106.27 ± 8.18 (3)	20.7 ± 3.5 (3)***	28338 ± 27202 **	-	<6	ND	
N43A	81.78 ± 8.45 (3)	2.6 ± 0.55 (3)***	7143.33 ± 764.56	120.23 ± 7.81 (4)	9.06 ± 0.48 (4) ***	ND	
N44A	83.7 ± 6.88 (3)	0.81 ± 0.17 (4)	6524.25 ± 587.67	92.16 ± 6.98 (4)	11.0 ± 0.1 (4)	ND	
G45A	118.64 ± 5.04 (3)	19.1 ± 3.1 (3)***	26505 ± 2304.5 **	135.94 ± 31.68 (4)	7.48 ± 0.57 (4) ****	ND	
W46A	112.30 ± 5.90 (3)	12.3 ± 1.4 (4)***	16020 ± 9989	109.6 ± 13.69 (3)	7.02 ± 0.18 (3) ****	ND	
F50A	101.09 ± 7.03 (4)	6.5 ± 0.76 (4)***	11469 ± 4305	91.9 ± 2.1 (4)*	9.45 ± 0.07 (4)***	65.6 ± 5.6 (6)	6.60 ± 0.15 (6)
D51A	89.77 ± 8.97 (4)	0.73 ± 0.11 (3)	9483 ± 2029.5	96.5 ± 4.0 (3)	11.01 ± 0.56 (3)	79.4 ± 3.8 (4)	6.67 ± 0.11 (4)
K52A	90.25 ± 15.21 (4)	ND		154.63 ± 33.73 (5)	11.06 ± 0.11	ND	
F54A	118.21 ± 12.8 (3)	2.43 ± 0.46***	5626.2 ± 1209	104.89 ± 10.48 (4)	10.23 ± 0.13 (4)***	89.68 ± 11.93 (4)	6.72 ± 0.03 (4)
A55L	126.58 ± 19.22 (4)	1.67 ± 0.25 (3)**	9024.25 ± 1534	123.59 ± 8.51 (5)	10.75 ± 0.17 (5) *	111.9 ± 16.4 (3)	6.71 ± 0.03 (3)

A55S	137.4 ± 18.75 (4)**	0.80 ± 0.09 (3)	10424.3 ± 1733	154.43 ± 39.77 (5)	11.39 ± 0.13 (5)	ND	
Y57A	138.6 ± 7.34 (5)**	0.81 ± 0.22 (4)	7823 ± 1393	126.7 ± 8.46 (5)	10.93 ± 0.10 (5)	85.5 ± 6.4 (3)	6.76 ± 0.04 (3)
Y58A	91.88 ± 8.46 (3)	1.56 ± 0.1 (4)***	9513 ± 1429	89.14 ± 7.93 (3)	10.88 ± 0.09 (3)	108.3 ± 10.4 (3)	6.78 ± 0.01 (3)
M60A	93.79 ± 16.66 (3)	1.08 ± 0.21 (5)	3886 ± 500.09	118.2 ± 6.51 (4)	11.2 ± 0.03 (4)	104.8 ± 11.05 (4)	6.73 ± 0.04 (4)
T61A	127.22 ± 8.88 (5)*	0.69 ± 0.08 (3)	5850 ± 196.22	142.58 ± 15.97 (4)	11.15 ± 0.17 (5)	ND	
F66A	81.6 ± 7.45 (3)	ND		88.29 ± 3.52 (3)	11.20 ± 0.08 (3)	ND	
E67A	91.14 ± 7.86 (3)	ND		141.74 ± 27.08 (5)	11.13 ± 0.13 (5)	ND	
Double/triple Linker Mutants							
F54A/Y58A	95.09 ± 10.55 (3)	6.51 ± 1.33 (5)***,#,^	9009.6 ± 931.88	99.94 ± 2.19 (5)	9.87 ± 0.08 (5)***,#,^^	72.26 ± 3.24 (4)*	6.60 ± 0.08 (4)
F54A/Y58A/M60A	112.81 ± 14.69 (3)	6.09 ± 1.75 (3) ***,#,^	7220.8 ± 1141.82	106.27 ± 7.2 (4)	10.08 ± 0.12 (4) ***,#,^^	90.32 ± 2.97 (3)	6.57 ± 0.09 (3)
Insertion/Deletion Mutants							
Ins A40-41	97.10 ± 7.68 (4)	3.92 ± 0.82 (3)***	7755.67 ± 510.36	No activity		94.1 ± 7.2 (3)	6.77 ± 0.03 (3)
Ins A50-51	135.36 ± 12.81 (4)**	16.7 ± 5.8 (4)***	18803.8 ± 5705 *	93.62 ± 5.34 (3)	9.41 ± 0.13 (3)***	82.8 ± 7.8 (3)	6.85 ± 0.10 (3)
Ins A67-68	128.19 ± 18.28 (3)	ND		110.15 ± 6.43(3)	11.32 ± 0.04 (3)	ND	
Del A68	113.97 ± 14.5 (4)	ND		93.78 ± 3.19 (3)	11.18 ± 0.02 (3)	ND	

ND, not determined.

K_d values from Eu-H2 relaxin saturation binding experiments; cell surface expression data from receptor expression ELISA experiments; pEC50 and maximum activity (E_{max}) values for both H2 relaxin andML290 stimulated cAMP activity assays. The number of replicates of each experiment for each individual construct are shown in parentheses with data reported as mean ± s.e.m. Significance is calculated using one-way analysis of variance (ANOVA) and uncorrected Fisher's least squares difference multiple comparison test.

*P<0.05; **P<0.01; ***P<0.001; ****P<0.0001 versus RXFP1. #P<0.05 versus F54A, ^P<0.05 versus Y58A, ^^P<0.001 versus Y58A.

3.4 Discussion

Typically, Class A GPCRs are activated upon the binding of a ligand into an orthosteric pocket within the TMD, at varying depth [297] and while it is thought that relaxin can interact with the 7TM α helices around EL2 [251], this interaction alone is not sufficient to induce activation. In the absence of a correctly folded LDLa module, activation cannot occur in response to relaxin binding [200], and thus we have concluded that the LDLa module is in fact the true RXFP1 ligand, and that it remains tethered to the rest of the receptor. The actual mechanism of activation by the tethered LDLa module is still unclear, but evidence presented in this chapter and the accompanying publication [2] would suggest that the linker plays an important role.

The extreme loss of signal experienced by the double mutants G41A/D42A (1000-fold over wild-type), N43A/N44A (100-fold over wild type) and G45A/W46A (virtually no signal) suggested that this region of RXFP1 is of utmost importance to the activation mechanism. Breaking the double mutants into single alanine mutants revealed that residues Asp42, Asn43, Gly45 and Trp46 were most profoundly implicated (Table 3.3). We initially assumed that this implied a relaxin-binding interaction was occurring around this space. However, the loss of affinity seen in binding experiments did not match the severity of the signalling loss. The binding affinity of double mutants G41A/D42A and G45A/W46A, as well as their matching single mutants D42A, G45A and W46A all saw around a 10- to 30-fold reduction, while N43A/N44A and N43A bound ligand around 5-fold less tightly than wild type (Table 3.2, Table 3.3). This told us that the region may in fact not be directly involved with binding. A comparison of the fold-difference from wild-type RXFP1 in relaxin potency vs affinity of select mutants is given in Table 3.3, highlighting the distinct phenotypes of certain residues in the initial portion of linker in which the reduction in potency is not matched by an equivalent loss in relaxin affinity.

Table 3.3. Comparison of fold-difference from wild-type RXFP1 of select mutants with respect to relaxin potency vs affinity.

Receptor Mutant	Relaxin Potency (EC50)	Fold difference from wild-type	Relaxin Affinity (K_d nM)	Fold difference from wild-type
RXFP1	5.62 pM	-	0.64	-
G41A/D42A	55 nM	~1000	>15	~25
N43A/N44A	0.55 nM	~100	3.3	5
G45A/W46A	>1 µM	>150,000	>15	~25
D42A	>1 µM	>150,000	20.7	32
N43A	0.871 nM	~150	2.6	4
G45A	33.11 nM	~5000	19.1	30
W46A	95.5 nM	>15,000	12.3	20
F50A	0.35 nM	63	6.5	10
F54A	0.06 nM	10	2.43	4
Y58A	0.013 nM	2	1.56	3
F54A/Y58A	0.13 nM	24	6.51	10

NMR experiments in which relaxin was titrated into ^{15}N-labeled $RXFP1_{(1-72)}$ also revealed that a relaxin binding site was more likely to be located further down the linker in the direction of the C-terminus, due to the location of the residues undergoing chemical shift change and line-broadening [2]. While single-point mutations from this central region of the linker did not show large differences from wild-type, there were small reductions in binding affinity from F54A and Y58A (Figure 3.13, Table 3.2), both large, hydrophobic amino acids separated by three residues. We considered these as good candidates for the formation of a binding surface on a helix and we therefore combined F54A and Y58A as a double mutant. This mutant displayed

an accumulative effect whereby the reduction in relaxin affinity and potency was greater for the double mutant than for either mutant individually. Interestingly, the loss in potency on these residues matched very well with the loss in affinity, being around 4-fold for the single mutant F54A and 10-fold for the double mutant (Table 3.3). Y58A experienced around a 3-fold loss in affinity, but a significant drop in potency was not detected with the activity assay, although it tended towards a right-ward shift (Figure 3.12), and the actual value was roughly half as potent as wild-type (Table 3.3).

Based on this information we were able to roughly divide the linker into two regions: an activation region, encompassing the GDNNGW sequence, and a binding region covering at least Phe54 and Tyr58. The residue on the border of these regions is Phe50, and this presented an interesting case, since it was three residues upstream of the F54A/Y58A potential binding site, and also within four residues of Trp46, which is involved in activation. Comparing the signalling and binding data, we see that the mutant experienced a 12-fold loss in binding, and a somewhat larger 32-fold loss in potency in the activity assay. This, along with comparison with the RXFP2 sequence in which Phe50 is present, but not the rest of Region 2 (see Chapter 4) led us to suppose that this residue is potentially involved in activation, and work on the RXFP2 linker lent support to this notion.

The results from the insertion and deletion mutants further highlighted the difference between the two regions within the linker that was starting to become apparent. An insertion of alanine between the LDLa module and linker (Ins A40-41), in the same region as the most important residues in activation (Asp42, Gly45, Trp46), suppressed the signal entirely, even though binding was only lost to a small degree (~8-fold over wild-type). A milder phenotype was induced by an insertion after Phe50 (Ins A50-51), matching the F50A mutant itself, and no loss of signal was seen from either insertion or deletion around residue 67 (Ins A67-68 and Del A68). Single-point mutants in this region also showed the same phenotype as wild-type (Figure 3.16, Table 3.2). Together, this implies that any difference seen as a result of inserting or deleting residues was more related to activity specific to that region than to a general effect of changing the length of the linker.

Supporting the notion of a helix existing in the central linker was from comparison of the chemical shifts of the $^{13}C\alpha$ and $^{13}C\beta$ resonances of the LDLa-linker to those from random coil which showed positive and negative ($\Delta C\alpha$ - $\Delta C\beta$) smoothed values for helical and β-strand structure respectively [298]. In our NMR experiments the linker region was largely

unstructured in its apo state but contained a handful of residues around Q49-K52 that showed the presence of a turn of α helix. Upon addition of relaxin the region of helical structure was extended to include residues up to at least Ser56 (Figure 3.17A). Additionally, ^{15}N heteronuclear NOE (hetNOE) experiments [299] were carried out, in which values approximately of 0.8 correspond to ordered structure being present. These values are expected to trend to zero or negative values with increasing disorder. The persistence of hetNOEs > 0.5 suggested that residual structure was indeed present in the region of linker encompassed by L48-M60 (Figure 3.17B).

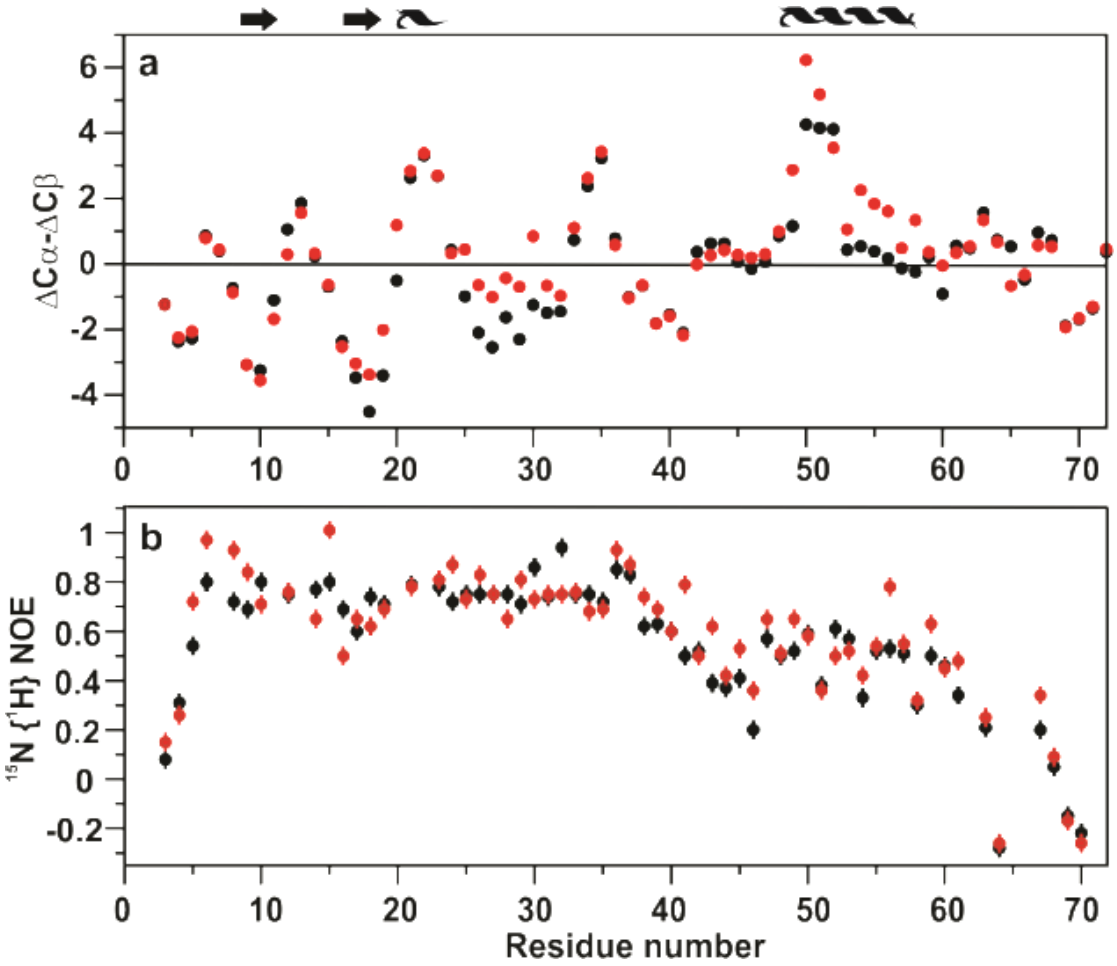

Figure 3.17. Plots of ^{13}Cαβ secondary chemical shifts and ^{15}N[^{1}H]-NOEs of RXFP1$_{(1-72)}$ in the absence (black) and presence (red) of three molar equivalents of H2 relaxin.

A) Deviations of the measured difference of ^{13}Cα and ^{13}Cβ chemical shifts from random coil (ΔCα - ΔCβ) where persistent positive or negative deviations indicate the presence of α-helix or β-strand respectively. Above this plot is schematically represented the known secondary structure of the LDLa module and included a region of α-helix that increases in the presence of H2 relaxin to spanning Leu48 to Lys59. B) Plot of ^{15}N[^{1}H]-NOEs that shows on addition of relaxin the ^{15}N[^{1}H]-NOEs increase for the region Gly41 to Lys59. Figure taken from [2].

The relaxin A-chain was implicated in the interaction, as evidenced from NMR experiments involving a paramagnetically-labelled relaxin [2]. In addition, competition experiments with various relaxin analogues showed that His12 and Val13 of the A-chain loop were involved, agreeing with earlier observations that replacing these and Gly14 with equivalent residues from insulin led to a significant loss in potency [300].

The presence of the relaxin binding site in the central portion of linker begged the question of how the LDLa module was actually activating the receptor. In order to identify an activation region, we turned to protein NMR once again. We used the recombinant protein that had been designed and characterized in our lab to display EL2 and part of EL1 of RXFP1 on a soluble scaffold based on the GB1 protein [251], referred to as ssRXFP1. We titrated $RXFP1_{(1-72)}$ with this construct and found that an interaction was occurring that involved the RXFP1 linker and EL2 of the soluble scaffold. The interaction was dependent on the correct formation of the disulphide bridge between the base of EL1 and EL2, typically seen in these GPCRs [301]. It was also severely reduced after mutation of EL2 residues Phe564 (ssRXFP1 residue Phe54) to alanine (Figure 3.18A – blue trace), which agreed with findings from mutation of the same residues in the whole receptor [251]. Similarly, mutations G41A/D42A, G45A/W46A and Ins A40-41, from the linker, all of which were highly detrimental to receptor signalling in whole receptors, starkly suppressed interactions between $RXFP1_{(1-72)}$ the soluble scaffold in NMR titrations (Figure 3.18A (red trace) and 3.18B), indicating that this initial portion of linker may be driving the binding event. The existence of a contact site between the linker and ELs may imply that the ectodomain, which is usually depicted in an open conformation, with the concave surface of the LRRs exposed to the extracellular medium, may exist at least in part in a closed conformation, with the high affinity binding site not as freely available to circulating relaxin as once thought.

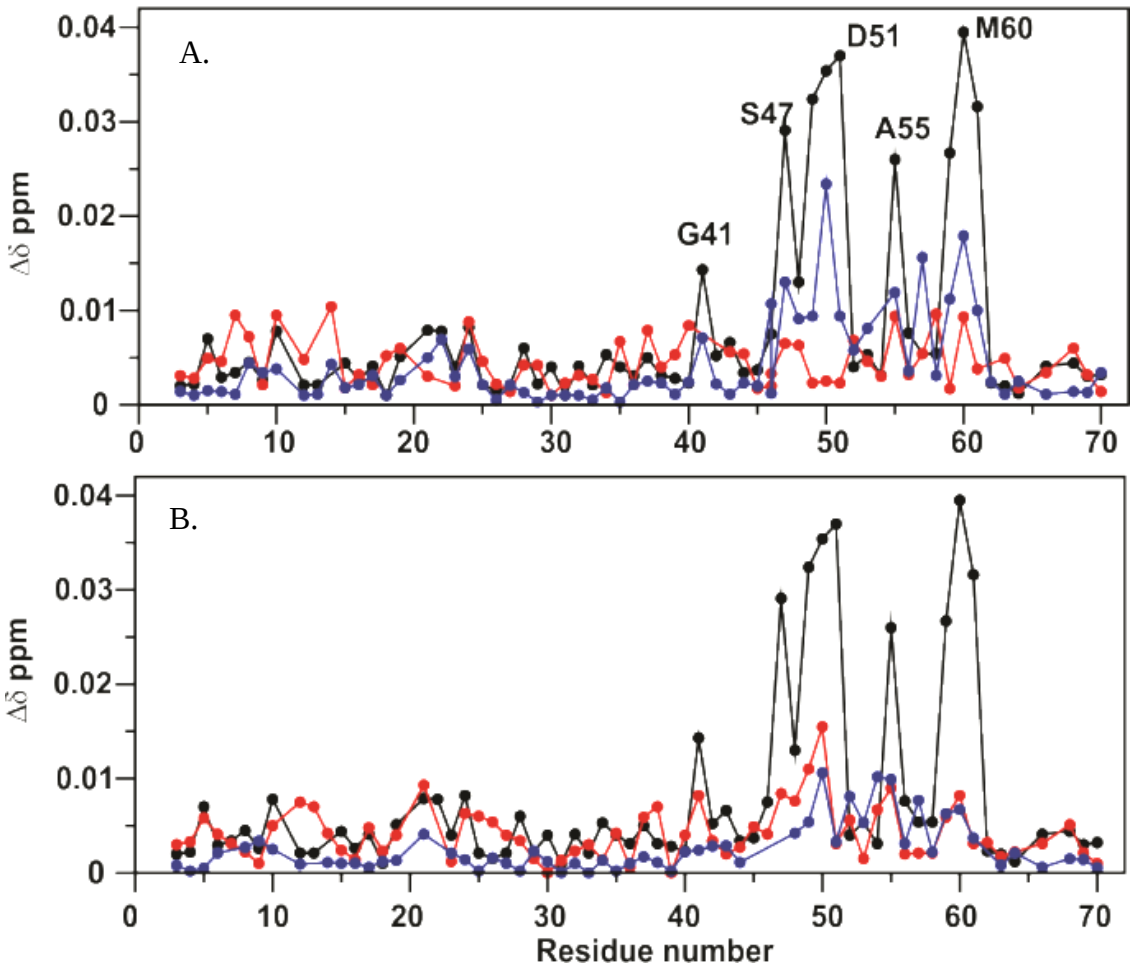

Figure 3.18. Chemical shift differences following a titration of ^{15}N-labelled RXFP1$_{(1-72)}$ with 20 molar equivalents of ssRXFP1

A. Chemical shift differences for wild Type RXFP$_{(1-72)}$ (black), ssRXFP1 F54A (blue), RXFP1$_{(1-72)}$ G41A/D42A (red). B. Wild type RXFP$_{(1-72)}$ (black), G45A/W46A (blue), C40Ains (red). Experiments were conducted at pH 6.8 and 25 ºC. Figure taken from [2].

Bringing the information together from mutagenesis and NMR we proposed a mechanism of activation in which the linker would be roughly divided into a relaxin binding domain (L48-M60) containing a transient α-helix that is stabilized in the presence of ligand, and an activation domain within the conserved GDNNGWxxxF (where x is any residue) motif that interacts with EL2 of the TM domain and brings about receptor activation (Figure 3.19). While the high-affinity binding site of relaxin to RXFP1 has previously been described within the LRR region, we hypothesize that this acts to capture the ligand from surrounding extracellular space. Relaxin would then come into contact with the linker via hydrophobic contacts including Phe54 and Tyr58, stabilizing the helix and bringing the activation domain into close proximity with the TM domain to allow LDLa-mediated RXFP1 activation.

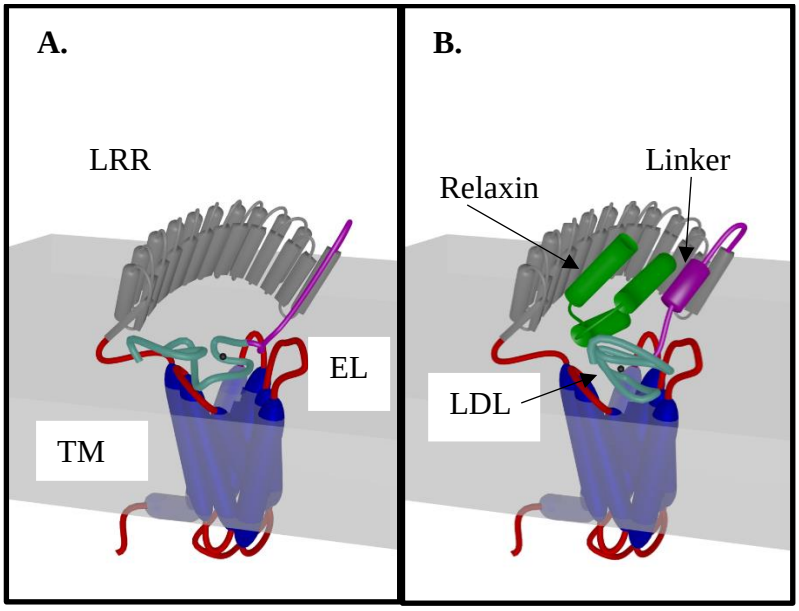

Figure 3.19. Proposed mechanism of RXFP1 activation.

(A) LDLa module (light blue) may be loosely bound to TM domain (dark blue/red loops) via contacts in linker. (B) Relaxin (green) binding at LRRs (grey) allows secondary binding at linker and the formation of a helix that helps position LDLa/linker to activate receptor TM domain. Figure adapted from [2].

An interesting side note is that the small molecule ML290 is able to bypass this entire system and activate RXFP1 via an interaction supposedly involving EL3 and TM helix 7 [166]. This implies that there may exist a binding pocket similar to those found in other Class A GPCRs, and even though the binding site of ML290 is distinct from that of the tethered LDLa-linker, and the two do not compete directly [142], there may be some overlap. This hypothesis is supported by the fact that it is a biased ligand [107], but it requires further exploration to be supported or disproven. The information is discussed in greater detail in chapter 5 and would most certainly help to further uncover details of the complex RXFP1 activation mechanism.

Chapter 4 Investigations into the INSL3 receptor: RXFP2

4.1 Introduction

In this chapter we turn our attention back to RXFP1's closest relative, the native receptor for the insulin-like peptide 3 (INSL3), RXFP2. As mentioned in the introduction to this thesis RXFP1 and RXFP2 are approximately 60% identical at an amino acid level, and contain an identical overall domain structure, with a large ectodomain taking up around half their size (Figure 1.1B). While they belong to the Leucine-rich repeat containing family of GPCRs (LGR), they are alone in their possession of an N-terminal LDLa module, which is imperative to their capacity to signal in response to their peptide ligands [200]. RXFP2 can be activated by both INSL3 and relaxin, although its affinity for its cognate ligand is around 10-fold higher than for relaxin. The physiological significance of the interaction of H2 relaxin with RXFP2 is unknown, and notably rodent relaxin peptides do not activate their RXFP2 equivalents [131, 132]. The small molecule ML290 does not activate RXFP2 [291], possibly due to differences in EL3 and TM7 compared with RXFP1 [166].

Given our findings with respect to the linker that joins the RXFP1 LDLa module with the LRRs we decided to perform a comparative study looking at the equivalent region of RXFP2. The structure of the RXFP2 LDLa module has been solved [197] (PDB 2M96; Figure 1.5B), and a sequence analysis reveals that the linker contains four of the initial six residues of linker, in a similarly conserved sequence, that we therefore refer to as the GDxxGW motif, where x is any residue (Figure 4.1A). This stretch of amino acids was defined in the previous chapter as linker region 1. Region 2, the proposed relaxin-binding sequence is not present in the RXFP2 linker however, and as such it is 7 residues shorter than its RXFP1 counterpart. It also has low sequence identity with human RXFP1 although it is relatively well conserved between mammalian species (Figure 4.1A).

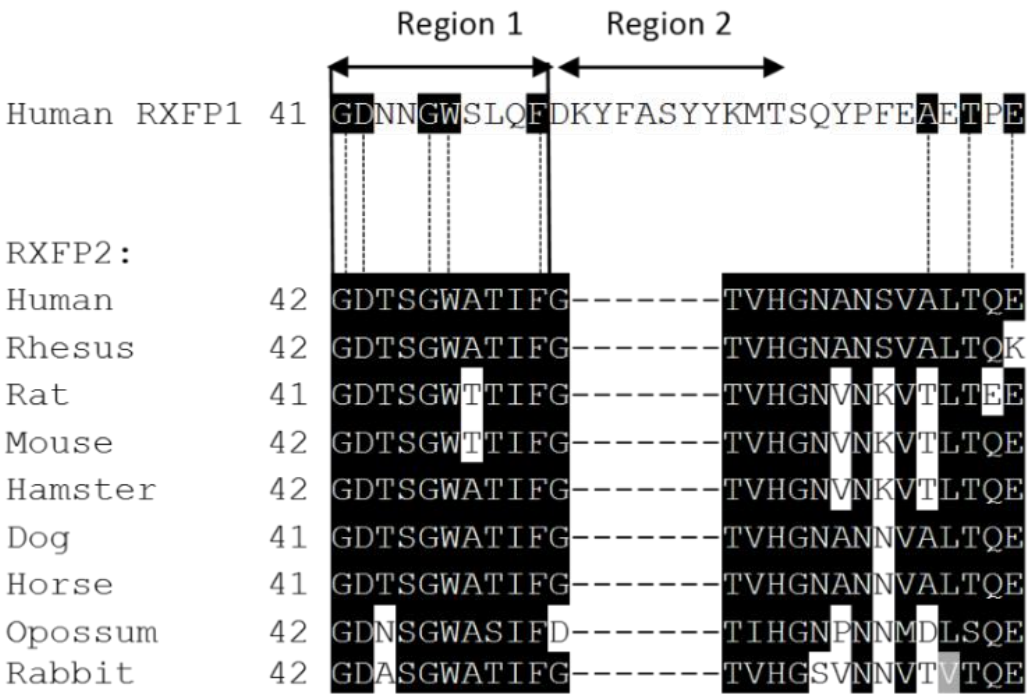

Figure 4.1. Sequence alignment of mammalian RXFP2 linker with RXFP1 human equivalent.

Two regions are defined, as marked by arrows above. Region 1 includes the GDxxGW motif as well as F50, and region 2 is thought to bind relaxin in RXFP1.

We decided to follow a similar rationale to that employed for our exploration of RXFP1 linker and we mutated the first six residues of the RXFP2 linker to alanine, as well as Phe51, equivalent to RXFP1's Phe50, which had proved instrumental in both binding and activation. These mutants were then submitted to binding and activity assays using both INSL3 and relaxin, in order to compare and contrast the behaviour of the receptor in response to either ligand. We then recapitulated our earlier study, designing and characterizing an LDLa/linker recombinant protein for RXFP2 ($RXFP2_{(1-65)}$) which was expressed with a cleavable N-terminal solubility tag (GB1). We also made a second version with a C-terminal GB1 moiety which was still attached during NMR experiments to help with solubility, but also as a mimic of the stabilizing effect of the LRRs in the whole receptor (Figure 4.2). This construct had also been made for the $RXFP1_{(1-72)}$ protein and was proving a superior tool, since it was easier to purify thanks to the addition of an N-terminal poly-HIS tag that could be used in affinity purification with a nickel or cobalt column, and the GB1 tag anchored the linker in solution without participating in any interactions measured. The characterized protein was used in titrations with relaxin to probe for an interaction.

Figure 4.2. Design of $RXFP2_{(1-65)}$ shown in N- to C-orientation.

Both ends of the RXFP2 LDLa and linker sequence (purple) have a GB1 tag (blue), and the N-terminus also has a His_6 tag (red), which together with the N-terminal GB1 is separated from RXFP2 sequence by a thrombin cleavage site (blue line).

We also wanted to discover if the RXFP2 LDLa-linker was able to interact with the receptor exoloops, and we therefore cloned these onto a GB1 soluble scaffold, following a similar rationale as that used to explore RXFP1 Exoloop:LDLa interactions [251] (Figure 4.3). The protein was purified and characterized and used in titration experiments with RXFP2$_{(1\text{-}65)}$-GB1. While two versions of the soluble scaffold protein were made (Figure 4.3B, C), final titrations were performed using RXFP1 and RXFP2 versions containing EL2 and partial EL1, and these were named ssRXFP1 and ssRXFP2 (Figure 4.3B).

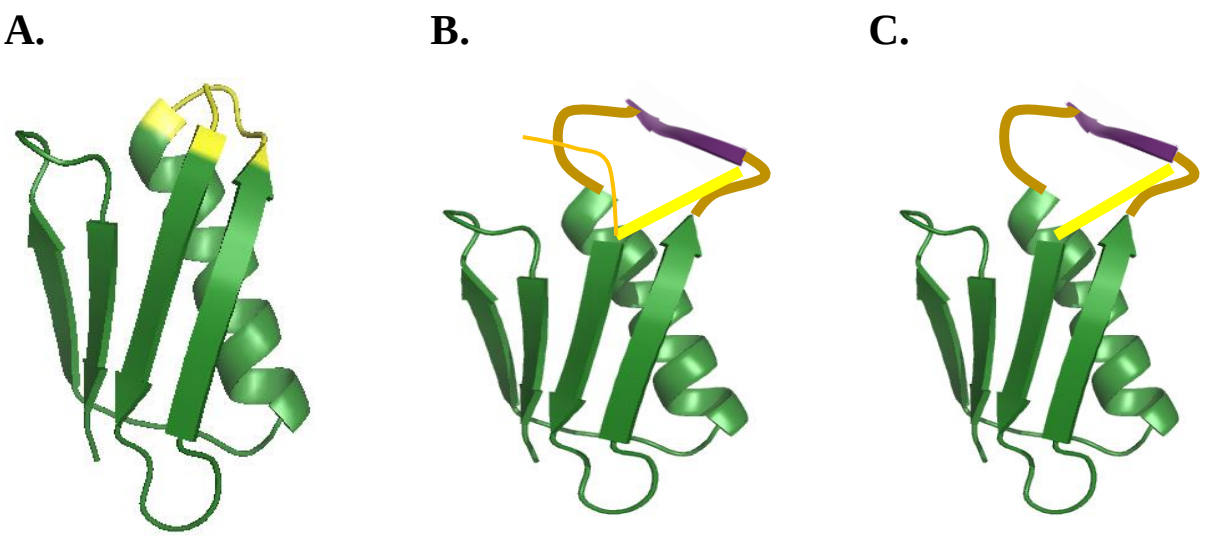

Figure 4.3. Design of ssRXFP1 and ssRXFP2

Thermostabilized GB1 (A) had C-terminus and loop sections (shown in yellow) replaced with sequence from RXFP1 or RXFP2 EL2 (brown/purple) (B,C) and EL1 (orange) (B) such that the disulphide bridge between the end of EL1 and EL2 would be maintained (yellow stripe). Only the construct with full EL2 and partial EL1 (B) was used in titration experiments.

The evidence so far (published in 2017 [3]) pointed to a different mode of activation being employed by RXFP2 in response to INSL3 as opposed to H2 relaxin, and we imagined that the response to H2 relaxin was occurring in an RXFP1-like manner. Making use of a bioluminescence resonance energy transfer (BRET) assay (Figure 4.4) we set out to dissect the kinetics of RXFP2-relaxin interactions. BRET partners Nanoluc™ (Nluc) and TAMRA were attached to the receptor N-terminus and relaxin respectively and the assay was validated using a Nanoluc-labelled RXFP2 as well as a similarly labelled splice variant (RXFP2-short [200]) and ectodomain only construct (RXFP2-ECD) [135], both previously characterized for relaxin binding. We then set about exploring the effect of inserting the supposed relaxin-binding site into the RXFP2 linker, creating two chimeric, extended linker receptors (named ExLink1 and ExLink2), which were tested for activity, binding and kinetic behaviour.

4.2 Materials and Methods

4.2.1 Receptor Expression on HEK293T cells and cell culture

Receptors were transiently transfected onto HEK293T cells using LipofectAmine® 2000 as described in section 3.2.2 and cells were cultured and plated out identically for all previously described assays. While total DNA per well was the same throughout all transfections, high levels of basal activity of RXFP2 in cAMP activity assays meant that lower quantities of receptor were used, the remainder being made up with empty vector pcDNA3.1. After some experimentation (see section 4.3.1) final proportions used for β-gal assays were 1:2:5 receptor:β-gal:pcDNA3.1, and thus cells for binding and cell surface assays (unless otherwise indicated) were transfected at 1:7 receptor:pcDNA3.1 for consistency. Transfection for NanoBRET experiments was achieved using polyethylenimine (PEI; Sigma Aldrich) at a ratio of 4.5 µl per µg of DNA in 300 µl Opti-MEM per well of a six-well plate. Cells were plated out at 400,000 cells per well and transfected with 0.5 µg DNA per well the following day. On the third day they were lifted and resuspended in 5 ml of complete DMEM before being plated out in 96-well white plates (Perkin Elmer) and allowed 18-24 hours' growth before assays were carried out.

4.2.2 Mutagenesis of RXFP2 and RXFP2$_{(1-65)}$

Mutants were constructed as per the protocol in section 3.2.3, with the exception of G42A, G46A and F51A. The two glycine mutants were both produced with single strands amplified in two separate PCR tubes, and then annealed together in a further reaction (1 minute at 95 °C followed by gradual cooling to anneal). F51A and ExLink constructs were produced according to the protocol outlined in [293] as described for insertion/deletion mutants in Chapter 3 of this thesis (section 3.2.3). Mutagenic primers are found in Table 4.1. Single-point linker mutants were produced by Nicholas Smith during his honours project under my training.

4.2.3 cAMP activity assays and Eu-relaxin/Eu-INSL3 saturation binding assays

Binding and activity assays were carried out as described in sections 3.2.6 and 3.2.7 respectively, using either recombinant relaxin, INSL3, Eu-relaxin or Eu-INSL3 as indicated. Honours student Nick Smith carried out activity and binding assays on the RXFP2 linker mutants under my supervision, while I analysed the data, determined statistical significance and prepared the figures for publication.

4.2.4 Cell Surface Expression Assay

Cell surface expression was either assessed using the B_{max} values from Eu-INSL3 saturation binding assays or using the same ELISA protocol outlined in section 3.2.5 of the previous chapter. Given the propensity of RXFP2 to show some level of constitutive activity in β-gal assays I set about establishing how much receptor would be expressed on cell surfaces as compared to total expression. I transfected HEK293T cells in 96-well plates using varying amounts of receptor DNA, making up the remainder to a total of 0.25 μg per well with pcDNA3.1 empty vector. Total expression was measured as for cell surface expression except that cells were lysed during the fixing step with the addition of 0.1% Triton-X 100 to buffer to expose intracellular receptor to the antibodies in subsequent steps. Data points were then plotted in GraphPad Prism and fit to a one-site saturation curve and normalized to the highest total expression levels measured.

4.2.5 Design, expression and purification of RXFP2$_{(1-65)}$ and RXFP2$_{(1-65)}$-GB1(P4F)

Within this project I attempted to express and purify both RXFP2$_{(1-65)}$, the first 65 residues of RXFP2 as a recombinant protein, and the LDLa plus linker of RXFP2 as designed according to the layout shown in Figure 4.2. For RXFP2$_{(1-65)}$ the solubility tag GB1 was attached at the N-terminus while for RXFP2$_{(1-65)}$-GB1 it was at both termini and a His tag consisting of 6 histidine residues (His$_6$) was also on the N-terminal, and this could be cleaved along with the N-terminal GB1 by overnight incubation with 5 units per mg of protein of thrombin (Sigma-Aldrich). While the vector containing RXFP2$_{(1-65)}$ was already available in the lab, the DNA for RXFP2$_{(1-65)}$-GB1 was purchased from Genscript (Nanjing, China) as an insert in pET15b expression vector using NcoI and NdeI restriction sites, and the insert sequence verified by sequencing upon reception.

Expression and purification proceeded as described in [3]. The constructs were expressed in BL21 (DE3)*trxB* cells (Novagen) that are commonly used when the target protein contains multiple disulphide bonds. An autoinduction protocol [302] was used for expression of the protein in shaker flasks. The method works by providing cells with enough glucose to nourish them until they begin exponential growth, at which time they are forced to switch to lactose, which will lead to induction of target protein expression since it is under control of the *lac* operon. The media used is named N-5052, and contains: 50 mM K_2HPO_4, 50 mM KH_2PO_4, 50 mM NH_4Cl (^{15}N labelled for HSQC experiments), 5 mM Na_2SO_4, 2 mM $MgSO_4$, 0.5% w/v glycerol, 0.05% w/v glucose, 0.2% w/v lactose and 0.2x trace metals. The flasks were inoculated with 1 ml of overnight culture of the cells in LB and grown in a shaking incubator at 37 °C for around 6 hours. They were then transferred to a shaking incubator at 16 °C and grown for at least one night or until growth stopped, as monitored by checking OD_{600} at regular intervals. At this point media was centrifuged at 5,000 × g for 20 minutes to harvest cells, which were then resuspended in TBS (20 mM Tris, pH 7.4, 150 mM NaCl, 5 mM imidazole) and stored at -20 °C until purification. ^{15}N,^{13}C-labelled RXFP2$_{(1-65)}$ was also produced by Ashish Sethi using the method outlined in [303].

The protein was purified after cells were lysed using an Avestin EmulsiFlex C3 cell crusher and soluble fraction separated by centrifuging down debris at 13,000 × g at 4 °C for 40 minutes. The supernatant was passed through a 0.45 µm filter and loaded onto 10 ml of pre-equilibrated IgG Sepharose resin (GE Healthcare) for RXFP2$_{(1-65)}$ or Talon Superflow resin (Takara Clontech) for RXFP2$_{(1-65)}$-GB1. Binding was allowed to occur at 4 °C for 1-2 hours on a rocking platform, and then the column washed by gravity flow with at least 10 column volumes

of NH_4Ac or TBS buffer. The bound protein was eluted 50 mM acetic acid ($RXFP2_{(1-65)}$) or with increasing concentrations of imidazole in TBS ($RXFP2_{(1-65)}$-GB1) and monitored by mixing with Bradford reagent and observing blue colour in the presence of protein. The elution was placed into a large volume (final concentration of protein 0.1-0.3 mg/ml) of mixed redox reaction containing reduced and oxidised glutathione (3 mM GSH, 0.3 mM GSSG, 50 mM Tris-HCl (pH8.5), 150 mM NaCl, 10 mM $CaCl_2$) overnight at 4 °C with stirring to encourage the correct formation of the three disulphide bonds and binding of Ca^{2+} ion necessary for correct folding of the LDLa module. This was preceded by a buffer exchange into TBS in the case of $RXFP2_{(1-65)}$. The following day the mix was concentrated to a final volume less than 10 ml using a 3 kDa MWCO Amicon® centrifugal concentrator (Millipore), and protein concentration measured using a spectrophotometer (at 280 nm) with flowthrough as blank. We then placed the liquid in a 15 ml tube and added 5 units of thrombin (Sigma-Aldrich) per mg of protein and left to cleave overnight at room temperature on a rocking platform. Different fractions from the purification were visualized by sodium dodecyl sulphate poly-acrylamide gel electrophoresis (SDS-PAGE) and final unfolded, folded and cleaved samples were analysed by mass spectrometry to verify correct molecular weight at each stage. The final stage of the purification was to separate the His-GB1 from the $RXFP2_{(1-65)}$-GB1 by first passing the mixture over the Talon resin a second time and collecting the flowthrough, which would contain the $RXFP2_{(1-65)}$-GB1 protein. The flowthrough was then purified by reversed-phase high performance liquid chromatography (RP-HPLC) (buffer A 0.1% trifluoro-acetic acid, buffer B acetonitrile with 0.1% trifluoro-acetic acid) with an Agilent Zorbax 300SB-C18 column, and the collected fractions assessed for purity and correct molecular weight by mass spectrometry. Fractions containing the protein of interest were collected in a Falcon ® tube and lyophilised overnight. Freeze-dried samples were kept at -20 °C and resuspended in 50 mM Imidazole, 10 mM $CaCl_2$, pH 6.8 for NMR analysis.

4.2.6 Design, expression and purification of ssRXFP1 and ssRXFP2

The GB1 protein was successfully used as a soluble scaffold to display the extracellular loops (EL) of RXFP1 and subsequently interrogate the interactions between the loops and relaxin as well as the LDLa module and linker [2, 251]. We therefore designed an RXFP2 version that would display EL2 and part of EL1 at equivalent positions on the scaffold protein (Figure 4.3). The resulting cDNA was cloned between NcoI and BamHI sites into the pET28a vector (Novagen Inc.) with an N-terminal His_6 tag, separable by a thrombin cleavage site (Genscript,

Nanjing, China). Upon arrival, DNA was sequenced before being amplified by miniprep (Wizard® SV kit, Promega), and expressed in BL21(DE3) cells. Cells were grown in LB medium in 2-L shaker flasks at 37 °C until reaching an OD_{600} of approximately 0.6. At this point isopropyl-D-1-thiogalactopyranoside (IPTG) was added to 1 mM, and the flasks were moved to 16 °C shaking incubators for around 16 hours. They were then harvested by centrifugation at 5000 × g for 20 minutes at room temperature and resuspended in TBS (20 mM Tris-HCl (pH 7.4), 150 mM NaCl, 5 mM Imidazole) and stored at -20 °C until purification.

Purification proceeded as described for $RXFP2_{(1-65)}$-GB1 using TALON Superflow resin and eluting with increasing concentrations of imidazole in TBS (pH 7.4). Elution was concentrated in a 3 kDa MWCO Amicon® centrifugal concentrator (Millipore) to less than 10 ml, and then placed in a 15 ml tube with 5 units of thrombin per mg of protein to cleave the His tag overnight at room temperature with rocking. The cleaved protein was then further purified by size exclusion chromatography (SEC) on a HiLoad 16/60 Superdex 75 prep grade column (GE Healthcare) in 20 mM Tris-HCl (pH 7.4), 150 mM NaCl. The purification was monitored by SDS-PAGE and final cleaved and uncleaved protein assessed and checked for purity and correct molecular weight using mass spectrometry, as well as correct fold by circular dichroism (CD).

4.2.7 Mass Spectrometry

Molecular weight was monitored on all protein products following purification. Where HPLC had been used 10 µl samples were taken directly from peak fractions and 2 µl were autoinjected into the Agilent 6220 electrospray ionization time-of-flight (ESI-TOF) mass spectrometer coupled to an Agilent 1100 LC system. If samples were in salt-containing buffer, a 10-minute separation on a short reverse-phase C18 column was used to ensure ionisation and injection of only protein into the machinery. Agilent MassHunter software was used for acquisition and analysis.

4.2.8 Circular Dichroism (CD)

Since ssRXFP2 had not previously been characterized we also submitted samples to CD analysis in order to compare predicted structure to the ssRXFP1 version as well as wild type GB1 (reported in [251]). Samples in 20 mM Tris-HCl (pH 7.4, 100 mM NaCl were diluted to

0.15 mg/ml and placed in a cell with 1 mm path length for wavelength scans from 260-190 nm at 1 nm intervals using an AVIV Model 410 SF spectropolarimeter (Biomed). Buffer only readings were subtracted as background and data were expressed as mean residue elipticity (MRE, [ϴ]) using the following equation:

Equation 1: $[\Theta] = (\Theta_{obs})/(l.c.n/M)$

where Θ_{obs} = observed elipticity (mdeg), l = path length (cm), n = number of amino acid residues, M = molecular weight and c = concentration. The online Dichroweb server was used for data analysis using the Selcon3 method and reference dataset 7 [304].

4.2.9 Nuclear Magnetic Resonance (NMR) spectroscopy

All NMR experiments were carried out by Ashish Sethi following the methods described in [2] and [3].

4.2.10 Cloning of Nluc-RXFP2, Nluc-RXFP2 short and Nluc-8BP

The RXFP2 cDNA from LDLa module to the end of the TM domain was amplified using Phusion™ polymerase (NEB Thermofisher) with primers that had restriction sites for BamHI (5') or XhoI (3') included as extensions (Table 4.1). The same strategy was employed to amplify the RXFP2 ectodomain attached to a single transmembrane helix from the CD8 protein (named RXFP2-ECD) and the splice variant of RXFP2 lacking the LDLa module [200] (named RXFP2-short). PCR reaction tubes were prepared in triplicate and contained 10 µl of 5x buffer, 1 µl of each primer at 25 µM concentration, 100 ng of template, 1 µl of dNTPs, 1.5 µl of DMSO, 1 µl of polymerase and dH_2O to a total of 50 µl. The amplification protocol was as follows: 30 sec at 98 °C, 30 rounds of 98 °C (5 sec), 66 °C (10 sec), 72 °C (30 sec), then 5 mins at 72 °C and a 4 °C hold. The DNA was cleaned using a gel purification kit (Bioline) and then digested with BamHI and XhoI and cleaned again to remove enzymes. Success was gauged by agarose gel electrophoresis. The resulting DNA was cloned into a pcDNA3.1 Zeo(+) vector containing a bovine prolactin signal sequence, FLAG tag, Nanoluc™ sequence and *sacB* gene, all following the multiple cloning site. Following cleavage with BamHI and XhoI at sites either

side of the *sacB* sequence, the amplified insert sequence was placed in a ligation reaction containing a 1:3 vector to insert ratio and 1 µl of T4 DNA ligase (Promega) at 4 °C overnight. The ligation mixtures were then frozen, and then used to transform competent DH5α cells and plated out on LB plates containing Ampicillin (1 µl per ml of agar gel) and 10% sucrose. The presence of sucrose meant that any vector that had re-ligated the *sacB* gene would not be able to grow on the plate, and the vectors with correct insertions would grow with near to 100% efficiency. Colonies were picked, and DNA isolated and entire insert sequences verified by sequencing.

4.2.11 NanoBRET saturation binding assay

After transfection and plating as described above, Nanoluc-tagged receptors were first tested for their ability to bind relaxin that had been labelled with the fluorophore TAMRA (TamRLX). Nanoluc and TAMRA are bioluminescence resonance energy transfer (BRET) partners (Figure 4.4) and donor and acceptor emission could be measured at 410-490 nm (donor) and >610 nm long pass (acceptor) respectively on the POLARstar Omega plate reader (BMG Labtech). Transfected HEK293T cells were washed with 100 µl per well of PBS (pH 7.4) and then incubated for 90 minutes at room temperature in low light with increasing concentrations of TamRLX suspended in relaxin receptor binding buffer (20 mM HEPES (pH 7.5), 50 mM NaCl, 1.5 mM $CaCl_2$) supplemented with 1% BSA. An excess of unlabelled relaxin was added to a subset of wells to establish non-specific binding levels. After the incubation, 10 µl of NanoGlo luciferase substrate at a 1 in 50 dilution in assay buffer was added to each well, and readings were taken at 1-minute intervals until an equilibrium was reached. BRET ratio was defined as acceptor emission over donor emission, and averages of duplicate measurements were plotted to a saturation binding equation using GraphPad Prism 7.

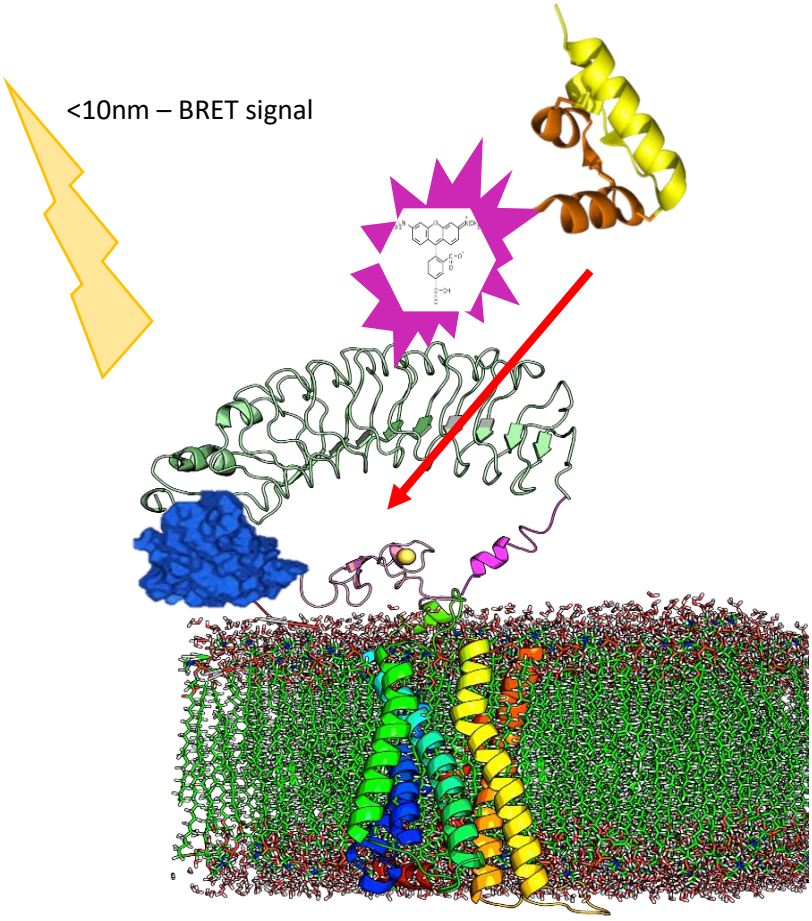

Figure 4.4. Basis of NanoBRET to probe RXFP2 ligand binding.

Receptor is tagged N-terminally with Nanoluc (blue), while relaxin A-chain is tagged with TAMRA moiety (mauve). Upon binding, transfer of luminescence occurs if a distance less than 10 nm exists between acceptor and donor. Models by Ashish Sethi.

4.2.12 NanoBRET dissociation assay

Cells were again transfected as described above and plated into white, 96-well plates. They were washed with PBS (100 µl per well) and then 100 µl of 13 µM TamRLX (and 1 in 500 dilution of NanoGlo substrate) was added and measurements taken every 30 seconds. Wells containing buffer and substrate only were included as base line. After 15 minutes of readings, unlabelled relaxin was added to a final concentration of 2 µM and dissociation monitored by continued readings for another 30 minutes. Wells with only TamRLX were used as 100%, and dissociation data were normalized to these. Dissociation curves were generated in GraphPad Prism and fit to either one- or two-site exponential decay functions as judged by observation of the associated residual plots of each one.

Table 4.1. Primers used in mutagenesis and cloning in this study.

Mutant	**Sense primer (5'-3')**
	Antisense primer (5'-3')
RXFP2-P4F	CACTTTTTCATGCCAAAAAGGATATTTTCCCTGTGGG
	CATGAAAAAGTGATCATGCTACCTTGGTCGACATC
RXFP2$_{(1-65)}$-P4F	GATCACCTTCAGCTGCCAAAAGGG
	GGCAGCTGAAGGTGATCATGCTAC
G42A	CTGTGCTGACACTAGTGGATGGGCGACCATATTTG
	GTGTCAGCACAGTTCTCTTCGTCCGCCCCG
D43A	GTGGTGCCACTAGTGGATGGGCGACCATATTTGGC
	CTAGTGGCACCACAGTTCTCTTCGTCCGCCC
T44A	GTGACGCTAGTGGATGGGCGACCATATTTGGCAC
	CACTAGCGTCACCACAGTTCTCTTCGTCCGC
S45A	CACTGCTGGATGGGCGACCATATTTGGCACAG
	CATCCAGCAGTGTCACCACAGTTCTCTTCGTCCG
G46A	CTAGTGCATGGGCGACCATATTTGGCACAGTGC
	CCCATGCACTAGTGTCACCACAGTTCTCTTCGTC
W47A	GTGGAGCGGCGACCATATTTGGCACAGTGCATGG
	GTCGCCGCTCCACTAGTGTCACCACAGTTCTCTTC
F51A	CCATAGCTGGCACAGTGCATGGAAATGCTAACAGC
	GTGCCAGCTATGGTCGCCCATCCACTAGTGTC
F574A	GTATGTGCCCCACTTTATTATGACCAAACAGAAGATATTGG
	GTGGGGCACATACTCCATTTTTCCCATAAAAGTTTCCAAAATAATC
P575A	GTTTCGCACTTTATTATGACCAAACAGAAGATATTGGAAGC
	CATAATAAAGTGCGAAACATACTCCATTTTTCCCATAAAAGTTTCC
ExLink1	GCGACCATATTTGGCAAATATTTTGCCACAGTGCATGGAAATGCTAACAGCGTGG
	TTTGCCAAATATGGTCGCCCATCCACTAGTGTCACCAC
ExLink2	GGCAAATATTTTGCCAGTTACTACACAGTGCATGGAAATGCTAACAG
	ACTGGCAAAATATTTGCCAAATATGGTCGCCCATCCAC
RXFP2$_{(1-65)}$-ExLink1	GCGACCATTTTCGGCAAATATTTTGCCACCGTGCACGGCAACGCG
	TTTGCCGAAAATGGTCGCCCAGCCGCTGGTATCACCG
RXFP2$_{(1-65)}$-ExLink2	GGCAAATATTTTGCCAGTTACTACACCGTGCACGGCAACGC
	ACTGGCAAAATATTTGCCGAAAATGGTCGCCCAGCCG
Clone	**Sense primer (BamHI forward) 5'-3'**
	Antisense primer (XhoI reverse) 5'-3'
RXFP2	CATCATCATGGATCCCAAGGTAGCATGATCACTCCTTC
	CATCATCATCTCGAGCTAGGAAACTGGTTTCATTATACTGTC
8BP	CATCATCATGGATCCCAAGGTAGCATGATCACTCCTTC
	GACGACCTCGAGTTAGACGTATCTGCCGAAAGG
RXFP2-short	CATCATGGATCCGACACTAGTGGATGGGCGAC
	CATCATCATCTCGAGCTAGGAAACTGGTTTCATTATACTGTC

Template for mutants was pcDNA3.1 containing FLAG- RXFP2.

4.3 Results

4.3.1 Cell Surface Expression of RXFP2

In the past, transfections of receptor into HEK293T cells in a 96-well plate format has used 0.25 µg of DNA per well, in accordance with the manufacturer's protocol provided with the transfection agent lipofectAMINE 2000^{TM}. However, at this expression level RXFP2 demonstrates high constitutive cAMP activity in the CRE reporter gene assay. I therefore set about exploring the expression levels induced by different quantities of DNA using the ELISA protocol described in the previous chapter (section 3.2.5). The results showed that beyond 25 ng of DNA per well, the amount of receptor expressed on the cell surface remained unchanged, at a maximum level around 23% of the maximum total receptor expression (Figure 4.5). Hence, for future assays only 1/8 total DNA was receptor, which should yield a maximum possible surface expression, with less than half the possible total expression.

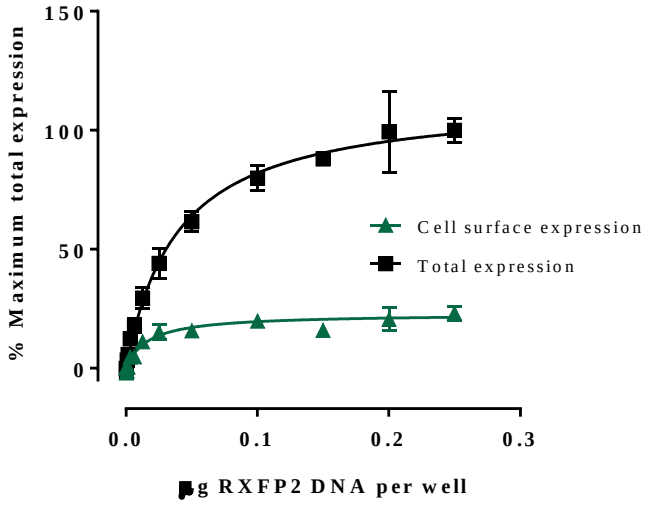

Figure 4.5 Total and cell surface expression of RXFP2 transfected at varying amounts into HEK293T cells in 96-well plates.

Points are mean ± SEM from three independent experiments each performed in triplicate.

4.3.2 INSL3 signalling and binding at RXFP2 linker mutants

We initially tested the ability of the linker mutants to bind INSL3 using an Eu-INSL3 whole-cell saturation binding assay. Wild-type RXFP2 bound Eu-INSL3 with an affinity around 1 nM, agreeing well with data previously published for this ligand [305] (Figure 4.6A, Table 4.2). The seven linker-mutant receptors also bound Eu-INSL3 like wild-type, and B_{max} values for all mutants were not different from the wild-type, showing that they were all correctly folded and expressed normally at the cell surface (Figure 4.6A, Table 4.2).

However, signalling by many of the mutants in response to INSL3 stimulation was greatly affected. Mutants D43A, G46A and W47A showed no cAMP response to concentrations up to 1 µM INSL3, while G42A and F51A had unchanged potency but their efficacy was around 40% of wild-type RXFP2 levels (Figure 4.6B,C, Table 4.2). Mutating the two middle residues Thr44 and Ser45 had no effect on INSL3 activity (Figure 4.6B,C, Table 4.2).

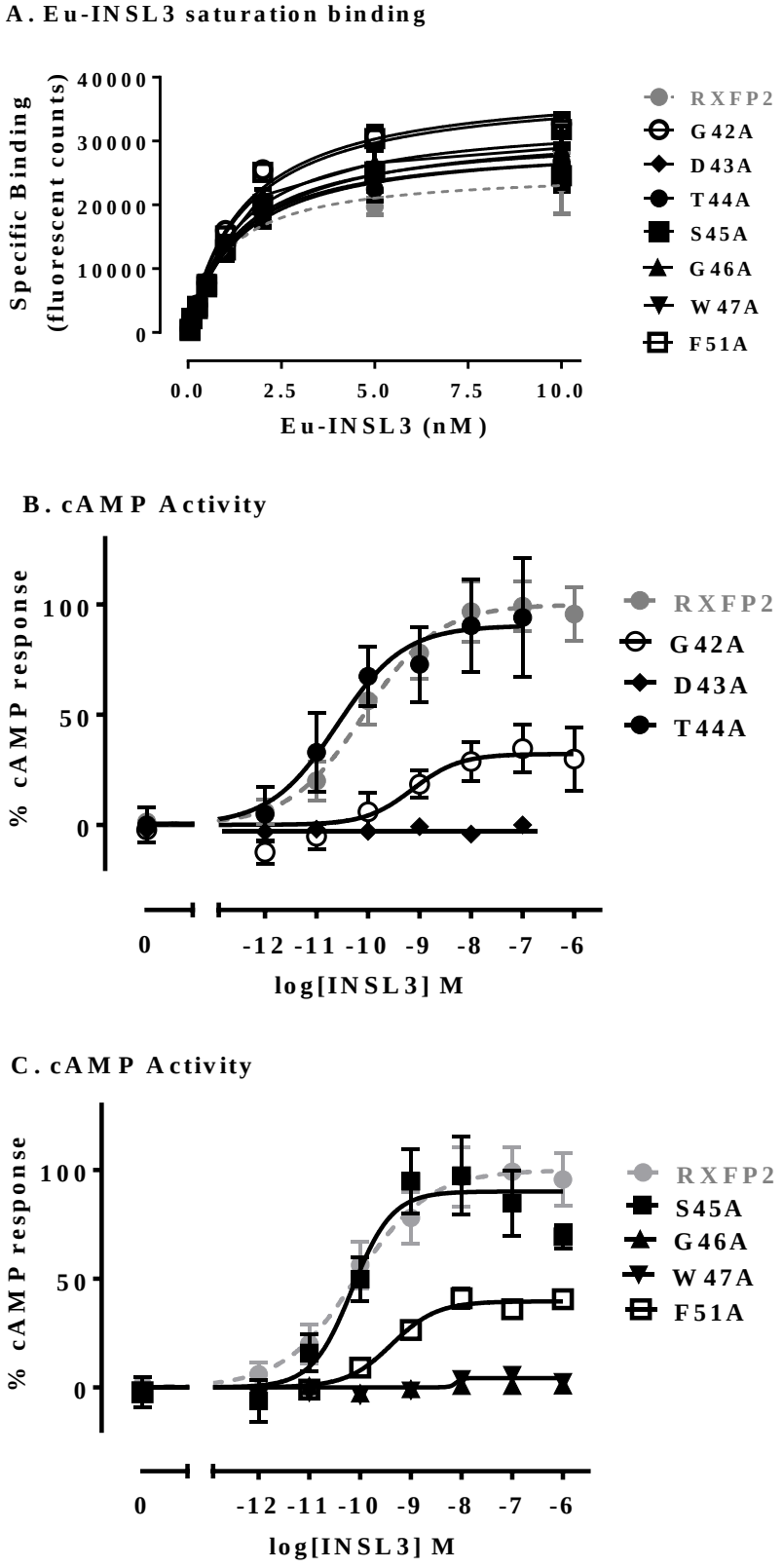

Figure 4.6 A. Eu-INSL3 Saturation binding and B, C. INSL3-stimulated cAMP activity from RXFP2 linker mutants compared to wild-type.

Points are mean ± SEM of at least three independent experiments performed in triplicate.

4.3.3 Relaxin signalling and binding at RXFP2 linker mutants

The binding of RXFP2 to Eu-relaxin highlighted the limitation of using the Europium-based assay to test binding to the non-native ligand relaxin. While a robust response was seen using concentrations up to 10 nM, inconsistency within the assay prevented us from using more ligand, and hence we could not see beyond the calculated K_d of relaxin to RXFP2 (Figure 4.7A, Table 4.2). Nevertheless, the assay was adequate to perceive the inability of the linker mutants D43A, G46A, W47A and F51A to bind relaxin at all at these concentrations (Figure 4.7A, Table 4.2), which was in stark contrast to the phenotype observed in response to Eu-INSL3 (Section 4.3.2).

The signalling profile of the mutants was quite similar to that of the INSL3 stimulations however, and no cAMP response was seen from D43A, G46A or W47A. Likewise T44A and S45A were equipotent with wild-type, although the efficacy of T44A was only around 50% of RXFP2 maximum response (Figure 4.7B,C, Table 4.2). The F51A mutant showed almost no activity in response to relaxin, despite having had only a reduction in INSL3-induced signalling (Figure 4.7C, Table 4.2). We therefore were able to observe that relaxin and INSL3 bind to and activate RXFP2 in distinct manners, with the behaviour of the mutants in response to relaxin mirroring more closely that of the equivalent mutants in RXFP1 in response to the cognate ligand (see Chapter 3 and [2]).

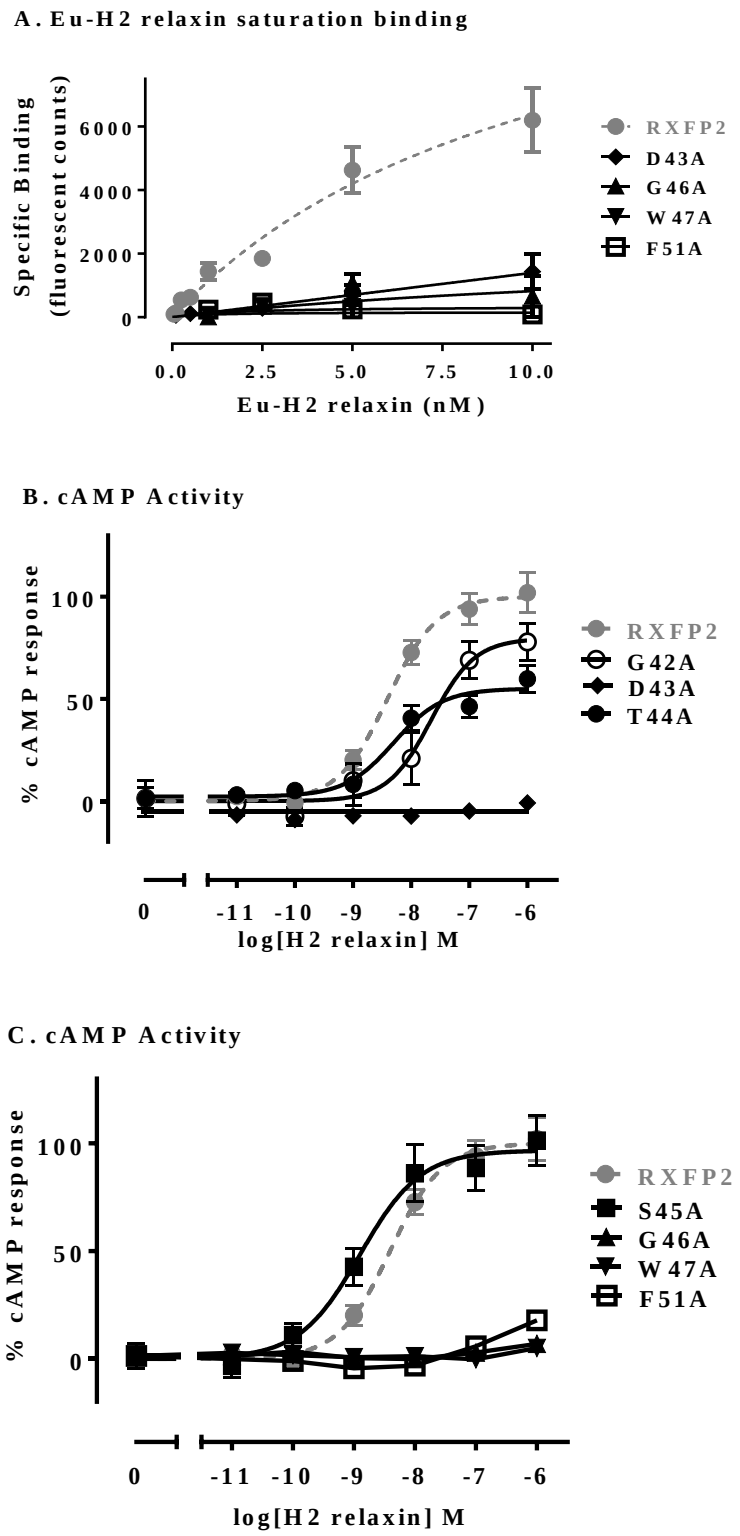

Figure 4.7 A. Eu-relaxin saturation binding and B, C. relaxin-stimulated cAMP activity of RXFP2 linker mutants compared to wild type.

Points are mean ± SEM of at least three independent experiments each performed in triplicate.

4.3.4 Characterisation of RXFP2$_{(1-65)}$ and RXFP2$_{(1-65)}$-GB1

After establishing that mutation of the RXFP2 linker residues was indeed deleterious to relaxin binding, we decided to test the binding of relaxin to the RXFP2 LDLa module and linker using NMR with a recombinant LDLa-linker protein as we had done when investigating RXFP1 (see Chapter 3). Initially we were using RXFP2$_{(1-65)}$, an equivalent protein to that used in the RXFP1 study [2]. SDS-PAGE of the purification fractions showed that the majority of over-expressed protein was soluble, although small amounts were lost in the flowthrough after binding to the resin, some of which could be recovered with a second pass (Figure 4.8).

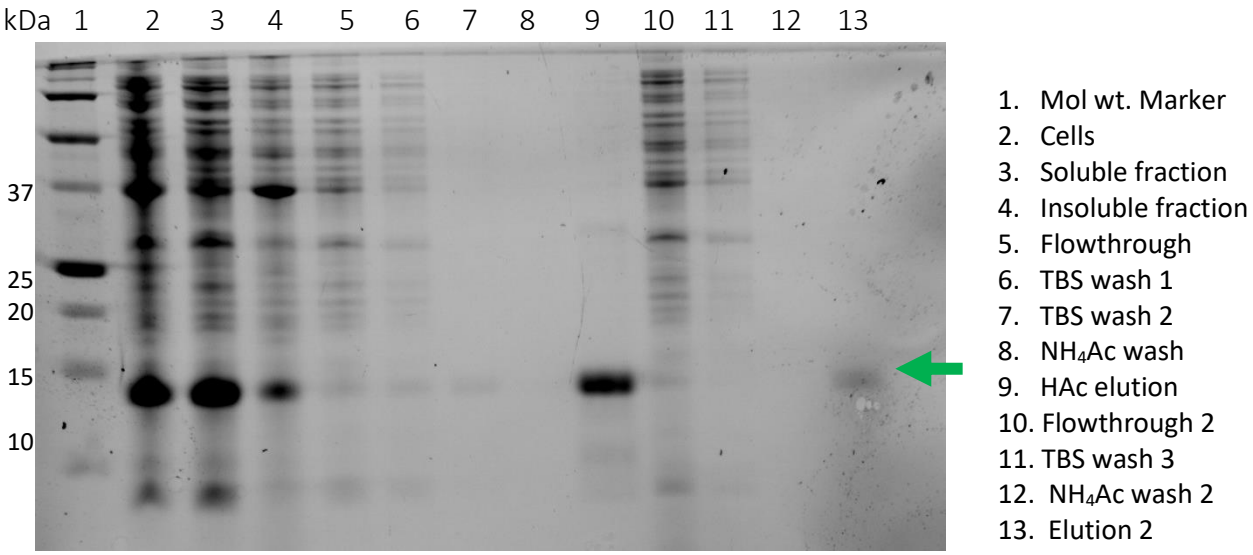

Figure 4.8 Stain-free 16% Tris-tricine SDS-PAGE gel from purification of RXFP2$_{(1-65)}$

Contents of lanes listed to the right of image. Green arrow shows band of protein of interest (molecular weight 14901.33 Da).

Following HPLC purification, the ^{15}N-labelled material was observed in a HSQC NMR experiment, and this revealed a split peak corresponding to the single tryptophan indole within the sequence (Figure 4.9A). There was also peak splitting observed in several of those assigned to glycine residues, indicating that the spectrum was heterogeneous, despite the fact that it looked well-dispersed and clean otherwise. This heterogeneity was thought to be indicative of either poor disulphide bond formation within the module, or cis-trans isomerisation of a proline residue. Given the overall quality of the spectrum, we suspected one of the two prolines within the sequence was undergoing isomerisation, and since Pro21 is conserved within RXFP1 where we had seen no evidence of this, we chose to focus on the proline at position 4. Despite its location at quite a distance from Trp47, we hypothesised that the initial part of the module may in fact wrap around to bring the termini into close association with one another. To test the

hypothesis, we mutated Pro4 to Phenylalanine, and purified the mutant protein as described above. Observation of the resulting HSQC spectrum revealed that the Trp indole resonance was visible as a single point, and the glycines had also collapsed into homogeneous points on the spectrum (Figure 4.9B). We made and tested an RXFP2-P4F mutant in activity assays, and thereby confirmed that the mutation did not disturb receptor-ligand binding or function (Figure 4.10) and proceeded to use this mutant protein for all remaining experiments.

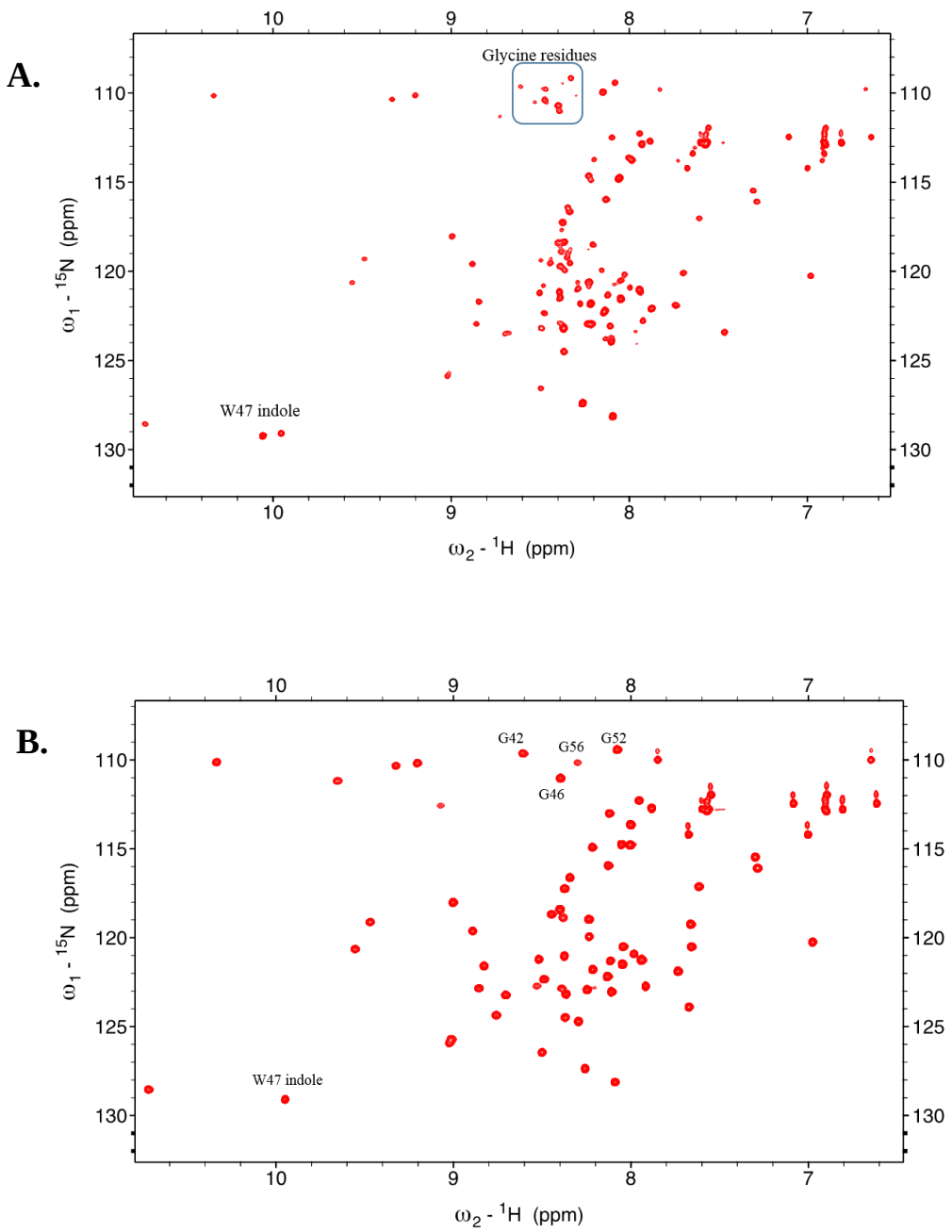

Figure 4.9. Full 2D ^{1}H-^{15}N HSQC spectra of A. RXFP2$_{(1-65)}$ and B. RXFP2$_{(1-65)}$ P4F

W47 indole and glycine residues are labelled to show effect of mutation of Pro4 to phenylalanine.

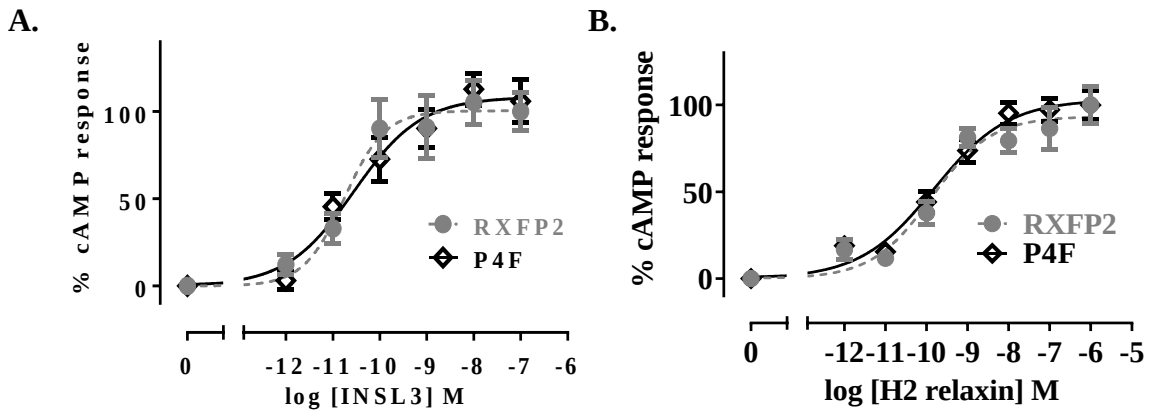

Figure 4.10. cAMP response to RXFP2 P4F compared to wild type in response to A. INSL3 and B. relaxin.

Points are mean ± SEM of at least three independent experiments each performed in triplicate.

Protein purification of RXFP2$_{(1\text{-}65)}$ had proved challenging due to its poor solubility and the use of the IgG column which required large quantities of 0.05 M acetic acid (pH 3.4) for elution. This was particularly damaging in the concentration steps, where the persistent presence of acid fumes contributed to the breakdown and subsequent replacement of the bench-top centrifuge. A new construct was designed that would contain a poly-Histidine tag at its N-terminus, meaning it would bind to a more amenable TALON resin and elute in buffer containing high concentrations of imidazole. An additional GB1 moiety was added to its C-terminus (Figure 4.2). This would remain attached after the N-terminal GB1 and His tag were removed by thrombin cleavage, likely affording extra solubility to the protein, as well as potentially mimicking the anchoring action of the native LRR domain. Initial purifications

showed that the protein was indeed expressed in the soluble fraction of expressed BL21(DE3)trxB cells, with very little in the pellet (lanes 3 and 4,

Figure 4.11). Significant quantities (assessed by spectrophotometric reading at 280 nm) were eluted in increasing concentrations of imidazole, with most being extracted by 100 mM and 200 mM elution buffers (lanes 9 and 10,

Figure 4.11).

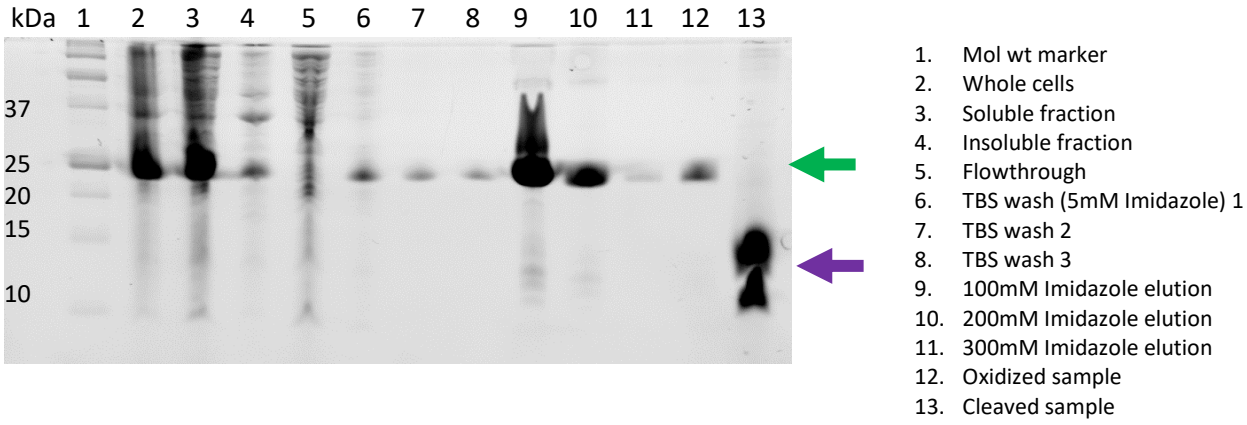

Figure 4.11 Stain-free 16% Tris-tricine SDS-PAGE gel from purification of RXFP2$_{(1-65)}$-GB1(P4F)

Contents of lanes listed to the right of image. Green and purple arrows show location of uncleaved GB1-RXFP2$_{(1-65)}$-GB1 (P4F) and cleaved RXFP2$_{(1-65)}$-GB1 (P4F) respectively. Expected mass 21348 Da (uncleaved) and 13131 Da (cleaved).

A correctly folded LDLa module requires the formation of three conserved disulphide bonds as well as binding of a single Ca^{2+} ion. To achieve this, the eluted protein was placed in a mixed redox reaction containing 10 mM $CaCl_2$ with stirring overnight. The presence of calcium in the buffer allows the fold to occur, and the reduced and oxidised glutathione drive disulphide bond formation. We could observe the oxidation of at least two of the three disulphide bonds by mass spec analysis, which showed an actual mass (21343.79) that was almost 5 daltons smaller

than the calculated expected mass (21348.27) (Figure 4.12A). Initial attempts to separate the components using a single run on RP-HPLC proved unsuccessful, as the hydrophobicity of the His-tagged GB1 and RXFP2-GB1 was too similar for satisfactory separation to be achieved. This was overcome by passing the cleaved sample over the TALON resin a second time, in which the His-tagged GB1 would bind, but the RXFP2-GB1 would flow through and be collected in the wash buffer. Mass spectrometry showed that the GB1 (expected value 8235; measured value 8236) still contained a component of uncleaved sample (Figure 4.12C), as well as some unidentified fragments, while the $RXFP2_{(1\text{-}65)}$ was comparatively pure, with a single major peak of mass 13127, being 4 daltons less than the calculated mass of 13131, accounting for at least two of the three disulphide bonds being formed (Figure 4.12B) on this occasion. However, NMR spectra showed a well-dispersed set of resonances, consistent with a correctly folded module (Figure 4.13).

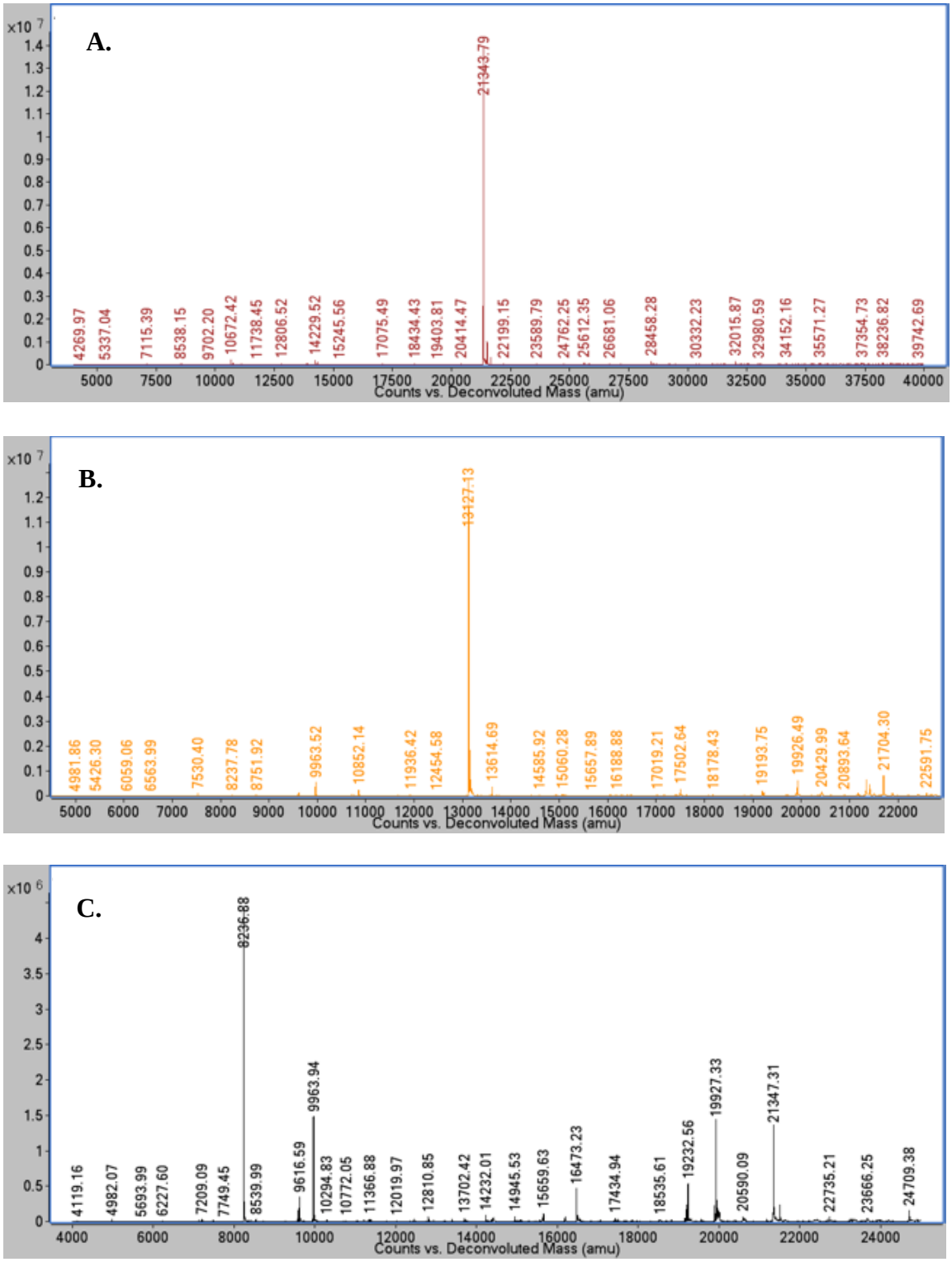

Figure 4.12. Deconvoluted reading from Mass spectrophotometer analysis of purified cleaved and uncleaved GB1-RXFP2$_{(1-65)}$

A. Uncleaved, oxidized GB1-RXFP2$_{(1-65)}$, showing mass of major peak as 21343.79 daltons. B. Cleaved RXFP2$_{(1-65)}$, with major peak mass13127.13, C. Cleaved GB1, with major peak 8236.88.

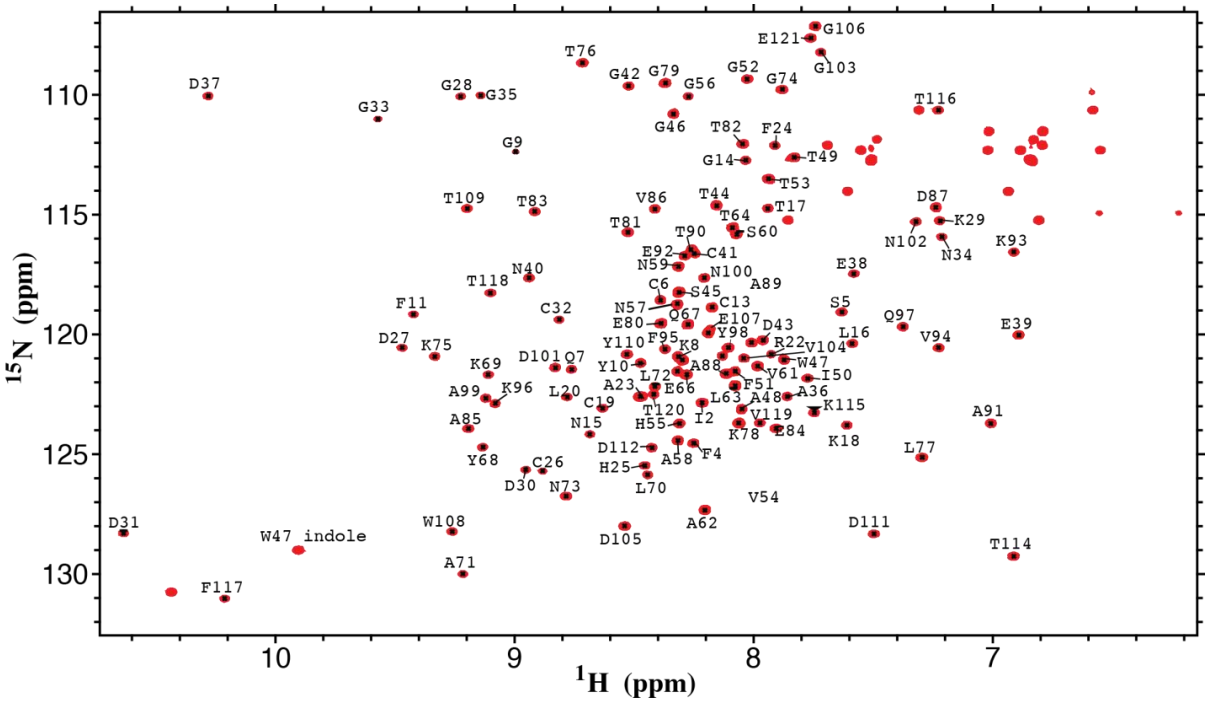

Figure 4.13. Full ^{1}HN ^{15}N HSQC spectrum of RXFP2$_{(1-65)}$ GB1 (P4F) with residue assignments.

Figure taken from [3].

4.3.5 Signalling of B5-29 [B-K 9 R,A-K9/17R] (truncated) relaxin

We were provided with a truncated, monomeric version of relaxin (termed truncated relaxin) to use in NMR experiments as the inherent capacity of relaxin to dimerise [306] can interfere with titrations when using high concentrations of the peptide. The superiority of truncated relaxin was seen when comparing 2D ^{1}H NOESY and TOCSY spectra and observing more cross peaks than those seen when using H2 relaxin, indicating that it is indeed monomeric. As a precaution I tested the peptide in activity assays on both RXFP1 and RXFP2, which revealed that it behaved the same as H2 relaxin on both receptors (Figure 4.14).

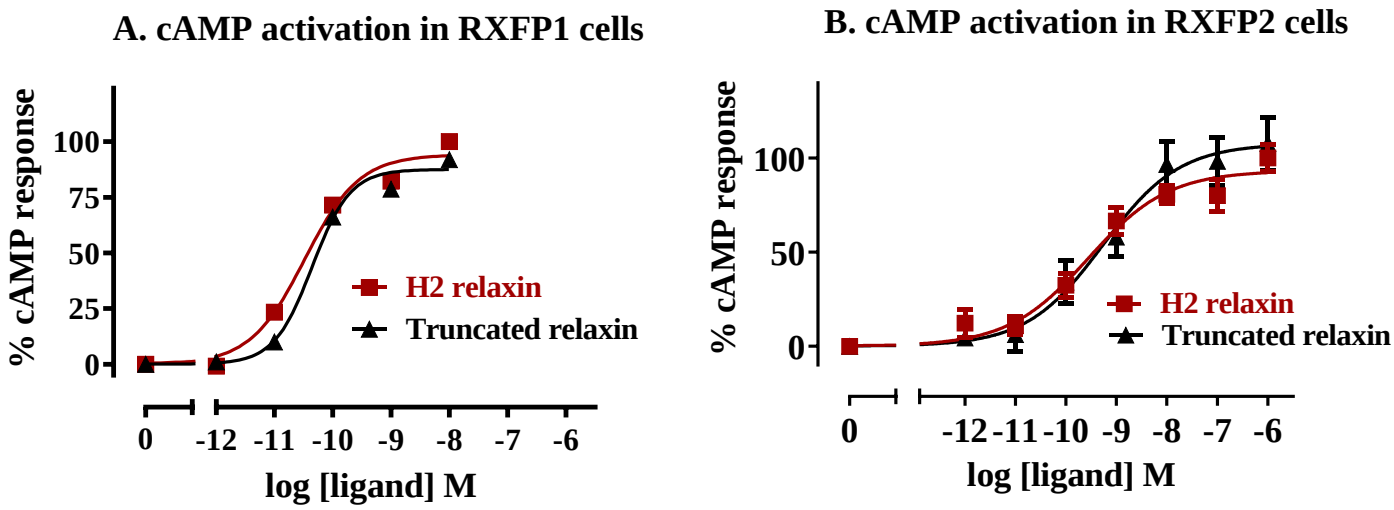

Figure 4.14. Activity of truncated relaxin compared to H2 relaxin on cells expressing A. RXFP1 and B. RXFP2.

Points are mean ± SEM from at least three independent experiments each performed in triplicate.

4.3.6 Characterisation of ssRXFP2

In addition to testing for an interaction between $RXFP2_{(1-65)}$ and relaxin, we also wanted to probe the protein's ability to interact with the extracellular loops (EL) of both RXFP1 and RXFP2. We sought to achieve this by expressing the relevant residues of the receptor extracellular loops on a soluble scaffold based on the thermostabilized GB1 protein (Figure 4.3). We decided to include a partial EL1 and full-length EL2, since this was the construct that was used to explore the same interaction on RXFP1 [2, 251]. We designed the construct based on the RXFP1 soluble scaffold version (known as ssRXFP1) and called it ssRXFP2 (Figure 4.3,

Figure 4.15).

```
ssRXFP1      MGSSHHHHHHSSGLVPRGSHMAQLWMESTHCQGGAQFKLIINGKTLKGEITIEAGG              56
ssRXFP2      MGSSHHHHHH---LVPRGSHMALLWMESVQCRGGAQFKLIINGKTLKGEITIEAGG              53
tGB1         -GSSHHHHHHSSGLVPRG-------------SGAQFKLIINGKTLKGEITIEAV-               37

ssRXFP1      EFFKNYYGTNGVCFPLHSEDTESIGAQGGAAEAEKIFKQYANDNGIDGEWTYDDATKTFTVTE       119
ssRXFP2      DYFGNFYGKNGVCFPLYYDQTEDIGSKGGAAEAEKIFKQYANDNGIDGEWTYDDATKTFTVTE       116
tGB1         ----------------------------DAAEAEKIFKQYANDNGIDGEWTYDDATKTFTVT-       75
```

Figure 4.15. Sequence alignment of ssRXFP1 with ssRXFP2 and tGB1, with truncated EL1 shown in red and EL2 in blue.

Alignment was constructed using Clustal Omega online server.

The purification of the construct was performed using TALON Superflow resin, and monitored by SDS-PAGE, which revealed that most of the protein eluted in 100 mM imidazole (Figure 4.16A), with the size matching the expected mass of 12729 Daltons. This was further confirmed by mass spectrometry (Figure 4.16B). The final characterization was performed using CD and comparing the structural components with those seen in the ssRXFP1 construct previously, as well as the tGB1 protein alone. The results revealed that ssRXFP2 indeed maintained its three-dimensional structure, with 23.4% being attributed to α-helix, 34.5% β-strand, 10.7% turns and 21.8% disordered (Figure 4.16C, D). This compared well to ssRXFP1 and tGB1, although tGB1 had relatively greater α-helix (35.5%) and less β-strand (14.7%).

A.

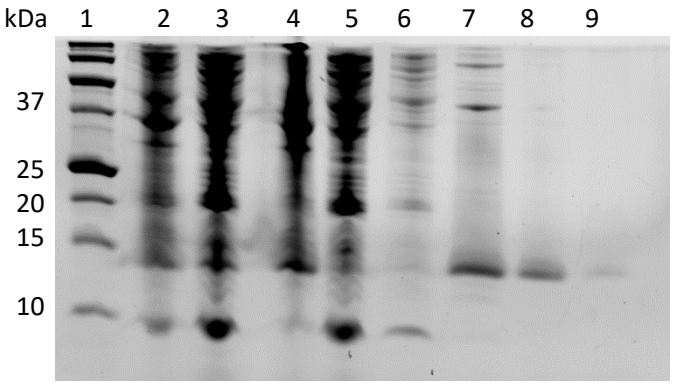

1. Mol weight marker
2. Whole cells
3. Soluble fraction
4. Insoluble fraction
5. Flowthrough
6. 5mM imid. Wash
7. 100mM Imid. Elution
8. 200mM imid elution
9. 300mM imid elution

B.

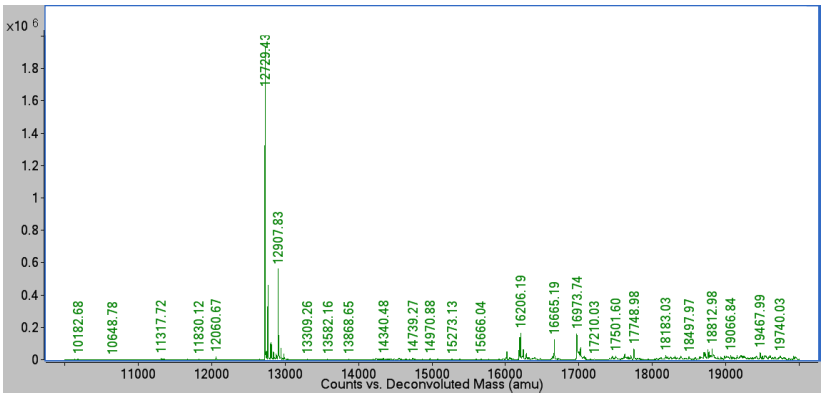

C.

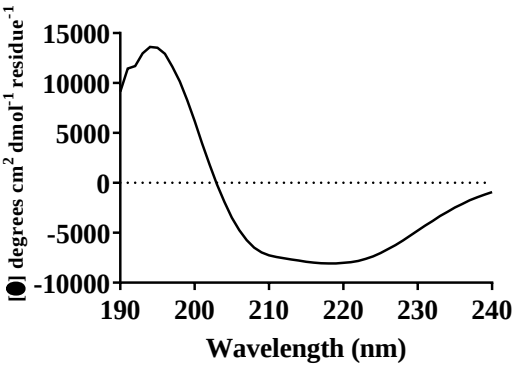

D.

α-Helix	β-Strand	Turns	Disordered
23.4	34.5	17.8	21.8

Figure 4.16. Characterisation of ssRXFP2.

A. SDS-PAGE gel (16% tris-tricine) of purification fractions from ssRXFP2. Lanes are numbered above with corresponding contents listed to the right. Molecular weight sizes are shown beside the bands in lane 1. B. Mass spec result of ssRXFP2, showing mass of 12729.43. C. CD analysis of ssRXFP2, with D. associated structural components calculated using Dichroweb online server with Selcon3 and reference set 7.

4.3.7 Interaction of RXFP2$_{(1-65)}$-GB1(P4F) with relaxin and soluble scaffolds

Although the NMR titrations were carried out and analysed by Ashish Sethi, it is important to present the results as part of the narrative thus far, since we now have our RXFP2 LDLa-linker recombinant protein, RXFP2$_{(1-65)}$-GB1, with P4F mutation (RXFP2$_{(1-65)}$-GB1(P4F)), truncated relaxin and two soluble scaffold proteins with RXFP1 and RXFP2 ELs, called ssRXFP1 and ssRXFP2. Titrations were performed of each of the soluble scaffold constructs as well as truncated relaxin with RXFP2$_{(1-65)}$-GB1(P4F), revealing that an interaction was occurring that was specific to the RXFP2 portion of the protein, as the residues mapped to GB1 did not respond with any chemical shift change beyond background noise (Figure 4.17). In all cases, the residues most affected were localized around the C-terminal end of the LDLa module, with C26 showing significant chemical shift change in response to all titrants. Acidic residues moved in the relaxin titration, including Asp43, from within the linker residues (specifically the GDxxGW motif), but the mechanism was seen as distinct from that seen in RXFP1 titrations, where the central portion of linker moved to a much greater degree. The K_d of the interaction between relaxin and RXFP2$_{(1-65)}$-GB1(P4F) was estimated at 330 ± 10 µM by plotting movement of resonances showing the greatest chemical shift change and fitting a single-site saturation curve (Figure 4.17B). This was weaker than that reported for the RXFP1 LDLa-linker with relaxin (90 µM [3]), as expected given that RXFP2 is not the native receptor for relaxin, and that the linker residues responsible for the RXFP1 interaction are missing.

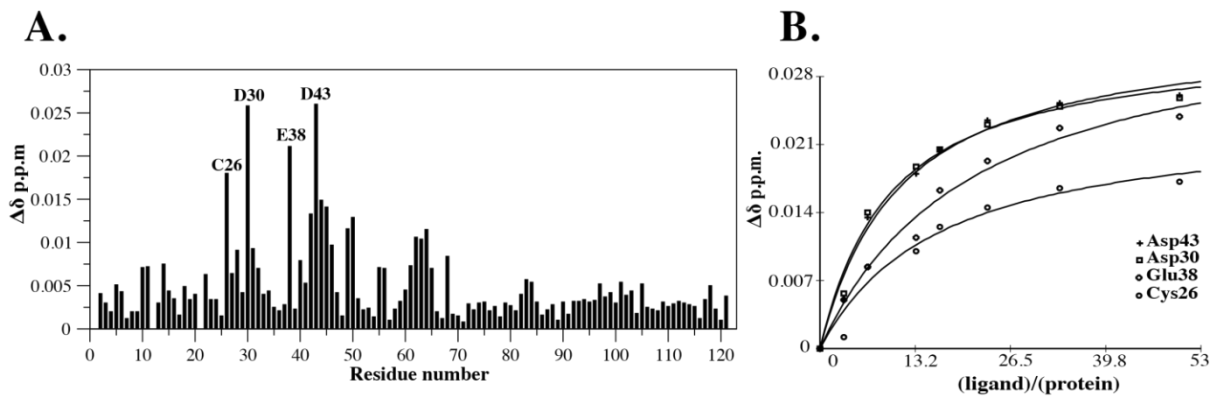

Figure 4.17. A. Graph of the average change in ^{1}HN and ^{15}N chemical shifts after titration of ^{15}N-RXFP2$_{(1-65)}$-GB1(P4F) with 50 equivalents of monomeric relaxin. B. Saturation binding curves for resonances showing the largest chemical shift changes while remaining resolved throughout the titration. Figure adapted from [3].

The two soluble scaffold proteins also showed an interaction with RXFP2$_{(1-65)}$-GB1(P4F) that was most apparent around the N-terminus, which again differed from what was seen with RXFP1 (Figure 4.18). This pointed to a different mechanism driving the interaction between the TM domain and LDLa module/linker between the two similar receptors.

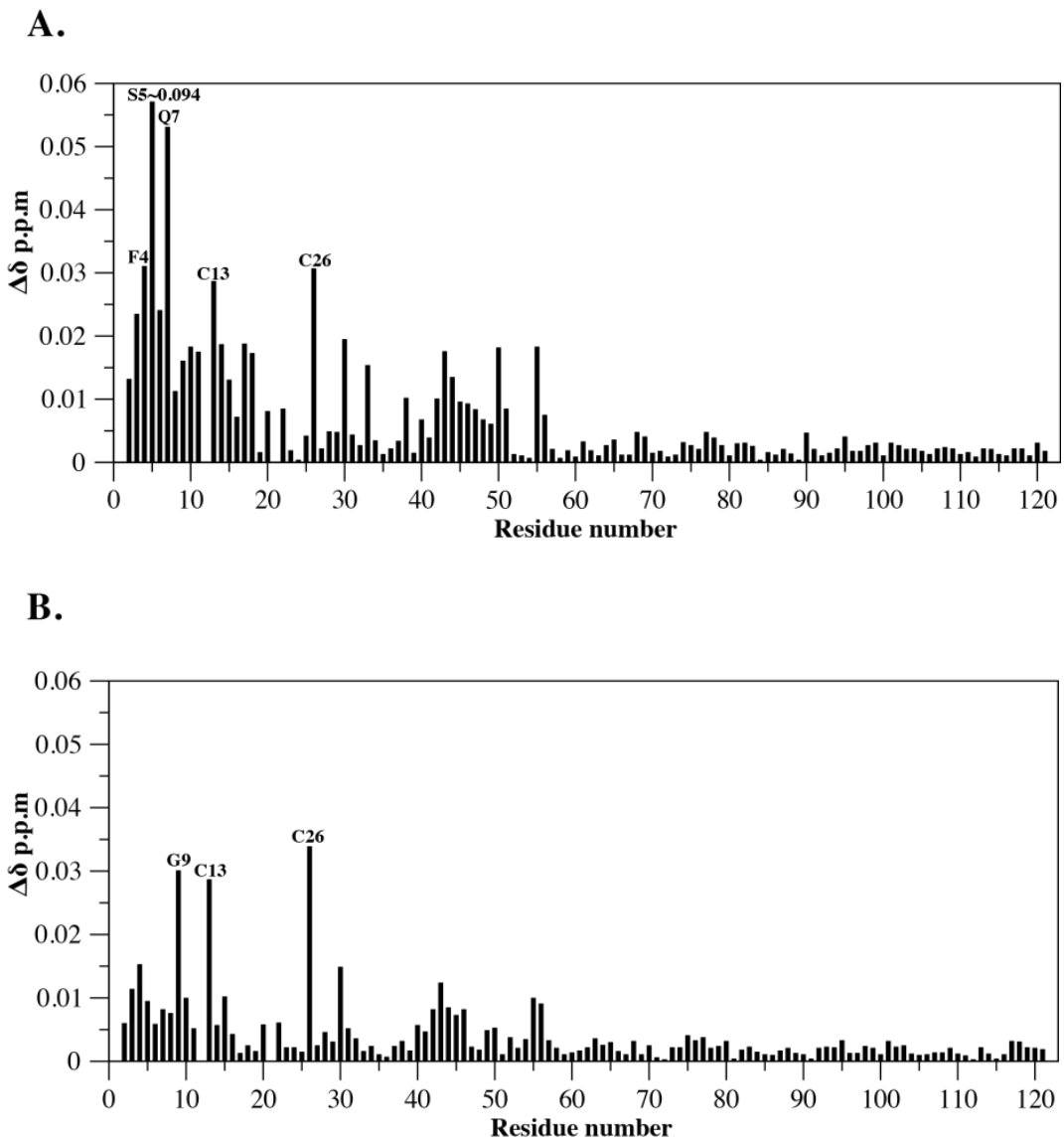

Figure 4.18. Graph of the change in average ^{1}HN and ^{15}N chemical shifts following titration of ^{15}N-RXFP2$_{(1-65)}$-GB1(P4F) with 20 equivalents of A. ssRXFP1 and B. ssRXFP2.

Figure taken from [3].

4.3.8 Signalling of loop mutants F574A and P575A

During the exploration of the interaction between RXFP1 LDLa/linker and the ELs, two residues from EL2 were identified as important, namely Phe564 and Pro565 [1, 251]. We tried to establish if the same residues from EL2 of RXFP2 (Phe574 and Pro575) were implicated, and mutated these to alanine. F574A experienced a significant loss of efficacy in response to either ligand (51.42 ± 3.16% of RXFP2 response for INSL3 ($p<0.01$); 52.91 ± 9.76% of RXFP2 response for relaxin ($p<0.05$); Figure 4.19) and while relaxin potency of F574A was lower than wild type (pEC_{50} = 8.63 ± 0.48), this difference was not significant and INSL3 potency was normal (Figure 4.19, Table 4.2). The differences in efficacy of F574A could potentially be explained by the apparent low expression of the mutants on the surface of cells, as evidenced by the B_{max} values in Eu-INSL3 saturation binding assays (F574A: ~15%; P575A: 47% of wild type expression). The respective K_d values were not significantly different from wild-type in the Eu-INSL3 saturation binding assay (Figure 4.19C, Table 4.2). While the residues within EL2 may be involved in receptor trafficking, the results did not warrant further exploration in the context of this study. It seemed that once again the mechanism of RXFP2 activation was distinct from that of RXFP1.

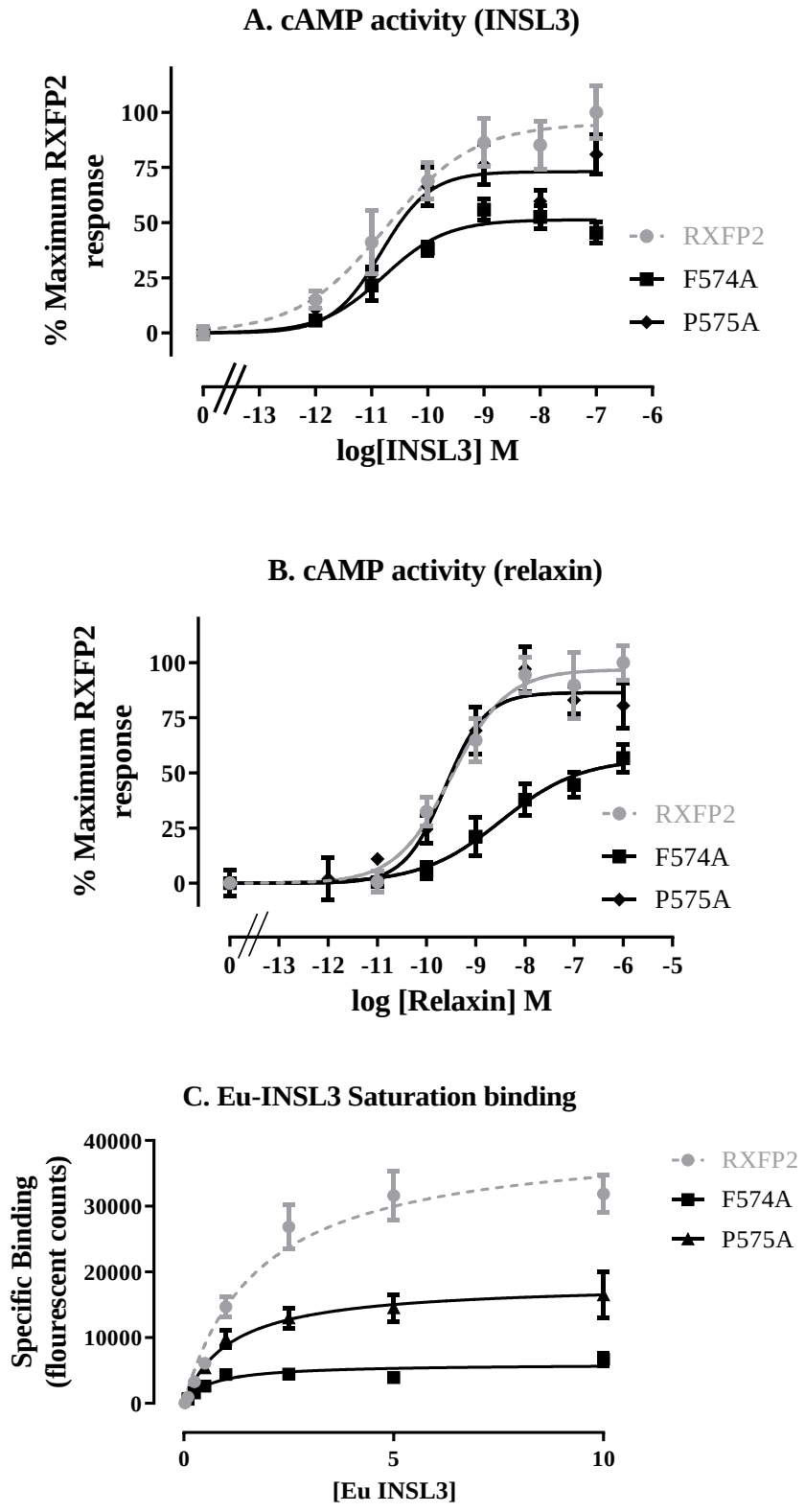

Figure 4.19. A,B. cAMP activity assay and C. Eu-INSL3 binding assay of loop mutants F574A and P575A in comparison to RXFP2.

Points are mean ± SEM of at least three independent experiments each performed in triplicate.

4.3.9 RXFP2 Extended Linker (ExLink) signalling

In order to explore the role of the RXFP1 linker in relaxin signalling further, we decided to insert the residues thought to encompass the identified binding site into an equivalent position in the RXFP2 linker. This was done in two rounds of mutagenesis, and so we ended up with two constructs, one with a four-residue insertion including Phe54, the first residue implicated in RXFP1 relaxin binding, and the other with seven residues including both Phe54 and Tyr58 from RXFP1 linker region 2 (Figure 4.20A). The chimeras were tested for relaxin signalling and compared to wild type RXFP1 and RXFP2 on the same plate with identical transfection protocols used. Despite large variation in efficacy seen from the ExLink constructs, the potency consistently fell between wild type RXFP1 (pEC_{50} = 11.02 ± 0.08) and RXFP2 (pEC_{50} = 8.57 ± 0.26), with ExLink1 having a slightly lower potency (pEC_{50} = 9.48 ± 0.36) than ExLink2 (pEC_{50} = 9.74 ± 0.24), such that they approached RXFP1 levels in a progressive manner (Figure 4.20B, Table 4.2). Neither of the chimeras showed significant difference from wild type in response to INSL3 stimulation (Figure 4.20C, Table 4.2). ExLink2 showed normal binding to Eu-INSL3 compared to wild type (Figure 4.20D, Table 4.2), and although their expression levels were significantly lower than those of wild type RXFP2, which expressed at 303.8% of RXFP1 levels, they were nonetheless still expressed more highly than wild type RXFP1, (ExLink1 = 145.52 ± 13.31% RXFP1 expression; ExLink2 = 206.27 ± 10.68% RXFP1 expression) (Figure 4.20E, Table 4.2).

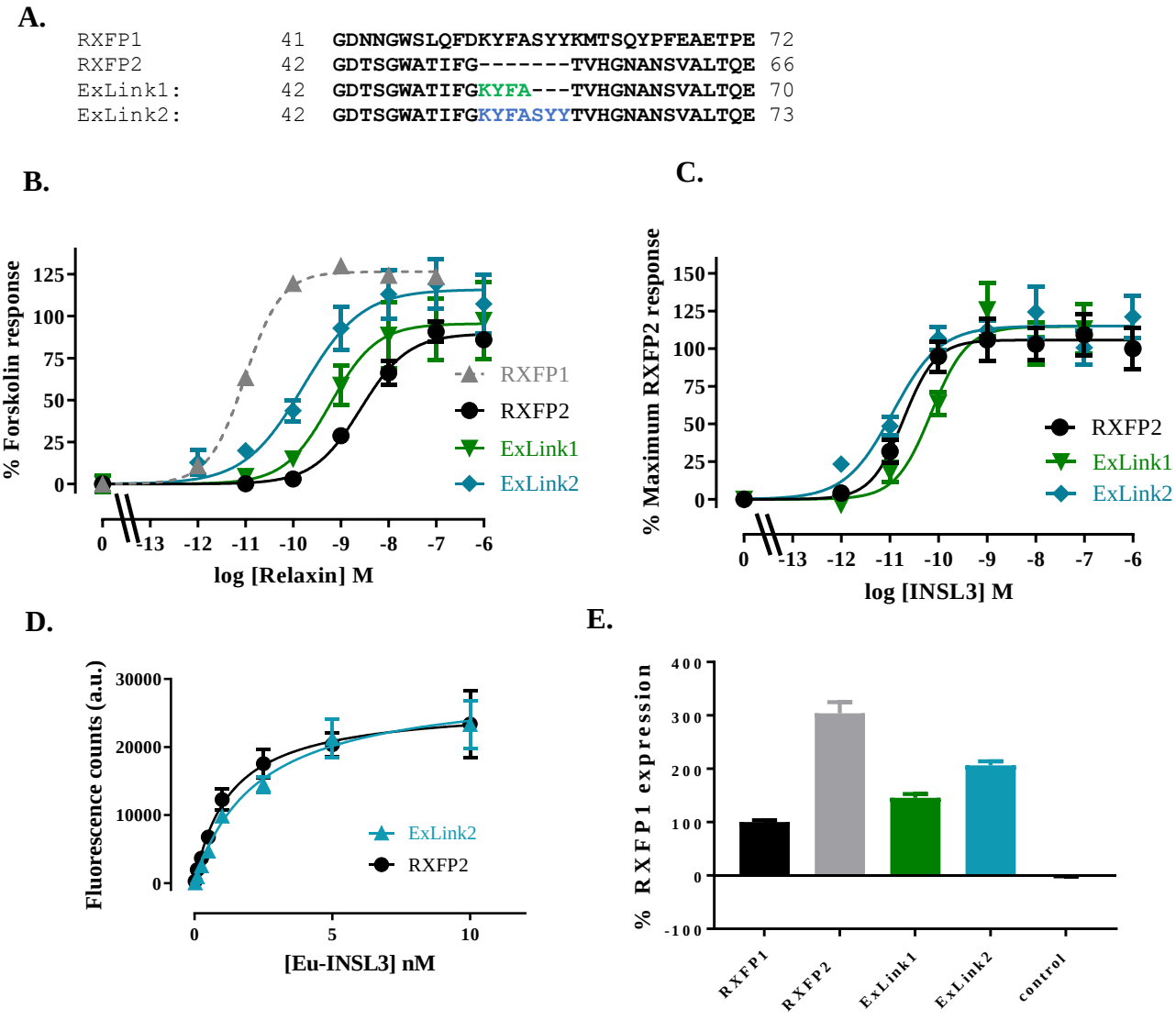

Figure 4.20. Characterization of ExLink1 and ExLink2.

A. Sequence alignment showing RXFP1 and RXFP2 linkers and ExLink1, with inserted residues shown in green and ExLink2, with inserted residues shown in teal. B, C. Activity assays of RXFP2 ExLink constructs compared to both RXFP1 and RXFP2 in response to relaxin (B), and compared to RXFP2 in response to INSL3 (C). D. Eu-INSL3 binding of ExLink2 compared to RXFP2. E. Relative cell surface expression of chimeras and RXFP2 as a percentage of RXFP1 expression levels. Points are mean ± SEM of at least three independent experiments each performed in triplicate.

4.3.10 Characterisation of Nluc-RXFP2 and variants

Given the shortcomings of the Eu-relaxin binding assay for RXFP2 (see section 4.3.3), we chose to use a newly developed NanoBRET assay to assess relaxin binding (section 4.2.11). This assay was established and optimised by Bradley Hoare using RXFP1, and he discovered that transfecting lower quantities of Nanoluc-tagged receptor led to a higher BRET signal, which could be explained by the reduction of intracellular pools of receptor that would contribute to luminescence but not BRET (Figure 4.21).

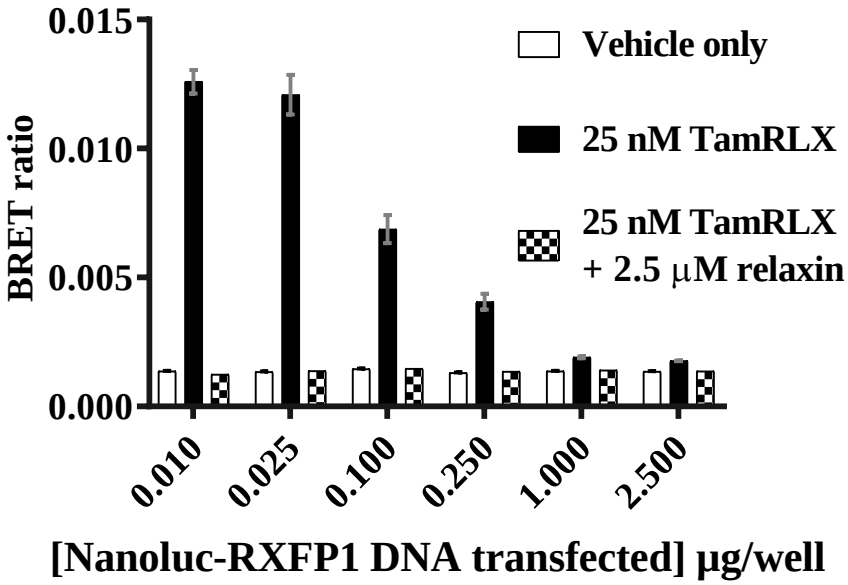

Figure 4.21. BRET ratio of HEK293T cells transfected with varying amounts of Nanoluc-tagged RXFP1 DNA.

Wells are incubated with either vehicle or 2.5 μM relaxin to exclude non-specific binding. Data pooled from 4 independent experiments each performed in duplicate. From [4].

For RXFP2, we had already observed that intracellular accumulation of receptor could occur with high amounts of DNA (section 4.3.1), and so we decided to use the less efficient (and more cost-effective) transfection agent PEI [307]. A quantity of 0.5 µg Nanoluc-RXFP2 DNA per well of a 6-well plate was found to give a robust BRET signal, which led to a saturation curve that was effective up to concentrations of 100 nM, being 10 times more than those being used in the Eu-relaxin saturation binding assay. Saturation was achieved and the K_d calculated (RXFP2 vs TamRLX = 10.74 ± 1.64 nM; Figure 4.22A, Table 4.3) matched well with that measured using Eu-relaxin (~10 nM – Table 4.2) as well as that previously reported in the literature [135]. We then assayed Nluc-RXFP2 for activity using our reporter gene assay to ensure the addition did not affect the receptor's capacity to signal, which was the case (Figure 4.22B, Table 4.2). We also tested the BRET partner TamRLX for its ability to illicit a cAMP response in FLAG-tagged RXFP2. This assay was only performed twice due to the low availability of TamRLX, but again it produced an equivalent response to unlabelled relaxin (Figure 4.22C, Table 4.2).

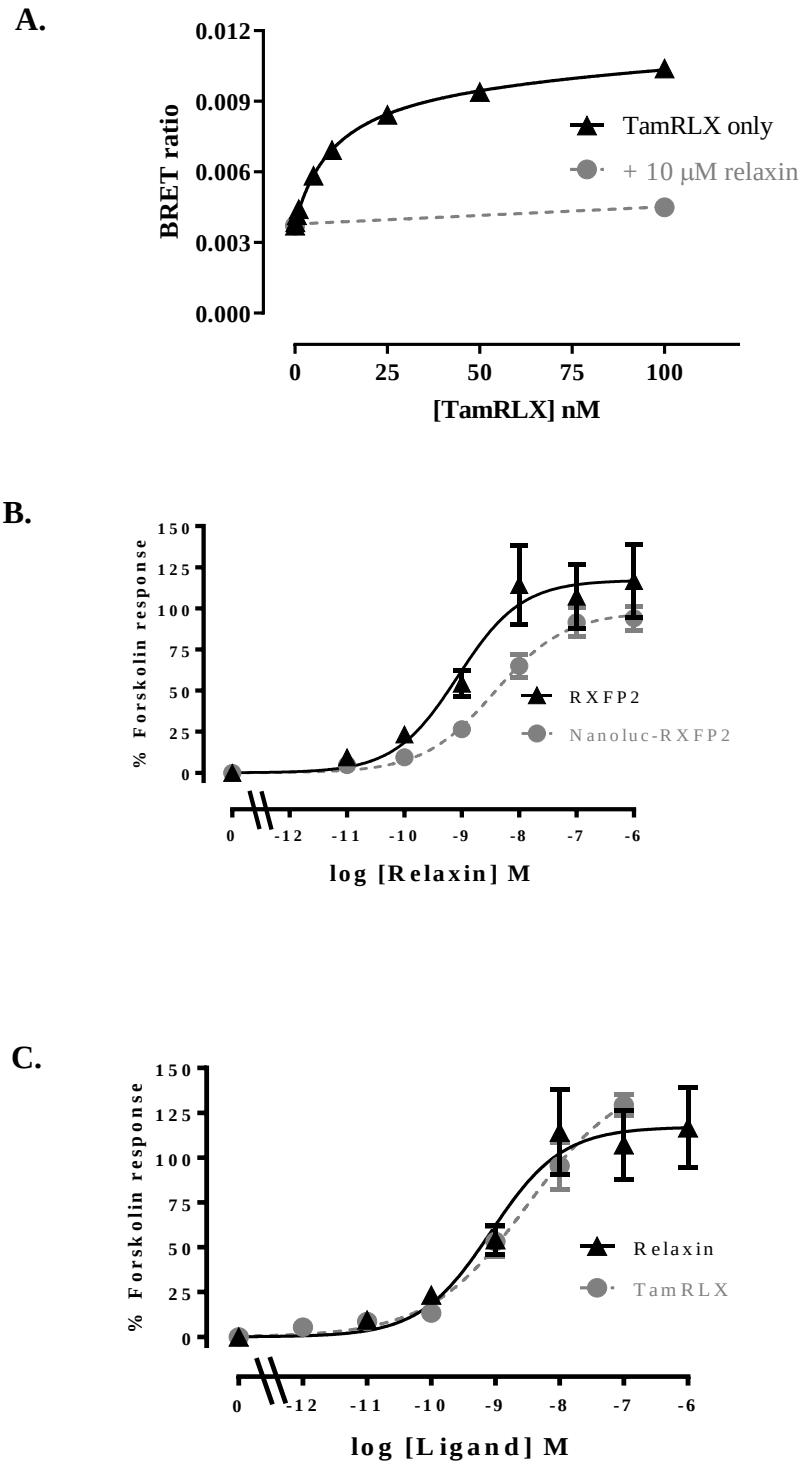

Figure 4.22. Validation of Nluc-RXFP2 and TamRLX as ligand at RXFP2.

A. Saturation binding assay of TamRLX to Nluc-RXFP2 transiently expressed in HEK293T cells. cAMP reporter gene assay of B. RXFP2 and Nanoluc-RXFP2 stimulated by relaxin and C. RXFP2 stimulated by relaxin vs TamRLX. Points are mean ± SEM of at least two independent experiments each performed in triplicate.

We also inserted the Nanoluc moiety onto the N-terminus of two RXFP2 variants, these being RXFP2-short, a naturally occurring splice variant [200], and RXFP2-ECD, which is the extracellular domain of RXFP2 attached to a single transmembrane helix that comes from protein CD8 [135]. By performing saturation binding assays with TamRLX we hoped to confirm the known affinities of the constructs for relaxin and further validate the NanoBRET system for use with RXFP2. RXFP2-short had only been characterized using a competition binding assay, which showed that the affinity for relaxin was slightly lower than that of RXFP2 (pIC_{50} 8.22 vs 8.92 for wild type [200]). This phenotype was confirmed using the NanoBRET assay, with a K_d of 15.25 ± 1.26 nM, only slightly weaker than that of RXFP2 wild type (Figure 4.23A, Table 4.3). In the case of the ectodomain-only construct, Nluc-RXFP2-ECD, the affinity was found to increase drastically, with a K_d of 0.21 ± 0.02 nM (Figure 4.23B, Table 4.3). This was around 10-fold stronger than the previously published affinity of relaxin for the RXFP2 ectodomain (K_d = 1.91 nM [135]), which had been attributed to the binding of ligand to a high-affinity site within the whole receptor, stated as being separable from another, low-affinity site, presumably within the TMD ELs. Interestingly, an improved affinity was also observed using NanoBRET to compare relaxin binding with RXFP1-ECD to the full length RXFP1 receptor, although it was not so dramatic (Nanoluc-RXFP1 K_d = 0.42 nM vs Nanoluc-RXFP1-ECD K_d = 0.28 nM, unpublished data).

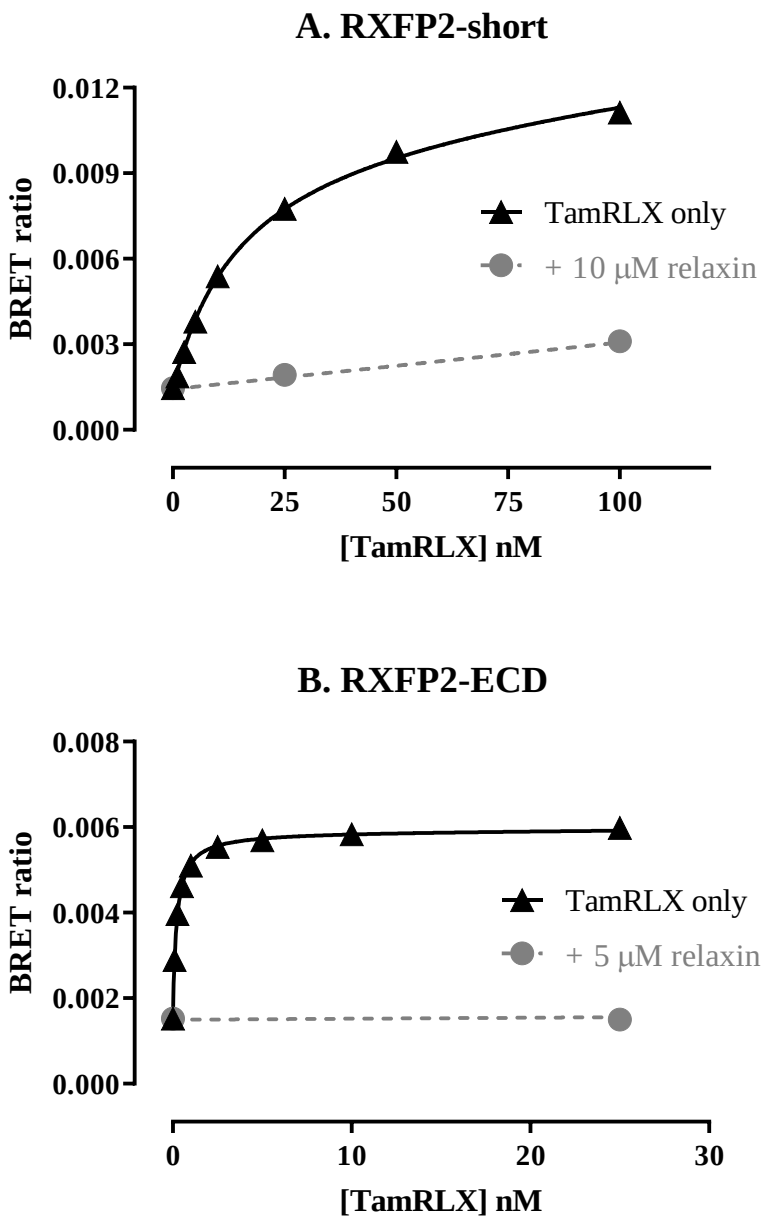

Figure 4.23. NanoBRET saturation binding curves for A. Nanoluc-RXFP2-short and B. Nanoluc-RXFP2-ECD with non-specific binding.

Points are mean ± SEM of at least two representative experiments each performed in duplicate.

4.3.11 NanoBRET saturation binding assays on ExLink1 and ExLink2

The extended linker constructs ExLink1 and ExLink2 were tested for relaxin binding using NanoBRET, which proved reliable using concentrations up to 100 nM. The results reflected those seen in activity assays, with a progressive increase in affinity for relaxin seen as more linker residues were introduced. The K_d of relaxin for Nanoluc-ExLink1 was 2.74 ± 0.52 nM, being around 5-fold stronger affinity than wild type, and that for Nanoluc-ExLink2 was 1.17 ± 0.2 nM, or twice as strong again (Figure 4.24, Table 4.3).

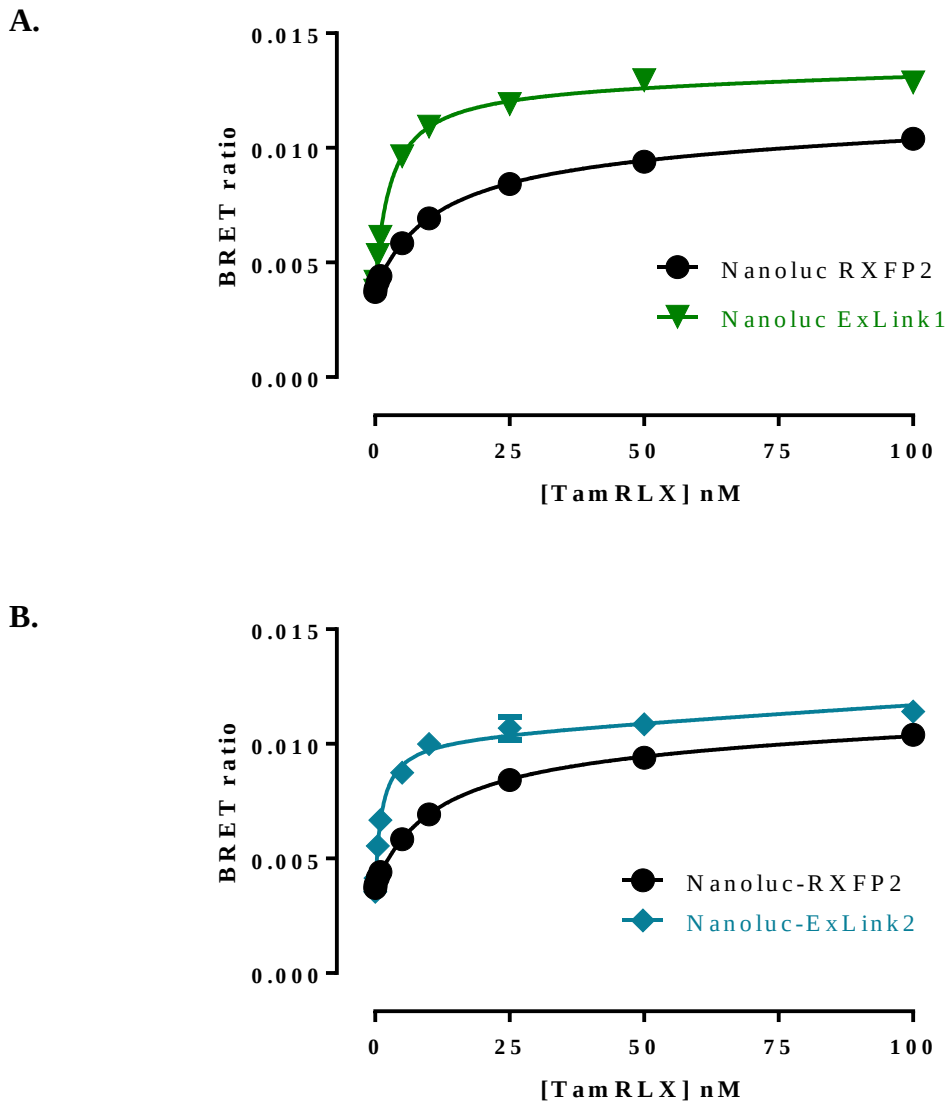

Figure 4.24. NanoBRET saturation binding assay of TamRLX to A.Nanoluc-ExLink1 compared to Nanoluc-RXFP2 and B. Nanoluc-ExLink2 compared to Nanoluc-RXFP2.

Points are mean ± SEM of four independent experiments each performed in duplicate.

4.3.12 NanoBRET dissociation assays

The NanoBRET system also allowed us to dissect the kinetics of the interaction between TamRLX and RXFP2. An interesting discovery made in the lab leading up to this study was that TamRLX dissociation from RXFP1 was best fit to a two-phase exponential decay function rather than a function fitting a single phase, as determined by comparison of the time-invariant distribution of residuals (Figure 4.25).

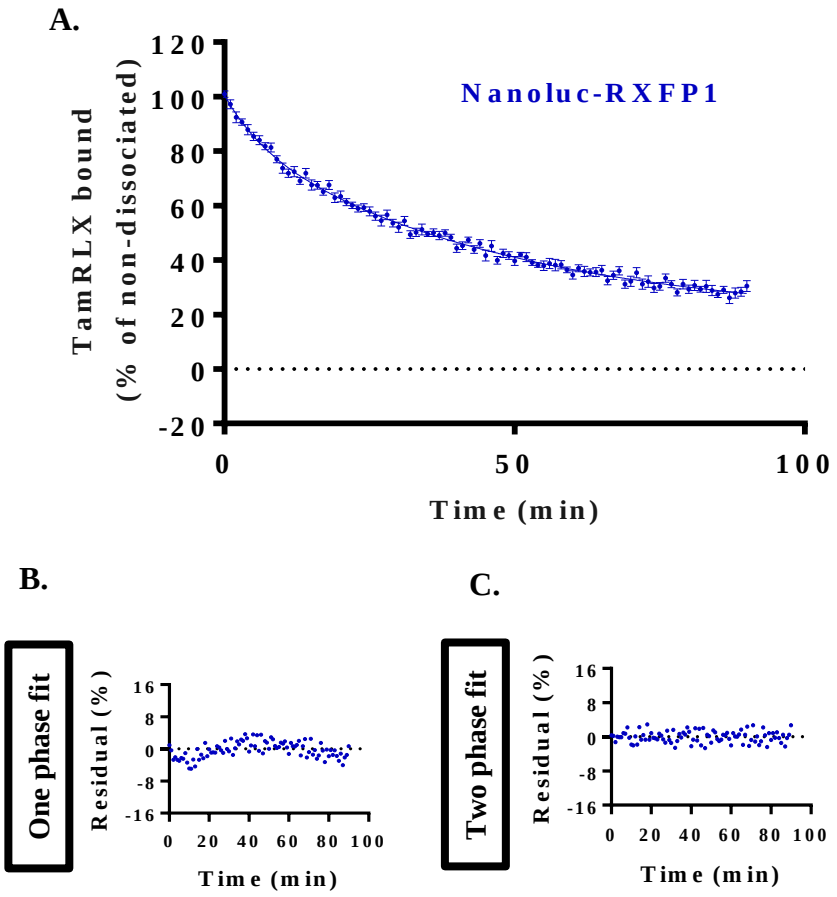

Figure 4.25. NanoBRET dissociation experiment of TamRLX from Nanoluc-RXFP1.

A. Dissociation as initiated by removal of unbound TamRLX and addition of 10 µM unlabelled relaxin. Data is pooled from 4-5 independent experiments and shown as mean ± SEM. B,C. Mean residuals for one phase decay and two phase decay respectively. From [4].

We found that dissociation of TamRLX from Nluc-RXFP2 or Nluc-RXFP2-short both fit equally well to a one- or two-phase decay function (Figure 4.26, Table 4.3), but that insertion of the RXFP1 linker residues reinstated the two-phase dissociation profile seen in RXFP1 (Figure 4.27, Table 4.3), thus highlighting the importance of the linker in the overall binding mechanism of RXFP1 as opposed to RXFP2. The rate of dissociation was somewhat faster in RXFP2 (k_{off} = 0.43 ± 0.05 min^{-1}) (Table 4.3) than that seen for RXFP1 ($k_{off\ FAST}$ = 0.15 ± 0.05 min^{-1}), probably due to the lower affinity of the ligand, but the fast component for the ExLink constructs were very similar to the off-rate of RXFP2 (ExLink1 $k_{off\ FAST}$ = 0.46 ± 0.05 min^{-1}; ExLink2 $k_{off\ FAST}$ = 0.47 ± 0.09 min^{-1}) (Table 4.3), while the percentage assigned to the fast component decreased as more linker residues were inserted (ExLink1 % fast = 79 ± 1; ExLink2 % fast = 49 ± 12; RXFP1 % fast = 19 ± 4) (Table 4.3), indicating that the presence of linker increased the influence of the slow component to the dissociation as a whole.

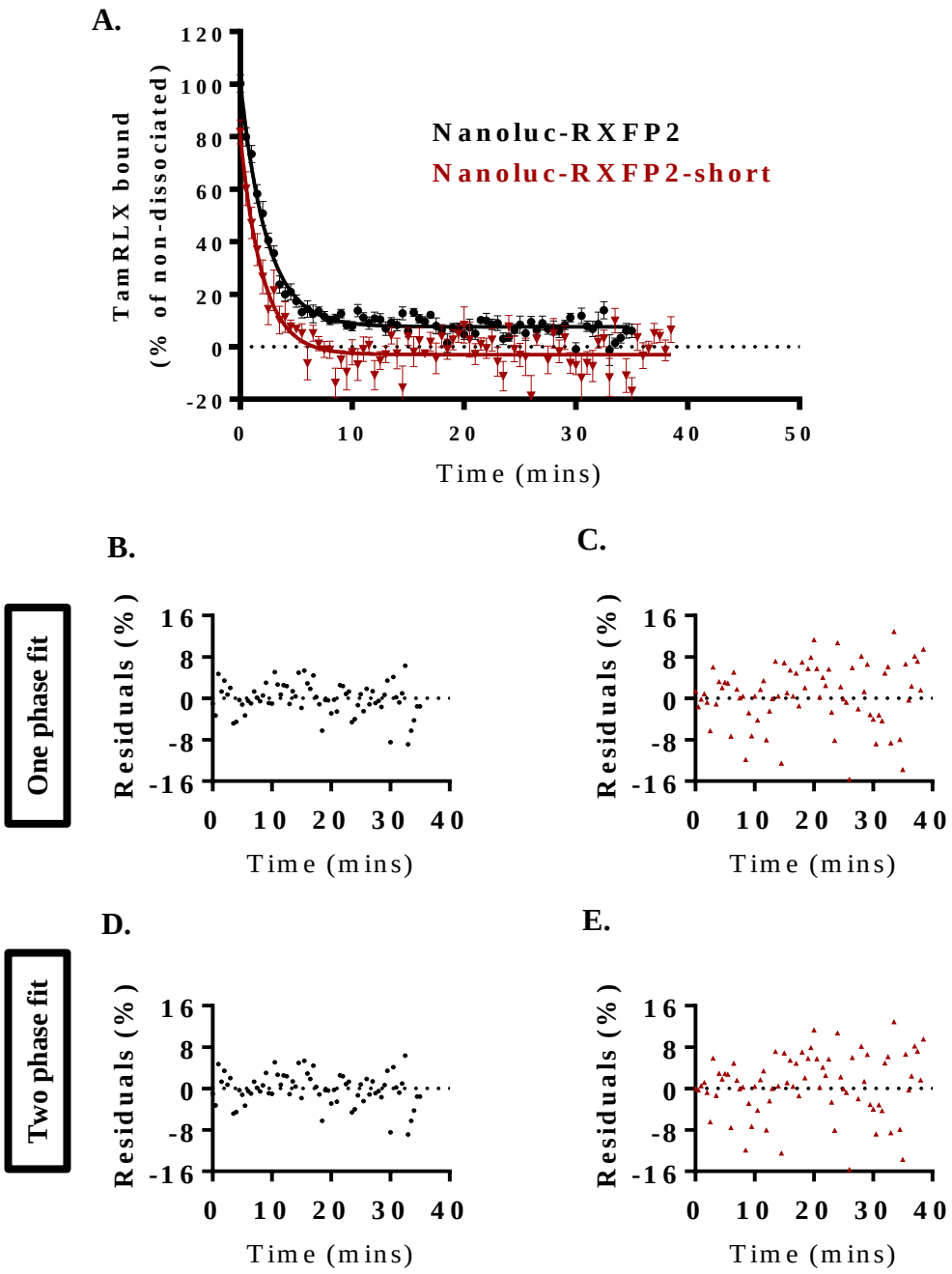

Figure 4.26. NanoBRET dissociation experiment of TamRLX from Nanoluc-RXFP2 (black) and Nanoluc-RXFP2-short (maroon),

A. Dissociation as initiated by addition of 10 µM unlabelled relaxin. Data is pooled from at least three different experiments each performed in triplicate and data is shown as mean ± SEM B, C, D, E. Associated mean residual plots for one-phase decay and two-phase decay (as labelled).

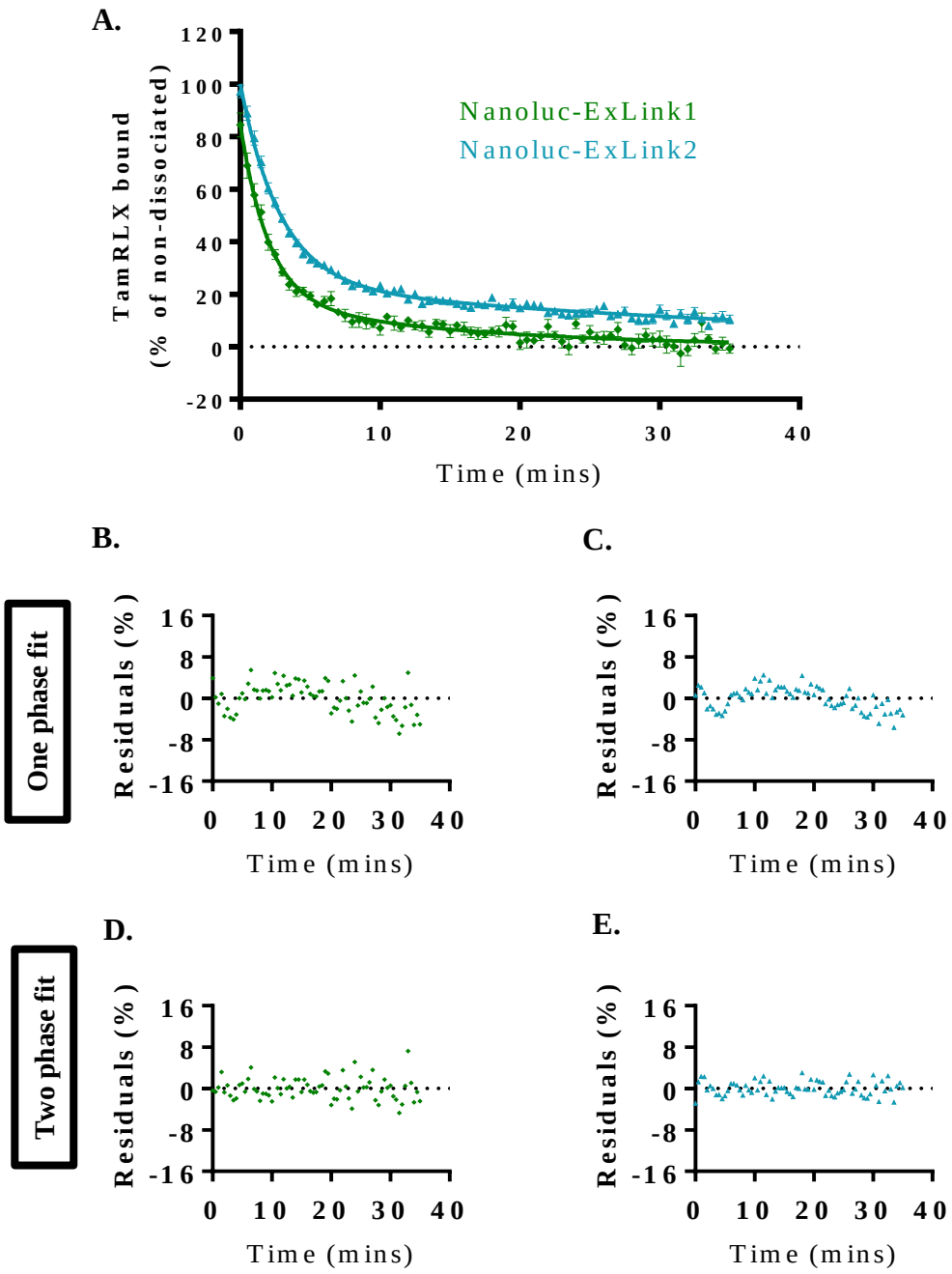

Figure 4.27. NanoBRET dissociation experiment of TamRLX from Nanoluc-ExLink1 (green) and Nanoluc-ExLink2 (teal).

A. Dissociation as initiated by addition of 10 µM unlabelled relaxin. Data is pooled from at least four different experiments each performed in triplicate and data is shown as mean ± SEM B, C, D, E. Associated mean residual plots for one-phase decay and two-phase decay (as labelled).

4.3.13 Numerical summary of data presented in this chapter

Table 4.2. Activity data for RXFP2 mutants compared to wild-type RXFP2.

Construct	Eu-INSL3 binding		Eu-relaxin binding		INSL3 activation		Relaxin activation	
	B_{max} (AU)	K_d nM	B_{max}	K_d nM	E_{max} (% RXFP2)	pEC_{50}	E_{max}† (% RXFP2)	pEC_{50}
RXFP2	23675 ± 5961 (3)	1.07 ± 0.22 (3)	19543 ± 3673 (3)	9.96 ± 0.62 (3)	100 (6)	9.99 ± 0.40 (6)	100 (6)	8.45 ± 0.15 (6)
							129.28 ± 7.1 (2) **(TamRLX)**	8.46 ± 0.25 (2) **(TamRLX)**
P4F	ND	ND	ND	ND	108.3 ± 7.62 (3)	10.55 ± 0.61 (3)	112.64 ± 21.28 (3)	9.63 ± 0.23 (3)
G42A	35678 ± 7441 (3)	1.93 ± 0.69 (3)	ND	ND	29.72 ± 7.04 (3) **	9.81 ± 0.53 (3)	75.21 ± 12.02 (3)	7.98 ± 0.55 (3)
D43A	25734 ± 10412 (3)	1.18 ± 0.15 (3)	No binding (3)		No activity (3)		No activity (3)	
T44A	32817 ± 4006 (3)	2.11 ± 0.63 (3)	ND	ND	98.66 ± 29.83 (4)	10.50 ± 0.44 (4)	53.02 ± 5.55 (3)	8.63 ± 0.40 (3)
S45A	26897 ± 5303 (3)	1.05 ± 0.20 (3)	ND	ND	92.15 ± 21.82 (3)	10.14 ± 0.20 (3)	106.95 ± 20.60 (4)	8.51 ± 0.42 (4)
G46A	34363 ± 2825 (3)	1.51 ± 0.43 (3)	No binding (3)		No activity (3)		No activity (3)	
W47A	40744 ± 10281 (3)	1.50 ± 0.41(3)	No binding (3)		No activity (3)		No activity (3)	
F51A	39612 ± 5290 (3)	1.55 ± 0.13 (3)	No binding (3)		39.76 ± 3.69 (3) *	9.36 ± 0.09 (3)	18.78 ± 5.0 (3) **	<6 (3)
F574A	6041 ± 316 (3) **	0.66 ± 0.06 (3) **	ND		51.42 ± 3.16 (3) **	10.82 ± 0.53 (3)	52.91 ± 9.76 (4) *	8.6 ± 0.48 (4)

P575A	18980 ± 5768 (3)*	1.27 ± 0.36 (3)	ND	80.56 ± 13.31 (3)	10.48 ± 0.5 (3)	86.62 ± 3.62 (3)	9.56 ± 0.29 (3)
ExLink1	ND	ND	ND	114.7 ± 7.47 (3)	10.15 ± 0.15 (3)	97.2 ± 37.8 (4)	9.48 ± 0.36 (4) *
ExLink2	48053 ± 18189 (3)	3.48 ± 1.38 (3)	ND	115 ± 5.45 (3)	10.94 ± 0.16 (3)	115 ± 27.3 (6)	9.74 ± 0.24 (6) **
Nanoluc-RXFP2	ND	ND	ND	ND	ND	99.8 ± 9.5 (3)	8.36 ± 0.12 (3)

* indicates p<0.05, ** indicates p≤0.01, *** indicates p≤0.001, **** indicates p≤0.0001 compared to RXFP2 as calculated by one-way ANOVA and uncorrected Fisher's LSD multiple comparison test. Emax: maximal cAMP response, % maximal RXFP2 activity; pEC50: H2/INSL3 potency of RXFP2 receptor ; Kd dissociation constant for relaxin or INSL3 binding; B_{max}: maximal binding; ND: not done. Number of individual assays performed in parentheses; † Max value based on 1μM activation.

Table 4.3. Summary of results from NanoBRET saturation binding and dissociation experiments performed on HEK293T cells transfected with Nanoluc-tagged receptors.

Nanoluc-tagged receptor	**Saturation binding**	**Dissociation Experiments**		
	K_d (nM)	**$k_{off\ FAST}$ (min^{-1})**	**$k_{off\ SLOW}$ (min^{-1})**	**Fast component (%)**
RXFP2	10.74 ± 1.64 (4)	*0.43 ± 0.05 (4)	-	-
ExLink1	2.74 ± 0.52 (4) ^	0.46 ± 0.05 (5)	0.04 ± 0.01	79 ± 1
ExLink2	1.17 ± 0.2 (4) ^	0.47 ± 0.09 (12)	0.085 ± 0.03	49 ± 12
RXFP2-short	15.25 ± 1.26 (3) ^	*0.61 ± 0.17 (3)	-	-
RXFP2-ECD	0.21 ± 0.02 (4) ^	ND	ND	ND

^ p < 0.0001 compared to Nluc RXFP2 as calculated by one-way ANOVA and uncorrected Fisher's LSD multiple comparison test; *k_{off} from a one-phase decay fit. Number of individual assays performed in parentheses.

4.4 Discussion

The exploration of the role of the RXFP2 linker was necessarily done with reference to the equivalent region of the homologous receptor RXFP1, since the techniques were freely available in the laboratories, and the previous study had proved so fruitful. The obvious difference between the two linkers was the length, and according to our sequence alignment, an important region of RXFP1 linker was missing from the RXFP2 counterpart. Hence, while we wanted to begin our investigation by performing an alanine scan, our experience with RXFP1 had shown that the residues of the motif GDxxGW were the most important, so we focussed our attention on these. We tested the residues individually since in RXFP1 the double mutants gave some ambiguity as to which one of the amino acids mutated was responsible for the phenotype seen, and by splitting them we were able to effectively resolve this issue. We included Phe51 in the scan as its RXFP1 equivalent had proved particularly important to relaxin signalling and binding. This shorter alanine scan for a shorter linker unveiled distinct differences in the manner in which RXFP2 responds to relaxin as opposed to INSL3, since activity was lost in a number of the linker mutants in response to either ligand (Figure 4.6B, C, Figure 4.7B, C, Table 4.2); as well as relaxin binding (Figure 4.7A, Table 4.2), but INSL3 binding was consistently maintained (Figure 4.6A, Table 4.2). This implied that the GDxxGWxxxF sequence plays an important role in RXFP2 signalling, and that this functioning is intimately connected to the relaxin binding event, despite INSL3 binding being unaffected by the mutations. Effectively, while the RXFP1 linker relaxin-binding region is absent, the non-native ligand is still able to bind in a fashion that can be interrupted by the mutation of the initial linker residues of RXFP2. Relaxin binding was therefore interrogated using our previously characterized NMR titration paradigm with a similarly designed LDLa-linker protein, $RXFP2_{(1\text{-}65)}$-GB1.

Initial HSQC spectra on $RXFP2_{(1\text{-}65)}$ showed distinct heterogeneity, particularly evidenced by the splitting of the indole resonance from W47 in the lower left corner of the spectrum (Figure 4.9A). We suspected that this was due to the cis-trans isomerisation of the peptide bond preceding Pro4, which although distant in the sequence, could be proximal to Trp47 in the folded structure, and so we mutated this to phenylalanine and observed a resulting homogeneous spectrum supporting this idea (Figure 4.9B). The same mutation did not alter the activity of the receptor in whole-cell assays (Figure 4.10) and so all further NMR work was done using this mutant. Titrations of monomeric relaxin showed a weak affinity interaction mostly involving acidic residues from the LDLa module itself, but also Asp43 from the linker.

LDLa module residues Asp30 and Glu38 are involved in calcium ligation, and thus contribute to the structural integrity of the module [258]. It would be completely conceivable for these residues to additionally interact with protein, since this is a duality commonly seen in calcium binding residues from LDLa modules on other proteins [308-310].

In order to interrogate the relaxin binding site within the RXFP1 linker more closely, we inserted the given residues into the RXFP2 linker and tested the resulting chimeras for activity and binding, making use of the newly developed NanoBRET system available in our lab. As expected, the presence of residues KYFAASY, which includes both Phe54 and Tyr58, markedly improved relaxin binding (Figure 4.24) and relaxin-induced activity in RXFP2 ExLink constructs (Figure 4.20), thus producing a more RXFP1-like version of the homologous receptor. The kinetics of the linker binding site was further explored using a dissociation assay and comparing off-rates and dynamics of dissociation of the two wild-type receptors and the extended linker versions of RXFP2. It was found that the simple addition of seven, or even just four residues from the RXFP1 linker was sufficient to alter the RXFP2 dissociation profile such that it resembled the RXFP1 profile more closely (Figure 4.27).

The titrations of $RXFP2_{(1\text{-}65)}$-GB1(P4F) with the soluble scaffold protein displaying truncated EL1 and EL2 from either RXFP1 (ssRXFP1) or RXFP2 (ssRXFP2) both showed an interaction, as expected given the interchangeability of the modules (see Chapter 2), and these interactions were highly similar to each other. There were two sites where chemical shift change was greatest, one being in the N-terminal region of the LDLa module, and the other in the linker (Figure 4.18). The fact that the two regions were distant to one another in sequence may be further evidence for the apparent wrapping around of the termini of the construct to be near to one another in the three-dimensional context. Site-directed mutagenesis of the EL2 residues Phe574 and Pro575, shown to be important to the RXFP1 linker:loop interaction, did not conclusively indicate their involvement, although the apparent low cell surface expression of the F574A mutant could mask its functional significance (Figure 4.19). Interestingly, recent results from mutagenesis of the neighbouring EL2 loop residue Leu576 (and Leu566 in RXFP1) to alanine showed a dramatic loss of signal in response to both INSL3 and relaxin, although the mutants were expressed normally on cell surfaces and ML290 activated RXFP1 L566A normally (A. Agoulnik – personal communication with supervisor). We can imagine that the conserved hydrophobic patch in EL2 may in fact be contributing to relaxin and INSL3 binding after all, whether through the peptides themselves, or residues of the linker.

The fact that there is an apparent interaction between both RXFP1 and RXFP2 LDLa-linker regions and the TM domain leads to the hypothesis that the receptors may in fact exist in a closed conformation, with a certain level of interaction occurring in the absence of ligand. The importance of a connection between the N-terminal region of the receptor ectodomain, relaxin and the transmembrane domain could also be underscored by the study of the Nanoluc-tagged receptors Nluc-RXFP2-short and Nluc-RXFP2-ECD. The minor but significant (Figure 4.23, Table 4.3) loss in relaxin affinity after removal of the LDLa module in the short receptor is consistent with the existence of a weak-affinity interaction between relaxin and the LDLa module. Conversely, the 50-fold stronger affinity for relaxin to RXFP2-ECD, compared to RXFP2 (Figure 4.23, Table 4.3), suggests that this protein may exist in an open conformation that is easily accessible to the peptide. Supporting this is the fact that INSL3, which binds RXFP1 poorly, is able to bind an equivalent RXFP1-ECD construct with relatively high affinity (pK_d = 9.28 ± 0.36) [135, 245]. This idea does suggest that the portion of linker at the N-terminus of RXFP2-short (LRR cap to Asp43) is sufficient to maintain this ectodomain in its closed conformation, such that we see a weakening and not a strengthening in binding affinity here.

Prior work focussing on relaxin and INSL3 peptide analogues shows some striking similarities to the discoveries made here. Truncation of the A-chain of relaxin gives rise to peptides that have loss in both binding and signalling at RXFP1 and RXFP2 [311]; similar truncations on the INSL3 A-chain are still able to bind RXFP2 normally, but do not signal [312]. These results mirror very closely the phenotype we observed in the linker mutants that could bind INSL3 but not relaxin and could not signal at all. Interestingly, removal of the first 9 residues of the INSL3 A-chain leads to an antagonist of INSL3, as do some B-chain only versions [252], and replacement of either the INSL3 A- or B-chain with the relaxin equivalent gives chimeric peptides that activate RXFP2 poorly [313]. A recent study on chimeric RXFP1/2 receptors in which various parts of the ectodomain were exchanged revealed that the binding of the peptide B-chains to receptor LRRs occurs in different orientations, with the relaxin B-chain α-helix sitting across the face of the LRRs at around a 45° angle, while INSL3 binds RXFP2 LRRs closer to a 90° angle [245]. The evidence presented here suggests that relaxin may bind RXFP2 in a manner more closely resembling its interaction with RXFP1 than that of INSL3 with RXFP2, but that in the absence of the correct linker sequence it cannot take on an entirely native conformation.

We propose a model in which the binding of INSL3 to RXFP2 directs reorientation of the LDLa module such that it can work in conjunction with the A-chain of INSL3 to activate the TMD. By contrast, relaxin would bind the LRRs and central portion of the linker to allow the various elements of the ectodomain (LDLa module and linker) to activate the receptor. The relaxin-RXFP2 interaction would therefore involve a binding event between relaxin and the GDxxGWxxxF motif, which then allows for the reorientation of the N-terminus of the LDLa module to participate in binding to the TMD and activating it via the exoloop interaction (Figure 4.28).

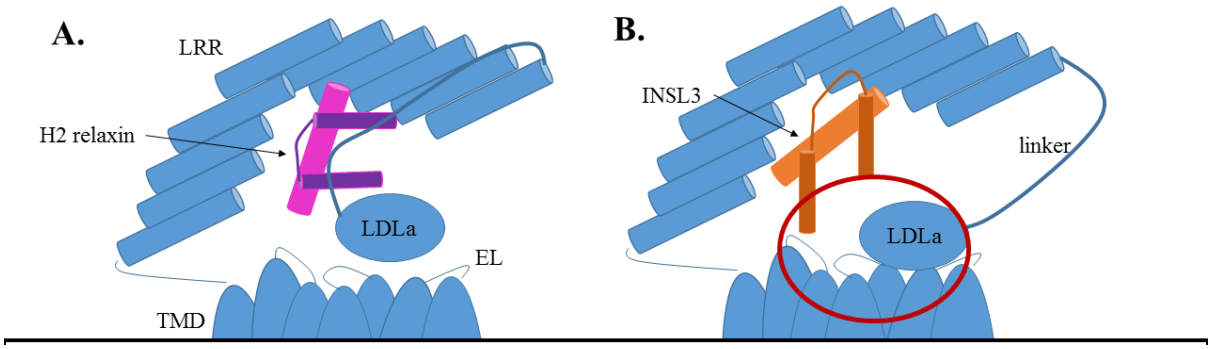

Figure 4.28. Diagrammatic representation of the extracellular portion of RXFP2 (blue) demonstrating proposed mechanism of activation in response to H2 relaxin and INSL3.

Relaxin A- and B-chains are coded purple and pink respectively, and INSL3 A- and B-chains are dark and light orange respectively. The B-chain of the two peptides sit at different orientations to one another, with relaxin at a 45° angle across a more restricted portion of the LRRs than INSL3, which requires more contacts and sits perpendicular to the LRR concave surface. While the final active conformation of receptor in response to relaxin is driven primarily by the LDLa module, the INSL3 response also involves key residues in the N-terminus of the A-chain (circled in red). From [3].

Chapter 5 General Discussion

Relaxin and INSL3 are two hormones with fundamental roles in reproductive biology. While the pleiotropic actions of relaxin throughout the body are becoming ever-more well recognized, it is now also clear that INSL3 performs a multitude of activities outside of the gonads, particularly in males. An understanding of how they function to activate their receptors at a molecular level is not only fascinating, but it paves the way for the manipulation of these systems for therapeutic benefit.

5.1 The LDLa module: a shared activation mechanism

The G-protein coupling and subsequent signal cascades initiated by hormone binding to RXFP1 and RXFP2 are mediated by their archetypal 7TM domains which, like other GPCRs, undergo a conformational change that renders them active. Rather than this change being a direct result of ligand binding however, it appears that for these unusual receptors, the final active conformation is driven by the correct positioning of their tethered LDLa modules. It has long been known that the LDLa modules of both RXFP1 and RXFP2 are required for hormone-induced activity, but prior to the start of the work presented here it was believed that the LDLa module of each of the receptors was unique to itself and could not be replaced by any similar module, and that the linkers joining the LRRs and LDLa modules were simple spacers without a functional role.

The construction of the chimeric receptors in Chapter 2 put paid to both suppositions. Firstly, we showed that we could replace the LDLa modules with that of the homologous receptor and the resulting chimeras were able to be expressed on the surfaces of cells, bind hormone and signal, although the RXFP1 receptor with an RXFP2 LDLa module (RXFP211) experienced a drop in relaxin-mediated potency and efficacy (Figure 2.4). And secondly, the design of the novel receptors such that only the LDLa modules were exchanged, with none of the neighbouring linker residues included in the swap, demonstrated the intrinsic importance of the RXFP1 linker. The exchange of the linker for the shorter RXFP2 equivalent in the experiment performed by Kern et al. [256] was very likely the reason that their chimeric receptor was non-functional.

Knowing that the receptors could in fact tolerate the replacement of their LDLa module with that of their closest relative informed us of the similarities in their activation mechanism. We went a step further, replacing the TMDs of the chimeric receptors such that they would match the non-native LDLa module, creating the constructs RXFP121 and RXFP212 (Figure 2.2). While the activity at RXFP212 upon relaxin stimulation was restored to full efficacy, its potency declined compared to RXFP211, indicating that the presence of a different TMD was detrimental to the relaxin-induced cAMP activity (Figure 2.3). The case of RXFP121 was truer to expectations, as the potency at both INSL3 and relaxin stimulation was higher than for RXFP122 where the LDLa module and TMD did not match (Figure 2.5). Nevertheless, the behaviour of all the chimeras in activity, binding and cell-surface expression assays was similar enough to that of the wild-type receptors to highlight a comparable mechanism of action with regards to their gross domain architecture.

The identification of a hydrophobic binding surface on the face of the RXFP1 LDLa module by loss- and gain-of-function studies using mutagenesis on wild-type and LB2-containing receptor [257] led to some confusion. While two of the three residues are conserved in the RXFP2 module (Figure 1.10), a similar function for these could not be found [197], which was contrary to expectations, and implied that another mechanism of LDLa-driven receptor activation must exist. This evidence, along with the inactivity of the previously characterised RXFP1-LDL2 chimera pointed to distinct differences in the modes of activation of the highly similar receptors.

5.2 The linker activation domain

Our attention was drawn to the linker, in particular the initial section with the sequence GDxxGWxxxF, that is conserved between RXFP1 and 2 and across species (Figure 1.12). Our mutagenesis campaign on the two linkers showed that the aspartic acid at linker position 2, glycine at position 5 and tryptophan at position 6 were all intimately involved in the activation of both receptors in response to either active peptide ligand. Relaxin binding at these mutants was also compromised, although for RXFP1 the affinity loss did not match the loss in signalling potency and the Eu-relaxin binding assay was not sensitive enough to show if this was the case or not for RXFP2. The result told us that the region was involved in relaxin binding to some degree but was probably not a binding site, a view that was confirmed by NMR analysis on the LDLa-linker of both receptors. Rather, we supposed that the GDxxGW motif, and possibly

also the conserved phenylalanine might make up an activation domain and be directly involved in an interaction with the TM domains. It is highly likely that the LDLa-linker occupies a peptide binding pocket within the TMD, which typically involves EL interactions [314].

5.2.1 Mapping an interaction site

The hypothesis that the LDLa-linker interacts with EL2 was supported by NMR titrations of LDLa-linker with the receptor exoloops, as displayed on the GB1 soluble scaffold. Both LDLa-linker proteins showed an interaction with EL2 of their respective loop constructs without any ligand being present. Mutagenesis on the RXFP1$_{(1\text{-}72)}$ protein confirmed the involvement of linker residues Asp42 (with Gly41), Gly45 and Trp46, and loop residue Phe564 in particular [2]. The insertion of an alanine between Cys40 and Gly41 also led to a loss of interaction, mirroring its effect in whole receptors (Figure 3.1). Given the knowledge that RXFP1 EL2 residues F564 and P565 were involved in the interaction between the LDLa module and ELs of the receptor [166, 251], we decided to test equivalent RXFP2 residues Phe574 and Pro575, mutating each one to alanine. Indeed, F574A showed some perturbation in efficacy in relaxin- and INSL3-induced cAMP signalling assays, to imply a level of involvement in this interaction, however its cell surface expression was compromised, as evidenced by the low B_{max} in Eu-INSL3 binding assays (Figure 4.19). Nevertheless, the mutant was able to elicit a cAMP signal that was not significantly different in potency from wild-type RXFP2 in response to both ligands (Figure 4.19), reflecting once again the subtle differences between the binding surface of RXFP1 compared to RXFP2.

The RXFP2$_{(1\text{-}65)}$-GB1 (P4F) protein was nevertheless able to interact with soluble scaffolds containing loops from both RXFP1 and RXFP2, reconfirming the interchangeability of the LDLa modules. However, the residues that showed the greatest chemical shift changes were all located within the LDLa module, in particular two cysteines, Cys13 and Cys26, and various C-terminal residues (Figure 4.15). This may seem to imply that LDLa residues, and not those from the linker, are interacting with EL2, however caution should be taken when making conclusions based on the movement of chemical shift positions in HSQC spectra. The divergence of certain residues on the spectrum simply shows that something has changed in the chemical environment surrounding them, and this can occur due to structural changes happening remotely within the molecule. The residue Cys26 was observed to move in all three titrations of RXFP2$_{(1\text{-}65)}$-GB1 (P4F) and this could be indicative that it is a marker of more

generalized movement within the module. Indeed, in the RXFP1$_{(1-72)}$ titration with scaffold protein, residues Met60 and others within the linker showed the greatest chemical shift change, but the mutagenesis data suggests that the interaction was localised within the GDNNGW motif (Figure 3.18).

It is also important to consider that the LDLa-linker proteins are three-dimensional structures, and that part of the linker may wrap around the rest of the module. This was implied by the splitting of the Trp46 indole as well as glycine residues in initial HSQC spectra of RXFP2$_{(1-65)}$, presumably due to the cis-trans isomerisation of the peptide bond of Pro4 in the RXFP2 sequence (Figure 5.1). If this is the case, it is easy to envisage that relaxin binding in the NMR titration could lead to chemical shift changes being observed at sequentially distant positions of the protein. A region of chemical shift change was indeed found within the RXFP2 linker and we have every reason to believe that the activation domain involving the GDxxGWxxxF sequence is conserved between RXFP1 and RXFP2, and that they have a similar modality of activation in this context. It seems reasonable to suggest that the tethered ligand occupies a classic binding pocket within the TMD, and that this pocket varies its architecture between the two receptors.

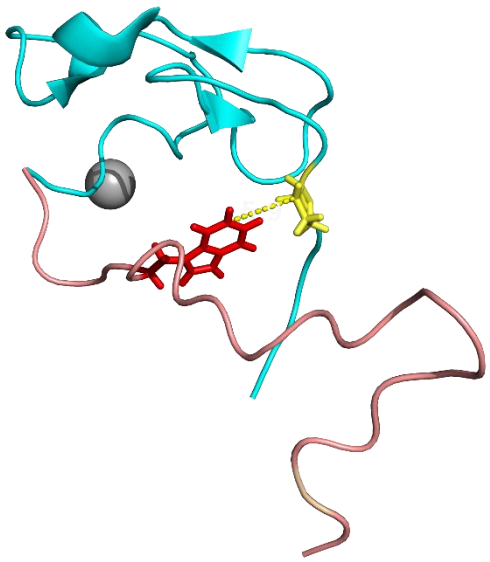

Figure 5.1. Model of RXFP2 LDL module (cyan) and linker (pink) showing potential "wrapping around" of first few residues of the linker.

In this model the side chains of Pro4 (yellow) and Trp47 (red) are within 6 Å of each other (distance shown by dotted yellow line, calculated as 5.9 Å in Pymol molecular graphics program).

Interestingly, RXFP1 loop mutant F564A also had compromised activity in response to the small molecule ML290, lending support to the notion of an overlapping binding site between the small molecule and the receptor linker, however in that study the mutant also showed poor cell surface expression consistent with a loss of structural integrity [166]. Recent developments from a collaborating lab would suggest that RXFP1-Leu566 and its RXFP2 counterpart Leu576 are implicated. The conserved leucine and phenylalanine (Phe564) residues may form a hydrophobic patch on EL2 that could interact with hydrophobic residues such as Trp46 and Phe50 from the linker. This in turn may be part of a larger binding site that corresponds in some ways to peptide-binding sites found across other Class A GPCR family members [315]. The small molecule ML290 (see section 1.6) binding site has been mapped in some detail on RXFP1, and it sits into a pocket encompassing residues from TM3, 5, 6 and 7 as well as EL2 and EL3 [316] (Figure 5.3), some of which could very well turn out to be interacting with the

linker as well. Notably, many of the residues identified are conserved in RXFP2, with some exceptions including the EL3 residue Gly659, which together with Thr660 was able to restore the affinity and activity for ML290 of mouse RXFP1 when mutated back to the human sequence [142]. This shows that while ML290 does not activate RXFP2, there could still be some shared residues in its linker binding pocket with the ML290 binding-site of RXFP1.

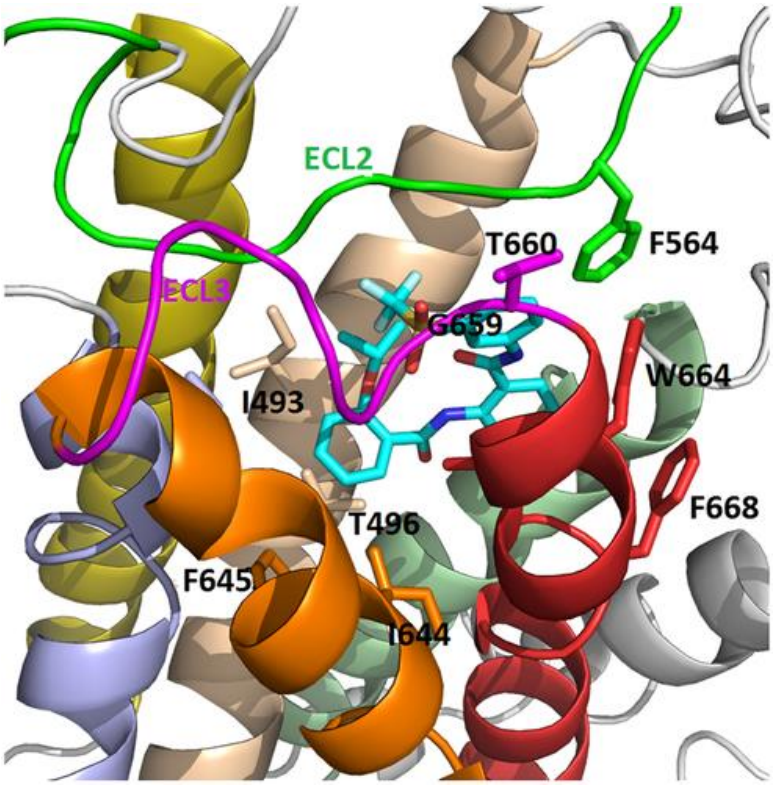

Figure 5.2. Model of binding site of ML290 with human RXFP1.

ML290 is shown in cyan with O atoms in red and N in blue. Key residues involved in the binding interaction are labelled and receptor parts are colour-coded with TM3 brown, TM5 blue, TM6 orange, TM7 red, EL2 green and EL3 in magenta. Figure taken from [316].

5.2.2 Is the ectodomain open or closed?

The interactions between the RXFP1 and RXFP2 LDLa-linker and the ELs as displayed on the soluble scaffold proteins ssRXFP1 and ssRXFP2, occurred in the absence of external peptide ligand (Figure 4.18). This may be evidence of an interaction between the LDLa-linker and EL2 in the receptor Apo state, resulting in a closed conformation of the ectodomain (Figure 5.2). This theory is supported by the fact that the single-chain relaxin derivative B7-33 (see section 1.6) can bind to the ECD of both RXFP1 and RXFP2 when they are not accompanied by their respective TMDs, but rather attached to a single TM helix anchor. The affinity of B7-33 for the RXFP1-ECD (K_i = 8.9 nM) is still much stronger than that for the RXFP2-ECD (K_i = 400 nM), but when the receptors are whole it has a much weaker affinity for both when expressed in HEK cells (B7-33 on RXFP1 pK_i = 5.54; no activity at RXFP2 [139]). Further evidence for the closed conformation hypothesis is the high affinity of INSL3 for RXFP1-ECD (pK_d = 9.28) compared to its extremely low affinity for RXFP1 [135, 245].

A. **B.**

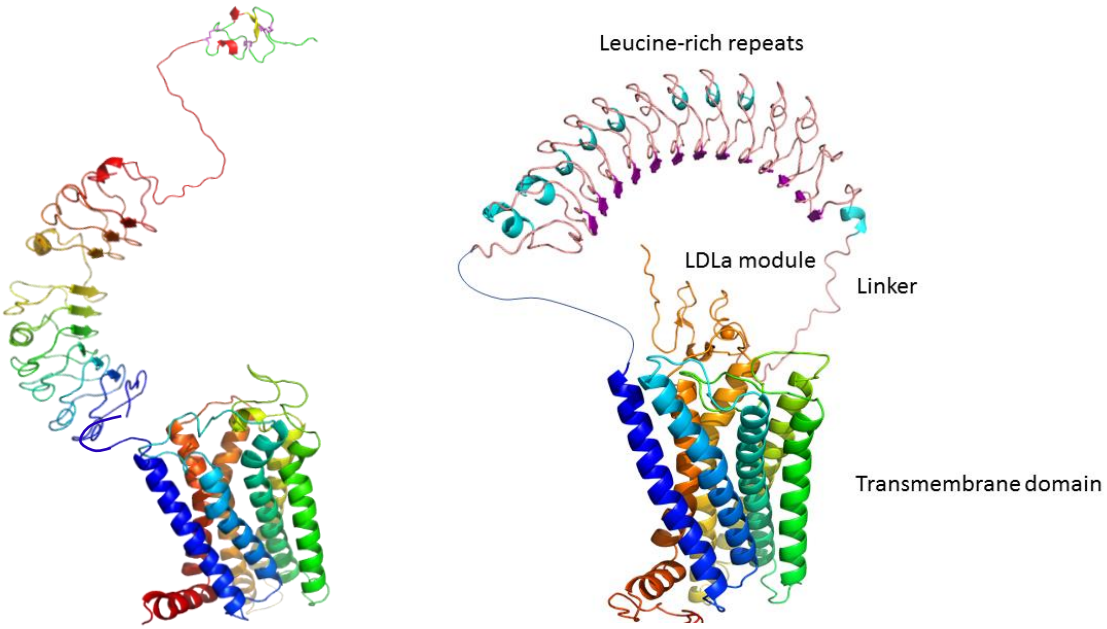

Figure 5.3. Models of RXFP1/RXFP2 demonstrating the concept of an open (A) versus closed (B) conformation.

An open receptor would have an ectodomain that protrudes into the extracellular space, with the LDLa module positioned far from the TMD, while a closed conformation is one where the LDLa module and/or linker is connected to the TMD via non-covalent interactions.

5.2.3 Differences in the mode of activation between RXFP1 and RXFP2

The differences between the responses of the linker mutants of RXFP2 to relaxin vs the native ligand INSL3 highlighted important differences in the way RXFP2 behaves depending on the ligand activating it, as well as its differences and similarities to RXFP1. The weakened relaxin potency of D43A, G46A, W47A and F51A of RXFP2 were slightly greater than that of the equivalent RXFP1 mutants, and this was closely mirrored in their inability to bind Eu-Relaxin at the concentrations we were able to use (Figure 3.9, Figure 4.7). However, while the INSL3 activity was also compromised to an enormous extent, there was no effect on Eu-INSL3 binding (Figure 4.6). Previous studies on mutant and truncated peptides of relaxin and INSL3 demonstrated remarkable similarities with this phenotype. Truncation of the A-chain of relaxin up to Cys9, which is involved in a disulphide bond, led to peptides that had a progressive reduction of both binding affinity and signalling potency at RXFP1 and RXFP2 as the A-chain grew shorter [255]. This gradual loss of function is similar to the activity loss of relaxin on mutants of both receptors from the GDxxGW motif in the linker. In contrast, A-chain truncations of INSL3 up to Cys10 were able to bind RXFP2 normally, while experiencing a severe reduction in their ability to stimulate cAMP [254]. This difference in function again reflects the activation profile of the GDxxGW linker mutants from RXFP2, all of which can bind INSL3 similar to wild-type, despite binding relaxin weakly and showing extremely diminished activity for both ligands. Interestingly, these INSL3 mutants were able to act as antagonists of INSL3-mediated RXFP2 activation, while the truncated relaxin analogues showed no such antagonist activity at either receptor [254, 255]. The findings from the peptide studies pointed to the presence of an activation region within the N-terminal tail of the INSL3 peptide, which when mutated mirrors the mutations within the RXFP2 activation region GDxxGWxxxF (Figure 5.5). It is yet to be shown whether these two regions interact with each other, or if they interact with unknown regions in the 7TM domain to bring about an active conformation of RXFP2.

5.3 The linker-relaxin binding site

Leaving the activation region behind, we identify a novel, yet integral relaxin binding site within the central portion of the RXFP1 linker. Comparing the relative loss of potency in signalling assays with affinity loss in binding assays by the mutants F54A and F54A/Y58A demonstrates that these were more likely to be directly involved in relaxin binding than the initial linker residues (GDNNGW), as the fold differences were very similar. We assumed that

this was an indication that the loss of relaxin binding was directly leading to the loss of signalling efficiency that we were observing, and again, the NMR data supported the hypothesis. Competition with A-chain derivatives of relaxin in the NMR titrations showed that the interaction was likely occurring here, and structural experiments showed that the linker around this region was helical. The helix would in turn be extended and stabilised in the presence of ligand (Figure 3.17).

One linker residue that may both directly bind relaxin and activate is the central phenylalanine RXFP1 Phe50 (or RXFP2 Phe51). As mentioned in Chapter 3, the residue has the capacity to contribute to the relaxin binding site, being that it is 3 residues upstream of our identified helix surface Phe54/Tyr58, but it is also close to Trp46 and conserved in RXFP2. Its activity at RXFP1 was more highly perturbed than its binding affinity for relaxin, suggesting a role in the activation region (Figure 3.12, 3.13), but at RXFP2 it was completely non-responsice to relaxin stimulation while maintaining its activity with INSL3 to a degree (Figure 4.6, 4.7). The insertion of an alanine residue beside Phe50 in RXFP1 similarly disrupted its activity and binding (Figure 3.16). It is possible that this residue forms a linkage between the two regions and can contribute to both relaxin binding and receptor activation.

The lack of a binding site for relaxin within the RXFP2 linker gave us the opportunity to further verify the functional role of the RXFP1 linker-relaxin binding site by inserting the implicated residues into an equivalent position of RXFP2. We did this in both the full-length receptor and the newly cloned Nanoluc-tagged RXFP2. The extended linker (ExLink) constructs showed improved relaxin activity and binding compared to RXFP2, approaching RXFP1 levels, although not reaching full RXFP1 equivalence, and the development of the BRET saturation binding assay allowed us to monitor this change accurately, using relaxin concentrations up to 100 nM. The remarkable 5-fold increase in affinity of relaxin for Nluc-ExLink1 and 10-fold increase for Nluc-ExLink2 (Figure 4.21) confirmed that this short stretch of amino acids was vital to the relaxin binding mode at RXFP1.

The other advantage of the BRET system was that it allowed us to do kinetic analysis of the interaction and compare dissociation rates and modes between the wild-type receptors and the ExLink chimeras. We found that while the off-rate was very similar at RXFP2 and the extended linker versions, reflecting their higher K_d's compared to RXFP1, the mode with which the ExLink receptors dissociated resembled that of RXFP1 more than that of RXFP2. We judged this parameter by observing the associated residual plots after fitting a one-phase or a two-

phase exponential decay function to the data. The fit of RXFP2 to these two functions was statistically the same (Figure 4.23), whereas RXFP1 and the two ExLinks both fit to a two-phase equation (Figure 4.24), suggesting a more complex binding mechanism. The splice variant RXFP2-short also showed no improvement in fit between the two different functions (Figure 4.23).

5.4 The binding and activation mechanisms of RXFP1 and RXFP2

It would be tempting to conclude that relaxin binds RXFP1 first at the LRRs, then at the linker and finally at the ELs, however we resist the urge to put the events into a given order. Based on the evidence at our disposal, we cannot say in what precise order the different contacts are being made, only that multiple components are involved at certain sites within the receptor and hormone. Now it is possible to map these sites with fairly high accuracy and to add insight to the existing models of hormone activation of these receptors.

For RXFP1, the highest affinity binding site remains that between the arginine cassette on the relaxin B-chain and the LRRs, as outlined in the general introduction. The extracellular loops, in particular EL2, probably interact with both relaxin and the LDLa-linker, but whether relaxin is instrumental in bringing the tethered ligand into contact with the ELs or simply assists in rearranging the pre-coupled receptor components into an active conformation is still unknown. It is fairly certain that EL2 is capable of interacting specifically with both relaxin and the LDLa-linker with K_d's in the micromolar range [2, 251], but the effect of one interaction on the other is less clear. Combining three components in an NMR tube provides data that is hard to disentangle and interpret. The linker interaction with relaxin is quite well defined at this point, with an approximate K_d of around 200 µM. We calculated that the LRR interaction must have an actual K_d around 1 µM such that the overall K_d of relaxin for its receptor be less than 1 nM. It was later shown using the Nluc-tagged ECD of RXFP1 that the K_d of the interaction between the LRRs and TamRLX is 121 ± 5.9 nM [4].

The mechanism of INSL3 activation of RXFP2 differs from both the relaxin-RXFP1 interaction and that of relaxin with RXFP2. The lack of a linker binding site is a major defining point, but the orientation of the hormone on the LRRs and therefore the positioning of the peptide and tethered ligand on the ELs and TMD may also be different. The presence of the INSL3 A-chain activation region defines a major difference in its functionality compared to that of relaxin. This may serve to explain why B-chain only analogues of INSL3 are antagonists

at RXFP2, since they compete for the LRR binding site, but cannot activate the receptor, while B7-33 is functional at RXFP1 (see section 1.6 and below) [139]. Figures 5.4 and 5.5 outline the current mechanisms of activation of RXFP1 and RXFP2 in response to their peptide ligands as elucidated during this project. The work presented here has highlighted the similarities and differences between the modes of activation between the receptors and also between the different hormone activity at RXFP2, but the details still require some clarification.

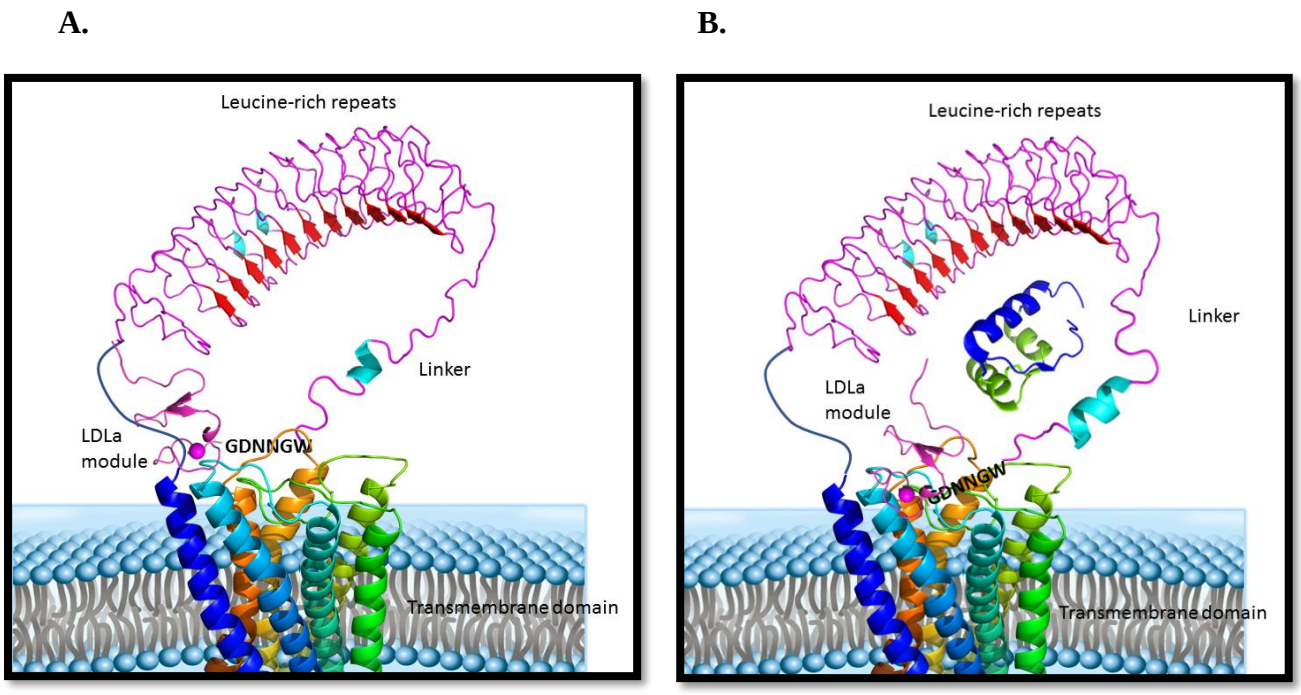

Figure 5.4. Models of the activation of RXFP1 in response to relaxin binding.

A. LDLa-linker (pink) may be pre-coupled to ELs and other parts of TMD via GDNNGW motif. Linker contains partial turn of a helix (cyan). B. Upon relaxin binding at LRRs (purple/red) via B-chain (blue), and at linker via A-chain (green), linker helix is extended and stabilized, and linker activation domain sinks deeper in peptide-binding pocket of TMD, inducing active conformation of receptor. Membrane image from [317].

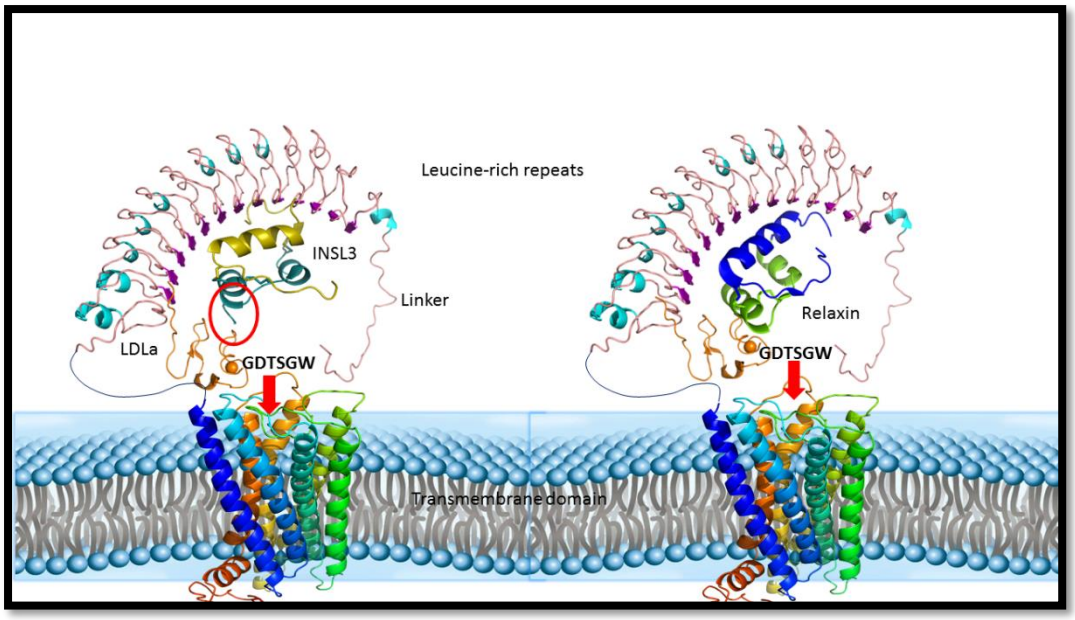

Figure 5.5. Differential activation of RXFP2 in response to INSL3 (left) and relaxin (right).

Unbound receptor may have LDLa-linker pre-coupled to TMD, and ligand binding occurs via B-chain (yellow-INSL3; blue-relaxin) at LRRs, but in different orientations. Combination of GDTSGW activation region of linker and INSL3 A-chain (circled in red) cause LDLa-linker to activate receptor via contacts within peptide-binding domain of TMD, including ELs, as shown by red arrows. Membrane image from [317].

5.5 Perspectives and future directions

This project has been instrumental in revealing important aspects of the complex activation mechanism of the GPCRs RXFP1 and RXFP2. Nevertheless, a caveat must be mentioned in order to put the new information into the context of the literature surrounding these receptors. The activity of the molecule B7-33, which can activate RXFP1 robustly in fibroblasts [139], puts doubt onto the necessity of the linker binding interaction in some native cells. The activation profile of B7-33 in HEK-RXFP1 cells and natively expressing THP-1 cells is similar to the response to relaxin in some of the linker mutants (B7-33 on human RXFP1 pEC50 = 5.12 ± 0.06; relaxin on RXFP1 (D42A) < 6; relaxin on RXFP1 (G45A) = 7.48 ± 0.57; relaxin on RXFP1 (W46A) = 7.02 ± 0.18) (Table 3.3.6). This implies that at high enough concentrations, the B-chain of relaxin can activate the receptor alone, without the requirement of the linker interaction, just as at high relaxin concentrations mutant RXFP1 can also be coaxed into an active conformation. Notably, the peptide can bind to the ectodomains of both

RXFP1 and RXFP2, giving credence to a closed ectodomain model for the receptors. B7-33 can also activate RXFP2 at 10 μM concentrations, fitting well with its affinity for RXFP2-ECD. It is perplexing then, that the response to B7-33 in fibroblasts is equivalent to that of relaxin, but we could postulate that the activation mechanism may differ according to cellular background, as reflected in the highly variable signalling profile observed in different contexts [104]. Alternatively, it could be a manifestation of ligand bias in different cell types. A similar cAMP response of RXFP2 linker mutants at high ligand concentration was not seen, with RXFP2 mutants D43A, G46A and W47A showing no activity up to the highest concentrations of relaxin or INSL3 used (Table 4.3.13), indicating that the linker activation domain is absolutely required for RXFP2 function, although no data exists in native cells to dispute this.

The other aspect that could contribute to the seeming functional selectivity of B7-33 is the presence of membrane-bound or other molecules that regulate RXFP1 function. Numerous splice variants have been identified that may play a role in modulating the actions of both receptors [199, 201], including the RXFP2-short construct used here, which decreases the signal when co-expressed with wild-type, as does a soluble RXFP1 LDLa module [200]. Multiple dimerization partners, and members of larger complexes may also contribute to receptor function, including those that have already been identified such as the angiotensin II receptors AT_1R and AT_2R [114, 116] and constituents of the RXFP1 signalosome [122], as well as the potential involvement of proteins identified with other GPCR function, such as the receptor-activity modulating proteins (RAMPs) [318]. RXFP1 and RXFP2 are known to be trafficked to the plasma membrane from the ER as obligate dimers, and to exist as both homo- and heterodimers *in vitro* [187, 188], and the possibility remains that they may also function as dimers in some contexts. This phenomenon may have some role in explaining why dose-response curves for relaxin are bell-shaped in a number of experimental and clinical paradigms [108]. The combination of multiple binding sites on the insulin and IGF receptors gives a symmetrical overall structure, that can still only bind a single ligand at a time, as it is subject to negative cooperativity and fits well to a harmonic oscillator model of activation [186]. A similar structure for the relaxin receptors is hard to envisage, and more recent work suggests that RXFP1 does not function as a dimer [189]. Nonetheless, negative cooperativity has been reported for both receptors [187, 188], and the possibility cannot be excluded.

The structural elucidation of the ectodomain components of RXFP1 and RXFP2 are helping to paint a fuller picture of these unusual receptors. The presence of a tethered ligand on a GPCR is not unique, and they are found in various forms on rhodopsin, PARs, adhesion GPCRs and the glycoprotein hormone receptors (GPHR) (reviewed in [319]). In these other GPCRs the tethered ligand is usually located close to the TMD, and some external signal allows it to meet the TM helices, either to relieve an inverse agonist action, or activate the receptor directly. The affinity of these tethered ligands is not needed to be very high, since they are present in equimolar concentration along with the receptor. In the case of RXFP1 and RXFP2, the tethered agonist is at the far end of the ectodomain, although it is possible that it is pre-coupled when the receptor is in its Apo state (see above). It is plausible that the LDLa-linker can make contacts with the ELs and TMD that change when they move from an inactive to an active state. However, RXFP1 variants lacking the LDLa-linker or entire ectodomain that are not constitutively active, can be activated by ML290 which also activates an RXFP1 TM only variant, indicating that the tethered ligand does not hold the receptor in an inactive state, and neither does the hinge region, as is the case with the GPHRs (see section 1.13).

Overall the hormone binding and activation of the receptors RXFP1 and RXFP2 is complex, involving multiple receptor domains and regions, as well as external factors that modulate their function. The two receptors are highly similar, and close evolutionary relatives, but they are not identical, and the way that they work is not the same. We have been able to drill down on a section of their large ectodomain, called, perhaps inappropriately, the linker, and reveal its integral involvement in both receptors' activation mechanism. This information is useful when trying to put together a detailed description of receptor function, especially given that structures of the whole receptors, or even their ectodomains are still lacking. The elucidation of a structure for one or both receptors would clarify several open questions about how they bind ligand and activate via LDLa and linker-mediated interactions with the TMD, but until then, we can continue to piece together the growing network of information at our disposal.

REFERENCES

1. Bruell, S., et al., *Chimeric RXFP1 and RXFP2 Receptors Highlight the Similar Mechanism of Activation Utilizing Their N-Terminal Low-Density Lipoprotein Class A Modules.* Front Endocrinol (Lausanne), 2013. **4**: p. 171.
2. Sethi, A., et al., *The complex binding mode of the peptide hormone H2 relaxin to its receptor RXFP1.* Nat Commun, 2016. **7**: p. 11344.
3. Bruell, S., et al., *Distinct activation modes of the Relaxin Family Peptide Receptor 2 in response to insulin-like peptide 3 and relaxin.* Sci Rep, 2017. **7**(1): p. 3294.
4. Hoare, B.L., et al., *Multi-component mechanism of H2 relaxin binding to RXFP1 through NanoBRET Kinetic analysis.* iScience, 2018.
5. Olinski, R.P., L.-G. Lundin, and F. Hallböök, *Conserved Synteny Between the Ciona Genome and Human Paralogons Identifies Large Duplication Events in the Molecular Evolution of the Insulin-Relaxin Gene Family.* Molecular Biology and Evolution, 2006. **23**(1): p. 10-22.
6. Bathgate, R.A.D., et al., *The relaxin receptor as a therapeutic target – perspectives from evolution and drug targeting.* Pharmacology & Therapeutics, 2018. **187**: p. 114-132.
7. Mita, M., et al., *A relaxin-like peptide purified from radial nerves induces oocyte maturation and ovulation in the starfish, Asterina pectinifera.* Proc Natl Acad Sci U S A, 2009. **106**(23): p. 9507-12.
8. Yegorov, S. and S. Good, *Using paleogenomics to study the evolution of gene families: origin and duplication history of the relaxin family hormones and their receptors.* PloS one, 2012. **7**(3): p. e32923.
9. Garelli, A., et al., *Imaginal Discs Secrete Insulin-Like Peptide 8 to Mediate Plasticity of Growth and Maturation.* Science, 2012. **336**(6081): p. 579-582.
10. Eigenbrot, C., et al., *X-ray structure of human relaxin at 1.5 A. Comparison to insulin and implications for receptor binding determinants.* J Mol Biol, 1991. **221**(1): p. 15-21.
11. Rosengren, K.J., et al., *Solution structure and novel insights into the determinants of the receptor specificity of human relaxin-3.* J Biol Chem, 2006. **281**(9): p. 5845-51.
12. Rosengren, K.J., et al., *Solution structure and characterization of the LGR8 receptor binding surface of insulin-like peptide 3.* J Biol Chem, 2006. **281**(38): p. 28287-95.
13. Haugaard-Jonsson, L.M., et al., *Structure of human insulin-like peptide 5 and characterization of conserved hydrogen bonds and electrostatic interactions within the relaxin framework.* Biochem J, 2009. **419**(3): p. 619-27.
14. Kong, R.C., et al., *Membrane receptors: structure and function of the relaxin family peptide receptors.* Mol Cell Endocrinol, 2010. **320**(1-2): p. 1-15.
15. Hisaw, F.L., *Experimental relaxation of the pubic ligament of the guinea pig.* Experimental Biology and Medicine, 1926. **23**(8): p. 661-663.
16. Hudson, P., et al., *Relaxin gene expression in human ovaries and the predicted structure of a human preprorelaxin by analysis of cDNA clones.* The EMBO Journal, 1984. **3**(10): p. 2333-2339.
17. Adham, I.M., et al., *Cloning of a cDNA for a novel insulin-like peptide of the testicular Leydig cells.* J Biol Chem, 1993. **268**(35): p. 26668-72.
18. Conklin, D., et al., *Identification of INSL5, a new member of the insulin superfamily.* Genomics, 1999. **60**(1): p. 50-6.
19. Hsu, S.Y., *Cloning of two novel mammalian paralogs of relaxin/insulin family proteins and their expression in testis and kidney.* Mol Endocrinol, 1999. **13**(12): p. 2163-74.
20. Ivell, R. and R.A.D. Bathgate, *Reproductive Biology of the Relaxin-Like Factor (RLF/INSL3) ¹*. Vol. 67. 2002: SPIE. 7.
21. Wilkinson, T.N., et al., *Evolution of the relaxin-like peptide family.* BMC Evolutionary Biology, 2005. **5**(1): p. 14.

22. Tang, J.-G., et al., *Human gene 2 relaxin chain combination and folding.* Biochemistry, 2003. **42**(9): p. 2731-2739.
23. Bullesbach, E.E., S. Yang, and C. Schwabe, *The receptor-binding site of human relaxin II. A dual prong-binding mechanism.* J Biol Chem, 1992. **267**(32): p. 22957-60.
24. Menting, J.G., et al., *How insulin engages its primary binding site on the insulin receptor.* Nature, 2013. **493**(7431): p. 241.
25. Bathgate, R.A., et al., *International Union of Pharmacology LVII: recommendations for the nomenclature of receptors for relaxin family peptides.* Pharmacol Rev, 2006. **58**(1): p. 7-31.
26. Good, S., et al., *New insights into ligand-receptor pairing and coevolution of relaxin family peptides and their receptors in teleosts.* International Journal of Evolutionary Biology, 2012. **2012**.
27. Matsumoto, M., et al., *The novel G-protein coupled receptor SALPR shares sequence similarity with somatostatin and angiotensin receptors.* Gene, 2000. **248**(1-2): p. 183-9.
28. Boels, K. and H.C. Schaller, *Identification and characterisation of GPR100 as a novel human G-protein-coupled bradykinin receptor.* Br J Pharmacol, 2003. **140**(5): p. 932-8.
29. Bathgate, R.A., et al., *Relaxin family peptides and their receptors.* Physiol Rev, 2013. **93**(1): p. 405-80.
30. Weiss, G., E.M. O'Byrne, and B.G. Steinetz, *Relaxin: a product of the human corpus luteum of pregnancy.* Science, 1976. **194**(4268): p. 948-9.
31. Stewart, D.R., et al., *Relaxin in the peri-implantation period.* J Clin Endocrinol Metab, 1990. **70**(6): p. 1771-3.
32. Khan-Dawood, F.S., et al., *Human corpus luteum secretion of relaxin, oxytocin, and progesterone.* J Clin Endocrinol Metab, 1989. **68**(3): p. 627-31.
33. Eddie, L.W., et al., *Radioimmunoassay of relaxin in pregnancy with an analogue of human relaxin.* Lancet, 1986. **1**(8494): p. 1344-6.
34. Eppel, W., E. Kucera, and C. Bieglmayer, *Relationship of serum levels of endogenous relaxin to cervical size in the second trimester and to cervical ripening at term.* Br J Obstet Gynaecol, 1999. **106**(9): p. 917-23.
35. Bogic, L.V., M. Mandel, and G.D. Bryant-Greenwood, *Relaxin gene expression in human reproductive tissues by in situ hybridization.* The Journal Of Clinical Endocrinology And Metabolism, 1995. **80**(1): p. 130-137.
36. Sherwood, O.D., et al., *Radioimmunoassay of relaxin throughout pregnancy and during parturition in the rat.* Endocrinology, 1980. **107**(3): p. 691-8.
37. Tashima, L.S., G. Mazoujian, and G.D. Bryantgreenwood, *Human Relaxins in Normal, Benign and Neoplastic Breast-Tissue.* Journal of Molecular Endocrinology, 1994. **12**(3): p. 351-364.
38. Sokol, R.Z., et al., *Immunohistochemical localization of relaxin in human prostate.* J Histochem Cytochem, 1989. **37**(8): p. 1253-5.
39. Ivell, R., et al., *Relaxin family peptides in the male reproductive system—a critical appraisal.* Molecular Human Reproduction, 2011. **17**(2): p. 71-84.
40. Hsu, S.Y., et al., *Activation of orphan receptors by the hormone relaxin.* Science, 2002. **295**(5555): p. 671-4.
41. Krajnc-Franken, M.A., et al., *Impaired nipple development and parturition in LGR7 knockout mice.* Molecular and cellular biology, 2004. **24**(2): p. 687-696.
42. Samuel, C.S. and E.P. Amento, *Relaxin knockout mice demonstrate delayed growth and have underdeveloped male reproductive tracts*, in *Relaxin 2000*. 2001, Springer. p. 221-223.
43. Steinetz, B., et al., *Hormonal regulation of the connective tissue of the symphysis pubis.* Biology of Relaxin and its Role in the Human, 1983: p. 71-92.
44. Bathgate, R., A. Hsueh, and O. Sherwood, *Physiology and molecular biology of the relaxin peptide family.* Physiology of reproduction, 2006: p. 679-770.
45. MacLennan, A.H., P. Grant, and G. Bryant-Greenwood, *hRLX-1. In vitro response of human and pig myometrium.* J Reprod Med, 1995. **40**(10): p. 703-6.

46. MacLennan, A.H., et al., *Ripening of the human cervix and induction of labor with intracervical purified porcine relaxin.* Obstet Gynecol, 1986. **68**(5): p. 598-601.
47. Bathgate, R.A.D., et al., *Relaxin family peptides and their receptors.* Physiological Reviews, 2013(1).
48. Einspanier, A., et al., *Relaxin supports implantation and early pregnancy in the marmoset monkey.* Ann N Y Acad Sci, 2009. **1160**: p. 140-146.
49. Johnson, M.R., et al., *Relaxin levels in ovum donation pregnancies.* Fertil Steril, 1991. **56**(1): p. 59-61.
50. Conrad, K.P. and J. Novak, *Emerging role of relaxin in renal and cardiovascular function.* American Journal of Physiology-Regulatory, Integrative and Comparative Physiology, 2004. **287**(2): p. R250-R261.
51. Teerlink, J.R., et al., *Serelaxin, recombinant human relaxin-2, for treatment of acute heart failure (RELAX-AHF): a randomised, placebo-controlled trial.* The Lancet, 2013. **381**(9860): p. 29-39.
52. Samuel, C.S., et al., *The Relaxin Gene-Knockout Mouse: A Model of Progressive Fibrosis.* Annals of the New York Academy of Sciences, 2005. **1041**(1): p. 173-181.
53. Samuel, C.S., et al., *The relaxin gene knockout mouse: a model of progressive scleroderma.* Journal of investigative dermatology, 2005. **125**(4): p. 692-699.
54. Kapila, S., W. Wang, and K. Uston, *Matrix Metalloproteinase Induction by Relaxin Causes Cartilage Matrix Degradation in Target Synovial Joints.* Ann N Y Acad Sci, 2009. **1160**: p. 322-328.
55. Bani-Sacchi, T., et al., *Relaxin-induced increased coronary flow through stimulation of nitric oxide production.* Br J Pharmacol, 1995. **116**(1): p. 1589-94.
56. Bani, D., et al., *Relaxin activates the L-arginine-nitric oxide pathway in vascular smooth muscle cells in culture.* Hypertension, 1998. **31**(6): p. 1240-7.
57. Ferlin, A., et al., *Relaxin stimulates osteoclast differentiation and activation.* Bone, 2010. **46**(2): p. 504-513.
58. Duarte, C., et al., *RELAXIN enhances differentiation and matrix mineralization through Relaxin/insulin-like family peptide receptor 2 (Rxfp2) in MC3T3-E1 cells in vitro.* Bone, 2014. **65**: p. 92-101.
59. Ferlin, A., et al., *Relaxin and insulin-like peptide 3 in the musculoskeletal system: from bench to bedside.* Br J Pharmacol, 2017. **174**(10): p. 1015-1024.
60. Ferlin, A., et al., *Relaxin and insulin-like peptide 3 in the musculoskeletal system: from bench to bedside.* British Journal of Pharmacology, 2017. **174**(10): p. 1015-1024.
61. Dschietzig, T., et al., *RXFP1-inactive relaxin activates human glucocorticoid receptor: further investigations into the relaxin-GR pathway.* Regulatory Peptides, 2009. **154**(1-3): p. 77-84.
62. Bartholome, B., et al., *Membrane glucocorticoid receptors (mGCR) are expressed in normal human peripheral blood mononuclear cells and up-regulated after in vitro stimulation and in patients with rheumatoid arthritis.* The FASEB journal, 2004. **18**(1): p. 70-80.
63. Ayrout, M., et al., *A novel non genomic glucocorticoid signaling mediated by a membrane palmitoylated glucocorticoid receptor cross talks with GnRH in gonadotrope cells.* Scientific Reports, 2017. **7**(1): p. 1537.
64. Dschietzig, T., et al., *Relaxin improves TNF-α-induced endothelial dysfunction: the role of glucocorticoid receptor and phosphatidylinositol 3-kinase signalling.* Cardiovascular Research, 2012. **95**(1): p. 97-107.
65. Ma, S., et al., *Comparative localization of leucine-rich repeat-containing G-protein-coupled receptor-7 (RXFP1) mRNA and [33P]-relaxin binding sites in rat brain: Restricted somatic co-expression a clue to relaxin action?* Neuroscience, 2006. **141**(1): p. 329-344.
66. Piccenna, L., et al., *Localization of LGR7 Gene Expression in Adult Mouse Brain Using LGR7 Knock-out/LacZ Knock-in Mice: Correlation with LGR7 mRNA Distribution.* Annals of the New York Academy of Sciences, 2005. **1041**(1): p. 197-204.

67. Gundlach, A.L., et al., *Relaxin family peptides and receptors in mammalian brain.* Annals of the New York Academy of Sciences, 2009. **1160**(1): p. 226-235.
68. Thanasupawat, T., et al., *RXFP1 is targeted by complement C1q tumor necrosis factor-related factor 8 in brain cancer.* Frontiers in endocrinology, 2015. **6**: p. 127.
69. Kumagai, J., et al., *INSL3/Leydig insulin-like peptide activates the LGR8 receptor important in testis descent.* J Biol Chem, 2002. **277**(35): p. 31283-6.
70. Gorlov, I.P., et al., *Mutations of the GREAT gene cause cryptorchidism.* Hum Mol Genet, 2002. **11**(19): p. 2309-18.
71. Nef, S. and L.F. Parada, *Cryptorchidism in mice mutant for Insl3.* Nat Genet, 1999. **22**(3): p. 295-9.
72. Zimmermann, S., et al., *Targeted disruption of the Insl3 gene causes bilateral cryptorchidism.* Mol Endocrinol, 1999. **13**(5): p. 681-91.
73. Anand-Ivell, R., et al., *Insulin-like factor 3 levels in amniotic fluid of human male fetuses.* Human Reproduction, 2008. **23**(5): p. 1180-1186.
74. Tomboc, M., et al., *Insulin-like 3/relaxin-like factor gene mutations are associated with cryptorchidism.* J Clin Endocrinol Metab, 2000. **85**(11): p. 4013-8.
75. Harris, R.M., et al., *A missense mutation in LRR8 of RXFP2 is associated with cryptorchidism.* Mamm Genome, 2010. **21**(9-10): p. 442-9.
76. Bogatcheva, N.V., et al., *T222P mutation of the insulin-like 3 hormone receptor LGR8 is associated with testicular maldescent and hinders receptor expression on the cell surface membrane.* American Journal of Physiology-Endocrinology and Metabolism, 2007. **292**(1): p. E138-E144.
77. Ayers, K., et al., *Familial bilateral cryptorchidism is caused by recessive variants in <em>RXFP2</em&gt.* Journal of Medical Genetics, 2019: p. jmedgenet-2019-106203.
78. Ferlin, A., et al., *Paracrine and endocrine roles of insulin-like factor 3.* J Endocrinol Invest, 2006. **29**(7): p. 657-64.
79. Ferlin, A., et al., *Changes in serum insulin-like factor 3 during normal male puberty.* J Clin Endocrinol Metab, 2006. **91**(9): p. 3426-31.
80. Sedaghat, K., et al., *Leucine-rich repeat-containing G-protein-coupled receptor 8 in the rat brain: Enrichment in thalamic neurons and their efferent projections.* Neuroscience, 2008. **156**(2): p. 319-33.
81. Fu, P., et al., *Leucine-rich repeat-containing G-protein-coupled receptor 8 in mature glomeruli of developing and adult rat kidney and inhibition by insulin-like peptide-3 of glomerular cell proliferation.* Journal of endocrinology, 2006. **189**(2): p. 397-408.
82. Ferlin, A., et al., *Mutations in the insulin-like factor 3 receptor are associated with osteoporosis.* J Bone Miner Res, 2008. **23**(5): p. 683-93.
83. Spanel-Borowski, K., et al., *Increase in final stages of follicular atresia and premature decay of corpora lutea in Insl3-deficient mice.* Mol Reprod Dev, 2001. **58**(3): p. 281-6.
84. Kawamura, K., et al., *Paracrine regulation of mammalian oocyte maturation and male germ cell survival.* Proceedings of the National Academy of Sciences of the United States of America, 2004. **101**(19): p. 7323-7328.
85. Irving-Rodgers, H.F., et al., *Dynamic Changes in the Expression of Relaxin-Like Factor (Insl3), Cholesterol Side-Chain Cleavage Cytochrome P450, and 3ß-Hydroxysteroid Dehydrogenase in Bovine Ovarian Follicles During Growth and Atresia1.* Biology of Reproduction, 2002. **66**(4): p. 934-943.
86. Ivell, R. and R. Anand-Ivell, *Insulin-like peptide 3 (INSL3) is a major regulator of female reproductive physiology.* Human reproduction update, 2018.
87. Anand-Ivell, R., et al., *Circulating insulin-like factor 3 (INSL3) in healthy and infertile women.* Hum Reprod, 2013. **28**(11): p. 3093-102.
88. Wilkinson, T.N. and R.A. Bathgate, *The evolution of the relaxin peptide family and their receptors.* Adv Exp Med Biol, 2007. **612**: p. 1-13.

89. Burazin, T.C., et al., *Restricted, but abundant, expression of the novel rat gene-3 (R3) relaxin in the dorsal tegmental region of brain.* J Neurochem, 2002. **82**(6): p. 1553-7.
90. Sudo, S., et al., *H3 relaxin is a specific ligand for LGR7 and activates the receptor by interacting with both the ectodomain and the exoloop 2.* J Biol Chem, 2003. **278**(10): p. 7855-62.
91. Liu, C., et al., *Identification of Relaxin-3/INSL7 as an Endogenous Ligand for the Orphan G-protein-coupled Receptor GPCR135.* Journal of Biological Chemistry, 2003. **278**(50): p. 50754-50764.
92. Liu, C., et al., *Identification of Relaxin-3/INSL7 as a Ligand for GPCR142.* Journal of Biological Chemistry, 2003. **278**(50): p. 50765-50770.
93. Smith, C.M., et al., *Review: Relaxin-3 systems in the brain—The first 10 years.* Journal of Chemical Neuroanatomy, 2011. **42**: p. 262-275.
94. Liu, C., et al., *INSL5 Is a High Affinity Specific Agonist for GPCR142 (GPR100).* Journal of Biological Chemistry, 2005. **280**(1): p. 292-300.
95. Grosse, J., et al., *Insulin-like peptide 5 is an orexigenic gastrointestinal hormone.* Proc Natl Acad Sci U S A, 2014. **111**(30): p. 11133-8.
96. Burnicka-Turek, O., et al., *INSL5-deficient mice display an alteration in glucose homeostasis and an impaired fertility.* Endocrinology, 2012. **153**(10): p. 4655-65.
97. Belgi, A., et al., *Preliminary Structure--Function Relationship Studies on Insulin-Like Peptide 5 (INSL5).* International Journal of Peptide Research and Therapeutics, 2013(1): p. 71.
98. Ang, S.Y., et al., *The actions of relaxin family peptides on signal transduction pathways activated by the relaxin family peptide receptor RXFP4.* Naunyn-Schmiedeberg's archives of pharmacology, 2017. **390**(1): p. 105-111.
99. Janneau, J. and o. and, *Cloning of a new member of the insulin gene superfamily (INSL4) expressed in human placenta.* Genomics, 1995(2): p. 465.
100. Lok, S., et al., *Identification of INSL6, a new member of the insulin family that is expressed in the testis of the human and rat.* Biology Of Reproduction, 2000. **62**(6): p. 1593-1599.
101. *UTILITY OF INSULIN-LIKE 6 (INSL6) FOR THE TREATMENT OF AUTOIMMUNE DISEASES*. 2014.
102. Beavo, J.A. and L.L. Brunton, *Cyclic nucleotide research - still expanding after half a century*. 2002, NATURE PUBLISHING GROUP: Great Britain. p. 710.
103. Halls, M.L., et al., *Relaxin activates multiple cAMP signaling pathway profiles in different target cells.* Ann N Y Acad Sci, 2009. **1160**: p. 108-11.
104. Valkovic, A.L., et al., *Real-time examination of cAMP activity at relaxin family peptide receptors using a BRET-based biosensor.* Pharmacology Research & Perspectives, 2018. **6**(5): p. e00432.
105. Heng, K., et al., *Relaxin signalling in primary cultures of human myometrial cells.* MHR: Basic science of reproductive medicine, 2008. **14**(10): p. 603-611.
106. Halls, M.L., et al., *Relaxin Activates Multiple cAMP Signaling Pathway Profiles in Different Target Cells.* Annals of the New York Academy of Sciences, 2009. **1160**(1): p. 108-111.
107. Kocan, M., et al., *ML290 is a biased allosteric agonist at the relaxin receptor RXFP1.* Scientific reports, 2017. **7**(1): p. 2968.
108. Halls, M.L., et al., *International Union of Basic and Clinical Pharmacology. XCV. Recent advances in the understanding of the pharmacology and biological roles of relaxin family peptide receptors 1-4, the receptors for relaxin family peptides.* Pharmacol Rev, 2015. **67**(2): p. 389-440.
109. Chow, B.S., et al., *Relaxin signals through a RXFP1-pERK-nNOS-NO-cGMP-dependent pathway to up-regulate matrix metalloproteinases: the additional involvement of iNOS.* PLoS One, 2012. **7**(8): p. e42714.
110. Mookerjee, I., et al., *Relaxin inhibits renal myofibroblast differentiation via RXFP1, the nitric oxide pathway, and Smad2.* The FASEB Journal, 2009. **23**(4): p. 1219-1229.
111. Heeg, M.H.J., et al., *The antifibrotic effects of relaxin in human renal fibroblasts are mediated in part by inhibition of the Smad2 pathway2.* Kidney International, 2005. **68**(1): p. 96-109.

112. Baccari, M.C. and D. Bani, *Relaxin and nitric oxide signalling.* Curr Protein Pept Sci, 2008. **9**(6): p. 638-45.
113. Sarwar, M., et al., *Serelaxin-mediated signal transduction in human vascular cells: bell-shaped concentration–response curves reflect differential coupling to G proteins.* British journal of pharmacology, 2015. **172**(4): p. 1005-1019.
114. Chow, B.S.M., et al., *Relaxin requires the angiotensin II type 2 receptor to abrogate renal interstitial fibrosis.* Kidney International, 2014. **86**(1): p. 75-85.
115. Jones, E.S., M.J. Black, and R.E. Widdop, *Influence of Angiotensin II Subtype 2 Receptor (A T 2 R) Antagonist, PD123319, on Cardiovascular Remodelling of Aged Spontaneously Hypertensive Rats during Chronic Angiotensin II Subtype 1 Receptor (A T 1 R) Blockade.* International journal of hypertension, 2012. **2012**.
116. Chow BSM, K.M., Shen M, Wang Y, Chew HLJ, Wang C, Bosnyak S, Mirabito-Colafella KM, Barsha G, Wigg B, Johnstone EKM, Hossain MA, Pfleger KDG, Denton KM, Widdop RE, Summers RJ, Bathgate RAD, Hewitson TD, Samuel CS, *Evidence of AT1R-AT2R-RXFP1 Functional Crosstalk in Myofibroblasts and its Impact on the Therapeutic Targeting of Renal and Cardiac Fibrosis. .* Journal of the American Society of Nephrology, 2019.
117. Sassoli, C., et al., *Relaxin prevents cardiac fibroblast-myofibroblast transition via notch-1-mediated inhibition of TGF-beta/Smad3 signaling.* PLoS One, 2013. **8**(5): p. e63896.
118. Boccalini, G., et al., *Relaxin protects cardiac muscle cells from hypoxia/reoxygenation injury: involvement of the Notch-1 pathway.* FASEB J, 2015. **29**(1): p. 239-49.
119. Wei, X., et al., *Relaxin ameliorates high glucose-induced cardiomyocyte hypertrophy and apoptosis via the Notch1 pathway.* Exp Ther Med, 2018. **15**(1): p. 691-698.
120. Singh, S., R.L. Simpson, and R.G. Bennett, *Relaxin activates peroxisome proliferator-activated receptor gamma (PPARgamma) through a pathway involving PPARgamma coactivator 1alpha (PGC1alpha).* J Biol Chem, 2015. **290**(2): p. 950-9.
121. Lehrke, M. and M.A. Lazar, *The many faces of PPARgamma.* Cell, 2005. **123**(6): p. 993-9.
122. Halls, M.L., *Constitutive formation of an RXFP1-signalosome: a novel paradigm in GPCR function and regulation.* Br J Pharmacol, 2012. **165**(6): p. 1644-58.
123. Sherwood, O.D., *Relaxin's physiological roles and other diverse actions.* Endocr Rev, 2004. **25**(2): p. 205-34.
124. Ivell, R., R. ANAND-IVELL, and O. Bartsch, *Relaxin signaling from natural receptors.* Annals of the New York Academy of Sciences, 2005. **1041**(1): p. 280-287.
125. Nguyen, B.T., et al., *Phosphoinositide 3-kinase activity is required for biphasic stimulation of cyclic adenosine 3', 5'-monophosphate by relaxin.* Molecular endocrinology, 2003. **17**(6): p. 1075-1084.
126. Nistri, S. and D. Bani, *Relaxin receptors and nitric oxide synthases: search for the missing link.* Reproductive Biology and Endocrinology, 2003. **1**(1): p. 5.
127. Dodge, K.L. and B.M. Sanborn, *Evidence for inhibition by protein kinase A of receptor/Gαq/phospholipase C (PLC) coupling by a mechanism not involving PLCβ2.* Endocrinology, 1998. **139**(5): p. 2265-2271.
128. Gellersen, B. and J. Brosens, *Cyclic AMP and progesterone receptor cross-talk in human endometrium: a decidualizing affair.* Journal of Endocrinology, 2003. **178**(3): p. 357-372.
129. Callander, G.E., W.G. Thomas, and R.A. Bathgate, *Prolonged RXFP1 and RXFP2 signaling can be explained by poor internalization and a lack of β-arrestin recruitment.* American Journal of Physiology-Cell Physiology, 2009. **296**(5): p. C1058-C1066.
130. Halls, M.L., R.A. Bathgate, and R.J. Summers, *Relaxin family peptide receptors RXFP1 and RXFP2 modulate cAMP signaling by distinct mechanisms.* Mol Pharmacol, 2006. **70**(1): p. 214-26.
131. Scott, D., et al., *Characterization of the rat INSL3 receptor.* Annals of the New York Academy of Sciences, 2005. **1041**(1): p. 13-16.

132. Scott, D., et al., *Characterization of the mouse and rat relaxin receptors.* Annals of the New York Academy of Sciences, 2005. **1041**(1): p. 8-12.
133. Huang, Z., et al., *Mechanisms of INSL3 signaling in male reproductive organs.* Ital J Anat Embryol, 2013. **118**(1 Suppl): p. 32-3.
134. Ferlin, A., et al., *Profiling Insulin Like Factor 3 (INSL3) Signaling in Human Osteoblasts.* PLoS ONE, 2011. **6**(12): p. 1-11.
135. Halls, M.L., et al., *Multiple binding sites revealed by interaction of relaxin family peptides with native and chimeric relaxin family peptide receptors 1 and 2 (LGR7 and LGR8).* J Pharmacol Exp Ther, 2005. **313**(2): p. 677-87.
136. Shemesh, R., et al., *Discovery and validation of novel peptide agonists for G-protein coupled receptors.* Journal of Biological Chemistry, 2008.
137. Pini, A., et al., *Prevention of bleomycin-induced pulmonary fibrosis by a novel antifibrotic peptide with relaxin-like activity.* Journal of Pharmacology and Experimental Therapeutics, 2010. **335**(3): p. 589-599.
138. Glogowska, A., et al., *C1q-tumour necrosis factor-related protein 8 (CTRP8) is a novel interaction partner of relaxin receptor RXFP1 in human brain cancer cells.* The Journal of Pathology, 2013. **231**(4): p. 466-479.
139. Hossain, M.A., et al., *A single-chain derivative of the relaxin hormone is a functionally selective agonist of the G protein-coupled receptor, RXFP1.* Chemical Science, 2016. **7**(6): p. 3805-3819.
140. Tietjens, J. and J.R. Teerlink, *Serelaxin and acute heart failure.* Heart, 2016. **102**(2): p. 95-9.
141. Xiao, J., et al., *Discovery, optimization, and biological activity of the first potent and selective small-molecule agonist series of human relaxin receptor 1 (RXFP1)*, in *Probe Reports from the NIH Molecular Libraries Program*. 2010: Bethesda (MD).
142. Xiao, J., et al., *Identification and optimization of small-molecule agonists of the human relaxin hormone receptor RXFP1.* Nat Commun, 2013. **4**: p. 1953.
143. Huang, Z., et al., *Activation of Relaxin Family Receptor 1 from different mammalian species by relaxin peptide and small molecule agonist ML290.* Frontiers in Endocrinology, 2015. **6**(128).
144. van der Westhuizen, E.T., et al., *The Relaxin Family Peptide Receptor 3 Activates Extracellular Signal-Regulated Kinase 1/2 through a Protein Kinase C-Dependent Mechanism.* Molecular Pharmacology, 2007. **71**(6): p. 1618-1629.
145. Kocan, M., S.Y. Ang, and R.J. Summers, *Orthosteric, Allosteric and Biased Signalling at the Relaxin-3 Receptor RXFP3.* Neurochem Res, 2016. **41**(3): p. 610-9.
146. Kocan, M., et al., *Signalling profiles of H3 relaxin, H2 relaxin and R3 (BΔ23–27) R/I5 acting at the relaxin family peptide receptor 3 (RXFP3).* British journal of pharmacology, 2014. **171**(11): p. 2827-2841.
147. Ang, S.Y., et al., *Signal transduction pathways activated by insulin-like peptide 5 at the relaxin family peptide RXFP4 receptor.* British journal of pharmacology, 2017. **174**(10): p. 1077-1089.
148. Garber, S.L., et al., *Relaxin decreases renal interstitial fibrosis and slows progression of renal disease.* Kidney Int, 2001. **59**(3): p. 876-82.
149. McGuane, J.T., et al., *Relaxin induces rapid dilation of rodent small renal and human subcutaneous arteries via PI3 kinase and nitric oxide.* Endocrinology, 2011. **152**(7): p. 2786-96.
150. Conrad, K.P., *Unveiling the vasodilatory actions and mechanisms of relaxin.* Hypertension, 2010. **56**(1): p. 2-9.
151. Seibold, J.R., et al., *Recombinant human relaxin in the treatment of scleroderma. A randomized, double-blind, placebo-controlled trial.* Ann Intern Med, 2000. **132**(11): p. 871-9.
152. McGorray, S.P., et al., *A randomized, placebo-controlled clinical trial on the effects of recombinant human relaxin on tooth movement and short-term stability.* American Journal of Orthodontics and Dentofacial Orthopedics, 2012. **141**(2): p. 196-203.
153. Teichman, S.L., et al., *Relaxin: review of biology and potential role in treating heart failure.* Curr Heart Fail Rep, 2010. **7**(2): p. 75-82.

154. Tietjens, J. and J.R. Teerlink, *Serelaxin and acute heart failure.* Heart, 2015: p. heartjnl-2014-306786.
155. Devarakonda, T. and F.N. Salloum, *Heart Disease and Relaxin: New Actions for an Old Hormone.* Trends in Endocrinology & Metabolism, 2018. **29**(5): p. 338-348.
156. McCullough, P.A., *How trialists and pharmaceutical sponsors have failed us by thinking that acute heart failure is a 48-hour illness*. 2017, Elsevier.
157. Snowdon, V.K., et al., *Serelaxin as a potential treatment for renal dysfunction in cirrhosis: Preclinical evaluation and results of a randomized phase 2 trial.* PLOS Medicine, 2017. **14**(2): p. e1002248.
158. Alexiou, K., et al., *Relaxin is a candidate drug for lung preservation: relaxin-induced protection of rat lungs from ischemia-reperfusion injury.* The Journal of Heart and Lung Transplantation, 2010. **29**(4): p. 454-460.
159. Popkov, V.A., et al., *Pregnancy protects the kidney from acute ischemic injury.* Scientific Reports, 2018. **8**(1): p. 14534.
160. Marshall, S.A., et al., *Relaxin treatment reduces angiotensin II-induced vasoconstriction in pregnancy and protects against endothelial dysfunction.* Biology of reproduction, 2017. **96**(4): p. 895-906.
161. Marshall, S.A., et al., *B7-33 replicates the vasoprotective functions of human relaxin-2 (serelaxin).* European Journal of Pharmacology, 2017. **807**: p. 190-197.
162. Domińska, K., et al., *Regulation of mRNA gene expression of members of the NF-κB transcription factor gene family by angiotensin II and relaxin 2 in normal and cancer prostate cell lines.* Molecular medicine reports, 2017. **15**(6): p. 4352-4359.
163. Guo, X., et al., *Serum relaxin as a diagnostic and prognostic marker in patients with epithelial ovarian cancer.* Cancer Biomarkers: Section A Of Disease Markers, 2017. **21**(1): p. 81-87.
164. Fue, M., et al., *Relaxin 2/RXFP1 Signaling Induces Cell Invasion via the β-Catenin Pathway in Endometrial Cancer.* International Journal of Molecular Sciences, 2018. **19**(8): p. N.PAG-N.PAG.
165. Binder, C., et al., *Relaxins enhance growth of spontaneous murine breast cancers as well as metastatic colonization of the brain.* Clinical & Experimental Metastasis, 2014. **31**(1): p. 57-65.
166. Hu, X., et al., *Structural Insights into the Activation of Human Relaxin Family Peptide Receptor 1 by Small-Molecule Agonists.* Biochemistry, 2016. **55**(12): p. 1772-1783.
167. Yoshida, T., et al., *Relaxin ameliorates salt-sensitive hypertension and renal fibrosis.* Nephrology Dialysis Transplantation, 2011. **27**(6): p. 2190-2197.
168. Dean, J.D., et al., *The I nternational S ociety for S exual M edicine's Process of Care for the Assessment and Management of Testosterone Deficiency in Adult Men.* The journal of sexual medicine, 2015. **12**(8): p. 1660-1686.
169. De Toni, L., et al., *INSL3 in the muscolo-skeletal system*. 2019. p. 12-17.
170. Ferlin, A., et al., *Testicular function and bone metabolism--beyond testosterone.* Nat Rev Endocrinol, 2013. **9**(9): p. 548-54.
171. Gambineri, A., et al., *Insulin-like factor 3: a new circulating hormone related to luteinizing hormone-dependent ovarian hyperandrogenism in the polycystic ovary syndrome.* The Journal of Clinical Endocrinology & Metabolism, 2007. **92**(6): p. 2066-2073.
172. Shaikh, N., et al., *Polymorphisms and haplotypes of insulin-like factor 3 gene are associated with risk of polycystic ovary syndrome in Indian women.* Gene, 2016. **577**(2): p. 180-186.
173. Ivell, R. and R. Anand-Ivell, *Insulin-like peptide 3 (INSL3) is a major regulator of female reproductive physiology.* Human Reproduction Update, 2018. **24**(6): p. 639-651.
174. Ivell, R. and R. Anand-Ivell, *Biology of insulin-like factor 3 in human reproduction.* Human Reproduction Update, 2009. **15**(4): p. 463-476.
175. Hombach-Klonisch, S., et al., *INSL-3 is expressed in human hyperplastic and neoplastic thyrocytes.* International Journal of Oncology, 2003. **22**(5): p. 993-1001.

176. Lottrup, G., et al., *Expression patterns of DLK1 and INSL3 identify stages of Leydig cell differentiation during normal development and in testicular pathologies, including testicular cancer and Klinefelter syndrome.* Human Reproduction, 2014. **29**(8): p. 1637-1650.
177. Klonisch, T., et al., *INSL3 in the benign hyperplastic and neoplastic human prostate gland.* International journal of oncology, 2005. **27**(2): p. 307-315.
178. Rossato, M., M. Barban, and R. Vettor, *Elevated plasma levels of the novel hormone INSL3 in a woman with metastatic ovarian cancer.* The International journal of biological markers, 2007. **22**(2): p. 159-160.
179. Rovira, X., J.-P. Pin, and J. Giraldo, *Opinion: The asymmetric/symmetric activation of GPCR dimers as a possible mechanistic rationale for multiple signalling pathways.* Trends in Pharmacological Sciences, 2010. **31**: p. 15-21.
180. Bouvier, M. and T.E. Hebert, *CrossTalk proposal: Weighing the evidence for Class A GPCR dimers, the evidence favours dimers.* Journal of Physiology, 2014(12): p. 2439.
181. Kniazeff, J., et al., *Associate editor: Ulrik Gether: Dimers and beyond: The functional puzzles of class C GPCRs.* Pharmacology and Therapeutics, 2011. **130**: p. 9-25.
182. de Lau, W., et al., *Lgr5 homologues associate with Wnt receptors and mediate R-spondin signalling.* Nature, 2011. **476**: p. 293.
183. Fan, Q.R. and W.A. Hendrickson, *Structure of human follicle-stimulating hormone in complex with its receptor.* Nature, 2005. **433**: p. 269.
184. De Meyts, P. and P. De Meyts, *The insulin receptor: a prototype for dimeric, allosteric membrane receptors?* Trends in Biochemical Sciences, 2008. **33**: p. 376-384.
185. Siddle, K., *Signalling by insulin and IGF receptors: supporting acts and new players.* 2011. **47**(1): p. R1.
186. Kiselyov, V.V., et al., *Harmonic oscillator model of the insulin and IGF1 receptors' allosteric binding and activation.* Molecular Systems Biology, 2009. **5**(1).
187. Svendsen, A.M., et al., *Negative cooperativity in H2 relaxin binding to a dimeric relaxin family peptide receptor 1.* Mol Cell Endocrinol, 2008. **296**(1-2): p. 10-7.
188. Svendsen, A.M., et al., *Cooperative binding of insulin-like Peptide 3 to a dimeric relaxin family peptide receptor 2.* Endocrinology, 2008. **149**(3): p. 1113-20.
189. Hoare, B.L., et al., *Using the novel HiBiT tag to label cell surface relaxin receptors for BRET proximity analysis.* Pharmacology Research & Perspectives, 2019. **7**(4): p. e00513.
190. Halls, M.L. and D.M. Cooper, *Sub-picomolar relaxin signalling by a pre-assembled RXFP1, AKAP79, AC2, beta-arrestin 2, PDE4D3 complex.* EMBO J, 2010. **29**(16): p. 2772-87.
191. Luttrell, L.M. and R.J. Lefkowitz, *The role of β-arrestins in the termination and transduction of G-protein-coupled receptor signals.* Journal of Cell Science, 2002. **115**(3): p. 455-465.
192. Rong Huang, J.U.N., et al., *Regulation of Prolactin Production by Progestin, Estrogen, and Relaxin in Human Endometrial Stromal Cells*.* Endocrinology, 1987. **121**(6): p. 2011-2017.
193. Sunn, N., et al., *Circulating relaxin acts on subfornical organ neurons to stimulate water drinking in the rat.* Proceedings of the National Academy of Sciences, 2002. **99**(3): p. 1701-1706.
194. Tan, Y.Y., et al., *Comparison of relaxin receptors in rat isolated atria and uterus by use of synthetic and native relaxin analogues.* British journal of pharmacology, 1998. **123**(4): p. 762-770.
195. Hartley, B.J., et al., *Resolving the Unconventional Mechanisms Underlying RXFP1 and RXFP2 Receptor Function.* Annals of the New York Academy of Sciences, 2009. **1160**: p. 67-73.
196. Yan, Y., et al., *Identification of the N-linked glycosylation sites of the human relaxin receptor and effect of glycosylation on receptor function.* Biochemistry, 2008. **47**(26): p. 6953-68.
197. Kong, R.C., et al., *Mapping key regions of the RXFP2 low-density lipoprotein class-A module that are involved in signal activation.* Biochemistry, 2014. **53**(28): p. 4537-48.

198. Kern, A. and G.D. Bryant-Greenwood, *Mechanisms of Relaxin Receptor (LGR7/RXFP1) Expression and Function.* Annals of the New York Academy of Sciences, 2009. **1160**(1): p. 60-66.
199. Muda, M., et al., *Splice variants of the relaxin and INSL3 receptors reveal unanticipated molecular complexity.* MHR: Basic science of reproductive medicine, 2005. **11**(8): p. 591-600.
200. Scott, D.J., et al., *Characterization of novel splice variants of LGR7 and LGR8 reveals that receptor signaling is mediated by their unique low density lipoprotein class A modules.* J Biol Chem, 2006. **281**(46): p. 34942-54.
201. Kern, A.s., et al., *Cloning, Expression, and Functional Characterization of Relaxin Receptor (Leucine-Rich Repeat-Containing G Protein-Coupled Receptor 7) Splice Variants from Human Fetal Membranes.* Endocrinology, 2008. **149**(3): p. 1277-1294.
202. Zhu, J., et al., *Identification of the domains in RXFP4 (GPCR142) responsible for the high affinity binding and agonistic activity of INSL5 at RXFP4 compared to RXFP3 (GPCR135).* European Journal of Pharmacology, 2008. **590**(1): p. 43-52.
203. Belgi, A., et al., *Structure and Function Relationship of Murine Insulin-like Peptide 5 (INSL5): Free C-Terminus Is Essential for RXFP4 Receptor Binding and Activation.* Biochemistry, 2011. **50**(39): p. 8352-8361.
204. Patil, N.A., et al., *The C-terminus of the B-chain of human insulin-like peptide 5 is critical for cognate RXFP4 receptor activity.* Amino Acids, 2016. **48**(4): p. 987-992.
205. Kuei, C., et al., *R3 (BΔ23–27) R/I5 Chimeric Peptide, a Selective Antagonist for GPCR135 and GPCR142 over Relaxin Receptor LGR7 IN VITRO AND IN VIVO CHARACTERIZATION.* Journal of Biological Chemistry, 2007. **282**(35): p. 25425-25435.
206. Wong, L., et al., *Distinct but overlapping binding sites of agonist and antagonist at the relaxin family peptide 3 (RXFP3) receptor.* The Journal of biological chemistry, 2018.
207. Haugaard-Kedstrom, L.M., et al., *Design, synthesis, and characterization of a single-chain peptide antagonist for the relaxin-3 receptor RXFP3.* Journal of the American Chemical Society, 2011. **133**(13): p. 4965-4974.
208. Hu, M.-J., et al., *Interaction mechanism of insulin-like peptide 5 with relaxin family peptide receptor 4.* Archives of Biochemistry and Biophysics, 2017. **619**: p. 27-34.
209. Hojo, K., et al., *Development of a single-chain peptide agonist of the relaxin-3 receptor using hydrocarbon stapling.* Journal of medicinal chemistry, 2016. **59**(16): p. 7445-7456.
210. Jayakody, T., et al., *Hydrocarbon stapled B chain analogues of relaxin-3 retain biological activity.* Peptides, 2016. **84**: p. 44-57.
211. Liu, C., et al., *Relaxin-3/insulin-like peptide 5 chimeric peptide, a selective ligand for G protein-coupled receptor (GPCR) 135 and GPCR142 over leucine-rich repeat-containing G protein-coupled receptor 7.* Molecular pharmacology, 2005. **67**(1): p. 231-240.
212. Hu, M.-J., et al., *Mechanism for insulin-like peptide 5 distinguishing the homologous relaxin family peptide receptor 3 and 4.* Scientific reports, 2016. **6**: p. 29648.
213. Kobe, B. and A.V. Kajava, *The leucine-rich repeat as a protein recognition motif.* Current Opinion in Structural Biology, 2001. **11**(6): p. 725-732.
214. Hsu, S.Y., et al., *The three subfamilies of leucine-rich repeat-containing G protein-coupled receptors (LGR): identification of LGR6 and LGR7 and the signaling mechanism for LGR7.* Molecular endocrinology, 2000. **14**(8): p. 1257-1271.
215. Hsu, S.Y., S.-G. Liang, and A.J. Hsueh, *Characterization of two LGR genes homologous to gonadotropin and thyrotropin receptors with extracellular leucine-rich repeats and a G protein-coupled, seven-transmembrane region.* Molecular endocrinology, 1998. **12**(12): p. 1830-1845.
216. de Lau, W., et al., *Lgr5 homologues associate with Wnt receptors and mediate R-spondin signalling.* Nature, 2011. **476**(7360): p. 293.
217. Glinka, A., et al., *LGR4 and LGR5 are R-spondin receptors mediating Wnt/β-catenin and Wnt/PCP signalling.* EMBO reports, 2011. **12**(10): p. 1055-1061.

218. Simoni, M., J.r. Gromoll, and E. Nieschlag, *The follicle-stimulating hormone receptor: biochemistry, molecular biology, physiology, and pathophysiology.* Endocrine reviews, 1997. **18**(6): p. 739-773.
219. Ascoli, M., F. Fanelli, and D.L. Segaloff, *The lutropin/choriogonadotropin receptor, a 2002 perspective.* Endocrine reviews, 2002. **23**(2): p. 141-174.
220. Harfst, E., et al., *The use of the amplifiable high-expression vector pEE14 to study the interactions of autoantibodies with recombinant human thyrotrophin receptor.* Molecular and cellular endocrinology, 1992. **83**(2-3): p. 117-123.
221. Wang, D., et al., *Structural basis for R-spondin recognition by LGR4/5/6 receptors.* Genes & development, 2013. **27**(12): p. 1339-1344.
222. Gong, X., et al., *LGR6 is a high affinity receptor of R-spondins and potentially functions as a tumor suppressor.* PloS one, 2012. **7**(5): p. e37137.
223. Petrie, E.J., et al., *In a Class of Their Own – RXFP1 and RXFP2 are Unique Members of the LGR Family.* Frontiers in Endocrinology, 2015. **6**(137).
224. Costagliola, S., et al., *Tyrosine sulfation is required for agonist recognition by glycoprotein hormone receptors.* The EMBO journal, 2002. **21**(4): p. 504-513.
225. Jiang, X., et al., *Structure of follicle-stimulating hormone in complex with the entire ectodomain of its receptor.* Proceedings of the National Academy of Sciences, 2012. **109**(31): p. 12491-12496.
226. Sanders, P., et al., *Crystal structure of the TSH receptor bound to a blocking type TSHR autoantibody.* Journal of molecular endocrinology, 2011: p. JME-10-0127.
227. Bonomi, M., et al., *Structural differences in the hinge region of the glycoprotein hormone receptors: evidence from the sulfated tyrosine residues.* Molecular endocrinology, 2006. **20**(12): p. 3351-3363.
228. Nurwakagari, P., et al., *A conformational contribution of the luteinizing hormone–receptor ectodomain to receptor activation.* Journal of molecular endocrinology, 2007. **38**(2): p. 259-275.
229. Peng, W.C., et al., *Structure of stem cell growth factor R-spondin 1 in complex with the ectodomain of its receptor LGR5.* Cell reports, 2013. **3**(6): p. 1885-1892.
230. Xu, J.-G., et al., *Crystal Structure of LGR4-Rspo1 Complex: INSIGHTS INTO THE DIVERGENT MECHANISMS OF LIGAND RECOGNITION BY LEUCINE-RICH REPEAT G-PROTEIN-COUPLED RECEPTORS (LGRs).* Journal of Biological Chemistry, 2015. **290**(4): p. 2455-2465.
231. Peng, Weng C., et al., *Structure of Stem Cell Growth Factor R-spondin 1 in Complex with the Ectodomain of Its Receptor LGR5.* Cell Reports, 2013. **3**(6): p. 1885-1892.
232. Ruffner, H., et al., *R-Spondin potentiates Wnt/ß-catenin signaling through orphan receptors LGR4 and LGR5.* PloS one, 2012. **7**(7): p. e40976.
233. McKern, N.M., et al., *Structure of the insulin receptor ectodomain reveals a folded-over conformation.* Nature, 2006. **443**: p. 218.
234. Adams, T.E., et al., *Structure and function of the type 1 insulin-like growth factor receptor.* Cellular and Molecular Life Sciences CMLS, 2000. **57**(7): p. 1050-1093.
235. De Meyts, P. and J. Whittaker, *Structural biology of insulin and IGF1 receptors: implications for drug design.* Nature Reviews Drug Discovery, 2002. **1**(10): p. 769.
236. De Meyts, P., *Insulin and its receptor: structure, function and evolution.* Bioessays, 2004. **26**(12): p. 1351-1362.
237. Kristensen, C., et al., *Functional Reconstitution of Insulin Receptor Binding Site from Non-binding Receptor Fragments.* Journal of Biological Chemistry, 2002. **277**(21): p. 18340-18345.
238. De Meyts, P., *The insulin receptor: a prototype for dimeric, allosteric membrane receptors?* Trends in Biochemical Sciences, 2008. **33**(8): p. 376-384.
239. De Meyts, P., *The structural basis of insulin and insulin-like growth factor-I receptor binding and negative co-operativity, and its relevance to mitogenic versus metabolic signalling.* Diabetologia, 1994. **37**(2): p. S135-S148.

240. Croll, Tristan I., et al., *Higher-Resolution Structure of the Human Insulin Receptor Ectodomain: Multi-Modal Inclusion of the Insert Domain.* Structure, 2016. **24**(3): p. 469-476.
241. Smith, B.J., et al., *Structural resolution of a tandem hormone-binding element in the insulin receptor and its implications for design of peptide agonists.* Proceedings of the National Academy of Sciences, 2010. **107**(15): p. 6771.
242. Menting, J.G., et al., *Structural Congruency of Ligand Binding to the Insulin and Insulin/Type 1 Insulin-like Growth Factor Hybrid Receptors.* Structure, 2015. **23**(7): p. 1271-82.
243. Bullesbach, E.E. and C. Schwabe, *The trap-like relaxin-binding site of the leucine-rich G-protein-coupled receptor 7.* J Biol Chem, 2005. **280**(14): p. 14051-6.
244. Scott, D.J., G.W. Tregear, and R.A. Bathgate, *Modeling the primary hormone-binding site of RXFP1 and RXFP2.* Annals of the New York Academy of Sciences, 2009. **1160**(1): p. 74-77.
245. Scott, D.J., K.J. Rosengren, and R.A. Bathgate, *The different ligand-binding modes of relaxin family peptide receptors RXFP1 and RXFP2.* Mol Endocrinol, 2012. **26**(11): p. 1896-906.
246. Scott, D.J., et al., *Defining the LGR8 residues involved in binding insulin-like peptide 3.* Mol Endocrinol, 2007. **21**(7): p. 1699-712.
247. Chan, L.J., et al., *The Importance of Tryptophan B28 in H2 Relaxin for RXFP2 Binding and Activation.* International Journal of Peptide Research and Therapeutics, 2013(1): p. 55.
248. Halls, M.L., et al., *Identification of binding sites with differing affinity and potency for relaxin analogues on LGR7 and LGR8 receptors.* Ann N Y Acad Sci, 2005. **1041**: p. 17-21.
249. Bullesbach, E.E. and C. Schwabe, *The relaxin receptor-binding site geometry suggests a novel gripping mode of interaction.* J Biol Chem, 2000. **275**(45): p. 35276-80.
250. Bullesbach, E.E. and C. Schwabe, *The mode of interaction of the relaxin-like factor (RLF) with the leucine-rich repeat G protein-activated receptor 8.* J Biol Chem, 2006. **281**(36): p. 26136-43.
251. Diepenhorst, N.A., et al., *Investigation of interactions at the extracellular loops of the relaxin family peptide receptor 1 (RXFP1).* J Biol Chem, 2014. **289**(50): p. 34938-52.
252. Del Borgo, M.P., et al., *Analogs of Insulin-like Peptide 3 (INSL3) B-chain Are LGR8 Antagonists in Vitro and in Vivo.* Journal of Biological Chemistry, 2006. **281**(19): p. 13068-13074.
253. Shabanpoor, F., et al., *Design and development of analogues of dimers of insulin-like peptide 3 B-chain as high-affinity antagonists of the RXFP2 receptor.* Peptide Science, 2011. **96**(1): p. 81-87.
254. Bullesbach, E.E. and C. Schwabe, *LGR8 signal activation by the relaxin-like factor.* J Biol Chem, 2005. **280**(15): p. 14586-90.
255. Hossain, M.A., et al., *The A-chain of human relaxin family peptides has distinct roles in the binding and activation of the different relaxin family peptide receptors.* J Biol Chem, 2008. **283**(25): p. 17287-97.
256. Kern, A., A.I. Agoulnik, and G.D. Bryant-Greenwood, *The low-density lipoprotein class A module of the relaxin receptor (leucine-rich repeat containing G-protein coupled receptor 7): its role in signaling and trafficking to the cell membrane.* Endocrinology, 2007. **148**(3): p. 1181-94.
257. Kong, R.C., et al., *The relaxin receptor (RXFP1) utilizes hydrophobic moieties on a signaling surface of its N-terminal low density lipoprotein class A module to mediate receptor activation.* J Biol Chem, 2013. **288**(39): p. 28138-51.
258. Hopkins, E.J., et al., *The NMR solution structure of the relaxin (RXFP1) receptor lipoprotein receptor class A module and identification of key residues in the N-terminal region of the module that mediate receptor activation.* J Biol Chem, 2007. **282**(6): p. 4172-84.
259. Yamamoto, T., et al., *The human LDL receptor: a cysteine-rich protein with multiple Alu sequences in its mRNA.* Cell, 1984. **39**(1): p. 27-38.
260. Sudhof, T.C., et al., *The LDL receptor gene: a mosaic of exons shared with different proteins.* Science, 1985. **228**(4701): p. 815-822.

261. Martínez-Oliván, J., et al., *Intradomain Confinement of Disulfides in the Folding of Two Consecutive Modules of the LDL Receptor.* PLoS One, 2015. **10**(7): p. 1-17.
262. Bieri, S., et al., *Folding, calcium binding, and structural characterization of a concatemer of the first and second ligand-binding modules of the low-density lipoprotein receptor.* Biochemistry, 1998(31): p. 10994.
263. Bates, P., J.A. Young, and H.E. Varmus, *A receptor for subgroup A Rous sarcoma virus is related to the low density lipoprotein receptor.* Cell, 1993. **74**(6): p. 1043-1051.
264. Demczuk, S., et al., *Cloning of a balanced translocation breakpoint in the DiGeorge syndrome critical region and isolation of a novel potential adhesion receptor gene in its vicinity.* Human molecular genetics, 1995. **4**(4): p. 551-558.
265. Zhang, W., et al., *Agrin Binds to the N-terminal Region of Lrp4 Protein and Stimulates Association between Lrp4 and the First Immunoglobulin-like Domain in Muscle-specific Kinase (MuSK).* Journal of Biological Chemistry, 2011. **286**(47): p. 40624-40630.
266. Guttman, M., et al., *Decoding of Lipoprotein—Receptor Interactions: Properties of Ligand Binding Modules Governing Interactions with Apolipoprotein E.* Biochemistry, 2010. **49**(6): p. 1207-1216.
267. Rudenko, G. and J. Deisenhofer, *The low-density lipoprotein receptor: ligands, debates and lore.* Current Opinion in Structural Biology, 2003. **13**(6): p. 683-689.
268. Bogatcheva, N.V., et al., *T222P mutation of the insulin-like 3 hormone receptor LGR8 is associated with testicular maldescent and hinders receptor expression on the cell surface membrane.* Am J Physiol Endocrinol Metab, 2007. **292**(1): p. E138-44.
269. Liebscher, I., et al., *A Tethered Agonist within the Ectodomain Activates the Adhesion G Protein-Coupled Receptors GPR126 and GPR133.* Cell Reports, 2014. **9**(6): p. 2018-2026.
270. Stoveken, H.M., et al., *Adhesion G protein-coupled receptors are activated by exposure of a cryptic tethered agonist.* Proceedings of the National Academy of Sciences, 2015. **112**(19): p. 6194-6199.
271. Adams, M.N., et al., *Structure, function and pathophysiology of protease activated receptors.* Pharmacol Ther, 2011. **130**(3): p. 248-82.
272. Shaw, G., et al., *Preferential transformation of human neuronal cells by human adenoviruses and the origin of HEK 293 cells.* The FASEB Journal, 2002. **16**(8): p. 869-871.
273. Stevens, R.C., et al., *The GPCR Network: a large-scale collaboration to determine human GPCR structure and function.* Nature Reviews Drug Discovery, 2013. **12**(1): p. 25-34.
274. Overington, J.P., B. Al-Lazikani, and A.L. Hopkins, *How many drug targets are there?* Nature Reviews Drug Discovery, 2006. **5**(12): p. 993-996.
275. Hsu, S.Y., et al., *Activation of orphan receptors by the hormone relaxin.* Science, 2002. **295**(5555): p. 671-674.
276. Svendsen, A.M., et al., *Dimerization and Negative Cooperativity in the Relaxin Family Peptide Receptors.* Ann N Y Acad Sci, 2009. **1160**(1): p. 54-59.
277. Svendsen, A.M., et al., *Negative cooperativity in H2 relaxin binding to a dimeric relaxin family peptide receptor 1.* Molecular and Cellular Endocrinology, 2008. **296**(1–2): p. 10-17.
278. Bathgate, R.A.D., et al., *Relaxin Family Peptides and Their Receptors.* Physiological Reviews, 2013. **93**(1): p. 405-480.
279. Fisher, C., N. Beglova, and S.C. Blacklow, *Structure of an LDLR-RAP Complex Reveals a General Mode for Ligand Recognition by Lipoprotein Receptors.* Mol. Cell, 2006. **22**(2): p. 277-283.
280. Kong, R.C., et al., *The relaxin receptor (RXFP1) utilises hydrophobic moieties on a signalling surface of its N-terminal low density lipoprotein class A module to mediate receptor activation.* J Biol Chem, 2013. **First Published on August 7, 2013, doi:10.1074/jbc.M113.499640**.
281. Shabanpoor, F., et al., *Solid-Phase Synthesis of Europium-Labeled Human INSL3 as a Novel Probe for the Study of Ligand−Receptor Interactions.* Bioconjugate Chemistry, 2008. **19**(7): p. 1456-1463.

282. Shabanpoor, F., et al., *Site-specific conjugation of a lanthanide chelator and its effects on the chemical synthesis and receptor binding affinity of human relaxin-2 hormone.* Biochem Biophys Res Commun, 2012. **420**(2): p. 253-6.
283. Chen, W.B., et al., *A Colorimetric Assay for Measuring Activation of Gs- and Gq-Coupled Signaling Pathways.* Analytical Biochemistry, 1995. **226**(2): p. 349-354.
284. Blacklow, S.C., *Versatility in ligand recognition by LDL receptor family proteins: advances and frontiers.* Curr Opin Struct Biol, 2007. **17**(4): p. 419-26.
285. Yasui, N., T. Nogi, and J. Takagi, *Structural Basis for Specific Recognition of Reelin by Its Receptors.* Structure. **18**(3): p. 320-331.
286. Scott, D.J., K.J. Rosengren, and R.A. Bathgate, *The different ligand-binding modes of relaxin family peptide receptors RXFP1 and RXFP2.* Molecular Endocrinology, 2012. **26**(11): p. 1896-906.
287. Wilkinson, T.N., et al., *Coevolution of the relaxin-like peptides and their receptors.* Ann N Y Acad Sci, 2005. **1041**: p. 534-9.
288. Nair, V.B., et al., *Human relaxin-2: historical perspectives and role in cancer biology.* Amino Acids, 2012. **43**(3): p. 1131-40.
289. Teerlink, J.R., et al., *Serelaxin, recombinant human relaxin-2, for treatment of acute heart failure (RELAX-AHF): a randomised, placebo-controlled trial.* Lancet, 2013. **381**(9860): p. 29-39.
290. Scott, D.J., et al., *Characterization of novel splice variants of LGR7 and LGR8 reveals that receptor signaling is mediated by their unique LDLa modules.* J Biol Chem, 2006. **281**: p. 34942-34954.
291. Chen, C.Z., et al., *Identification of small-molecule agonists of human relaxin family receptor 1 (RXFP1) by using a homogenous cell-based cAMP assay.* J Biomol Screen, 2013. **18**(6): p. 670-7.
292. Zheng, L., U. Baumann, and J.L. Reymond, *An efficient one-step site-directed and site-saturation mutagenesis protocol.* Nucleic Acids Res, 2004. **32**(14): p. e115.
293. Liu, H. and J.H. Naismith, *An efficient one-step site-directed deletion, insertion, single and multiple-site plasmid mutagenesis protocol.* BMC Biotechnol, 2008. **8**: p. 91.
294. Chen, W., et al., *A colorimetric assay for measuring activation of Gs- and Gq-coupled signaling pathways.* Anal Biochem, 1995. **226**(2): p. 349-54.
295. Dong, C., Z. Liu, and F. Wang, *Radioligand saturation binding for quantitative analysis of ligand-receptor interactions.* Biophysics reports, 2015. **1**(3): p. 148-155.
296. Cunningham, B.C. and J.A. Wells, *High-resolution epitope mapping of hGH-receptor interactions by alanine-scanning mutagenesis.* Science, 1989. **244**: p. 1081+.
297. Deupi, X. and J. Standfuss, *Structural insights into agonist-induced activation of G-protein-coupled receptors.* Curr Opin Struct Biol, 2011. **21**(4): p. 541-51.
298. Metzler, W.J., et al., *The Three-Dimensional Solution Structure of the SH2 Domain from p55 blk Kinase.* Biochemistry, 1996. **35**(20): p. 6201-6211.
299. Kai, L., D. Torchia, and A. Bax, *Backbone dynamics of proteins as studied by 15N inverse detected heteronuclear NMR spectroscopy: application to staphyloccal nuclase.* Biochemistry, 1989. **28**: p. 8972.
300. Bullesbach, E.E. and C. Schwabe, *Structural contribution of the A-chain loop in relaxin.* Int J Pept Protein Res, 1995. **46**(3-4): p. 238-43.
301. Wheatley, M., et al., *Lifting the lid on GPCRs: the role of extracellular loops.* British journal of pharmacology, 2012. **165**(6): p. 1688-1703.
302. Studier, F.W., *Protein production by auto-induction in high density shaking cultures.* Protein Expr Purif, 2005. **41**(1): p. 207-34.
303. Cai, M., et al., *An efficient and cost-effective isotope labeling protocol for proteins expressed in Escherichia coli.* J Biomol NMR, 1998. **11**(1): p. 97-102.

304. Sreerama, N., S.Y. Venyaminov, and R.W. Woody, *Estimation of protein secondary structure from circular dichroism spectra: inclusion of denatured proteins with native proteins in the analysis.* Anal Biochem, 2000. **287**(2): p. 243-51.
305. Shabanpoor, F., et al., *Solid-phase synthesis of europium-labeled human INSL3 as a novel probe for the study of ligand-receptor interactions.* Bioconjug Chem, 2008. **19**(7): p. 1456-63.
306. Haugaard-Kedstrom, L.M., et al., *Solution structure, aggregation behavior, and flexibility of human relaxin-2.* ACS Chem Biol, 2015. **10**(3): p. 891-900.
307. Varga, C.M., et al., *Quantitative comparison of polyethylenimine formulations and adenoviral vectors in terms of intracellular gene delivery processes.* Gene Therapy, 2005. **12**(13): p. 1023-1032.
308. Yasui, N., T. Nogi, and J. Takagi, *Structural basis for specific recognition of reelin by its receptors.* Structure, 2010. **18**(3): p. 320-331.
309. Fisher, C., N. Beglova, and S.C. Blacklow, *Structure of an LDLR-RAP complex reveals a general mode for ligand recognition by lipoprotein receptors.* Molecular cell, 2006. **22**(2): p. 277-283.
310. Dagil, R., et al., *Gentamicin Binds to the Megalin Receptor as a Competitive Inhibitor Using the Common Ligand Binding Motif of Complement Type Repeats INSIGHT FROM THE NMR STRUCTURE OF THE 10TH COMPLEMENT TYPE REPEAT DOMAIN ALONE AND IN COMPLEX WITH GENTAMICIN.* Journal of Biological Chemistry, 2013. **288**(6): p. 4424-4435.
311. Hossain, M.A., et al., *A-chain of Human Relaxin Family Peptides Has Distinct Roles in the Binding and Activation of the Different Relaxin Family Peptide Receptors.* Journal of biological chemistry, 2008(25).
312. Büllesbach, E.E. and C. Schwabe, *LGR8 signal activation by the relaxin-like factor.* The Journal Of Biological Chemistry, 2005. **280**(15): p. 14586-14590.
313. Hossain, M.A., J.D. Wade, and R.A. Bathgate, *Chimeric relaxin peptides highlight the role of the A-chain in the function of H2 relaxin.* Peptides, 2012. **35**(1): p. 102-6.
314. Berthold, M. and T. Bartfai, *Modes of Peptide Binding in G Protein-Coupled Receptors.* Neurochemical Research, 1997. **22**(8): p. 1023-1031.
315. Wu, F., et al., *Structure and function of peptide-binding G protein-coupled receptors.* Journal of molecular biology, 2017. **429**(17): p. 2726-2745.
316. Agoulnik, A.I., et al., *Synthetic non-peptide low molecular weight agonists of the relaxin receptor 1.* Br J Pharmacol, 2017. **174**(10): p. 977-989.
317. Sadava, D.E., et al., *Life: The science of biology*. 2008: MacMillan.
318. Hay, D.L., D.R. Poyner, and P.M. Sexton, *GPCR modulation by RAMPs.* Pharmacology & Therapeutics, 2006. **109**(1): p. 173-197.
319. Schöneberg, T., G. Kleinau, and A. Brüser, *What are they waiting for?—Tethered agonism in G protein-coupled receptors.* Pharmacological Research, 2016. **108**: p. 9-15.